Université de Lille

Numéro d'ordre:

UNIVERSITÉ DE LILLE

École doctorale **Sciences Pour l'Ingénieur**

Unité de recherche **CRIStAL** UMR 9189

Thèse présentée par

Ayad AL-DUJAILI

Soutenue le 19 mars 2018

En vue de l'obtention du grade de docteur de l'Université de Lille

Discipline **Informatique, automatique**

Fault Diagnosis and Fault Tolerant Control Design for Physically Linked 2WD Mobile Robots Systems

Membres du jury:

Rapporteurs

Ghaleb Hoblos	Enseignant-Chercheur à l'ESIGELEC
Benoit Marx	Maître de conférences à l'Université de Lorraine

Examinateurs

Reine Talj	Chargé de recherche CNRS à l'HEUDIASYC
Rochdi Merzouki	Professeur à l'Université de Lille

Directeurs

Vincent Cocquempot	Professeur à l'Université de Lille
Maan El Badaoui El Najjar	Professeur à l'Université de Lille

ABSTRACT

In harsh environments resulting from natural disasters or industrial accidents, reducing human interventions by increasing robotic operations is desirable. The main challenges to be considered are not only that the robots should be able to go over long distances and operate for relatively long periods, but also make the global system tolerant to actuators' failures. In this thesis, to overcome these challenges, systems composed of multi-linked two-wheel drive (2WD) mobile robots are considered. The objective of these multi-robot systems is to asymptotically track a reference trajectory, despite the presence of actuator faults. In this thesis, we design original Fault Tolerant Control (FTC) schemes. Some of them are passive methods, i.e. robust control laws to given failures, and other ones are active FTC which include a Fault Diagnosis (FD) algorithm that detects, localizes and estimates the faults, and adapts the control actions to the faulty situations.

Several passive FTC strategies are proposed to deal with the unknown failure pattern matrix in the dynamic control law. Firstly, multiple dynamic controllers are designed for two-linked 2WD mobile robots, each one aiming at compensating a specific combination of actuator faults; a switching mechanism selects the proper controller. Secondly, a control solution which is well-suited for n-linked robots ($n \geq 2$) is presented. The provided solution is based on transforming the considered model into the canonical chained form, then a recursive technique is used to derive the kinematic control law. Based on this, multiple dynamic controllers are designed considering all possible failure cases. From these dynamic controllers, an appropriate one is selected to generate the applied control signal by the control switching mechanism. Thirdly, in order to design a FTC for multi-linked 2WD mobile robots with friction and actuator faults, the same kinematic control law is used, but another dynamic control which does not use the control switching mechanism is proposed. To cover all possible actuator failures and to deal with friction, a multi design integration based adaptive method is proposed.

An active FTC scheme is designed where a nonlinear adaptive observer is used to estimate the actuator faults, which are modeled as multiplicative and additive faults changing the torque inputs on the wheels, and also to estimate the states of the system,

making the non-measured states available for the feedback control law. The proposed active FTC scheme provides fault estimation and fault tolerance.

Simulation results are presented all along the thesis to verify the validity of the proposed control algorithms and to show the performance of the FTC schemes.

Keywords: Fault-tolerant control; Fault diagnosis; Chained form; Multi-linked mobile robots, Mobile robotics, Modeling.

List of Figures

1.1 Different applications of wheeled mobile robots……1
1.2 Multiple swarm robotics……...4
1.3 Multiple wheeled mobile robots……...5
1.4 Tractor-trailer mobile robots……6
1.5 Application of articulated wheeled vehicle……...7
1.6 Articulated mobile robots……8
1.7 Tractor-trailer mobile robots……9
1.8 Snake robots……...10
1.9 Multi-linked 2WD mobile robots……...11

2.1 2WD mobile robot……..23
2.2 Equivalent circuit of a DC motor with a free body attached……..27
2.3 Two-linked 2WD mobile robots……28
2.4 Three-linked 2WD mobile robots……...32
2.5 Multi-linked 2WD mobile robots……...35

3.1 Multiple-model compensation scheme for the case of two-linked mobile robots...50
3.2 Structure of the control switching mechanism……57
3.3 Robot trajectories in (x, y) plane……62
3.4 Tracking errors: $x - x_d, y - y_d$ and $\theta_2 - \theta_d$……62
3.5 Control torques generated by the robot 1……63
3.6 Control torques generated by the robot 2……63
3.7 Orientation error between two robots ……64
3.8 Control switching index ……64
3.9 Multiple-model compensation scheme for the case of three-linked mobile robots.68
3.10 Robot trajectories in (x, y) plane……..80
3.11 Tracking errors……80
3.12 Control torques generated by the robot 1, robot 2, robot 3……81
3.13 Control switching index ……...81
3.14 Block diagram of the fault compensation control scheme……82

3.15 Robot trajectories for the circle reference in (X, Y) plane 94
3.16 Tracking errors for the circle reference 94
3.17 Orientation error between two robots for the circle reference 95
3.18 Control torques for the circle reference 95
3.19 Robot trajectories for the eight-like reference in (X, Y) plane 96
3.20 Tracking errors for the eight-like reference 96
3.21 Orientation error between two robots for the eight-like reference 97
3.22 Control torques for the eight-like reference 97
3.23 Robot trajectories in (X, Y) plane 99
3.24 Control torques generated by robot 1, robot 2 and robot 3.....99
3.25 Tracking errors 100
3.26 Orientation error between each two robots 100

4.1 Active fault tolerant control scheme for fault estimation 106
4.2 Trajectories of the mobile robots and tracking errors for the case of two robots..112
4.3 State estimation error 113
4.4 Estimations of ρ and $\bar{u}$.....114
4.5 Applied torques and control signals of robot 1.....115
4.6 Applied torques and control signals of robot 2.....116
4.7 Linear velocities of robot 1 and robot 2.....117
4.8 Angular velocities of robot 1 and robot 2.....117
4.9 Trajectories of the mobile robots and tracking errors for the case of three robots..120
4.10 State estimation error 121
4.11 Estimations ρ (unfiltered).....122
4.12 Estimations ρ (filtered).....122
4.13 Control signals 123
4.14 Comparison torque-control of robot 1.....124
4.15 Comparison torque-control of robot 2.....125
4.16 Comparison torque-control of robot 3.....126
4.17 Linear velocities of robot 1, 2 and robot 3.....127
4.18 Angular velocities of robot 1, 2 and robot 3.....127

List of Tables

4.1 Actuators' faults (the case of two-linked 2WD mobile robots) ……111

4.2 Actuators' faults (the case of three-linked 2WD mobile robots) ……...119

Notations

The following table describes the different acronyms used in this manuscript.

Acronym	Description of the acronym
FTC	Fault Tolerant Control
FD	Fault Diagnosis
WMR	Wheeled Mobile Robot
JPL	Jet Propulsion Laboratory
CAMPOUT	Control Architecture for Multirobot Planetary Outposts
2WD	Two-Wheel Drive
4WD	Four-Wheel Drive
FDD	Fault Detection and Diagnosis
FDI-PC	Fault Detection, Isolation and Path Correction
DOF	Degrees of Freedom

TABLE OF CONTENTS

1 General Introduction

1.1 Multi-linked mobile robots 1

1.1.1 Motivations to use multi-linked mobile robots..... 1

1.1.2 Articulated mobile robots..... 7

1.1.3 Literature review on FTC and FD for multi-linked mobile robots..... 11

1.2 Thesis objectives 15

1.3 Original contributions 16

1.4 Thesis outline 17

2 System Modeling and Model Transformation 18

2.1 Introduction 19

2.2 Nonholonomic constraint 20

2.3 Kinematic and dynamic models for 2WD mobile robots 22

2.3.1 Kinematic modeling 23

2.3.2 Dynamic modeling..... 24

2.3.3 Actuator modeling..... 26

2.4 Modeling of multi-linked 2WD mobile robots..... 28

2.4.1 Modeling of two-linked 2WD mobile robots 29

2.4.1.1 Kinematic modeling..... 30

2.4.1.2 Dynamic modeling 31

2.4.2 Modeling of three-linked 2WD mobile robots 31

2.4.2.1 Kinematic modeling..... 32

2.4.2.2 Dynamic modeling 33

2.4.3 Modeling of n-linked 2WD mobile robots 34

2.4.3.1 Kinematic modeling..... 35

2.4.3.2 Dynamic modeling..... 36

2.5 Model transformation into the canonical chained form 37

2.5.1 Transformation of the kinematic model of n-linked robots into the chained form.38

2.5.2 Illustration for three-linked robots 41

2.6 Actuator fault model for multi-linked 2WD mobile robots..... 42

2.7 Conclusion 44

3 Passive Fault Tolerant Control **45**

3.1 Introduction 47

3.2 Actuator FTC compensation for the case of two-linked robots 49

3.2.1 Problem formulation 49

3.2.2 Fault tolerant control design 51

3.2.2.1 Kinematic controller design 51

3.2.2.2 Multiple dynamic controllers design 54

3.2.2.3 Control switching mechanism design 56

3.2.2.4 Overall system performance analysis 58

3.2.3 Simulation studies 60

3.3 Actuator FTC compensation for the case of three-linked robots 65

3.3.1 Multiple model actuator FTC compensation for three-linked robots 65

3.3.1.1 Problem formulation 65

3.3.1.2 Trajectory generation 66

3.3.1.3 Fault tolerant control design 69

3.3.1.3.1 Kinematic controller design 69

3.3.1.3.2 Multiple dynamic controllers design 76

3.3.1.3.3 Control switching mechanism design 77

3.3.1.3.4 Overall system performance analysis 78

3.3.1.4 Simulation studies 78

3.3.2 Multiple-design integration based adaptive FTC for three-linked robots 82

3.3.2.1 Problem formulation and FTC objective 3 82

3.3.2.2 Fault tolerant control design 83

3.3.2.2.1 Kinematic controller design 83

3.3.2.2.2 Dynamic controller design 84

3.3.2.2.3 Stability analysis 88

3.3.2.3 Simulation studies 92

3.4 Design steps of a passive FTC for n-linked 2WD mobile robots ($n > 1$) 101

3.5 Conclusion 101

4 Active Fault Tolerant Control **103**

4.1 Introduction..... 104

4.2 FD and FTC in three-linked 2WD mobile robots..... 105

4.2.1 Problem formulation 105

4.2.2 Nonlinear adaptive observer and fault diagnosis 107

4.2.2.1 State-space representation 107

4.2.2.2 Nonlinear adaptive observer design..... 108

4.2.2.3 Fault estimation.....109

4.2.3 Fault tolerant control design 109

4.2.3.1 Kinematic controller..... 109

4.2.3.2 Dynamic controller..... 109

4.2.4 Simulation studies 110

4.3 Generalization of FD and FTC for n-linked 2WD mobile robots 128

4.3.1 Nonlinear adaptive observer and fault diagnosis..... 128

4.3.1.1 Nonlinear adaptive observer..... 129

4.3.1.2 Fault estimation.....129

4.3.2 Fault tolerant control design..... 129

4.4 Conclusion 130

5 Conclusions and Future Work **131**

Appendix A: Input transformation matrix $B(q)$ in (2.43) 134

Appendix B: System inertia matrix $M(q)$, and Coriolis forces vector $C(q,\dot{q})$ in (2.43) 135

Appendix C: Input transformation matrix $B(q)$ in (2.69) 137

Appendix D: System inertia matrix $M(q)$ in (2.67) and Coriolis forces $C(q,\dot{q})$ in (2.68)139

Appendix E: Proof of theorem 2.1 141

Appendix F: Diffeomorphism in (3.19)-(3.22) 145

Appendix G: Obtaining T_α and f_α in (3.23) 146

List of bibliographic references **147**

CHAPTER 1

General Introduction

Contents

1.1 Multi-linked mobile robots 1

1.1.1 Motivations to use multi-linked mobile robots..... 7

1.1.2 Articulated mobile robots..... 7

1.1.3 Literature review on FTC and FD for multi-linked mobile robots..... 11

1.2 Thesis objectives 15

1.3 Original contributions 16

1.4 Thesis outline 17

Chapter content

This chapter introduces the objectives and motivations of the thesis, the considered problems and challenges and provides the requirements to derive solutions. Different kinds of articulated mobile robots are described. A review of the relevant literature on wheeled mobile robots and multi-linked wheeled mobile robots are presented. Afterwards, the research questions and objectives that this thesis aims to solve are discussed. Finally, the organisation of the thesis and the contributions in each chapter are outlined.

1.1 Multi-linked mobile robots

1.1.1 Motivation to use multi-linked mobile robots

The applications of Wheeled Mobile Robots (WMR) have expanded steadily over the last two decades, including planetary exploration, search and rescue, demining, and operation in remote and hazardous environments as shown in Fig. 1.1. However, these complex systems, which have numerous sensors and actuators, could never be immune to system faults, which may result in mission failures [1]. So, some sort of strategy must be adopted

Figure 1.1: Different applications of wheeled mobile robots [2, 3].

to mitigate the effect of the faults.

Due to the harsh environment, it is difficult, even impossible, to send human operators to repair a faulty robot. However, in the situation where there are partial failures and degradation in some subsystems, instead of aborting the mission, one may decide that the group of robots operates at lower efficiencies, or even completes parts of the whole mission with a smaller set of available resources. To achieve this, we need fault tolerant control systems, where the robots continue to operate despite the occurrence of faults.

Let us consider the following illustrative example. On March 2011, a severe nuclear accident happened after that a very strong earthquake and accompanying tsunami have impacted the Fukushima Daiichi Nuclear Power Plants. An enormous amount of radioactive particles were released at the plant site, and the environmental conditions accordingly were very harsh [4]. In this emergency situation, the objective of the first disaster response mission was to assess the damages to the target environment. However, the site was very dangerous for humans because of the potential for high radiation exposure. Therefore, the exploration using mobile robot technologies was crucial [5]. Mobile robots were used extensively to explore the environment at Fukushima Nuclear Power Plants, as well as to try to regain control of the plant and conduct decontamination in selected areas.

However, robots were frequently impaired by the following reasons [6]:

1) Mobility limitations arose when robots were faced with obstructions such as rubble piles, tree roots, and doors.
2) The presence of radiation results in degraded electronics and cameras within a few meters of highly radioactive material.
3) Mission durations were short due to the limited battery lives of robots, while robots that were charging continuously throughout their missions had very limited ranges.
4) Blocked transmissions caused by buildings and degradation of communication networks created difficulties in communicating with robots.

However, the hardware reliability, communication systems, and sensors were considered inadequate for operations as part of the disaster response effort in Fukushima. It was impossible to know without testing how long the equipment in the robots could operate in such an extreme environment [7].

For two years after the accident occurred in Fukushima, more than thirty robots have been deployed to the Fukushima area (or site). In these, five robots could not return and some robots could not complete the mission because of some faults [8]. Rendering robots more tolerant to faults, more nimble, more autonomous, less vulnerable to radiation, able to negotiate obstacles, and to evolve in hazardous environments with fewer support requirements would be helpful to avoid the consequences of a nuclear disaster such as in Fukushima.

One of the possibilities to reduce, even avoid the effect of faults in the robots that were sent to the Fukushima Daiichi Nuclear Power Plants would have been to link two or more robots together. This is because compared to one alone robot, a multi-robot system has intrinsic fault tolerance ability due to the redundant actuators and sensors, can carry more easily needed supplies and equipments, and can carry more heavy loads.

There are many potential advantages of a group of robots over a single robot including greater flexibility, adaptability, robustness, sharing the sensor data, and operating in parallel [9]. These advantages are enforced when the robots are physically linked. Furthermore, added interests will result in the cooperating robots when the tasks are inherently too complex for a single system. Comparing with one single and large system, multi-robot systems can be simpler, more flexible, and fault-tolerant systems.

A short summary describing some important multi-robot capabilities is given below [10]:

- Distribution: work in many places at the same time.
- Multitasking: execute a myriad of tasks simultaneously.
- Fault tolerance: superposition of functions in order to maintain the overall functionality even in the case of the loss of some functions.
- Flexibility: the operationality can be changed very easily just rearranging the robots.
- Cost-effectiveness: taking advantage of small cheap robots with different (and possibly low) capabilities, the group of (linked-) robots can deal with difficult missions that could require one expensive big complex robot.

In summary, multi-robot systems can often deal with tasks that are difficult, if not impossible, to be accomplished by a single robot. A multi-linked robot has most of the advantages of the multi-robot systems, furthermore, it has other advantages.

Hence, when using mobile robots in harsh environments, one strategy in order to mitigate the effect of the faults is to send some swarm robotics. If we have a redundant number of robots, even if some robots are lost due to failures they will still be able to perform autonomously some operations such as bring some equipment's or help human operators in rescue and repairing missions.

Taking cues from nature, like ants that are linked when they are bringing together a big object, swarm manipulation commonly consists of many small robots working cooperatively toward a similar goal but with little information of their fellow robots. Each robot of the swarm is a fully autonomous mobile robot capable of performing basic tasks such as autonomous navigation, perception of the environment and grasping of objects [11].

A swarm-bot is a group of mobile robots, equipped with a gripper, also known as s-bots, that can connect each s-bot to the other. A swarm-bot is more suitable to deal with missions that are hard to do for a unique s-bot. As shown in Fig. 1.2, the physically linked system can overcome a ground gap or carry heavy loads, which could not be performed by a single s-bot [12].

This swarm robotics are effective in certain conditions, but there is a risk of damaging the robot or the transported object if unsafe magnitudes of force are applied. The robots are subject to tremendous stress under those conditions and internal failures often occur.

In the following are presented some control problems with the multiple cooperative robots including, tracking control, force control or grasping or transporting objects.

Figure 1.2: Multiple swarm robotics [12].

In [13, 14] the NASA Jet Propulsion Laboratory (JPL) developed an autonomous multi robot system, under hard constraints on power, mass, communication, and computing, to help infrastructure construction for exploration of Mars. Two heterogeneous holonomic mobile robots (physically linked through a shared payload), with independent four-wheel drive and steering motors, a four degree-of-freedom arm, and a gripper with a 3-axis force torque sensor, operated autonomously using a leader-follower control architecture called CAMPOUT (Control Architecture for Multirobot Planetary Outposts) [13].

In this NASA application, one of the main tasks of the two robots is the transportation of long beams for building structures. The two robots, as shown in Fig. 1.3, move into transport formation and orient themselves toward the goal location. The advantages of using multiple versus a single robot for such tasks are: efficient use of system resources, parallel execution of multiple tasks, complementary capabilities provided by a group of robots, reliability and fault-tolerance to failure of individual components (including failure of single robots).

Jet Propulsion Laboratory has successfully demonstrated the effectiveness of this control system in their planetary robotics laboratory through experiments [13, 14]. However, the controller was designed without considering fault-tolerant control methods.

In [15], the authors proposed a re-configuration strategy for the controllers of the healthy mobile robots, assigning to them the tasks that were going to be lost when there is a faulty robot. For this team of mobile robots, each of them has the same risk to fail. If some robots are faulty, they will become obstacles which makes the rescue mission more difficult and less efficient to be performed.

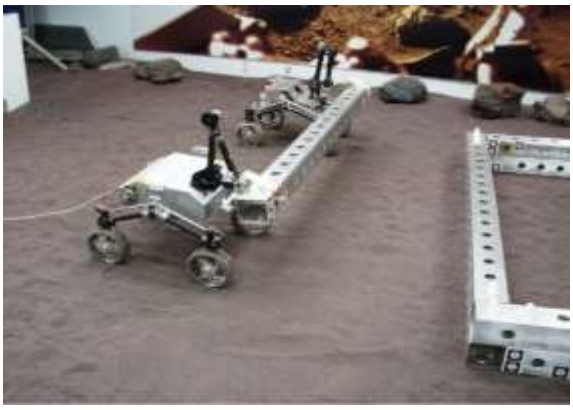

Figure 1.3: Multiple wheeled mobile robots [14].

The robots need to independently detect and isolate internal failures and utilize the remaining functional capabilities to automatically overcome the limitations imposed by the failures. In this case, identifying the faults and adopting a strategy for the compensation of their effects are highly recommended in order to guarantee the accomplishment of the tasks with satisfactory performance.

Fault diagnosis for robots is a complex problem, because the set of possible faults is very large; actuators' and sensors' faults, environment conditions are uncertain; and there is limited computation time and power.

Two-wheel drive (2WD) mobile robots are often used in multiple cooperative robotic systems due to their low cost, simplicity, efficiency, and flexibility. However, such a robot becomes uncontrollable when an actuator is totally faulty, which results in the free rolling of the wheel or a blocking in a fixed position with undesirable frictions with the ground. To avoid such an uncontrollable situation, additional actuators are needed.

One possible solution is to physically link multiple 2WD mobile robots. This physical interaction between robots makes the global system more tolerant to total failures of actuators and thus provides ability to complete a mission in presence of actuator faults, rather than aborting the entire mission. The robots may be linked initially or when needed.

Multi-linked 2WD mobile robots are similar to a tractor-trailer, as shown in Fig. 1.4. Indeed, they can be understood as equivalent systems when the multi-linked system has just one actuated robot. These robotic systems can accomplish dexterous and complex tasks which are impossible to realize by a single robot, improve the performance and create a lot of advantages. The potential advantages of such system are flexibility (robots may be

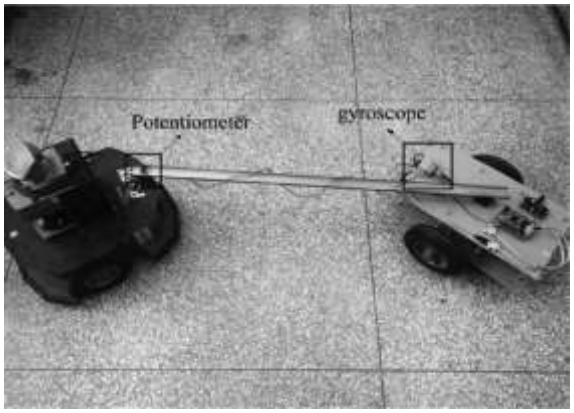

Figure 1.4: Tractor-trailer mobile robots [16].

attached or separated very easily), improvement of the disturbance-rejection capabilities, robustness to failure, adaptability, intrinsic system redundancy, moving facilities in harsh environments and fault tolerance. As an over-actuated system, the linked robots system can reconfigure itself when partial faults occur, to be able to continue the mission.

In this work, the 2WD mobile robots are physically linked to deal with faulty actuators. This architecture can carry the faulty WMRs up to their targets, without missing any of them, guaranteeing the availability of their specialized tools and instruments, which might be essential for the mission. The physically linked 2WD mobile robots system is a kind of articulated mobile robot which will be described in the next section.

1.1.2 Articulated mobile robots

An articulated mobile robot consists of linked elements, similar to a snake with active wheels providing propulsion. These kinds of robots can easily adapt themselves to aggressive terrains and pass through many kinds of obstacles. This is possible because of their joint servomechanisms, that give them a great mobility, allowing to move in open fields or to crawl in restricted spaces such as pipes. Thus, the articulated robots are recommended in many search and rescue missions inside buildings [17].

The connection of multiple active wheeled vehicles in a train-like configuration is a common strategy to increase the traction. Applications in this field are reported since 1950, as for example the enormous trains from R. G. LeTourneau Inc shown in Fig. 1.5, with enhanced traction provided by electric motors that are attached to each wheel [17].

Figure 1.5: Application of articulated wheeled vehicle (one of the R. G. LeTourneau trackless trains LCC-1) [17].

In the following we present some strategies of the work with articulated mobile robots, including self-reconfigurable robots, tractor-trailer mobile robots and snake robots. We are also going to present the multi-linked 2WD mobile robot as an advanced tractor-trailer mobile robot and as a kind of articulated mobile robots.

The self-assembly as the examples shown in Fig. 1.6, is another useful concept, where the core idea is the use of modular robots that have the capability of autonomously connecting one to the other. By this way, the missions can be performed by a connected structure or by a group of single modules, accordingly to the necessities, as for example the requirements imposed by the ground conditions [18].

Modular self-reconfigurable robot systems have the promise of making significant technological advances to the field of robotics in general. Their characteristics of high versatility, high value, and high robustness may lead to a radical change in automation.

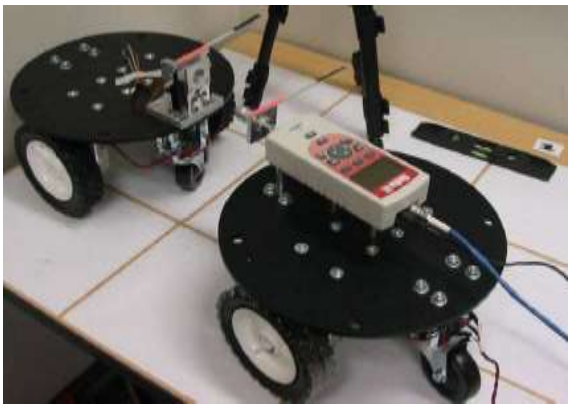

Figure 1.6: Articulated mobile robots [18, 19, 20].

A tractor-trailer mobile robot is another kind of articulated mobile robot system, as shown in Fig. 1.7, a tractor with multiple passive trailers which is the simplest kind of articulated mobile robots [3]. The passive trailers have two main advantages, including: 1) Low cost, since no additional costs have to be paid on the actuators of the trailers. 2) The passive trailers can be extended more easily, if more trailers are required, they can be directly hooked to the rear part of the system [16].

However, the major drawbacks of the passive trailers are that they require more space to travel and more traction power for the tractor. Another drawback is that the overall width of the system increases with the number of the trailers, making difficult the turning movements. If additional trailers are hitched, the maximal lateral deviation of the trailers from the trajectory of the tractor may increase. This may result in a collision between the additional trailers and the obstacles. As a result, the path replanning has to be considered. Furthermore, due to the added trailers, the robot may fail to find a collision free path in replanning [16].

On the other hand, active trailers can be used. There exist two types of active trailers. A first type is to actuate wheels of trailers, where the connecting joints are passive, and two-wheel drive (2WD) robots can be used as active trailers. By using this type of active trailers, accurate path following control can be achieved. The second type is to actuate the connecting joints, as the work in [16, 21] where the wheels of the trailer are passively driven. By appropriate actuation of the connecting joints, the mobile robot can move without wheel actuation, by snake like motions.

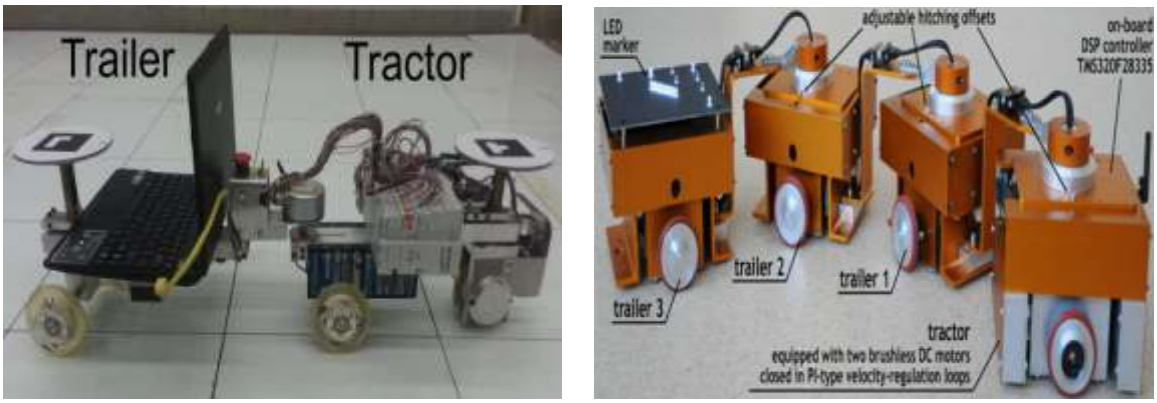

Figure 1.7: Tractor-trailer mobile robots [21, 22].

In summary, compared with the active trailers, the passive trailers have much less manoeuvrability, which is the biggest problem of the passive trailers from the viewpoint of real application. Moreover, actuator faults in the tractor can make the tractor-trailer useless.

Snakes are a good inspiration for systems that need to locomote in rough environments. That's because they have a great adaptability that allows them to overcome different kinds of barriers, such as stones, holes, or others. Then, robotic systems that can imitate the motion of biological snakes are very attractive for applications that face the same motion limitations, such as those arising from natural disasters [23]. This robot configuration is shown in Fig. 1.8.

Physical links between robots, are essential for solving many collective tasks. For example, connecting several robots results in increasing the system power which leads to be able to carry heavy loads. Also, for navigation on a rough terrain, physical links can serve to pass across wide gaps. More important, multi-linked wheeled mobile robots provide actuator and sensor redundancies which improve the fault tolerance of the system. If some robots are faulty, the other ones may link to them and can help continue moving. By physically linking multiple 2WD mobile robots and building an over-actuated system, those ones with faulty motors may stay usable. Using this concept of linked robots makes the mobile system more flexible, more efficient and gives better fault tolerance capabilities to faults.

Robustness refers to the ability of a system to be insensitive to external disturbances while fault tolerance refers to the ability of a system to detect and compensate for system

Figure 1.8: Snake robots [24].

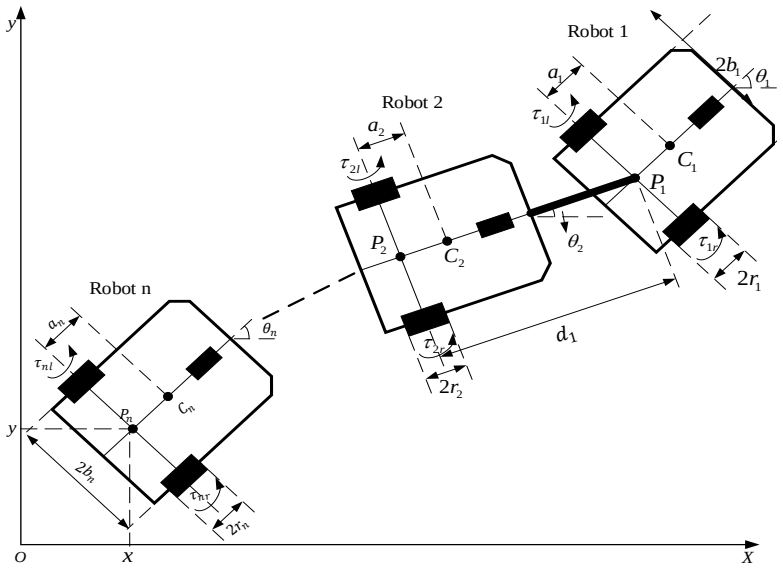

Figure 1.9: Multi-linked 2WD mobile robots.

failures. Requiring robustness and fault tolerance in a cooperative architecture emphasizes the need to build multi-linked wheeled mobile robots that reduce their vulnerability to individual robot faults.

In order to exploit these fault tolerance capabilities, efficient control algorithms have to be used. Designing such Fault Tolerant Control Schemes for multi-linked wheeled mobile robot systems, as shown in Fig. 1.9, is the objective of this thesis. These FTC algorithms may either include a Fault Diagnosis (FD) layer (we speak about Active FTC in that case) or do not use any FD (we qualify this as Passive FTC).

1.1.3 Literature review of FTC and FD for multi-linked mobile robots

This section presents a review of the relevant literature on control design methods for wheeled mobile robots and multi-linked wheeled mobile robots in order to put a foundation for our work and justify the new developments made in this thesis. First, a review on trajectory tracking control of wheeled mobile robots will be presented, followed by a brief review on trajectory tracking control of multiple mobile robots. Then several Fault Tolerant Control (FTC) and Fault Detection and Diagnosis (FDD) algorithms with application to mobile robots and multi-linked mobile robots will be presented.

Some control problems were studied for autonomous navigation of wheeled mobile robots, examples are trajectory tracking, path following, and point stabilization. In this

thesis, we focus ourselves on trajectory tracking control for a wheeled mobile robot and multi-linked wheeled mobile robots. Trajectory tracking control of a mobile robot refers to the actual position/orientation of a mobile robot converging to a reference path which may be fixed or generated by a moving target.

The 2WD mobile robots are known to be nonholonomic systems, which are characterized by kinematic constraints that are not integrable, i.e., the constraints cannot be written as time derivatives of some functions of the generalized coordinates [25].

Based on whether a kinematic model or a dynamic model is used to describe the system behaviour, the tracking control problem is classified as either a kinematic or a dynamic tracking control problem. Using kinematic models of nonholonomic mobile robots, different approaches such as neural networks [26], neural-fuzzy [27], backstepping [28], have been proposed to solve the tracking control problem. These solutions rely on the assumption that the control inputs, usually motor voltages, instantaneously establish the desired robot velocities. Based on the dynamic feedback linearization and the differential flatness concept, the dynamic controllers are proposed in [29] and [30]. This outlook totally ignores the robot dynamics and is usually known as perfect velocity tracking [31].

In contrast, dynamic control schemes are based on a full dynamic model which captures entirely the behaviour of the real mobile robot by accounting for dynamic effects due to mass, inertia, and friction, which are otherwise neglected by kinematic control. In [32], the dynamic tracking problem of a wheeled mobile robot is studied, and a neural network based controller is proposed. The dynamic tracking control problem of nonholonomic mobile robot with uncertainties in both kinematics and dynamics is proposed in [33]. In [34] and [35] the dynamic tracking problem of a class of the nonholonomic system with unknown parameters has been considered.

For a multibody vehicle which consists of a unicycle-like tractor with multiple trailers, a survey on the various control strategies may be found in [36]. In [37] the controllability of these systems has been studied; the concept of flatness for multibody mobile robot has been discussed in [38]; and nonholonomic motion planning has been discussed in [39]. In [40], the method to facilitate the design of the controller, is based on coordinate and input transformations to another equivalent control system with a simpler structure (known as chained system).

Several authors have studied the kinematic control design methods. In [41] an alternative idea to stabilize nonholonomic systems that is based on so-called transverse functions was presented, and the tracking control for double steering tractor-trailer mobile robots with on-axle hitching was studied in [16]. A kinematic and dynamic control scheme is developed in [42] for a tractor with one trailer, and in [43] for a tractor with two trailers. However, these control methods are developed without considering actuator faults.

Two bibliographical reviews on FTC design methods may be found in [44], [45], and various effective design methods are presented for different applications in [46-48].

Fault tolerant control schemes were proposed for mobile robots, see for examples [49-53] and the references therein. Fault detection and diagnosis (FDD) and fault tolerant control (FTC) topics for such vehicles were discussed in [49], [50]. A sensor fault accommodation scheme is presented in [51]. A sliding mode FTC using a fault hiding approach based on the kinematic model of a nonholonomic mobile robot is presented in [52]. A fault-tolerant controller design method is presented in [53], as a two-step procedure to provide alternative steering and reuse the nominal controller in a way that resembles a crab-like driving mode. Three fault modes are injected (one, two, and three failed steering joints) in the real wheeled planetary rovers to evaluate the response of the non-reconfigured and reconfigured control systems in face of these faults.

In the field of wheeled mobile robotics, the subject of faults occurring in wheeled locomotion has attracted significant attention because of its vital impact on the functionality for a robot [54]. A robust adaptive fault-tolerant control approach for WMR is presented in [55], to deal with time-varying unknown control gain and parametric/non-parametric uncertainties of WMR, together with output constraints and actuation/propulsion failures. A hybrid fault adaptive control is designed to accommodate partial faults and degradation for 2WD robots in [56]. An adaptive fault tolerant control for 2WD mobile robots under partial loss of actuator effectiveness is presented in [57]. In [58], both kinematic and dynamic models are considered to detect faults under uncertainties on the mechanical parameters of the 2WD mobile robots. Sensors, actuators, controller, and communication faults are considered in [59] and a fault-tolerant controller for a wheeled mobile robot dealing with agricultural environments is designed. In [60-62], fault tolerant control design methods for four-wheel drive (4WD) mobile robots are discussed.

Besides the fault compensation, Fault Diagnosis (FD) also must be considered, both for maintenance purposes, in order to make repairs and prevent a total failure of the system, or to improve the control law, in order to act more precisely against the fault effects. Fault diagnosis includes three tasks, namely fault detection (determining whether there is a fault in the system, in addition to the time at which the fault occurs), fault isolation (determining the location of the faulty component), and fault estimation (providing information about the type, size, and shape of the fault) [63].

Several books ([64], [65], [66]) and survey papers ([67], [68], [69]) make extensive reviews on fault diagnosis methods. In [70], the methods are categorized into model-based, signal-based, knowledge-based, hybrid, and active fault diagnosis.

The observer-based methods play a key role in model-based fault diagnosis. Such techniques were considered for WMR diagnosis in [71], where an observer-based actuator fault detection and isolation method is proposed following the approach presented in [72]. In [73], it is suggested to combinate two approaches, namely local model networks for modeling and change-detection algorithms for residual generation. This provides an efficient method for fault detection and diagnosis, and is applied on the wheels subsystem of a 2WD mobile robot. A model-based actuator fault diagnosis for a four-wheel skid steering mobile robot was presented in [74]. In [75], a multiple-fault diagnosis method for a mobile robot system in the presence of hide effect, is proposed. In [76], it is developed a discrete event dynamic system diagnosis to cope with two faulty conditions in an autonomous mobile robot task. A fault diagnosis algorithm that estimates the abnormal conditions before a breakdown occurs is presented in [77].

In [78], multiple models of the robot are used, each one corresponding to a specific sensor or actuator fault and the state estimation is performed with Kalman filters. In [79], a model-based Fault Detection, Isolation and Path Correction Module (FDI-PC) is presented, for 2WD robots. Simulation results demonstrate that a robot is able to navigate in an indoor building after a fault occurs on one of its wheels by compensating the effects of the fault with corrective input signals. In [80], a neural network is trained when the robot is operating normally and then trained again when the robot is operating under different faults. The results show that the neural network is able to detect the occurrence of faults.

1.2 Thesis objectives

Fault detection and diagnosis (FDD) and fault tolerant control (FTC) are increasingly important for wheeled mobile robots (WMRs), especially those moving in unknown environments. Fault detection, diagnosis, and accommodation play a key role in the operation of WMRs. Due to the importance of reliability and safe operation of WMRs, FDD & FTC are developed in this thesis for multi-linked 2WD mobile robots under unknown environments.

One of the fundamental issues in the motion of mobile robots is trajectory tracking, which can be achieved with minimal error by the aid of a proper feedback controller. In case of faulty actuators, trajectory tracking with acceptable performance requires a fault tolerant feedback control law.

One can notice that there are very few literatures on fault diagnosis and fault tolerant control design for multi-linked mobile robots [81, 82, 83]. In these work, only the case of two linked robots is treated.

The objective of the presented thesis is to develop passive and active fault tolerant control schemes for multi-linked 2WD mobile robots, to asymptotically track a reference trajectory, despite the presence of actuator faults.

Three different fault compensation strategies are developed:

1) Switching between multiple dynamic control laws, each one compensating a specific actuator fault.
2) Using an adaptive control law with a multi integration mechanism that incorporates the compensation of all the considered faults.
3) Using a nonlinear adaptive observer which can estimate the actuator gains, the additive faults and the state variables. The estimated variables are used to update the dynamic control law and guarantee the trajectory tracking under faulty conditions.

The faults addressed in this thesis include mechanical component faults, such as broken motors, and faults due to environmental interactions, such as a wheel introducing friction. This thesis involves modeling, simulation variables and parameters, parameter estimation, and control design tasks.

1.3 Original contributions

The original contributions of the presented thesis are follows:

1) The configuration of n $(n > 1)$ physically linked 2WD mobile robots is proposed to deal with the actuator faults.
2) The kinematic and dynamic models of multi-linked 2WD mobile robots are proposed.
3) FTC compensation schemes are designed for multi-linked 2WD mobile robots (two or more linked 2WD mobile robots):
    - One proposed solution is based on converting the kinematic model of the multi-linked 2WD mobile robots into the canonical chained form. It consists in transforming the nonlinear model into an equivalent linear one through a change of variables and a feedback transformation. The main difficulty is to find the diffeomorphism (state transformation) used to transform the kinematic model into the chained form.
    - A recursive algorithm is proposed to design the kinematic controller for n $(n > 1)$ linked robots to guarantee that all the system's states converge to their desired trajectories.
    - Dynamic control laws including actuator fault are designed, each of which is related to one specific failure pattern matrix. If the failure pattern which is used in the controller is consistent with the actual one, then the applied control signal can ensure the desired system performance. In the following, different strategies are proposed including multiple dynamic controllers and adaptive fault tolerant dynamic controller.
4) For failure compensation, multiple dynamic controllers are designed considering all possible failure cases. Among these dynamic controllers, an appropriate one is selected using the control switching mechanism and applied to ensure the desired system performance.
5) An adaptive fault tolerant dynamic controller based on a multi-design integration method is proposed to overcome, on one hand, the problem of uncertain system

friction and, on the other hand, the problem of multiple actuator faults while ensuring the overall system stability and asymptotic tracking properties.

6) An adaptive nonlinear observer is proposed to estimate the actuator faults, which are modeled as multiplicative and additive faults changing the torque inputs on the wheels, and also to estimate the states of the system, making the non-measured states available for the feedback control law. The estimated actuator gains and state variables are used to update the dynamic control law.

1.4 Thesis outline:

The outline of the thesis is given below

- **Chapter 1**: The motivations, contributions, literature review and thesis outline are presented in this chapter.
- **Chapter 2**: The description and modeling of multi-linked 2WD mobile robots are presented in this chapter. The transformation of the state representation into the chained form is also introduced [84, 85, 86].
- **Chapter 3**: This chapter presents two passive fault tolerant control methods, including multiple dynamic controllers [85, 86] and adaptive fault tolerant dynamic controller [84] for the purpose of actuator fault compensation in multi-linked 2WD mobile robots. Simulation results are presented to show the efficiency of the proposed passive FTC methods.
- **Chapter 4**: This chapter presents active fault tolerant control methods in multi-linked 2WD mobile robots including actuator fault estimation and compensation using a nonlinear adaptive observer. The observer is used to estimate both the actuator faults and the states of the system to be able to construct the feedback control. Simulation results are presented to show the efficiency of the proposed FD observer and active FTC method.
- **Chapter 5**: This chapter concludes the thesis and discusses potential improvements of the presented methods and possible future research developments in fault diagnosis and fault tolerant control for multi-linked 2WD mobile robots.

CHAPTER 2

System Modeling and Model Transformation

Contents

2.1 Introduction 19

2.2 Nonholonomic constraint 20

2.3 Kinematic and dynamic models for 2WD mobile robot 22

2.3.1 Kinematic modeling 23

2.3.2 Dynamic modeling 24

2.3.3 Actuator modeling 26

2.4 Modeling of multi-linked 2WD mobile robots 28

2.4.1 Modeling of two-linked 2WD mobile robots 29

2.4.1.1 Kinematic modeling 30

2.4.1.2 Dynamic modeling 31

2.4.2 Modeling of three-linked 2WD mobile robots 31

2.4.2.1 Kinematic modeling 32

2.4.2.2 Dynamic modeling 33

2.4.3 Modeling of n-linked 2WD mobile robots 34

2.4.3.1 Kinematic modeling 35

2.4.3.2 Dynamic modeling 36

2.5 Model transformation into the canonical chained form 37

2.5.1Transformation of the kinematic model of n-linked robots into the chained form.38

2.5.2 Illustration for three-linked robots..... 41

2.6 Actuator fault model for multi-linked 2WD mobile robots..... 42

2.7 Conclusion 44

Chapter content

This chapter is dedicated to the models used in the current research. First, the kinematic and the dynamic models of a 2WD mobile robot are given, followed by the model of the system actuators. Then a methodology is described to obtain the kinematic and dynamic models of a multi-linked mobile robots system. The models are first derived for a simple case with two-linked 2WD mobile robots. In the sequel, the model is extended to the case of three-linked 2WD mobile robots in order to show the effect of adding one new robot. This will emphasize the difficulties in multi-linked robots modeling when three-linked robots and more are considered. The models of n-linked 2WD mobile robots are thus proposed. Then, a diffeomorphism is proposed to transform the initial state space representation of the kinematic model into the canonical chained form. This new state space representation will emphasize the link between the kinematic and dynamic models which will be used for the FTC design. The actuator fault model is finally presented.

2.1 Introduction

The motion of a mechanical system can be described by a set of dynamic equations, containing the forces or torques the system is subjected to. The dynamics of a mechanical system has been discussed in numerous scholar literatures related to engineering mechanics and analytical mechanics. The study of this subject is important due to the problem of controlling the system, which is in contact with its environment. Indeed, the design of a controller for such system depends heavily on the mathematical model.

Many researchers have developed methodologies for the kinematic and dynamic modeling of wheeled mobile robots. An extensive study of this subject was published in [87]. In [88], structural properties and a classification of the kinematic and dynamic models for wheeled mobile robots are presented. The relation between the rigid body motion of the robot and the steering and drive rates of wheels was developed in [89] based on nonholonomic constraint as, for example, rolling without sliding.

A systematic method for kinematic and dynamic modeling of a three-wheeled 2-DOF mobile robot was presented in [90]. In [91, 92], the kinematics and a set of differential equations for the dynamics modeling of a wheeled mobile robot are presented. Using a

recursive formulation, the kinematic model of wheeled mobile robots with a global singularity analysis is carefully discussed in [93].

In general, the dynamic model of a 2WD mobile robots is derived from the Euler-Lagrange equations [94-97], Newton's laws of motion [98, 99] or Kane's method [100]. The classical assumptions are ideal rigid body dynamics, flat and horizontal ground surface, zero-wheel slip and no friction [101].

For the case of tractor-trailer mobile robots, the kinematic models of the tractor with and without steering trailer are presented in [102] and the dynamic model of the tractor with steering trailer is presented in [103]. The kinematic and dynamic models of the tractor with one trailer are presented in [42]. These models of a tractor with n trailers are presented in [104].

2.2 Nonholonomic constraint

Nonholonomic systems are nonlinear systems that frequently appear in robotics (for instance, mobile robots, robot manipulators, wheeled vehicles and underwater robots). To perform locomotion of mobile robots the use of wheels is the most common mechanism. If we suppose that the wheels are rolling without slipping (classical hypothesis), the mobile robot can only move in a direction perpendicular to the axle connecting the wheels. For instance, a classical car can reach any final position in its non-constrained plane, but it can never move sideways. Hence, it requires to perform a series of maneuvers (such as parallel parking) to reach the desired state [105].

The motion of many mechanical systems is subjected to constraints on the position and the velocity. These constraints restrict the motion of the system by limiting the set of paths which the system can follow. Generally speaking, a constraint is said to be *holonomic* if it restricts the motion of the system in a smooth hypersurface in the (unconstrained) configuration space Q [106].

It will be convenient to adopt some terms and notations from the differential geometry, so this smooth hypersurface is called a *manifold*. Locally, a holonomic constraint can be represented as a set of algebraic constraints on the configuration space, as follows

$$h_i(q) = 0, \qquad i = 1, 2, \cdots, k \tag{2.1}$$

where q is the generalized coordinate vector, and h_i is a mapping from Q to $\mathbb{R}$ which restricts the motion of the system. The dimension of the manifold on which the motion of the system evolves is $n-k$. We assume that the constraints are linearly independent and consequently the matrix

$$\frac{\partial h}{\partial q} = \begin{bmatrix} \frac{\partial h_1}{\partial q_1} & \cdots & \frac{\partial h_1}{\partial q_n} \\ \vdots & \ddots & \vdots \\ \frac{\partial h_k}{\partial q_1} & \cdots & \frac{\partial h_k}{\partial q_n} \end{bmatrix} \tag{2.2}$$

is full row rank (i.e., $\det\left(\frac{\partial h}{\partial q}\right) \neq 0$).

Since holonomic constraints define a smooth hypersurface in the configuration space, it is possible to "eliminate" these constraints by choosing a set of coordinates corresponding to this surface. These new coordinates parameterize all allowable motions of the system and are not subject to any further constraints.

More generally, for a system with the configuration space Q, velocity constraints of the following form may be considered

$$\omega_i(q)\dot{q} = 0, \qquad i = 1, 2, \cdots, k \tag{2.3}$$

where the $\omega_i(q)$ are row vectors. We assume that the ω_i are linearly independent at each point $q \in \mathbb{R}^n$, since if they are not, the dependent constraints may be eliminated. Each ω_i describes one constraint on the directions in which $\dot{q}$ is permitted to take values.

We say that the k Pfaffian constraints of the form of equation (2.3) are integrable if there exist functions h_i: $\mathbb{R}^n \to \mathbb{R}$, $i = 1, \cdots, k$ such that

$$h_i\,(q(t)) = 0 \iff \omega_i(q)\dot{q} = 0, \qquad i = 1, 2, \cdots, k \tag{2.4}$$

Thus, a set of Pfaffian constraints is integrable if it is equivalent to a set of holonomic constraints. As a consequence, an integrable Pfaffian constraint is often called a holonomic constraint, although strictly speaking the former is described by a set of velocity constraints and the latter by a set of functions. A set of Pfaffian constraints is said to be *nonholonomic* if it is not equivalent to a set of holonomic constraints [106].

A car is an example of a system with nonholonomic constraints. The kinematics of a car is constrained because the front and rear wheels are only allowed to roll and spin, but not to slide sideways. As a consequence, the car itself is not capable of sliding sideways,

or rotating in place. Despite this, we know from our own experience that we can park an automobile at any position and orientation. Thus, the constraints are not holonomic since the motion of the system is unrestricted. Finding an actual path between two given configurations is an example of a *nonholonomic motion planning problem*. Note that equation 2.4 is not satisfied for the car.

If the system is nonholonomic, the number of Degrees of Freedom (DOF) (or the number of independent velocity) is equal to the number of independent generalized coordinates minus the number of nonholonomic constraints [105].

Throughout the thesis, we assume that the wheels satisfy the nonholonomic constraints relative to the pure rolling conditions at each contact wheel/ground, without slipping effects. This implies that we suppose that the contact forces between the ground and the wheels take the right values allowing the satisfaction of these conditions; this is an ideal model. In reality, the contact forces appear as a consequence of local slipping, according to phenomenological contact force models. Using a singular perturbation approach, it can be shown that these slipping effects correspond to fast dynamics, i.e., to dynamical effects with characteristic times that are quite short with respect to the dynamics of the global motion of the robot, and can therefore be neglected, at least when using the ideal model for control design purpose [3].

Assumption 2.1 [3]*: For the linked mobile robots, we assume that the wheels satisfy the nonholonomic constraints relative to the pure rolling conditions at each contact wheel/ground, without slipping effects. This implies that the contact forces between the ground and the wheels take the right values allowing the satisfaction of these conditions.*

2.3 Kinematic and dynamic models for 2WD mobile robots

Modeling of a 2WD mobile robot consists of kinematic and dynamic modeling in addition to the modeling of the system actuators. Kinematic modeling deals with the geometric relationships that govern the system and studies the mathematics of motion without considering the affecting forces. On the other hand, dynamic modeling is the study of the motion in which forces and energies are modeled and included. Actuator modeling is needed to find the relationship between the control signal and the mechanical system's input [107].

2.3.1 Kinematic modeling

A 2WD mobile robot, as shown in Fig. 2.1, consists of two individually propelled wheels and a third wheel called *castor wheel* needed for mobile robot stability, that can move freely in space. By adjusting the power applied to each motor, the robot can go forward, rotate in place or perform movement on any arbitrary curve in plane.

Consider a differential drive mobile robot which has two wheels, with radius R, placed at a distance L from the robot center. The center of mass of the robot is assumed to be located at a distance a from the center of the driving wheels axis. (A, x_r, y_r) is the reference frame fixed to the mobile robot and (A, x_l, y_l) is the global inertial reference frame. The mobile robot has a total mass m and a moment of inertia I_c around its center of mass. The configuration of the robot, can be described by five generalized coordinates

$$q = [x_c, y_c, \theta, \varphi_r, \varphi_l]^T \tag{2.5}$$

where (x_c, y_c) are the coordinates of the center of mass in the inertial reference frame, θ is the heading angle of the robot, and (φ_r, φ_l) are the rotation angles of respectively the right and left driving wheels.

The translational velocity v and rotational velocity ω of the 2WD mobile robot, in the local frame, are found using the velocities of the right and left driving wheels

$$v = \frac{R}{2}(\dot{\varphi}_r + \dot{\varphi}_l) \tag{2.6}$$

$$\omega = \dot{\theta} = \frac{R}{2L}(\dot{\varphi}_r - \dot{\varphi}_l) \tag{2.7}$$

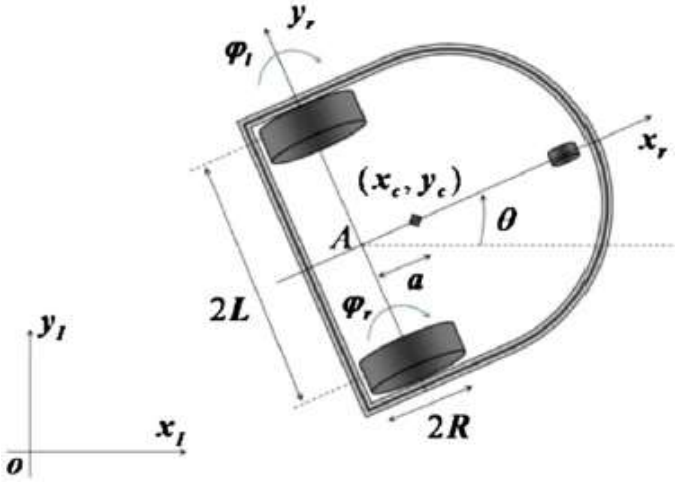

Figure 2.1: 2WD mobile robot.

The nonholonomic constraint of the 2WD mobile robot states that the robot can only move in the direction normal to the axis of the driving wheels, i.e., the mobile robot satisfies the conditions of pure rolling and non-slipping.

The no lateral slip constraint is given by

$$\dot{y}_c \cos\theta - \dot{x}_c \sin\theta - a\dot{\theta}=0 \tag{2.8}$$

where $\dot{y}_c$ and $\dot{x}_c$ are of the robot's center of mass. This constraint means that the velocity of the robot center A is in the direction of the symmetry axis and the motion along the orthogonal axis does not exist.

The pure rolling constraint is expressed by the following two equations

$$\dot{x}_c \cos\theta + \dot{y}_c \sin\theta + L\dot{\theta}= R\dot{\varphi}_r \tag{2.9}$$

$$\dot{x}_c \cos\theta + \dot{y}_c \sin\theta - L\dot{\theta}= R\dot{\varphi}_l \tag{2.10}$$

This constraint shows that the driving wheels do not slip.

To summarize, the three nonholonomic constraints can be written in the following form:

$$A(q)\dot{q} =0 \tag{2.11}$$

where

$$A(q) = \begin{bmatrix} -\sin\theta & \cos\theta & -a & 0 & 0 \\ \cos\theta & \sin\theta & L & -R & 0 \\ \cos\theta & \sin\theta & -L & 0 & -R \end{bmatrix} \tag{2.12}$$

2.3.2 Dynamic modeling

We now derive the dynamic equations for the 2WD mobile robots. The energy-based Lagrangian approach can be used to derive the dynamic model of the 2WD mobile robot which is represented in the following general form [108]:

$$M(q)\ddot{q} + C(q,\dot{q})\dot{q} + F(\dot{q}) + G(q) = B(q)\tau + A^T(q)\lambda \tag{2.13}$$

where

$M(q) \in \Re^{3\times3}$ is the symmetric positive definite inertia matrix, $C(q,\dot{q}) \in \Re^{3\times1}$ is the centripetal and Coriolis forces matrix, $F(\dot{q})$ is the surface friction matrix, $G(q)$ is the gravitational vector, $B(q) \in \Re^{3\times2}$ is the input transformation matrix, $\tau \in \Re^{2\times1}$ is the vector of control torques, $A(q) \in \Re^{3\times1}$ is the system constraint matrix, $\lambda \in \Re^{2\times1}$ is the Lagrange multipliers vector.

Because the trajectory of the mobile robot is constrained to the horizontal plane, i.e., since the system cannot change its vertical position, its potential energy U remains constant. This provides the elimination of the gravity term in the dynamic equation:

$$G(q) = 0 \tag{2.14}$$

Assuming that the surface friction may be neglected, we have

$$F(\dot{q}) = 0 \tag{2.15}$$

The system in equation (2.13) can be transformed into a more proper representation for control and simulation purposes. From (2.6)-(2.10) we can obtain

$$\dot{q} = \begin{bmatrix} \dot{x}_c \\ \dot{y}_c \\ \dot{\theta} \\ \dot{\varphi}_r \\ \dot{\varphi}_l \end{bmatrix} = S(q)\eta = \begin{bmatrix} cos\,\theta & -asin\,\theta \\ sin\,\theta & acos\,\theta \\ 0 & 1 \\ \frac{1}{R} & \frac{L}{R} \\ \frac{1}{R} & -\frac{L}{R} \end{bmatrix} \begin{bmatrix} \upsilon \\ \omega \end{bmatrix} \tag{2.16}$$

where υ is the longitudinal velocity of the robot along the axis of symmetry and $S(q)$ is the forward kinematic matrix.

It can be proved that

$$S(q)^T A(q)^T = 0 \tag{2.17}$$

The above equation is useful to eliminate the constraint term from the main dynamic equation as shown in the following procedure.

Differentiating equation (2.16), we have

$$\ddot{q} = \dot{S}(q)\eta + S(q)\dot{\eta} \tag{2.18}$$

Substituting the above equation in (2.13) results in the following equation:

$$M(q)\dot{S}(q)\eta + M(q)S(q)\dot{\eta} + C(q,\dot{q})S(q)\eta = B(q)\tau + A^T(q)\lambda \tag{2.19}$$

In order to eliminate the constraint $A^T(q)\lambda$, equation (2.19) is left-multiplied by $S(q)^T$ it gives:

$$\begin{aligned} [S(q)^T M(q)S(q)]\dot{\eta} + \left[S(q)^T M(q)\dot{S}(q) + S(q)^T C(q,\dot{q})S(q)\right]\eta \\ = S(q)^T B(q)\tau + S(q)^T A^T(q)\lambda \end{aligned} \tag{2.20}$$

which is equivalent to

$$[S(q)^T M(q) S(q)]\dot{\eta} + \left[S(q)^T M(q)\dot{S}(q) + S(q)^T C(q,\dot{q}) S(q)\right]\eta = S(q)^T B(q)\tau \tag{2.21}$$

This equation may be rewritten as:

$$\bar{\boldsymbol{M}}(\boldsymbol{q})\dot{\boldsymbol{\eta}} + \bar{\boldsymbol{C}}(\boldsymbol{q},\dot{\boldsymbol{q}})\boldsymbol{\eta} = \bar{\boldsymbol{B}}(\boldsymbol{q})\boldsymbol{\tau} \tag{2.22}$$

where

$$\bar{M}(q) = S(q)^T M(q) S(q) \tag{2.23}$$

$$\bar{C}(q,\dot{q}) = S(q)^T M(q)\dot{S}(q) + S(q)^T C(q,\dot{q}) S(q) \tag{2.24}$$

$$\bar{B}(q) = S(q)^T B(q) \tag{2.25}$$

2.3.3 Actuator modeling

DC motors are the main type of actuators used in mobile robots. Consequently, it is important to analyze and integrate their dynamics into the mobile robot model. There are two types of DC motors:

1) Field current controlled.
2) Armature current controlled.

In a field current controlled motor, the armature current i_a is kept constant while the field current is controlled using field voltage v_f signals.

On the other hand, in an armature current controlled motor, the armature voltage v_a is the signal to control the armature current while keeping the field current i_f constant. Consequently, we have the following equations for the DC motor model:

$$\tau_m = k_m i_a \tag{2.26}$$

$$v_a = k_b \omega_m \tag{2.27}$$

where

τ_m is the rotor torque.

i_a is the armature current.

ω_m is the angular speed of the motor.

The parameters k_m and k_b are the torque constants and the back Electromotive Force (EMF) constant respectively. Note that with consistent units, $k_m = k_b$ in the case of ideal electrical to mechanical energy conversion at the motor rotor. Armature current controlled DC motors are more common choice in mobile robots.

The equation for the armature rotor circuit is as follows:

$$v_a = R_a i_a + L_a \frac{di_a}{dt} + v_b \tag{2.28}$$

where

v_a is the supply voltage to the armature.

v_b is the back e.m.f. voltage.

R_a is the resistance of the armature winding.

L_a is the leakage inductance in the armature winding.

It should be noted here that the leakage inductance is usually neglected.

The mechanical equation of the motor as shown in Fig. 2.2, is obtained by applying the Newton's second law as follows:

$$J_m \frac{d\omega_m}{dt} = \tau_m - \tau_l - b_m \omega_m \tag{2.29}$$

where

J_m is the rotor inertia.

b_m is the equivalent damping constant of the rotor.

τ_l is the load torque of the motor rotor.

Equations (2.26), (2.27), (2.28) and (2.29) represent the model of the DC motor. However, their effect on the system dynamic will be neglected in the future FTC design methods because the dynamic of this actuator is faster compared with the robot dynamic. However, this model has been integrated in the simulation scheme to have simulation results as close as possible to actual system behaviour.

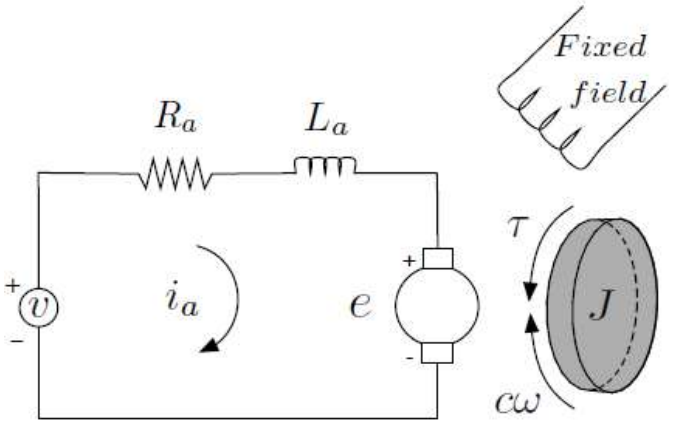

Figure 2.2: Equivalent circuit of a DC motor with a free body attached.

2.4 Modeling of multi-linked 2WD mobile robots

In this section, a methodology is presented to obtain the kinematic and dynamic models of multi-linked systems. First, the models are derived for the simple case with two-linked 2WD mobile robots. In the sequel, the idea is extended to the case of three-linked robots in order to show the effect of adding one new robot. Then, the model is generalized for n-linked robots.

2.4.1 Modeling of two-linked 2WD mobile robots

In this subsection, the kinematic and dynamic models are given for a two-linked 2WD robots system. For each robot, the front passive caster is omitted and the two rear wheels are actuated. The orientation of the first robot is independent (the physical link rotates freely at the attached point), but in the other robot the orientation is constrained by the fixed link.

It can be seen in Fig. 2.3, the configuration of a system with two physically linked 2WD mobile robots. For the ith ($i = 1, 2$) robot, P_i is the centered point between the wheels, C_i is the geometrical center of mass, a_i is the distance between P_i and C_i, b_i is half of the distance between the wheels, r_i is the radius of the wheels, θ_i is the orientation of the robot, and τ_{il} and τ_{ir} are the control torques applied to the left and right actuated wheels, respectively. In addition, d is the distance between P_1 and P_2, frame OXY is the inertial frame, and (x, y) denotes the position of P_2 in frame OXY.

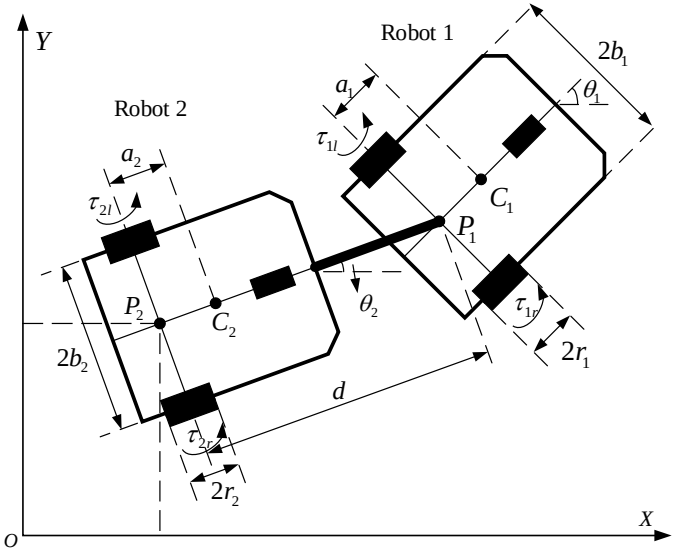

Figure 2.3: Two-linked 2WD mobile robots.

This system can be represented by the generalized coordinate vector

$$q = [x, y, \theta_2, \theta_1]^T \tag{2.30}$$

Note that q, x, y, θ_2 and θ_1 are time-dependent signals but the time variable is omitted in the notation for sake of simplicity.

2.4.1.1 Kinematic modeling

Let v_1 and v_2 be the linear velocities of P_1 and P_2, which also denote the linear velocities of the two robots, respectively, with $v_2 = v_1 \cos(\theta_1 - \theta_2)$.

The output of the kinematic model is the generalized coordinate q and the input is conveniently defined as $\eta = [v_2, \omega_1]^T$, where v_2 is the linear velocity of robot 2 and ω_1 is the angular velocity of robot 1. Thus, the kinematic equations of the two linked 2WD mobile robots shown in Fig. 2.3 are given by

$$\dot{x} = v_2 \cos\theta_2 \tag{2.31}$$

$$\dot{y} = v_2 \sin\theta_2 \tag{2.32}$$

$$\dot{\theta}_2 = \frac{v_2}{d}\tan(\theta_1 - \theta_2) \tag{2.33}$$

$$\dot{\theta}_1 = \omega_1 \tag{2.34}$$

The kinematic equations in (2.31) -(2.34) can be rewritten as

$$\dot{\boldsymbol{q}} = \boldsymbol{S}(\boldsymbol{q})\boldsymbol{\eta} \tag{2.35}$$

where $S(q) \in \Re^{4\times 2}$ is given by

$$S(q) = \begin{bmatrix} \cos\theta_2 & \sin\theta_2 & \frac{1}{d}\tan(\theta_1 - \theta_2) & 0 \\ 0 & 0 & 0 & 1 \end{bmatrix}^T \tag{2.36}$$

Let (x_1, y_1) be the position of P_1, we have $\dot{x}_1 = v_1 \cos\theta_1$ and $\dot{y}_1 = v_1 \sin\theta_1$. Then with (2.31) and (2.32), the system constraints are

$$\dot{x}_1 \sin\theta_1 - \dot{y}_1 \cos\theta_1 = 0 \tag{2.37}$$

$$\dot{x}\sin\theta_2 - \dot{y}\cos\theta_2 = 0 \tag{2.38}$$

with $x_1 = x + d\cos\theta_2$ and $y_1 = y + d\sin\theta_2$, equation (2.37) can be rewritten as

$$\dot{x}\sin\theta_1 - \dot{y}\cos\theta_1 - \dot{\theta}_2 d\cos(\theta_1 - \theta_2) = 0 \tag{2.39}$$

Then (2.38) and (2.39) can be expressed as

$$A(q)\dot{q} = 0 \tag{2.40}$$

where $A(q) \in \Re^{2\times 4}$ is the system constraint matrix given by

$$A(q) = \begin{bmatrix} sin\,\theta_1 & -cos\,\theta_1 & -d\,cos(\theta_1 - \theta_2) & 0 \\ sin\,\theta_2 & -cos\,\theta_2 & 0 & 0 \end{bmatrix} \tag{2.41}$$

Furthermore, the kinematic model respects the natural orthogonal complement property

$$S(q)^T A(q)^T = 0 \tag{2.42}$$

which is related to the nature of the constraints.

In many applications, the kinematic model of a WMR is sufficient to design a controller for trajectory tracking with satisfactory performance. However, many nonholonomic systems in reality have non-negligible dynamics, therefore a dynamic model of the system must be taken into account, in order to properly deal with the actuator faults changing the torque inputs.

2.4.1.2 Dynamic modeling

From the Lagrange method, the differential equation governing the dynamics of the two physically linked 2WD mobile robots is derived as:

$$M(q)\ddot{q} + C(q,\dot{q}) = B(q)\tau + A(q)^T\lambda \tag{2.43}$$

where
$M(q) \in \Re^{4\times 4}$ is the system inertia matrix, $C(q,\dot{q}) \in \Re^{4\times 1}$ is the matrix that multiplied by $\dot{q}$ gives the centripetal and Coriolis forces vector, $B(q) \in \Re^{4\times 4}$ is the input transformation matrix, $\tau \in \Re^{4\times 1}$ is the vector of control torques. $A(q) \in \Re^{2\times 4}$ is the system constraint matrix, $\lambda \in \Re^{2\times 1}$ Lagrange multipliers vector.

$$M(q) = \begin{bmatrix} m_1 + m_1 & 0 \\ 0 & m_1 + m_1 \\ -(a_2 m_2 + d m_1)\sin\theta_2 & (a_2 m_2 + d m_1)\cos\theta_2 \\ -a_1 m_1 \sin\theta_2 & a_1 m_1 \cos\theta_1 \end{bmatrix}$$

$$\begin{bmatrix} -(a_2 m_2 + d m_1)\sin\theta_2 & -a_1 m_1 \sin\theta_2 \\ (a_2 m_2 + d m_1)\cos\theta_2 & a_1 m_1 \cos\theta_1 \\ m_2 {a_2}^2 + m_1 d^2 + I_{m2} & a_1 d m_1 \cos(\theta_1 - \theta_2) \\ a_1 d m_1 \cos(\theta_1 - \theta_2) & m_1 {a_1}^2 + I_{m1} \end{bmatrix}$$

$$C(q,\dot{q})=\begin{bmatrix} -a_1 m_1 \dot{\theta}_1^2 \cos\theta_1 - (a_2 m_2 + d m_1)\dot{\theta}_2^2 \cos\theta_2 \\ -a_1 m_1 \dot{\theta}_1^2 \sin\theta_1 - (a_2 m_2 + d m_1)\dot{\theta}_2^2 \sin\theta_1 \\ -a_1 d m_1 \dot{\theta}_1^2 \sin(\theta_1 - \theta_2) \\ a_1 d m_1 \dot{\theta}_2^2 \sin(\theta_1 - \theta_2) \end{bmatrix}$$

$$B(q) = \begin{bmatrix} \frac{\cos\theta_1}{r_1} & \frac{\cos\theta_1}{r_1} & \frac{\cos\theta_2}{r_2} & \frac{\cos\theta_2}{r_2} \\ \frac{\cos\theta_1}{r_1} & \frac{\cos\theta_1}{r_1} & \frac{\cos\theta_2}{r_2} & \frac{\cos\theta_2}{r_2} \\ \frac{d\sin(\theta_1-\theta_2)}{r_1} & \frac{d\sin(\theta_1-\theta_2)}{r_1} & \frac{b_2}{r_2} & -\frac{b_2}{r_2} \\ \frac{b_1}{r_1} & -\frac{b_1}{r_1} & 0 & 0 \end{bmatrix}$$

where m_1 and m_2 are the masses of the robot 1 and robot 2, and I_{m1} and I_{m2} are the corresponding inertia parameters.

The details to obtain $M(q)$, $C(q,\dot{q})$ and $B(q)$, are given in Appendix A and B.

Substituting (2.35) into (2.43), and left-multiplying by $S(q)^T$, $A(q)^T\lambda$ is eliminated with (2.42). Then, the dynamic equation (2.43) becomes

$$\bar{\boldsymbol{M}}_{\boldsymbol{1}}(\boldsymbol{q})\dot{\boldsymbol{\eta}} + \bar{\boldsymbol{M}}_{\boldsymbol{2}}(\boldsymbol{q})\boldsymbol{\eta} + \bar{\boldsymbol{C}}(\boldsymbol{q},\dot{\boldsymbol{q}}) = \bar{\boldsymbol{B}}(\boldsymbol{q})\boldsymbol{\tau} \tag{2.44}$$

where

$$\bar{M}_1(q) = S(q)^T M(q) S(q) \tag{2.45}$$

$$\bar{M}_2(q) = S(q)^T M(q) \dot{S}(q) \tag{2.46}$$

$$\bar{C}(q,\dot{q}) = S(q)^T C(q,\dot{q}) \tag{2.47}$$

$$\bar{B}(q) = S(q)^T B(q) \tag{2.48}$$

2.4.2 Modeling of three-linked 2WD mobile robots

With the objective to derive in the next section the kinematic and dynamic models for a n-linked 2WD robots system (where n is any integer greater than 2), let first consider the case of three-linked robots. For each robot, the front passive caster is omitted and the two rear wheels are actuated. The leader robot is robot 1, while the followers are robots 2 and 3. The orientations of robots 2 and 3 are consistent with the physical links, but the orientation of robot 1 is independent. The configuration of the whole system is completely described by $q = [x, y, \theta_3, \theta_2, \theta_1]$.

2.4.2.1 Kinematic modeling

The nonholonomic nature of a mobile robot is related to the assumption that the wheels of the mobile robots roll without slipping. They are subject to nonholonomic constraints involving the velocity. The system constraints take the matrix form as follows

$$A(q)\dot{q} = 0 \tag{2.49}$$

where

$$A(q) = \begin{bmatrix} sin\,\theta_3 & -cos\,\theta_3 & 0 & 0 & 0 \\ sin\,\theta_2 & -cos\,\theta_2 & -d_2\,cos(\theta_2 - \theta_3) & 0 & 0 \\ sin\,\theta_1 & -cos\,\theta_1 & -d_2 cos(\theta_1 - \theta_3) & -d_1\,cos(\theta_1 - \theta_2) & 0 \end{bmatrix} \tag{2.50}$$

The kinematic equations of three-linked mobile robots, as shown in Fig. 2.4, are given by

$$\dot{\boldsymbol{q}} = \boldsymbol{S}(\boldsymbol{q})\boldsymbol{\eta} \tag{2.51}$$

where $\eta = [\upsilon_3 \quad \omega_1]^T$, υ_3 is the linear velocity of robot 3, and ω_1 the rotational velocity of robot 1. and the matrix $S(q)$

$$S(q) = \begin{bmatrix} cos\,\theta_3 & sin\,\theta_3 & \frac{1}{d_2}tan(\theta_2 - \theta_3) & \frac{1}{d_1}tan(\theta_1 - \theta_2)\,/\,cos(\theta_2 - \theta_3) & 0 \\ 0 & 0 & 0 & 0 & 1 \end{bmatrix}^T \tag{2.52}$$

Moreover, we can show the following, which describes the natural orthogonal complement property

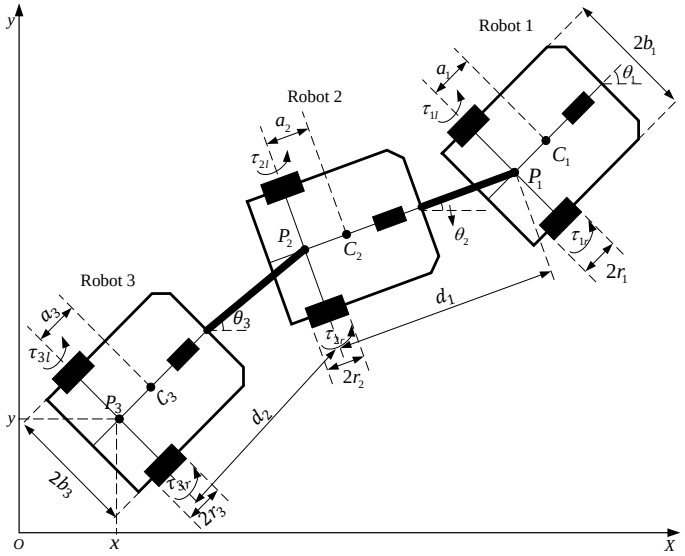

Figure 2.4: Three-linked 2WD mobile robots.

$$S(q)^T A(q)^T = 0 \tag{2.53}$$

2.4.2.2 Dynamic modeling

The dynamic model of three mobile robots with fixed links can be obtained using the Lagrange method in matrix form as

$$M(q)\ddot{q} + C(q,\dot{q}) = B(q)\tau + A(q)^T\lambda \tag{2.54}$$

where

$M(q) \in \Re^{5\times5}$ is the system inertia matrix, $C(q,\dot{q}) \in \Re^{5\times1}$ is the centripetal and Coriolis forces vector, $B(q) \in \Re^{5\times6}$ is the input transformation matrix, $\tau \in \Re^{6\times1}$ is the vector of control torques. $A(q) \in \Re^{3\times5}$ is the system constraint matrix, $\lambda \in \Re^{3\times1}$ Lagrange multipliers vector.

Matrices $M(q)$, $C(q,\dot{q})$ and $B(q)$ in (2.54) are

$$M(q) = \begin{bmatrix} m_1+m_2+m_3 & 0 \\ 0 & m_1+m_2+m_3 \\ -[(m_1+m_2)\,d_2 + a_3m_3]\ sin\,\theta_3 & [(m_1+m_2)d_2 + a_3m_3]\cos\theta_3 \\ -[d_1m_1 + a_2m_2]\sin\theta_2 & [d_1m_1 + a_2m_2]\cos\theta_2 \\ a_1m_1 sin\,\theta_1 & a_1m_1 cos\,\theta_1 \end{bmatrix}$$

$$\begin{bmatrix} -[(m_1+m_2)\,d_2 + a_3m_3]\ sin\,\theta_3 & -[d_1m_1 + a_2m_2]\sin\theta_2 & a_1m_1 sin\,\theta_1 \\ [(m_1+m_2)d_2 + a_3m_3]\cos\theta_3 & [d_1m_1 + a_2m_2]\cos\theta_2 & a_1m_1 cos\,\theta_1 \\ (m_1+m_2)d_2^2 + m_3a_3^2 + I_{m3} & (d_1m_1 + a_2m_2)\ d_2\cos(\theta_2-\theta_3) & a_1m_1d_2\cos(\theta_1-\theta_3) \\ (d_1m_1 + a_2m_2)\ d_2\cos(\theta_2-\theta_3) & m_1d_1^2 + m_2a_2^2 + I_{m2} & a_1m_1d_1\cos(\theta_1-\theta_2) \\ a_1m_1d_2\cos(\theta_1-\theta_3) & a_1m_1d_2\cos(\theta_1-\theta_3) & m_1a_1^2 + I_{m1} \end{bmatrix}$$

$$B(q) = \begin{bmatrix} \frac{cos\,\theta_1}{r_1} & \frac{cos\,\theta_1}{r_1} & \frac{cos\,\theta_2}{r_2} & \frac{cos\,\theta_2}{r_2} & \frac{cos\,\theta_3}{r_3} & \frac{cos\,\theta_3}{r_3} \\ \frac{sin\,\theta_1}{r_1} & \frac{sin\,\theta_1}{r_1} & \frac{sin\,\theta_2}{r_2} & \frac{sin\,\theta_2}{r_2} & \frac{sin\,\theta_3}{r_3} & \frac{sin\,\theta_3}{r_3} \\ \frac{d_2\,sin(\theta_1-\theta_3)}{r_1} & \frac{d_2\,sin(\theta_1-\theta_3)}{r_1} & \frac{d_2\,sin(\theta_2-\theta_3)}{r_2} & \frac{d_2\,sin(\theta_2-\theta_3)}{r_2} & \frac{b_3}{r_3} & \frac{b_3}{r_3} \\ \frac{d_1\,sin(\theta_1-\theta_3)}{r_1} & \frac{d_1\,sin(\theta_1-\theta_3)}{r_1} & -\frac{b_2}{r_2} & -\frac{b_2}{r_2} & 0 & 0 \\ \frac{b_1}{r_1} & -\frac{b_1}{r_1} & 0 & 0 & 0 & 0 \end{bmatrix}$$

$$C(q,\dot{q}) = [C_{ij}]_{5\times1}$$

where

$$\boldsymbol{c_{11}} = -[(m_1 + m_2)d_2 + a_3 m_3]\,\dot{\theta}_3^2\, cos\,\theta_3\,(d_1 m_1 + a_2 m_2)\dot{\theta}_2^2\, cos\,\theta_2 - a_1 m_1 \dot{\theta}_1^2\, cos\,\theta_1.$$

$$\boldsymbol{c_{21}} = -(d_1 m_1 + a_2 m_2) d_2 \dot{\theta}_2^2\, sin(\theta_2 - \theta_3) - a_1 m_1 d_2 \dot{\theta}_1^2\, sin(\theta_1 - \theta_3) + 2(d_1 m_1 + a_2 m_2 d_2 \dot{\theta}_2 \dot{\theta}_3 sin.$$

$$\boldsymbol{c_{31}} = -(d_1 m_1 + a_2 m_2) d_2 \dot{\theta}_2^2\, sin(\theta_2 - \theta_3) - a_1 m_1 d_2 \dot{\theta}_1^2\, sin(\theta_1 - \theta_3) + 2(d_1 m_1 + a_2 m_2)\, d_2 \dot{\theta}_2 \dot{\theta}_3 sin(\theta_2 - \theta_3) + 2a_1 m_1 d_2 \dot{\theta}_1 \dot{\theta}_3\, sin(\theta_1 - \theta_3).$$

$$\boldsymbol{c_{41}} = -(d_1 m_1 + a_2 m_2) d_2 \dot{\theta}_3^2\, sin(\theta_2 - \theta_3) - a_1 m_1 d_2 \dot{\theta}_1^2\, sin(\theta_1 - \theta_2) + 2m_1 d_1 \dot{\theta}_1 \dot{\theta}_3\, sin(\theta_1 - \theta_2).$$

$$\boldsymbol{c_{51}} = a_1 m_1 d_2 \dot{\theta}_3^2\, sin(\theta_1 - \theta_2) + a_1 m_1 d_1 \dot{\theta}_2^2\, sin(\theta_1 - \theta_2).$$

In order to remove the Lagrange multipliers, substituting from the derivative of (2.51) into (2.54), and multiplying by $S(q)^T$, the system dynamic equation takes the following form

$$\boldsymbol{\bar{M}_1(q)\dot{\eta} + \bar{M}_2(q)\eta + \bar{C}(q,\dot{q}) = \bar{B}(q)\tau} \tag{2.55}$$

where

$$\bar{M}_1(q) = S(q)^T M(q) S(q) \tag{2.56}$$

$$\bar{M}_2(q) = S(q)^T M(q) \dot{S}(q) \tag{2.57}$$

$$\bar{B}(q) = S(q)^T B(q) \tag{2.58}$$

$$\bar{C}(q,\dot{q}) = S(q)^T C(q,\dot{q}) \tag{2.59}$$

2.4.3 Modeling of n-linked 2WD mobile robots

We will now express the kinematic and dynamic models of n-linked robots ($n > 2$) as an extension of the models derived for three linked robots.

The following notations are used in the sequel. For the ith ($i = 1,\ 2, \dots, n$) robot: P_i is the center between two actuated wheels, C_i is the center of mass, a_i is the distance between P_i and C_i, b_i is half of the distance between two actuated wheels, r_i is the radius of wheels, θ_i is the orientation of the robot, and τ_{il} and τ_{ir} are the control torques applied to the left and right actuated wheels, respectively. In addition, d_i is the length of the physical links, the frame OXY is the inertial frame, (x, y) denotes the coordinates of point P_n that is the middle point of robot n (the last one) rear wheels.

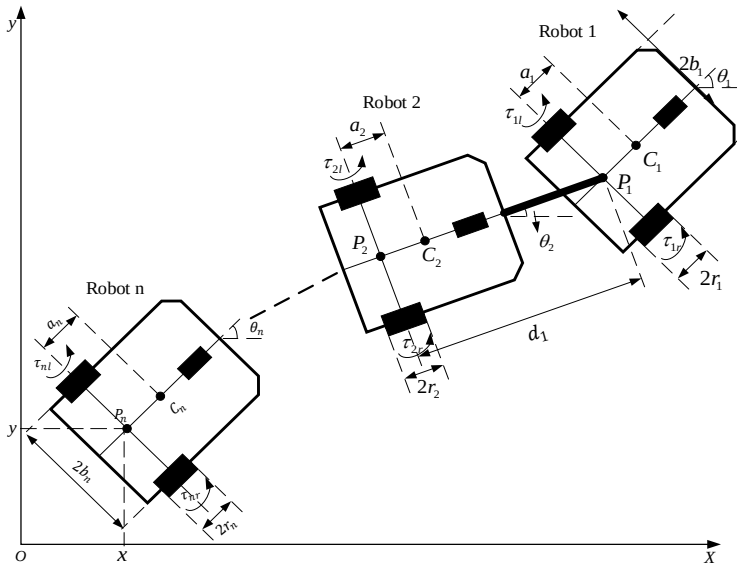

Figure 2.5: Multi-linked 2WD mobile robots.

2.4.3.1 Kinematic modeling

The configuration of the system, as shown in Fig. 2.5, can be expressed with the generalized coordinates vector

$$q = [x, y, \theta_n, \theta_{n-1}, \dots, \theta_1]^T \tag{2.60}$$

The main feature in kinematic models of wheeled mobile robots is the presence of nonholonomic constraints due to the rolling without slipping conditions between the wheels and the ground. The system constraints take the matrix form as follows

$$A(q)\dot{q} = 0 \tag{2.61}$$

where

$$A(q) = \begin{bmatrix} sin\,\theta_n & -cos\,\theta_n & 0 \\ sin\,\theta_{n-1} & -cos\,\theta_{n-1} & -d_n cos(\theta_{n-1} - \theta_n) \\ sin\,\theta_{n-2} & -cos\,\theta_{n-2} & -d_n cos(\theta_{n-2} - \theta_n) \\ \vdots & \vdots & \vdots \\ sin\,\theta_2 & -cos\,\theta_2 & -d_n cos(\theta_2 - \theta_n) \\ sin\,\theta_1 & -cos\,\theta_1 & -d_n cos(\theta_1 - \theta_n) \end{bmatrix}$$

$$\begin{bmatrix} 0 & \cdots & 0 & 0 \\ 0 & \cdots & 0 & 0 \\ 0 & \cdots & 0 & 0 \\ \vdots & \vdots & \vdots & \vdots \\ 0 & -d_2 cos(\theta_2 - \theta_3) & 0 & 0 \\ 0 & -d_2 cos(\theta_1 - \theta_3) & -d_1 cos(\theta_1 - \theta_2) & 0 \end{bmatrix} \tag{2.62}$$

The kinematic equations of the multi mobile robots with fixed links, are given by

$$\dot{\boldsymbol{q}} = \boldsymbol{S}(\boldsymbol{q})\boldsymbol{\eta} \tag{2.63}$$

where $\eta = [v_n \quad \omega_1]^T$; v_n is the linear velocity of robot n, and ω_1 is the rotational velocity of robot 1, and the matrix $S(q)$

$$S(q)=\begin{bmatrix} cos\,\theta_n & 0 \\ sin\,\theta_n & 0 \\ \frac{1}{d_{n-1}} tan(\theta_{n-1}-\theta_n) & 0 \\ \vdots & \vdots \\ \frac{1}{d_{n-k-1}} tan(\theta_{n-k-1}-\theta_{n-k}) / \prod_{i=n-k}^{n-1} cos(\theta_i-\theta_{i+1}) & 0 \\ \vdots & \vdots \\ \frac{1}{d_1} tan(\theta_1-\theta_2) / \prod_{i=1}^{n-1} cos(\theta_i-\theta_{i+1}) & 0 \\ 0 & 1 \end{bmatrix} \tag{2.64}$$

where $(k = 2,\ 3, \dots, n-2)$.

Moreover, the natural orthogonal complement property is expressed as

$$S(q)^T A(q)^T = 0 \tag{2.65}$$

2.4.3.2 Dynamic modeling

The dynamic model of multi mobile robots with fixed links can be obtained using the Lagrange method in matrix form as

$$M(q)\ddot{q} + C(q,\dot{q}) = B(q)\tau + A(q)^T\lambda \tag{2.66}$$

where

$M(q) \in \Re^{(n+2)\times(n+2)}$ is the symmetric, positive definite matrix, $C(q,\dot{q}) \in \Re^{(n+2)\times(1)}$ is the centripetal Coriolis matrix, $B(q) \in \Re^{(n+2)\times(2n)}$ is the input transformation matrix, $\tau \in \Re^{(2n)\times(1)}$ is the vector of control torque. $A(q) \in \Re^{n\times(n+2)}$ is the system constraint matrix, $\lambda \in \Re^{n\times 1}$ is the Lagrange multipliers vector. The matrices and vectors in (2.64) are given by

$$M(q) = \left[m_{ij}\right], i \text{ and } j \in \{1, 2, \cdots, n+2\} \tag{2.67}$$

$$C(q,\dot{q}) = [c_i], i \in \{1, 2, \quad \cdots, n+2\} \tag{2.68}$$

$$B(q) = \left[b_{ij}\right], i \in \{1, 2, \cdots, n+2\},\ j \in \{1, 2, \cdots, 2n\} \tag{2.69}$$

The details to obtain $M(q)$, $C(q,\dot{q})$ and $B(q)$, are given in Appendix C and D, respectively.

In order to remove the Lagrange multipliers, substituting from the derivative of (2.63) into (2.66), and multiplying by $S(q)^T$, the system dynamic equation takes the following form

$$\bar{\boldsymbol{M}}_{\boldsymbol{1}}(\boldsymbol{q})\dot{\boldsymbol{\eta}} + \bar{\boldsymbol{M}}_{\boldsymbol{2}}(\boldsymbol{q})\boldsymbol{\eta} + \bar{\boldsymbol{C}}(\boldsymbol{q},\dot{\boldsymbol{q}}) = \bar{\boldsymbol{B}}(\boldsymbol{q})\boldsymbol{\tau} \tag{2.70}$$

where

$$\bar{M}_1(q) = S(q)^T M(q) S(q) \tag{2.71}$$

$$\bar{M}_2(q) = S(q)^T M(q) \dot{S}(q) \tag{2.72}$$

$$\bar{B}(q) = S(q)^T B(q) \tag{2.73}$$

$$\bar{C}(q,\dot{q}) = S(q)^T C(q,\dot{q}) \tag{2.74}$$

When we aim to control a system using two models (kinematic and dynamic one for the same system), a link (in the form of a diffeomorphism) must be found between the control vectors of the two models in order to elaborate the control signals to be applied on the real system.

In the case of two-linked mobile robots, the diffeomorphism is simple to be found. But in the case of more than two robots, it is much more difficult. One solution is to use the transformation of the kinematic model into the canonical chained form which permits to find relatively simply the searched diffeomorphism. We have chosen to use the canonical chained form in order not only to find the needed diffeomorphism but also to design more easily the control law.

2.5 Model transformation into the canonical chained form

The commonly used approach for controller design of a nonholonomic system is to convert, with appropriate state and input transformations, the original system into a canonical form for which the controller design can be carried out more easily. One of the commonly used canonical form for robotic systems is the so-called chained form, where derivative of each state depends on the state directly above it [109, 110, 111, 112].

A special chained form is the two-input chained form which is expressed as follows

$$\dot{\xi}_1 = \alpha_1$$

$$\dot{\xi}_2 = \alpha_2$$

$$\dot{\xi}_3 = \xi_2 \alpha_1$$

$$\vdots$$

$$\dot{\xi}_m = \xi_{m-1} \alpha_1 \tag{2.75}$$

where $\xi = (\xi_1, \xi_2, \dots, \xi_m)$ is the state, α_1, α_2 are the two virtual control inputs, and m is the number of the states.

The two-input case is sufficiently broad to cover most of the kinematic models of practical wheeled mobile robots. For information on the other *multi-chain forms*, the reader is referred to [111], where these canonical forms were originally introduced.

The motivations to transform the initial state model into the canonical chained form are:

1) To determine a diffeomorphism, to link the kinematic and dynamic controllers for n-linked 2WD mobile robots ($n \geq 2$).
2) To design easily a backstepping control law, which allows controlling each state of the system.

In the next subsection, inspired by the exact linearization method of a nonlinear model presented in [110], we give a theorem which expresses the way to transform the kinematic model of a n-linked robots system into the chained form.

2.5.1 Transformation of the kinematic model of n-linked robots into the chained form

In this subsection, we give a theorem to derive the diffeomorphism which is used to transform the multi-linked 2WD mobile robots system in equation (2.63) into a chained form.

In [40], Sordalen shows how to transform the kinematic model of a car with n trailers into the chained form. We apply his method here for a n-linked 2WD mobile robots system.

The following assumption is needed:

Assumption 2.2*: The state* $q = [x, y, \theta_n, \theta_{n-1}, \dots, \theta_1]^T$ *is in a neighbourhood* D *of the origin where* D *is given by*

$$(x, y) \in R^2$$

$$\theta_i \in \left(-\frac{\pi}{4} + \epsilon, \frac{\pi}{4} - \epsilon\right), \quad i \in \{1, \cdots, n)$$

where ϵ *is a small constant.*

Let us introduce the transformed input v as

$$v = cos\theta_n \, v_n = cos\theta_n \prod_{j=2}^{n} cos\left(\theta_{j-1} - \theta_j\right) v_1 \tag{2.76}$$

The transformed input v is the velocity of robot n in the x-direction. This transformation from v_1 to v is non-singular and smooth in D, where v_1 is the linear velocity of robot 1 and it is considered as a virtual input to the system. The other virtual input is the angular velocity of the robot 1, ω_1.

The linear velocity of robot i, v_i can be written as

$$v_i = cos(\theta_{i-1} - \theta_i) \, v_{i-1} = \prod_{j=2}^{i} cos\left(\theta_{j-1} - \theta_j\right) v_1 \tag{2.77}$$

for $i \in \{2, \cdots, n\}$

Then equation (2.77) can be rewritten using equation (2.76) as follows

$$v_i = \frac{1}{cos\theta_n \prod_{j=i+1}^{n} cos\left(\theta_{j-1} - \theta_j\right)} v = \frac{1}{p_i(\Theta_i)} v \tag{2.78}$$

for $i \in \{1, \cdots, n\}$

where

$$\Theta_i \triangleq [\theta_i, \cdots, \theta_n]^T \tag{2.79}$$

$$p_i(\Theta_i) \triangleq cos\theta_n \prod_{j=i+1}^{n} cos(\theta_{j-1} - \theta_j) = \prod_{j=i}^{n} cos(\theta_j - \theta_{j+1}) \tag{2.80}$$

where $\theta_{n+1} \triangleq 0$.

Equation (2.78) then gives $v = p_1(\theta_1) v_1$.

Inspired by [40], we can now give the following theorem

Theorem 2.1*: The following nonlinear change of coordinates, $\xi = \phi(q)$, and feedback transformation, $\alpha = G(q)\eta$, convert locally the kinematic model (2.63) of the n-linked 2WD mobile robots system into the chained form (2.75)*

The change of coordinates, $\xi = \phi(q)$, is given by

$$\xi_1 = x \tag{2.81}$$

$$\xi_2 = \frac{tan(\theta_1 - \theta_2)}{c_2(\theta_2)} + r_2(\theta_2) \tag{2.82}$$

$$\vdots$$

$$\xi_i = \frac{tan(\theta_{i-2} - \theta_{i-1})}{c_i(\theta_{i-1})} + r_i(\theta_{i-1}) \tag{2.83}$$

$$\vdots$$

$$\xi_n = \frac{tan(\theta_{n-1} - \theta_n)}{d_{n-1}cos^3\theta_n} \tag{2.84}$$

$$\xi_{n+1} = tan\theta_n \tag{2.85}$$

$$\xi_{n+2} = y \tag{2.86}$$

where

$$c_i(\theta_{i-1}) = \prod_{j=2}^{n+1} cos^{j-i+3}(\theta_{j-1} - \theta_j) d_{n+i-j} = p_{i-1}^2(\theta_{i-1}) \prod_{j=i-1}^{n} d_j p_j(\theta_j) \tag{2.87}$$

$$r_i(\theta_{i-1}) = \frac{\partial \xi_{i+1}}{\partial \theta_i} f_i(\theta_{i-1}) \tag{2.88}$$

$$f_i(\theta_{i-1}) = \frac{1}{d_i} \frac{tan(\theta_{i-1} - \theta_i)}{p_i(\theta_i)} \tag{2.89}$$

The feedback transformation of the inputs, $\alpha = G(q)\eta$, is given by

$$\alpha_1 = p_1(\theta_1)v_1 \tag{2.90}$$

$$\alpha_2 = \frac{1}{cos^2(\theta_1 - \theta_2)c_2(\theta_2)\omega_1} + r_1(\theta_1)p_1(\theta_1)v_1 \tag{2.91}$$

The proof of *Theorem 2.1* is given in Appendix E.

By this way, we have all the parameters and we can build the model given by (2.75).

2.5.2 Illustration for three-linked robots

Let us consider the kinematic model of three-linked 2WD mobile robots (2.51). This model has a triangular structure, which can be transformed into the chained form. Equation (2.51) can be expressed as follows:

$$\dot{q}=g_1(q)v_3 + g_2(q)\omega_1 \tag{2.92}$$

where $q = [x, y, \theta_3, \theta_2, \theta_1]^T$,

$$g_1(q) = \left[cos\,\theta_3\ , sin\,\theta_3\ , \frac{1}{d_2}tan(\theta_2 - \theta_3)\ , \frac{1}{d_1}\frac{tan(\theta_1 - \theta_2)}{cos(\theta_2 - \theta_3)}, 0\right]^T$$

$$g_2(q) = [0, 0, 0, 0,1]^T$$

where v_3 is the linear velocity of robot 3, ω_1 is the angular velocity of robot 1, and the $g_1(q)$, $g_2(q)$ are smooth linearly independent vector field.

Applying *Theorem 2.1*, the following change of coordinates is considered

$$\xi_1 = x \tag{2.93}$$

$$\xi_2 = \frac{tan(\theta_1 - \theta_2)}{d_1 d_2 cos^4\theta_3\, cos^3(\theta_2 - \theta_3)} + \frac{1}{d_2^2 cos^4\theta_3}tan(\theta_2 - \theta_3)$$

$$. [3\, tan\,\theta_3 tan\,(\theta_2 - \theta_3) sec^2(\theta_2 - \theta_3)] \tag{2.94}$$

$$\xi_3 = \frac{tan(\theta_2 - \theta_3)}{d_2 cos^3\theta_3} \tag{2.95}$$

$$\xi_4 = tan\theta_3 \tag{2.96}$$

$$\xi_5 = y \tag{2.97}$$

together with the following input transformations

$$\alpha_1 = v_3\, cos\,\theta_3 \tag{2.98}$$

$$\alpha_2 = \beta_1 v_3 + \beta_2 \omega_1 \tag{2.99}$$

where

$$\beta_1 = \frac{1}{d_1 d_2} sec^4\theta_3 tan(\theta_1 - \theta_2) sec^4(\theta_2 - \theta_3)[\frac{1}{d_1}(3tan(\theta_2 - \theta_3)tan(\theta_1 - \theta_2)) + \frac{1}{d_2}(6tan\theta_3 sin(\theta_2 - \theta_3) - 2tan(\theta_2 - \theta_3)sin(\theta_2 - \theta_3) - sec(\theta_2 - \theta_3))] + \frac{1}{d_1 d_2} sec^4\theta_3 sec^2(\theta_1 - \theta_2) sec^3(\theta_2 - \theta_3)$$

$$\beta_2 = \frac{1}{d_1 d_2} sec^4\theta_3 sec^2(\theta_1 - \theta_2) sec^3(\theta_2 - \theta_3)$$

This transformation is a local diffeomorphism around the configurations for which the angle of each robot and the angles between each adjacent robot are different from $(\pi/2)$.

When applying the transformation to the system model in (2.92), we get the following system in chained form:

$$\dot{\xi}_1 = \alpha_1,$$

$$\dot{\xi}_2 = \alpha_2,$$

$$\dot{\xi}_3 = \xi_2 \alpha_1,$$

$$\dot{\xi}_4 = \xi_3 \alpha_1,$$

$$\dot{\xi}_5 = \xi_4 \alpha_1 \qquad (2.100)$$

2.6 Actuator fault model for multi-linked 2WD mobile robots

In this section, the actuator fault model is given for multi-linked 2WD mobile robots. Two types of actuator faults are considered: 1) Partial loss of effectiveness of the wheel motor; 2) Some motors totally lose power which will introduce additional frictions.

These actuator faults for one motor can be modeled as

$$\boldsymbol{\tau_j(t) = \sigma_j(t) u_j(t) + \bar{u}_j}, \qquad t \geq t_j \qquad (2.101)$$

for $j = 1r, 1l, \cdots, nr, nl$, where u_j is the applied control signal, $t_j > 0$ is the unknown fault occurring time instant, $0 \leq \sigma_j \leq 1$ is the unknown actuation effectiveness, and $\bar{u}_j$ is the unknown friction value that is introduced by the fault. Note that, the time interval of each faulty case is supposed to be long enough, and σ_j and $\bar{u}_j$ are piecewise constant.

One can remark that equation (2.101), is composed of two terms, one related to the direct effect of the faults, the second one caused by the resulting frictions.

The actuator fault model in (2.101) can describe many types of practical faults. For example, $\sigma_j = 1$ and $\bar{u}_j = 0$ represents the no fault situation; $\sigma_j = 0$ and $\bar{u}_j = 0$ denotes that the motor loses its power but can rotate freely; $\sigma_j = 0$ and $\bar{u}_j \neq 0$ is the situation when the motor introduces an additional friction between the wheel and the surface; $0 < \sigma_j < 1$ denotes partial loss of effectiveness faults, which may be caused by some interturn faults (open circuit or short circuit) or a low busbar voltage; and $\bar{u}_j \neq 0$ denotes the friction in the bearing. On the other hand, this fault model can also describe the following two classic faults: σ_j denotes a multiplicative fault while $\bar{u}_j$ denotes an additive fault.

Consider that all actuators may be potentially faulty. The control torque vector in equation (2.70) becomes

$$\tau(t) = \sigma(t)u(t) + \bar{u}(t) \tag{2.102}$$

where $\tau = [\tau_{1r}, \tau_{1l}, \tau_{2r}, \tau_{2l}, \cdots, \tau_{nr}, \tau_{nl}]^T$ is the torque vector generated by the motors, $u = [u_{1r}, u_{1l}, u_{2r}, u_{2l}, \cdots, u_{nr}, u_{nl}]^T$ is the control signals vector to be designed, $\sigma = \text{diag}\{\sigma_{1r}, \sigma_{1l}, \cdots, \sigma_{nr}, \sigma_{nl}\}$ is the uncertain control effectiveness matrix, and $\bar{u} = [\bar{u}_{1r}, \bar{u}_{1l}, \bar{u}_{2r}, \bar{u}_{2l}, \cdots, \bar{u}_{nr}, \bar{u}_{nl}]^T$ is the friction vector caused by actuator faults.

Assumption 2.3*: The dynamic subsystem in (2.70) for n-linked 2WD mobile robots has two control input (v_n, ω_1) to be controlled. Then, for the fault compensation design, the following actuation redundancy condition needs to be satisfied*

$$\boldsymbol{rank}(\bar{\boldsymbol{B}}\boldsymbol{\sigma}) = \mathbf{2} \tag{2.103}$$

where, v_n is the linear velocity of robot n, and ω_1 is the rotational velocity of robot 1.

Remark 2.1*: For two-linked 2WD mobile robots as case study, with $\bar{B}(q)$ in (2.48), the compensable fault cases satisfying the redundancy condition in (2.103) are:*

1) *Fault free case with four actuated wheels.*
2) *One actuator fails with three remaining actuated wheels.*
3) *Two actuators fail with two remaining actuated wheels.*

However, for case 3), if the two failed actuators are in robot 2, then the system is similar with a tractor-trailer system [42], and the faults may be tolerated; if each robot has one faulty actuator, then the faults are also compensable; but if the two failed actuators are both in robot 1, then the faults are un-compensable, because in this case, $rank(\bar{B}\sigma) = 1$ with $\sigma = \text{diag}\{\sigma_{1\text{r}}, \sigma_{1\text{l}}, \sigma_{2\text{r}}, \sigma_{2\text{l}}\}$ and ω_1 is uncontrollable.

Key technical issues: The key feature of the control problem is that the failure time t_j, the failure pattern σ_j, and the friction $\bar{u}_j$ are unknown, that is, the feedback control law does not know which component is faulty but is still expected to be able to achieve the desired performance for the closed-loop system.

An observer will be used later on chapter 4, to estimate the actuator gains, the additive faults and the state variables and update the feedback control law to improve the performance of the controlled system.

2.7 Conclusion

In this chapter, a brief review of modeling issues for mobile robots and multi-linked wheeled mobile robots was presented. Then the kinematic and dynamic models for a 2WD mobile robot and multi-linked 2WD robots were introduced. The different models which have been introduced in this chapter will be used in the following chapters to design the FTC laws. Finally, the actuator fault model and the transformation method of the multi-linked 2WD mobile robots system model into the chained form was presented.

After describing the system with an appropriate model, it is possible to design control schemes that guarantee the tracking performance under nonfaulty and faulty situations. Different FTC strategies are presented in the next chapters. Chapter 3 presents passive FTC approaches, which may be viewed as robust control schemes w.r.t the faults, while chapter 4 presents active control algorithms which use a fault diagnosis information.

CHAPTER 3

Passive Fault Tolerant Control

Contents

3.1 Introduction 47

3.2 Actuator FTC compensation for the case of two-linked robots 49

3.2.1 Problem formulation 49

3.2.2 Fault tolerant control design 51

3.2.2.1 Kinematic controller design 51

3.2.2.2 Multiple dynamic controllers design 54

3.2.2.3 Control switching mechanism design 56

3.2.2.4 Overall system performance analysis 58

3.2.3 Simulation studies 60

3.3 Actuator FTC compensation for the case of three-linked robots 65

3.3.1 Multiple model actuator FTC compensation for three-linked robots 65

3.3.1.1 Problem formulation 65

3.3.1.2 Trajectory generation for three-linked 2WD mobile robots 66

3.3.1.3 Fault tolerant control design 69

3.3.1.3.1 Kinematic controller design 69

3.3.1.3.2 Multiple dynamic controllers design 76

3.3.1.3.3 Control switching mechanism design 77

3.3.1.3.4 Overall system performance analysis 78

3.3.1.4 Simulation studies 78

3.3.2 Multiple-design integration based adaptive FTC for three-linked robots 82

3.3.2.1 Problem formulation and FTC objective 3..... 82

3.3.2.2 Fault tolerant control design ……..…….…..... 83

3.3.2.2.1 Kinematic controller design ……... 83

3.3.2.2.2 Dynamic controller design ……. 84

3.3.2.2.3 Stability analysis ……..... 88

3.3.2.3 Simulation studies ……...…… 92

3.4 Generalization of FTC for *n*-linked 2WD mobile robots ……... 101

3.5 Conclusion ……... 101

Chapter content

This chapter is devoted to passive FTC techniques for ***n-linked 2WD mobile robots****. Firstly, a multiple model actuator failure compensation scheme for two-linked 2WD mobile robots is developed in subsection 3.2 to compensate for actuator failures, consisting of a kinematic controller, multiple dynamic controllers and a control switching mechanism, which ensure system stability and asymptotic tracking properties.*

Secondly, a control solution which is well-suited for n-linked $(n > 2)$ *2WD mobile robots (we will start with the case of three-linked robots and further generalize for n-linked robots), is presented in subsection 3.3.1. The provided solution is based on the chained form model introduced in chapter 2. After that, a recursive technique is used to derive the kinematic control law. Based on this, multiple dynamic controllers are designed considering all possible failure cases. From these dynamic controllers, an appropriate one is selected to generate the applied control signal by the control switching mechanism using multiple reconstruction dynamic signals to ensure desired system performance.*

Thirdly, in subsection 3.3.2, in order to design a FTC for multi-linked 2WD mobile robots with friction and actuator faults, the same kinematic control law which is designed in Section 3.3.1 is used, but the dynamic control is different. Therefore, a new adaptive actuator failure compensation scheme is developed using a multi-design integration method. We employ adaptive laws to compensate for uncertain friction coefficients and faults in order to adapt online the single control law and to avoid the control switching mechanism used in the previous sections.

3.1 Introduction

Recently there has been a growing interest in the design and development of advanced feedback control laws for mobile robots. To achieve high precision path tracking control for a wheeled mobile robot, many advanced control approaches have been proposed in the last decade [113, 114]. These methods can be classified based on whether the wheeled mobile robot is described by a kinematic model or a dynamic model. The tracking control problem is therefore classified as either a kinematic or a dynamic tracking control problem.

The purpose of the kinematic controller is to produce velocity set point for the mobile robot to make the tracking error between the real and the reference trajectories converge to

zero. In many applications, the kinematic model of a wheeled mobile robot is sufficient to design a controller for trajectory tracking with satisfactory performance. However, in order to properly deal with the actuator faults changing the applied torque, a dynamic model of the system should be taken into account. The backstepping controller [27] is one of the earliest kinematic level controllers. To improve the overall performance of the backstepping controller and to guarantee the asymptotic convergence of the mobile robot with different reference trajectories, adaptive kinematic controllers have been proposed in [115]. There are also other kinematic control schemes presented in [116-119], which would not fall into the category of adaptive and backstepping controllers but provide stable tracking control structures dealing only with robot velocities.

The kinematic controller is designed in the following. For the simple case of two-linked robots, the kinematic controller is designed using a simple diffeomorphism. For more than two-linked robots, we use the chained form model derived from the initial kinematic model, as it was shown in chapter 2, and the controller is designed using a recursive technique based on the classical integrator backstepping method [120].

The dynamic controllers may be of different types, for example adaptive controllers, robust controllers, robust adaptive controllers and feedback linearization controllers. The dynamic adaptive controllers in [121-123], are adaptive extensions of the kinematic backstepping controller to deal with the unknown parameters. The dynamic robust controllers are designed to deal with uncertainties and disturbances [124] and use sliding mode [125, 126] and H_∞ [127] techniques. There are also some proposed controllers which have both robust and adaptive properties and use a combination of an intelligent controller and a sliding mode controller [128, 129]. The last group of dynamic controllers, uses the feedback linearization control, to compensate for the nonlinear system dynamics (see for instance [130]).

A dynamic controller which is also a torque controller is next designed based on the system dynamics such that the velocity of the mobile robot converges to the generated desired velocity. We are going to use an adaptive control algorithm whose principle may be found in the reference [131], considering two different fault compensation strategies: switching between multiple dynamic control laws, each one compensating a specific fault of a predefined set of actuator faults; designing an adaptive control law with a multi-

integration mechanism that incorporates the compensation of all the sets of predefined faults in just one control law.

3.2 Actuator FTC compensation for the case of two-linked robots

In this subsection, the multiple model actuator failure compensation scheme is developed for two-linked 2WD mobile robots.

3.2.1 Problem formulation

The kinematic model for a two-linked 2WD mobile robots [83] was derived in Section 2.4 (see chapter 2), and is recalled below

$$\dot{x} = \upsilon_2 \cos\theta_2 \tag{3.1}$$

$$\dot{y} = \upsilon_2 \sin\theta_2 \tag{3.2}$$

$$\dot{\theta}_2 = \frac{\upsilon_2}{d}\tan(\theta_1 - \theta_2) \tag{3.3}$$

$$\dot{\theta}_1 = \omega_1 \tag{3.4}$$

Fault-tolerant control objective 1

The fault-tolerant control objective 1 is to develop an actuator failure compensation scheme for two-linked 2WD mobile robots to asymptotically track a reference motion, despite the presence of some actuator failures. In other words, the control objective is to design a control signal $u(t)$ to guarantee that all closed-loop system signals are bounded and $\lim_{t\to\infty}\big(x(t) - x_d(t)\big) = 0$, $\lim_{t\to\infty}\big(y(t) - y_d(t)\big) = 0$ and $\lim_{t\to\infty}\big(\theta_2(t) - \theta_d(t)\big) = 0$ in the presence of uncertain $\sigma(t)$, where x_d, y_d, θ_d are reference trajectories.

The reference motion can be generated by a virtual robot as follows:

$$\dot{x}_d = \upsilon_d \cos\theta_d \tag{3.5}$$

$$\dot{y}_d = \upsilon_d \sin\theta_d \tag{3.6}$$

$$\dot{\theta}_d = \omega_d \tag{3.7}$$

where υ_d and ω_d are the linear velocity and angular velocity of the reference robot, respectively. By choosing appropriate υ_d, ω_d and initial values $x_d(0)$, $y_d(0)$, $\theta_d(0)$, the desired reference trajectories x_d, y_d and θ_d are determined. In this section, we consider the tracking problem (as described in [32]) of a two-robot system.

The following assumption is given for the reference trajectories.

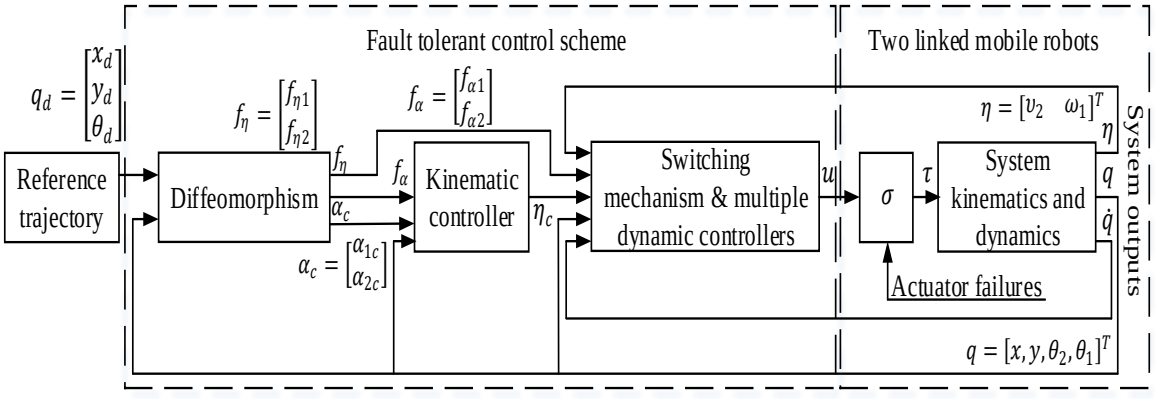

Figure 3.1: Multiple-model actuator failure compensation control scheme, for the case of two-linked 2WD mobile robots.

Assumption 3.1*: The reference trajectories x_d, y_d and θ_d, the velocities v_d, ω_d, and their derivatives are continuous and uniformly bounded, and $v_d \neq 0$.*

Remark 3.1*: In Assumption 3.1, it is imposed that $v_d \neq 0$ to avoid singularity in the controller for the trajectory tracking of the mobile robots. On the other hand, in order to stop the vehicle when the tracking mission is completed, the controller should be disabled.*

Remark 3.2*: The control objective 1 is focused on the tracking task for the rear robot, and the front robot can be seen to help the rear one to track the reference trajectory. The reason is the following: the states x, y are chosen to be the position of the rear robot (see chapter 2), based on which, the kinematics and dynamics are modelled, then the control scheme is designed. Furthermore, the position of the front robot can also be chosen as the states x and y, but the kinematic and dynamic models will change correspondingly. In this case, the control scheme should be redesigned.*

Design issues. Since the failure pattern matrix σ is uncertain, in this section, we will develop a multiple model control scheme covering all possible σ to achieve the fault-tolerant control objective 1, the structure of which is shown in Fig. 3.1. Our failure compensation control design employs three steps:

Step 1*:* For the kinematic equations, the linear velocity v_2 and the angular velocity ω_1 can be seen as intermediate control signals. So, we first design a kinematic control law $\eta_c = [v_{2c}, \omega_{1c}]^T$, such that when it is applied, the desired control performance can be ensured.

***Step 2**:* Then, multiple controllers are designed, each of which is designed using one possible failure pattern matrix. If the failure pattern used in the applied controller, is consistent with the actual one, the applied control signal can ensure $(\eta(t) - \eta_c(t)) \to 0$ as t goes to infinity and also can guarantee the desired system performance.

***Step 3**:* Finally, a control switching mechanism is established to select an appropriate controller to generate the applied control signal u.

3.2.2 Fault-tolerant control design

In this subsection, a multiple model actuator fault compensation scheme is developed for two-linked robots, which consists of three parts as shown in Fig. 3.1.

3.2.2.1 Kinematic controller design

***Kinematic control law**:*

Define the output tracking error as

$$\tilde{e} = \begin{pmatrix} \tilde{e}_x \\ \tilde{e}_y \\ \tilde{e}_\theta \end{pmatrix} = \begin{pmatrix} x - x_d \\ y - y_d \\ \theta_2 - \theta_d \end{pmatrix} \tag{3.8}$$

and a transformation matrix as

$$T_e = \begin{pmatrix} \cos\theta_d & \sin\theta_d & 0 \\ -\sin\theta_d & \cos\theta_d & 0 \\ 0 & 0 & 1 \end{pmatrix} \tag{3.9}$$

Then, a new error is defined as

$$e = [e_x \quad e_y \quad e_\theta]^T = T_e \tilde{e} \tag{3.10}$$

Note that, since det $[T_e]$ = 1 which means that T_e is nonsingular, $\lim_{t\to\infty} e(t) = 0$ implies $\lim_{t\to\infty} \tilde{e}(t) = 0$. With (3.1) -(3.4), (3.5)-(3.7) and (3.8)-(3.10), we have

$$\dot{e}_x = \omega_d e_y + \upsilon_2 \cos e_\theta - \upsilon_d \tag{3.11}$$

$$\dot{e}_y = -\omega_d e_x + \upsilon_2 \sin e_\theta \tag{3.12}$$

$$\dot{e}_\theta = \frac{\upsilon_2}{d}\tan(\theta_1 - \theta_2) - \omega_d \tag{3.13}$$

To develop a kinematic control law $\eta_c = [\upsilon_{2c}, \omega_{1c}]^T$ for $\eta = [\upsilon_2, \omega_1]^T$, we introduce the following diffeomorphism:

$$z_1 = e_x \tag{3.14}$$

$$z_2 = e_y \tag{3.15}$$

$$z_3 = \tan e_\theta \tag{3.16}$$

$$z_4 = \frac{tan(\theta_1 - \theta_2)}{d\, cos^3\, e_\theta} - \frac{\omega_d}{\upsilon_d d\, cos^2\, e_\theta} + e_y \tag{3.17}$$

and an input transformation:

$$\alpha = \begin{bmatrix}\alpha_1 \\ \alpha_2\end{bmatrix} = \begin{bmatrix}\upsilon_2 \cos e_\theta - \upsilon_d \\ \dot{z}_4\end{bmatrix} \tag{3.18}$$

Then, the derivatives of z_1, z_2, z_3 and z_4 are

$$\dot{z}_1 = \omega_d z_2 + \alpha_1 \tag{3.19}$$

$$\dot{z}_2 = -\omega_d z_1 + (\upsilon_d + \alpha_1) z_3 \tag{3.20}$$

$$\dot{z}_3 = \upsilon_d (z_4 - z_{2_1}) + (z_4 - z_2 + \frac{\omega_d}{\upsilon_d}(1 + z_3^2)) \tag{3.21}$$

$$\dot{z}_4 = \alpha_2 \tag{3.22}$$

The detailed computations to derive (3.19)-(3.22) are given in Appendix F.

From (3.17) and (3.18), we can obtain

$$\alpha = T_\alpha \eta + f_\alpha \tag{3.23}$$

where $T_\alpha \in \Re^{2\times 2}$ and $f_\alpha \in \Re^2$ are given in Appendix G.

Define a virtual kinematic control signal

$$\alpha_c = T_\alpha \eta_c + f_\alpha \tag{3.24}$$

and the velocity tracking error as

$$\eta_e = \eta - \eta_c \tag{3.25}$$

Then, we have

$$\alpha_e = [\alpha_{1e},\, \alpha_{2e}]^T = \alpha - \alpha_c = T_\alpha \eta_e \tag{3.26}$$

Now, we design the virtual kinematic signal $\alpha_c = [\alpha_{1c},\, \alpha_{2c}]^T$ as

$$\alpha_{1c} = -k_1 (z_1 + z_3 (z_4 + \frac{\omega_d}{\upsilon_d}(1 + z_3^2))) \tag{3.27}$$

$$\alpha_{2c} = -k_2 v_d z_3 - k_3 z_4 \tag{3.28}$$

where $k_1 > 0$, $k_2 > 0$ and k_3 are chosen to be constant gains. Note that, if v_d is too small, then α_{1c} may be very large which will result in a bad system transient response. So, for the practical situation, the reference velocity v_d should be chosen as an appropriate one that can contribute to a smooth system transient response. From (3.24), the kinematic control law is

$$\boldsymbol{\eta_c = T_\alpha^{-1}(\alpha_c - f_\alpha)} \tag{3.29}$$

The expression of T_α will be given in the overall system performance analysis.

***Preliminary analysis**:*

For the preliminary analysis of the performance of the designed kinematic control law, we choose a positive-definite function as

$$V_1 = \frac{1}{2}(z_1^2 + z_2^2 + z_3^2 + \frac{1}{k_2} z_4^2) \tag{3.30}$$

With (3.19)-(3.22), the time derivative of V_1 is

$$\begin{aligned}
\dot{V}_1 = & z_1\omega_d z_2 + z_1\alpha_1 - z_2\omega_d z_1 + z_2 v_d z_3 + z_2\alpha_1 z_3 + z_3 v_d z_4 - z_3 v_d z_2 \\
& + z_3\alpha_1 z_4 - z_3\alpha_1 z_2 + \frac{z_3\alpha_1\omega_d(1+z_3^2)}{v_d} + \frac{z_4}{k_2}\alpha_2 \\
= & (z_1 + z_3(z_4 + \frac{\omega_d}{v_d}(1+z_3^2)))\alpha_1 + v_d z_3 z_4 + \frac{z_4}{k_2}\alpha_2 \\
= & (z_1 + z_3(z_4 + \frac{\omega_d}{v_d}(1+z_3^2)))\alpha_{1c} + v_d z_3 z_4 + \frac{z_4}{k_2}\alpha_{2c} \\
& + (z_1 + z_3(z_4 + \frac{\omega_d}{v_d}(1+z_3^2)))\alpha_{2e} + \frac{z_4}{k_2}\alpha_{2e}
\end{aligned} \tag{3.31}$$

Letting $f_\eta = [z_1 + z_3(z_4 + \frac{\omega_d}{v_d}(1+z_3^2)), \frac{z_4}{k_2}]^T$ and substituting (3.27), (3.28) and (3.26) into (3.30) yield

$$\dot{V}_1 = -k_1(z_1 + z_3(z_4 + \frac{\omega_d}{v_d}(1+z_3^2)))^2 - \frac{k_3}{k_2} z_4^2 + f_\eta^T T_\alpha \eta_e \tag{3.32}$$

If there was no term $f_\eta^T T_\alpha \eta_e$, then $\dot{V}_1$ would be nonpositive. To eliminate this term and ensure desired system performance, we will design a dynamic controller in the next section.

3.2.2.2 Multiple dynamic controllers design

Since the faults are uncertain, which will cause an uncertainty of the control gain, it is difficult to ensure system stability and asymptotic tracking properties by using a single control law. To cover all possible failure patterns, we will design one specific control law for each failure pattern. Then, we will establish a control switching mechanism to select an appropriate control law to be the applied one.

***Multiple dynamic control laws**:*

Substituting (2.102) into (2.44) (see chapter 2), we have the following dynamic equation when actuator failures are considered:

$$\dot{\eta} = -\bar{M}_1^{-1}\bar{M}_2\eta - \bar{M}_1^{-1}\bar{C} + \bar{M}_1^{-1}\bar{B}\sigma u \tag{3.33}$$

where $u = [u_{1r}, u_{1l}, u_{2r}, u_{2r}]^T$ is the applied control signal to be designed.

With (3.25), the time derivative of the velocity tracking error is

$$\dot{\eta}_e = -\bar{M}_1^{-1}\bar{M}_2\eta - \bar{M}_1^{-1}\bar{C} + \bar{M}_1^{-1}\bar{B}\sigma u - \dot{\eta}_c \tag{3.34}$$

Let $\sigma_{(k)}$, $k = 1, 2, \dots, N$, denote the kth possible failure matrix satisfying actuation redundancy condition (2.103), where N is the number of all possible failure pattern matrices that are under consideration. Then, the dynamic control law corresponding to $\sigma_{(k)}$ is designed as

$$\boldsymbol{u_{(k)} = \left(\bar{M}_1^{-1}\bar{B}\sigma_{(k)}\right)^{+}\left[-k_4\eta_e - T_\alpha^T f_\eta + \bar{M}_1^{-1}\bar{M}_2\eta + \bar{M}_1^{-1}\bar{C} + \dot{\eta}_c\right]} \tag{3.35}$$

for $k = 1, 2, \dots, N$, where $k_4 > 0$ is chosen to be constant, and $\left(\bar{M}_1^{-1}\bar{B}\sigma_{(k)}\right)^{+}$ is the generalized inverse matrix satisfying $\bar{M}_1^{-1}\bar{B}\sigma_{(k)}\left(\bar{M}_1^{-1}\bar{B}\sigma_{(k)}\right)^{+} = I_2$. The performance of the dynamic control law in (3.35) is given next.

***Performance analysis**:* The performance of the designed dynamic control laws is given by the following lemma.

***Lemma 3.1**: If the applied control law matches with the actual failure pattern matrix, i.e., $\sigma = \sigma_{(a)}$ and $u = u_{(a)}$ for $a = 1, 2, \dots, N$, then the boundedness of all closed-loop signals is ensured, and $lim_{t\to\infty}\left(x(t) - x_d(t)\right) = 0$, $lim_{t\to\infty}\left(y(t) - y_d(t)\right) = 0$ and $lim_{t\to\infty}\left(\theta_2(t) - \theta_d(t)\right) = 0$ and $lim_{t\to\infty}\left(\eta(t) - \eta_c(t)\right) = 0$.*

***Proof**:* Consider $\sigma = \sigma_{(a)}$ and $u = u_{(a)}$, and choose the global Lyapunov function candidate as

$$V_{2(a)} = V_1 + \frac{1}{2}\eta_e^T \eta_e \tag{3.36}$$

Deriving equation (3.36) and using (3.32) and (3.34) lead to

$$\begin{aligned}\dot{V}_{2(a)} &= -k_1(z_1 + z_3(z_4 + \frac{\omega_d}{\upsilon_d}(1+z_3^2)))^2 - \frac{k_3}{k_2}z_4^2 + f_\eta^T T_\alpha \eta_e \\ &\quad + \eta_e^T\left[-\bar{M}_1^{-1}\bar{M}_2\eta - \bar{M}_1^{-1}\bar{C} + \bar{M}_1^{-1}\bar{B}\sigma_{(a)}u - \dot{\eta}_c\right] \\ &= -k_1(z_1 + z_3(z_4 + \frac{\omega_d}{\upsilon_d}(1+z_3^2)))^2 - \frac{k_3}{k_2}z_4^2 \\ &\quad + \eta_e^T\left(T_\alpha^T f_\alpha - \bar{M}_1^{-1}\bar{M}_2\eta - \bar{M}_1^{-1}\bar{C} + \bar{M}_1^{-1}\bar{B}\sigma_{(a)}u - \dot{\eta}_c\right)\end{aligned} \tag{3.37}$$

Substituting the dynamic control law in (3.35) with $k = a$ in the equation (3.37), we have

$$\dot{V}_{2(a)} = -k_1(z_1 + z_3(z_4 + \frac{\omega_d}{\upsilon_d}(1+z_3^2)))^2 - \frac{k_3}{k_2}z_4^2 - k_4\eta_e^T\eta_e \leq 0 \tag{3.38}$$

where $(z_1, \cdots, z_4)$ are the variables which we used to derive the kinematic control law.

The proof of equation (3.38) is as follows:

z_1, z_2, z_3, z_4, η_e, $(z_1 + z_3(z_4 + (\omega_d/\upsilon_d)(1+z_3^2))) \in L^\infty$, and z_4, η_e, $(z_1 + z_3(z_4 + (\omega_d/\upsilon_d)(1+z_3^2))) \in L^2$. The definitions of L^∞ and L^2 can be found in [131]. It follows from (3.16) and (3.17) that $\cos e_\theta \neq 0$ and $\tan(\theta_1 - \theta_2) \in L^\infty$ meaning $\cos(\theta_1 - \theta_2) \neq 0$. Then, from Appendix F, (3.11)-(3.29) and (3.33)-(3.35), we can obtain: T_α is bounded and nonsingular, and f_α, α_c, α_e, α, η_c, η, $\dot{z}_1$, $\dot{z}_2$, $\dot{z}_3$, $\dot{z}_4$, $\dot{\alpha}_c$, $\dot{\eta}_c$, $u(k)$, $\dot{\eta}_e$, $\dot{\alpha}_c$, $\dot{\alpha} \in L^\infty$ which also means that the time derivative of $(z_1 + z_3(z_4 + (\omega_d/\upsilon_d)(1+z_3^2)))$ is bounded. According to Barbalat's lemma [131], it is concluded that all closed-loop signals are bounded, and $(z_1 + z_3(z_4 + (\omega_d/\upsilon_d)(1+z_3^2)))$, $\lim_{t\to\infty} z_4 = 0$ and $\lim_{t\to\infty} \eta_e = 0$, which also implies $\lim_{t\to\infty} \alpha_e = 0$ and $\lim_{t\to\infty} \alpha_{c1} = 0$ with (3.26) and (3.27) meaning $\lim_{t\to\infty} \alpha_1 = 0$.

From (3.22), we have $\ddot{z}_4 = \dot{\alpha}_2 = \dot{\alpha}_{2c} + \dot{\alpha}_{2e} \in L^\infty$ with $\dot{\alpha}_{2c}$, $\dot{\alpha}_{2e} \in L^\infty$, which means that $\dot{z}_4$ is uniformly continuous, together with $\lim_{t\to\infty} \int_0^t \dot{z}_4(\tau)\, d\tau = z_4(\infty) - z_4(0) = -z_4(0)$, we can further obtain $\lim_{t\to\infty}\dot{z}_4 = \lim_{t\to\infty}\alpha_2 = \lim_{t\to\infty}(\alpha_{2c} + \alpha_{2e})=0$ according to Barbalat's lemma. Then, with $\lim_{t\to\infty}\alpha_e$, $\lim_{t\to\infty} z_4 = 0$, $\alpha_{2c} = -k_2\upsilon_2 z_3 - k_3 z_4$ and $|\upsilon_d| > 0$, we have $\lim_{t\to\infty} \alpha_{2c} = 0$ and $\lim_{t\to\infty} z_3 = 0$, it follows that $\lim_{t\to\infty} z_1 = 0$ with $\lim_{t\to\infty}(z_1 + z_3(z_4 + (\omega_d/\upsilon_d)(1+z_3^2)))$.

On the other hand, from $\dot{z}_3 = v_d(z_4 - z_2) + \alpha_1(z_4 - z_2 + (\omega_d/v_d)(1 + z_3^2)))$ in (3.21), we have $\ddot{z}_3 \in L^\infty$. Similarly, $\lim_{t\to\infty}\dot{z}_3 = 0$ is ensured according to Barbalat's lemma. Then, we can further obtain that $\lim_{t\to\infty} z_2 = 0$ with $\lim_{t\to\infty} z_4 = 0$, $\lim_{t\to\infty} \alpha_1 = 0$ and $|v_d| > 0$.

Finally, all the closed loop system signals are uniformly bounded, furthermore $\lim_{t\to\infty} z_i(t) = 0$, $(i = 1, 2, 3, 4)$ and $\lim_{t\to\infty}(\eta(t) - \eta_c(t)) = 0$, which also means $\lim_{t\to\infty}\big(x(t) - x_d(t)\big) = 0$, $\lim_{t\to\infty}\big(y(t) - y_d(t)\big) = 0$ and $\lim_{t\to\infty}\big(\theta_2(t) - \theta_d(t)\big) = 0$ with the diffeomorphism in (3.14)-(3.16) and the transformation in (3.10).

This concludes the proof of *lemma 3.1*. ■

Remark 3.3*: Choosing small controller parameters $k_1, \cdots, k_4$ may lead to a smooth system transient response but with a slow convergence speed of the tracking errors, while choosing large ones may contribute to fast convergent tracking errors but with a large transient response. To fully utilize these properties, $k_1, \cdots, k_4$ are chosen empirically. The system may be first simulated with different sets of parameters (small ones and large ones), then we can choose the most appropriate set that may ensure a good smooth system transient response and with an acceptable convergence speed of the tracking errors.*

Since the failure pattern is uncertain, that is, we do not know which $\sigma_{(k)}$, $k = 1, 2, \dots, N$, matches with the actual σ, a control switching mechanism is needed to select the most appropriate control law $u(k)$ from (3.35) as the applied control signal u.

3.2.2.3 Control switching mechanism design:

To develop the control switching mechanism, we first reconstruct the velocity vector η for each possible $\sigma_{(k)}$, $k = 1, 2, \dots, N$. Then, multiple cost functions are calculated from the reconstruction errors, and are employed to generate the control switching signal. So, the design of the switching mechanism includes the following three steps:

Step 1. ***Signal reconstruction****:* We first reconstruct the velocity vector η for all possible $\sigma_{(k)}, k = 1, 2, \dots, N$. Let us start with the dynamic equations in (3.33):

$$\dot{\eta} = -\bar{M}_1^{-1}\bar{M}_2\eta - \bar{M}_1^{-1}\bar{C} + \bar{M}_1^{-1}\bar{B}\sigma u \tag{3.39}$$

Choosing a stable filter $\frac{1}{s+\gamma}$ with $\gamma > 0$ and adding to both sides of equation (3.39), we have

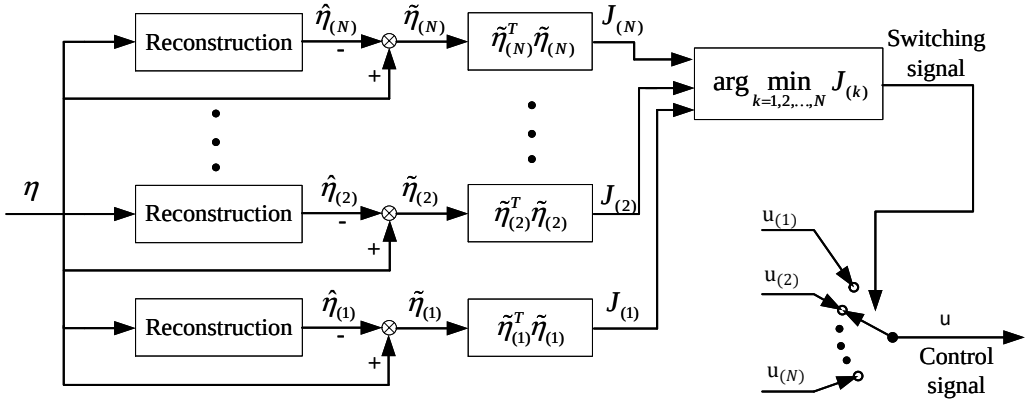

Figure 3.2: Structure of the control switching mechanism.

$$\frac{s}{s+\gamma}[\eta](t) = \frac{1}{s+\gamma}[-\bar{M}_1^{-1}\bar{M}_2\eta - \bar{M}_1^{-1}\bar{C}](t) + \frac{1}{s+\gamma}[\bar{M}_1^{-1}\bar{B}\ \sigma u\ ](t) \qquad (3.40)$$

where $\dot{\eta}(t) = s[\eta](t)$ and $\frac{1}{s+\gamma}[\chi](t)$ denotes the output of the filter $\frac{1}{s+\gamma}$ with the input $\chi(t)$ [131].

From (3.40), it can be further obtained

$$\eta(t) = \frac{\gamma}{s+\gamma}[\eta](t) + \frac{1}{s+\gamma}[-\bar{M}_1^{-1}\bar{M}_2\eta - \bar{M}_1^{-1}\bar{C}](t) + \frac{1}{s+\gamma}[\bar{M}_1^{-1}\bar{B}\ \sigma u](t) \qquad (3.41)$$

For each possible $\sigma_{(k)}, k = 1, 2, \ldots . N$, we reconstruct a signal as follows

$$\hat{\eta}_{(k)}(t) = \frac{\gamma}{s+\gamma}[\eta](t) + \frac{1}{s+\gamma}[-\bar{M}_1^{-1}\bar{M}_2\eta - \bar{M}_1^{-1}\bar{C}](t) + \frac{1}{s+\gamma}\left[\bar{M}_1^{-1}\bar{B}\ \sigma_{(k)}u\ \right](t) \qquad (3.42)$$

Define the reconstruction error, as shown in Fig. 3.2, as follows

$$\tilde{\eta}(t) = \eta(t) - \hat{\eta}(t) \qquad (3.43)$$

Then, consider that the actual failure pattern matrix is $\sigma_{(a)}$, then with (3.41) and (3.42), the matched reconstruction error takes the form of

$$\tilde{\eta}_{(a)}(t) = 0 \qquad (3.44)$$

and the unmatched reconstruction errors take the form of

$$\tilde{\eta}_{(b)}(t) = \frac{1}{s+\gamma}\left[\bar{M}_1^{-1}\bar{B}\sigma_{(a)}u - \bar{M}_1^{-1}\bar{B}\sigma_{(b)}u\right](t) \tag{3.45}$$

for $b = 1, 2, \ldots N, b \neq a,$ which may be not zero as compared with the matched reconstruction error.

Step 2. ***Multiple cost functions****:* For the cost functions, as shown in Fig. 3.2, calculated from the reconstruction errors, it is common to use quadratic error cost functions, which are chosen as

$$J_{(k)}(t) = \tilde{\eta}_{(k)}^{T}(t)\tilde{\eta}_{(k)}(t) \tag{3.46}$$

for $k = 1, 2, \ldots . N$.

Step 3. ***Control signal selection****:* The control switching, is implemented by comparing all the cost functions in (3.46), and determining the index k corresponding to the minimum one, that is

$$k(t) = \arg \min_{\mathrm{k=1,2,\ldots.N}} J_{(k)}(t) \tag{3.47}$$

Thus, we can select which $\sigma_{(k)}$ should be put in the dynamic control signal. Then the corresponding control law is selected as the applied control signal from (3.35), that is

$$u(t) = u_{(k)}(t) \tag{3.48}$$

Moreover, for practical robots, a waiting time T_{min} will be employed between every two switchings to prevent arbitrary fast switching.

3.2.2.4 Overall system performance analysis

This mobile robot system composed of two-linked 2WD robots may be in different failure situations. To deal with these actuator faults, multiple dynamic control laws and multiple nonnegative cost functions are designed, each of which matches with one possible failure situation. The control switching mechanism is implemented by comparing all the cost functions and applying the control law corresponding to the minimum one. The cost function matching with the actual system is theoretically zero which is the minimum value. So, the matched control law will be selected, which can ensure system stability and asymptotic tracking properties. In some specific situations, an unmatched control law may

be selected. This means that the corresponding unmatched cost function is minimum. In this case, the selected unmatched control law can also ensure the desired system performance. Therefore, the desired performance of the overall system is ensured by the developed multiple model-based control scheme.

The performance of the overall system is given as follows:

Theorem 3.1*: The developed multiple-model actuator failure compensation control scheme, constituted by the kinematic control law in (3.27) and (3.28), multiple dynamic control laws in (3.35) and the control switching mechanism implemented by (3.47) and (3.48) with multiple reconstructed signals in (3.42) and multiple cost functions in (3.46), applied to two-linked 2WD mobile robots, guarantees that all closed-loop signals are bounded and* $lim_{t\to\infty}\big(x(t)-x_d(t)\big)=0$, $lim_{t\to\infty}\big(y(t)-y_d(t)\big)=0$ *and* $lim_{t\to\infty}\big(\theta_2(t)-\theta_d(t)\big)=0$, *despite the presence of actuator faults whose time of occurrence and pattern are not known.*

Proof*:* Consider $\sigma=\sigma_{(a)}$. From (3.44) and (3.46), we have $J_{(a)}=0$ for the matched cost function. But for the unmatched functions $J_{(b)}, b=1,2,\dots N, b\neq a$, these zero properties may not hold due to (3.45). Since all cost functions are nonnegative, the matched cost function will generically become smaller than the other ones. Then, the matched control law $u_{(a)}$ will be selected as the applied one with (3.47) and (3.48). According to Lemma 3.1, the selected control law can guarantee that all closed-loop signals are bounded and $\lim_{t\to\infty}\big(x(t)-x_d(t)\big)=0$, $\lim_{t\to\infty}\big(y(t)-y_d(t)\big)=0$ and $\lim_{t\to\infty}\big(\theta_2(t)-\theta_d(t)\big)=0$, despite the presence of actuator failures. This is the generic (generally true) matched case. On the other hand, if the unmatched control law $u_{(b)}, b\neq a$ is selected as the applied one meaning $J_{(b)}(t)\leq J_{(a)}$, then there is a time interval $[T_1,T_2]$ such that $J_{(b)}(t)=0$ for $t\in[T_1,T_2]$, as $J_{(a)}(t)=0$. From (3.45), $J_{(b)}(t)=0$ means $\bar{M}_1^{-1}\bar{B}\,\sigma_{(a)}u_{(b)}-\bar{M}_1^{-1}\bar{B}\,\sigma_{(b)}u_{(b)}=0$ for $t\in[T_1,T_2]$, together with $\bar{M}_1^{-1}\bar{B}\sigma_{(b)}u_{(b)}=\bar{M}_1^{-1}\bar{B}\sigma_{(a)}u_{(a)}=-k_4\eta_e-T_\alpha^T f_\alpha+\bar{M}_1^{-1}\bar{M}_2\eta+\bar{M}_1^{-1}\bar{C}+\dot{\eta}_c$, it also means that: if $\sigma_{(a)}$ but $u_{(b)}$ is selected, then $u_{(b)}$ has the same control effectiveness for the dynamic system in (3.33) as compared with the matched control law $u_{(a)}$.

This concludes the proof of *Theorem 3.1*. ■

Remark 3.4*: The designed multiple model control scheme can also be applied when some actuator faults occur and disappear, i.e. intermittent faults. On the other hand, we would like to point out that the time intervals between every two different faulty cases should be long enough. This hypothesis means that the status of the actuators will not change quickly, which is also reasonable for actual robots. Moreover, for practical robots, an artificial waiting time* $T_{min} > 0$ *(as in [132]) may be employed between every two-control switchings to prevent arbitrarily fast switching. The proposed multiple-model control scheme only employs the switching of control signals, but not a switched system that will act among several subsystems. On the other hand, the control switchings in this section are independent on the waiting time but depend on the cost function-based control switching mechanism. So, we call* T_{min} *as a waiting time but not as a dwell-time that needs to be designed for switched systems.*

3.2.3 Simulation studies

To verify the effectiveness of the developed multiple model failure compensation scheme for two differentially driven wheeled mobile robots with fixed link, a simulation study is presented.

Simulation conditions

In this simulation studies, we assume that the two wheeled driven robots are the one used in [34], then the physical parameters of the two robots are chosen as: $a_1 = a_2 = 0.3\,m$, $b_1 = b_2 = 0.75\,m$, $r_1 = r_2 = 0.15\,m$, $m_1 = m_2 = 30\,kg$, $I_{m1} = I_{m2} = 15.625\,kg \cdot m^2$. The length of the link between the two robots is assumed to be $d = 1.7\,m$. The reference trajectory are generated by (3.5)-(3.7), with $v_d = 0.5\,m/s$, and $\omega_d = 0.1\,rad/s$.

In order to verify the failure compensation effectiveness of the developed multiple model control scheme, the following fault cases are simulated:

- no fault: $\sigma_{(1)} = \text{diag}\{1, 1, 1, 1\}$, $0 \leq \text{t} < 20\text{s}$;
- τ_{1r} fails: $\sigma_{(2)} = \text{diag}\{0, 1, 1, 1\}$, $20\text{s} \leq \text{t} < 50\text{s}$;
- τ_{1r}, τ_{2l} fail: $\sigma_{(3)} = \text{diag}\{0, 1, 1, 0\}$, $50\text{s} \leq \text{t} < 80\text{s}$;
- τ_{2l} fails: $\sigma_{(4)} = \text{diag}\{1, 1, 1, 0\}$, $80\text{s} \leq \text{t} < 110\text{s}$;
- τ_{2r}, τ_{2l}, fail: $\sigma_{(5)} = \text{diag}\{1, 1, 0, 0\}$, $\text{t} \geq 110\text{s}$.

There are five failure pattern matrices satisfying the actuation redundancy condition (see equation 2.103 in chapter 2), covering the cases of fault free, one actuator fails, both two actuators of robot 2 fail, and one actuator of each robot fails. Then we need five control laws in (3.35), reconstructed signals in (3.45) and cost functions in (3.46).

The initial conditions are chosen as:

$x_d(0) = 0, \quad y_d(0) = 0, \quad \theta_2(0) = 0 \text{ deg}, \quad \theta_1(0) = 0 \text{ deg}, \quad v_2(0) = 0, \quad \omega_d = 0.$

The control gains are chosen as:

$k_1 = 10, k_2 = 2, k_3 = 0.5$ and $k_4 = 3000,$ and the waiting time between every two switchings is $T_{min} = 0.01s$.

Simulation results

We apply the developed multiple model failure compensation control scheme to two-linked mobile robots. The following simulation results are obtained.

Fig. 3.3, shows the positions of robot 2, reference robot and robot 1, Fig. 3.4, shows the tracking errors of robot 2. From them, we can see that the desired system stability and asymptotic tracking properties are ensured despite the presence of uncertain actuator failures. Fig. 3.5 and Fig. 3.6, show the control torques generated by the wheels in robot 1 and robot 2, respectively, from which we can see that the actuator failures are consistent with the failure cases in simulation conditions.

Fig. 3.7, shows the orientation error between two robots. Fig. 3.8, shows the control switching index, the sequence of which is $1 \rightarrow 3 \rightarrow 2 \rightarrow 3 \rightarrow 4 \rightarrow 5$. We can see that the control switching index matches with the actual failure pattern index, although there is some wrong switchings at some short time intervals after the failure occurring time instants. The wrong control switching does not affect system stability and asymptotic tracking properties, which is consistent with the unmatched case in the proof of *Theorem 3.1*.

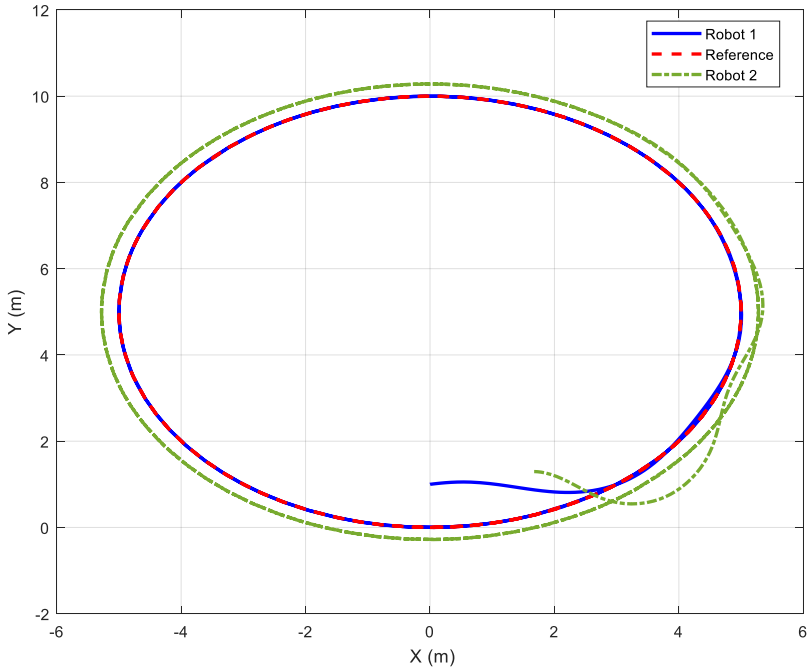

Figure 3.3: Robot trajectories in (x,y) plane.

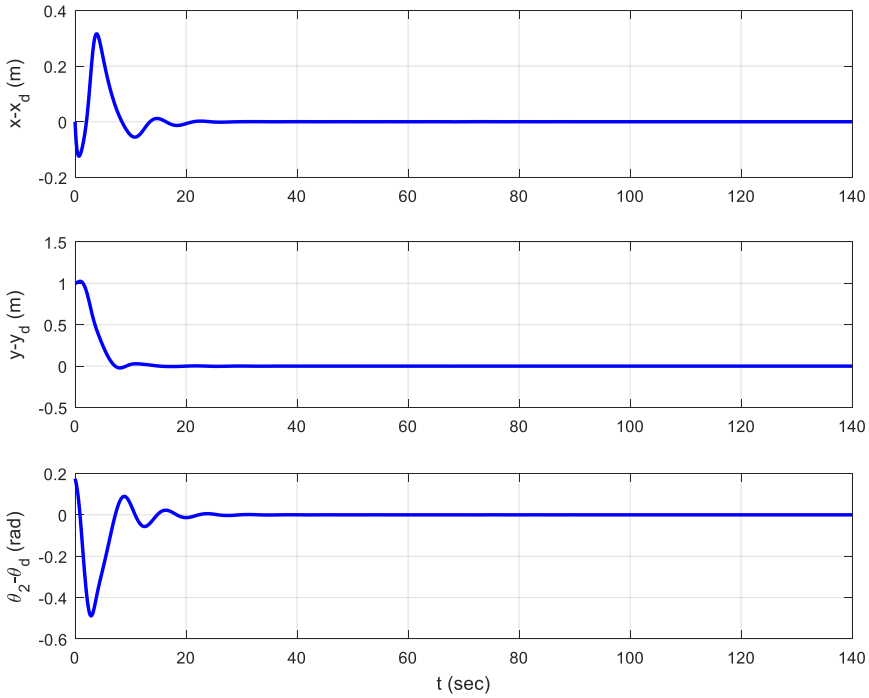

Figure 3.4: Tracking errors: $x - x_d$, $y - y_d$ and $\theta_2 - \theta_d$.

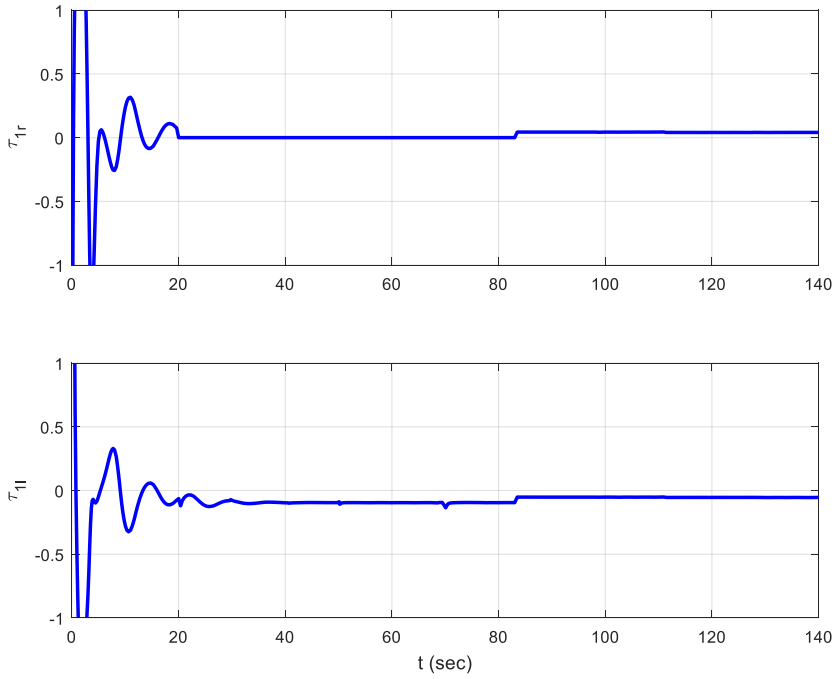

Figure 3.5: Control torques generated by the robot 1.

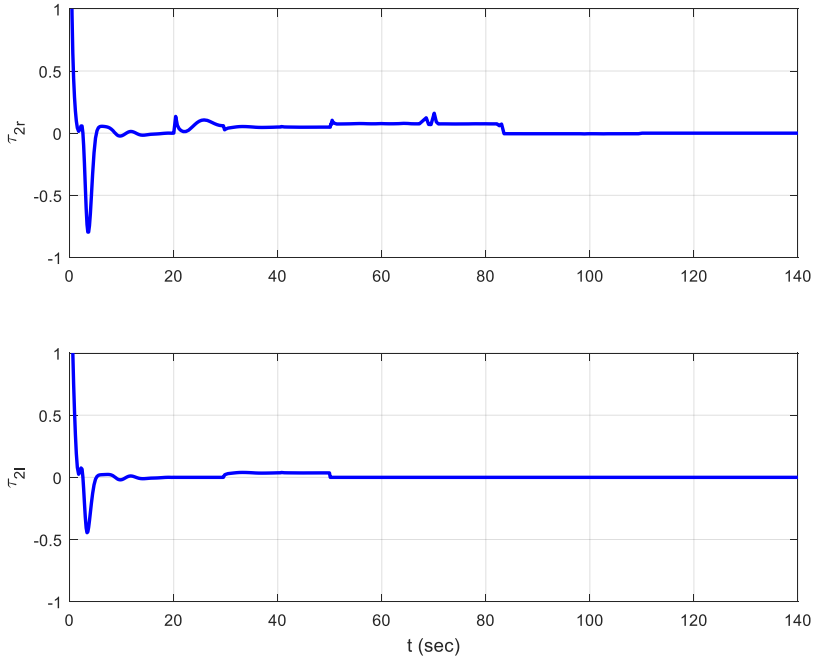

Figure 3.6: Control torques generated by the robot 2.

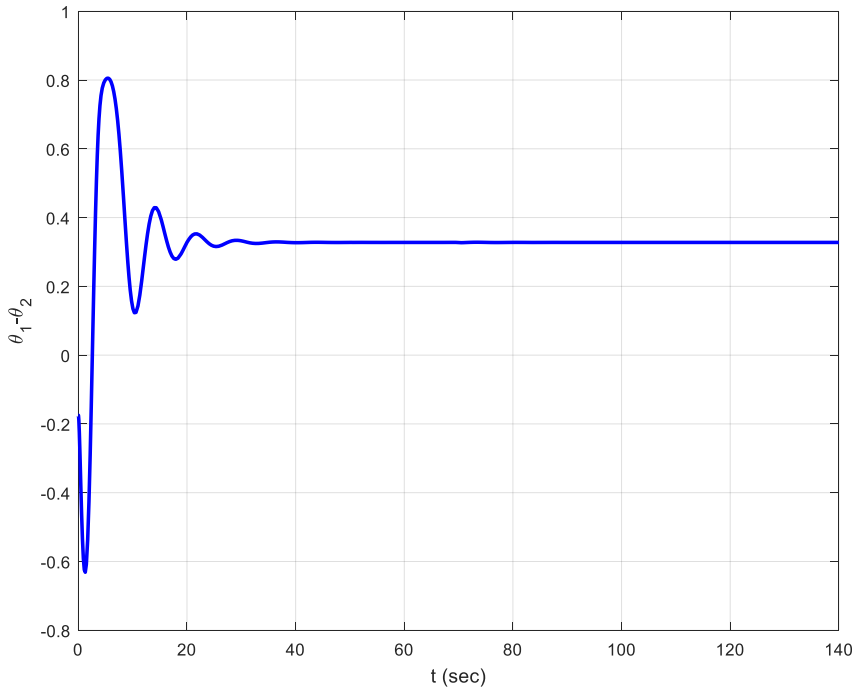

Figure 3.7: Orientation error between two robots.

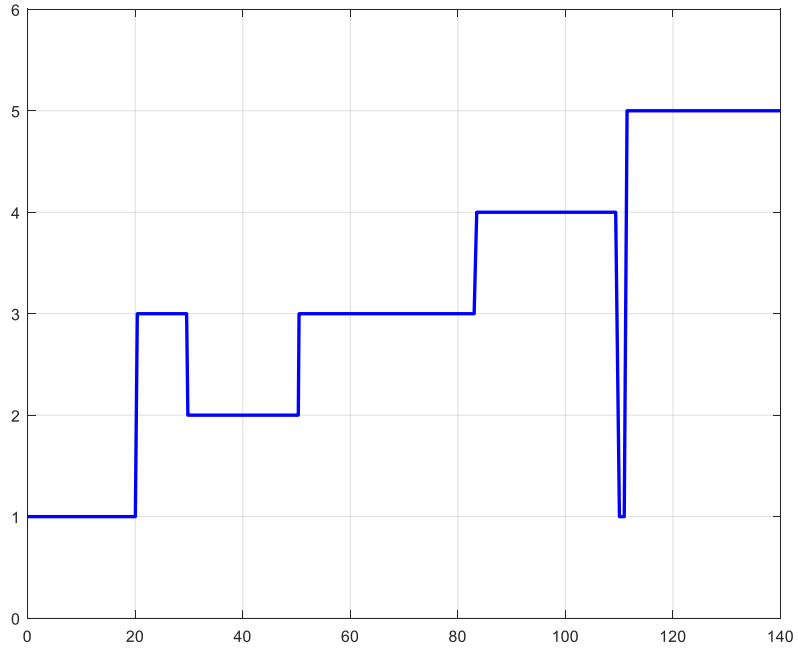

Fig. 3.8: Control switching index.

3.3 Actuator FTC compensation for the case of three-linked robots

In this section, a control solution which is well-suited for more than two-linked 2WD mobile robots ($n > 2$) is presented, where n is the number of robots. In the previous section, considering the case of two-linked robots it was found a diffeomorphism relating the kinematic and dynamic controllers. However, it is very difficult to find in the same way a diffeomorphism for more than two-linked 2WD mobile robots. Furthermore, even if we can find this diffeomorphism, the control objective will be always designed only for the last robot of the 2WD multi-linked mobile robots. In order to overcome these limitations, we are going to present in the sequel a solution that is based on the chained form representation of the kinematic model.

3.3.1 Multiple model actuator FTC compensation for three-linked robots

In this subsection, in order to achieve the desired control objective, we propose a compensation control scheme, consisting of a kinematic control and a dynamic control.

The provided solution is based on the transformation of the kinematic model of a multi-linked 2WD mobile robots system into the chained form [85] that was presented in chapter 2. Then, the recursive technique is used to derive the kinematic control law. Based on this, multiple dynamic controllers are designed considering all possible failure cases. From these dynamic controllers, an appropriate one is selected to generate the applied control signal by the control switching mechanism using multiple reconstruction dynamic signals to ensure desired system performance.

3.3.1.1 Problem formulation

The kinematic model for a three-linked 2WD mobile robots were derived in Section 2.4 (see chapter 2), and is recalled below

$$\dot{x} = v_3 \cos\theta_3 \tag{3.49}$$

$$\dot{y} = v_3 \sin\theta_3 \tag{3.50}$$

$$\dot{\theta}_3 = \frac{v_3}{d_2}\tan(\theta_2 - \theta_3) \tag{3.51}$$

$$\dot{\theta}_2 = v_3\, tan(\theta_{1d} - \theta_2)/\,(d_1 cos(\theta_2 - \theta_3)) \tag{3.52}$$

$$\dot{\theta}_1 = \omega_1 \tag{3.53}$$

Fault-tolerant control objective 2

The fault-tolerant control objective 2 is to develop an actuator failure compensation scheme for three-linked 2WD mobile robots to asymptotically track a reference motion, despite the presence of some actuator failures. In other words, the control objective is to design a control signal $u(t)$ to guarantee that the closed-loop system signals are bounded and $\lim_{t\to\infty}(x(t)-x_d(t))=0$, $\lim_{t\to\infty}(y(t)-y_d(t))=0$, $\lim_{t\to\infty}(\theta_3(t)-\theta_{3d}(t))=0$, $\lim_{t\to\infty}(\theta_2(t)-\theta_{2d}(t))=0$, $\lim_{t\to\infty}(\theta_1(t)-\theta_{1d}(t))=0$, in the presence of uncertain $\sigma(t)$, where x_d, y_d, θ_{3d}, θ_{2d}, θ_{1d}, are reference trajectories.

Remark 3.5*: Notice that in the fault-tolerant control objective 1 presented in subsection 3.2.1.2, only parameters of the rear robot were considered in the control objective. The fault-tolerant control objective 2 presented here considers the control of each robot of the multi-linked system.*

3.3.1.2 Trajectory generation for three-linked 2WD mobile robots

In this subsection, firstly, a feasible trajectories generation method for three-linked 2WD mobile robots is proposed. Secondly, the tracking ability of the trajectories is ensured while guaranteeing the controllability of the system and avoiding the system singularities.

Feasible desired trajectories are given in terms of the Cartesian positions of the point P_3 (the middle point of robot 3 rear wheels) and are denoted as x_d and y_d. Consequently, the state space vector q and system kinematic input vector η can be expressed algebraically as a function of the flat outputs and their derivatives up to a certain order [37]. A desired output trajectory is feasible if and only if it is a solution of the kinematic model [38].

Let us consider a given desired trajectory x_d, y_d. This trajectory is feasible if it is possible to find v_{3d}, θ_{3d}, θ_{2d}, θ_{1d} and ω_{1d} such that the following system is fulfilled.

$$\dot{x}_d = v_{3d}\cos\theta_{3d} \tag{3.54}$$

$$\dot{y}_d = v_{3d}\sin\theta_{3d} \tag{3.55}$$

$$\dot{\theta}_{3d} = \frac{v_{3d}}{d_2}\tan(\theta_{2d}-\theta_{3d}), \tag{3.56}$$

$$\dot{\theta}_{2d} = v_{3d}\tan(\theta_{1d}-\theta_{2d})/\left(d_1\cos(\theta_{2d}-\theta_{3d})\right) \tag{3.57}$$

$$\dot{\theta}_{1d} = \omega_{1d} \tag{3.58}$$

Necessary conditions for (x_d, y_d) to be a feasible trajectory are $(\theta_{2d} - \theta_{3d}) \neq (\pi/2)$, and $(\theta_{1d} - \theta_{2d}) \neq (\pi/2)$. Moreover, if x_d or y_d are not constant, υ_{3d} must be different from 0.

From the equations (3.54) and (3.55), it can be concluded that:

$$\theta_{3d} = \text{ATAN2}\{\dot{y}_d, \dot{x}_d\} \tag{3.59}$$

Using the equation (3.56), we can get:

$$\theta_{2d} = \theta_{3d} + \text{atan}(d_2\dot{\theta}_{3d}/\upsilon_{3d}) \tag{3.60}$$

Using the equation (3.57), we can get:

$$\theta_{1d} = \theta_{2d} + atan((d_1\dot{\theta}_{2d}\, cos(\theta_{2d} - \theta_{3d}))/\upsilon_{3d}) \tag{3.61}$$

Also, equations (3.54) and (3.55) yield:

$$\upsilon_{3d} = \sqrt{\dot{x}_d^2 + \dot{y}_d^2} \tag{3.62}$$

Differentiating equations (3.54) and (3.55), and combining the results so as to eliminate $\dot{\upsilon}_{3d}$, we obtain:

$$\dot{\theta}_{3d} = \frac{(\ddot{y}_d\dot{x}_d - \ddot{x}_d\dot{y}_d)}{\upsilon_{3d}^2} \tag{3.63}$$

Putting equations (3.59), (3.63) into equation (3.60), we obtain:

$$\theta_{2d} = \text{ATAN2}\{\dot{y}_d, \dot{x}_d\}\text{atan}\left(\frac{d_2(\ddot{y}_d\dot{x}_d - \ddot{x}_d\dot{y}_d)}{\upsilon_{3d}^3}\right) \tag{3.64}$$

Differentiating equation (3.64), we obtain:

$$\dot{\theta}_{2d} = \dot{\theta}_{3d} + \frac{d_2\upsilon_{3d}(\dddot{y}_d\dot{x}_d - \dddot{x}_d\dot{y}_d)\upsilon_{3d}^2 - 3(\ddot{y}_d\dot{x}_d - \ddot{x}_d\dot{y}_d)(\dot{x}_d\ddot{x}_d + \dot{y}_d\ddot{y}_d)}{\upsilon_{3d}^6 + d_2^2(\ddot{y}_d\dot{x}_d - \ddot{x}_d\dot{y}_d)^2} \tag{3.65}$$

Differentiating equation (3.61), we obtain:

$$\dot{\theta}_{1d} = \dot{\theta}_{2d} + \frac{d}{dt}\left[\frac{d_1\dot{\theta}_{2d}cos(\theta_{2d} - \theta_{3d})}{\upsilon_{3d}}\right] \tag{3.66}$$

Equations (3.59)-(3.66) express the constraints that the desired states and reference velocities must fulfill to make the desired trajectory a feasible trajectory.

Assumption 3.2*: The reference trajectory $x_d, y_d, \theta_{3d}, \theta_{2d}, \theta_{1d}$ and reference velocity and their derivatives are continuous and uniformly bounded. Moreover, reference velocity does not tend to zero as $t \longrightarrow \infty$.*

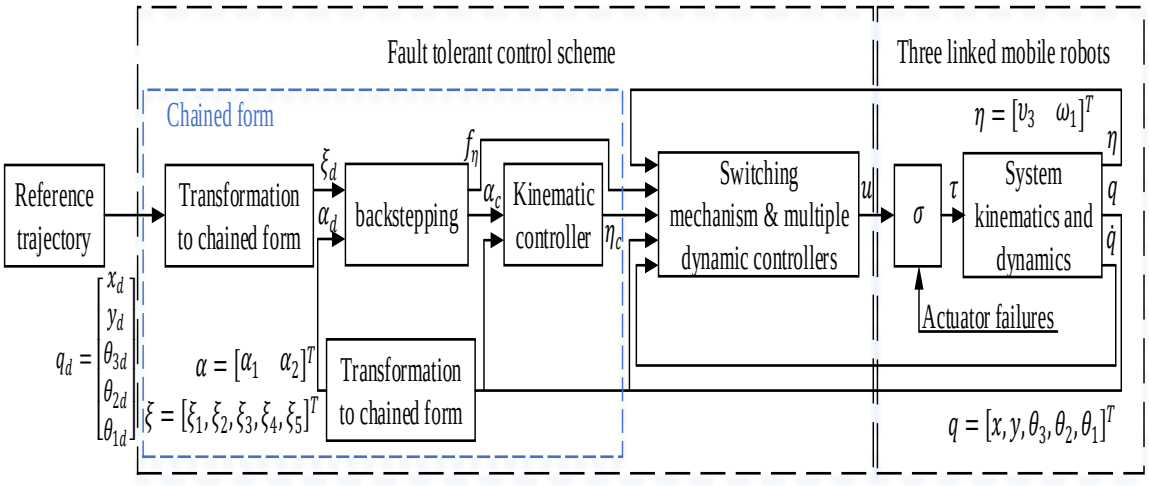

Figure 3.9: Block diagram of the fault compensation control scheme with coordinate and feedback transformations, for the case of three-linked mobile robots.

Design issues: The structure of the proposed actuator fault compensation scheme is shown in Fig. 3.9. To design such a fault tolerant control scheme, the following steps need to be solved:

1. The use of the chained form state-space permits to design a recursive technique, which allows controlling each variable of the state of the system, in order to derive the virtual kinematic control signal α_c. This is not possible using the same method used for the two-linked mobile robots to find the diffeomorphism.
2. The desired kinematic control law η_c is designed such that the desired control performance can be ensured.
3. Multiple dynamic controllers are designed, each of which is designed using one possible failure pattern matrix. If the failure pattern which is used for the controller design is consistent with the actual one, then the applied control signal can ensure $\eta \longrightarrow \eta_c$ and the desired system performance.
4. Finally, the control switching mechanism is used to select the appropriate controller in order to generate the applied control signal u.

This scheme exhibits the following differences with the preceding control scheme for two-linked 2WD mobile robots in Fig. 3.1:

1) The canonical chained form model is used as introduced in chapter 2.
2) backstepping technique is used to derive the kinematic control law.

3.3.1.3 Fault-tolerant control design

In this subsection, a multiple model actuator fault compensation scheme is developed for three-linked robots, as shown in Fig. 3.9.

3.3.1.3.1 Kinematic controller design

In order to derive the kinematic control, we use a recursive technique which appears to be an extension of the popular integrator backstepping idea to derive the kinematic control law for trajectory tracking.

Let us consider the kinematic model of the three-linked 2WD mobile robots. Applying the algorithm proposed in [40], using the change of coordinates in Section 2.5.2, the kinematic model of the system has the following chained form

$$\begin{aligned} \dot{\xi}_1 &= \alpha_1, \\ \dot{\xi}_2 &= \alpha_2, \\ \dot{\xi}_3 &= \xi_2 \alpha_1, \\ \dot{\xi}_4 &= \xi_3 \alpha_1, \\ \dot{\xi}_5 &= \xi_4 \alpha_1 \end{aligned} \tag{3.67}$$

where $\xi = (\xi_1, \xi_2, \dots, \xi_5)$ is the state and α_1, α_2 are the two control inputs.

The desired trajectory $\xi_d = (\xi_{1d}, \xi_{2d}, \dots, \xi_{5d})$ is generated after the change of coordinates, by applying

$$\begin{aligned} \dot{\xi}_{1d} &= \alpha_{1d}, \\ \dot{\xi}_{2d} &= \alpha_{2d}, \\ \dot{\xi}_{3d} &= \xi_{2d} \alpha_{1d}, \\ \dot{\xi}_{4d} &= \xi_{3d} \alpha_{1d}, \\ \dot{\xi}_{5d} &= \xi_{4d} \alpha_{1d} \end{aligned} \tag{3.68}$$

where $\alpha_d = (\alpha_{1d}, \alpha_{2d})$ are the reference control inputs.

Denote the tracking error as $\xi_e = \xi - \xi_d$. It is directly established that the ξ_e dynamics errors satisfy the following differential equations

$$\dot{\xi}_{1e} = \alpha_1 - \alpha_{1d}$$
$$\dot{\xi}_{2e} = \alpha_2 - \alpha_{2d}$$
$$\dot{\xi}_{3e} = \xi_{2e}\alpha_{1d} + \xi_2(\alpha_1 - \alpha_{1d})$$
$$\dot{\xi}_{4e} = \xi_{3e}\alpha_{1d} + \xi_3(\alpha_1 - \alpha_{1d})$$
$$\dot{\xi}_{5e} = \xi_{4e}\alpha_{1d} + \xi_4(\alpha_1 - \alpha_{1d}) \quad (3.69)$$

Our objective is to find a bounded smooth kinematic control law such that the system in equation (3.67) tracks the smooth reference desired trajectory in equation (3.68). Toward this end, the following tracking control problems is addressed.

Definition 3.1*: The tracking control problem will be said to be semi globally solvable [120] for system (3.67) if, given any compact set* $S \in \mathbb{R}^5$ *containing the origin, we can design appropriate continuous time-varying state feedback controllers of the form* $\alpha_1 = \mu_1(\xi)$ *and* $\alpha_2 = \mu_2(\xi)$*, such that for any initial tracking error* $\xi_e(0) = \xi(0) - \xi_d(0)$ *in S, all the signals of the closed loop system (3.69),* α_1 *and* α_2 *are uniformly bounded over* $[0, \infty)$*. Furthermore*

$$\lim_{t\to\infty}|\xi(t) - \xi_d(t)| = 0 \quad (3.70)$$

Kinematic control law*:*

The main purpose of this subsection is to design the kinematic control laws α_1 and α_2 for trajectory tracking of the considered system.

First, an error dynamic is considered for the tracking problem, second, a change of coordinates is proposed and system (3.69) is rearranged into a triangular form so that the integrator backstepping can be applied.

Denote $\tilde{\xi}_d = (\xi_{2d}, \cdots, \xi_{4d})$ and let $\Phi_1(.;\tilde{\xi}_d)$: $\mathbb{R}^5 \to \mathbb{R}^5$ be the mapping defined by

$$z_1 = \xi_{5e} - [\xi_{4e} + \xi_{4d}]\xi_{1e}$$
$$z_2 = \xi_{4e} - [\xi_{3e} + \xi_{3d}]\xi_{1e}$$
$$z_3 = \xi_{3e} - [\xi_{2e} + \xi_{2d}]\xi_{1e}$$
$$z_4 = \xi_{2e}$$
$$z_5 = \xi_{1e} \quad (3.71)$$

As it can be checked, $\Phi_1(.;\tilde{\xi}_d)$ is a global diffeomorphism for each $\tilde{\xi}_d \in \mathbb{R}^3$ [120] and its inverse $\Phi_1^{-1}(z;\tilde{\xi}_d)$ is given by

$$\xi_{1e} = z_5$$

$$\xi_{2e} = z_4$$

$$\xi_{3e} = z_3 + [z_4 + \xi_{2d}]z_5$$

$$\xi_{4e} = z_2 + [z_{3+}z_4z_5 + \xi_{2d}z_5 + \xi_{3d}]z_5$$

$$\xi_{5e} = z_1 + [z_2+(z_3 + z_4z_5 + \xi_{2d}z_5 + \xi_{3d})z_5 + \xi_{4d}]z_5 \quad (3.72)$$

The tracking error dynamics is transformed into the following system

$$\dot{z}_1 = \alpha_{1d}z_2 - \xi_3(\alpha_1 - \alpha_{1d})z_5$$

$$\dot{z}_2 = \alpha_{1d}z_3 - \xi_2(\alpha_1 - \alpha_{1d})z_5$$

$$\dot{z}_3 = \alpha_{1d}z_4 - \alpha_2 z_5$$

$$\dot{z}_4 = \alpha_2 - \alpha_{2d}$$

$$\dot{z}_5 = \alpha_1 - \alpha_{1d} \quad (3.73)$$

The backstepping algorithm is inspired by the one described in [120].

Let us formulate the backstepping design scheme for the system (3.73). In this aim, we need to consider an intermediate virtual control functions $\beta_i (1 \leq i \leq 3)$, which would make the subsystem stabilizable.

Step 1*:* Consider the z_1 subsystem of system (3.73)

$$\dot{z}_1 = \alpha_{1d}z_2 - \xi_3(\alpha_1 - \alpha_{1d})z_5 \quad (3.74)$$

Suppose the variable z_2 is a virtual control input and the variables α_{1d} and z_5 are time-varying functions.

Set $\bar{z}_1 = z_1$. Along the solutions of system (3.73), the time derivatives of the positive definite and proper functions

$$V_1(\bar{z}_1) = \frac{1}{2}\bar{z}_1^2 \quad (3.75)$$

satisfies

$$\dot{V}_1 = \alpha_{1d}\bar{z}_1 z_2 - \bar{z}_1\xi_3(\alpha_1 - \alpha_{1d})z_5 \quad (3.76)$$

Let us choose $\beta_1(z_1)$ as follows

$$\beta_1(z_1)=z_2 + \bar{z}_2 \quad (3.77)$$

with $\beta_1(z_1) = 0$, is a stabilizing function for the system (3.74) whenever $z_5 = 0$. Equation (3.76) becomes

$$\dot{V}_1 = \alpha_{1d}\bar{z}_1\bar{z}_2 - \bar{z}_1\xi_3(\alpha_1 - \alpha_{1d})z_5 \tag{3.78}$$

In the next steps, we apply the same procedure as step 1 recursively for the subsystem $(z_1, \dots, z_5)$ of system (3.73). The outputs of these steps are the functions (β_2, β_3), which are necessary for the computation of α_1 and α_2 in the steps 4 and 5.

Step 2*:* We apply the same procedure as step 1 for the (z_1, z_2) subsystem of system (3.73) with z_3 viewed as a virtual control input. To achieve this goal, let us choose the function

$$V_2(\bar{z}_1, \bar{z}_2) = V_1(\bar{z}_1) + \frac{1}{2}\bar{z}_2^2 \tag{3.79}$$

Differentiating the function V_2 along the solutions of system (3.73) yields

$$\dot{V}_2 = -\left[\bar{z}_1\xi_3 + \bar{z}_2\xi_2 - \bar{z}_2\frac{\partial\beta_1}{\partial z_1}\xi_3\right](\alpha_1 - \alpha_{1d})z_5 + \alpha_{1d}\bar{z}_2\left[\bar{z}_1 + z_3 - \frac{\partial\beta_1}{\partial z_1}z_2\right] \tag{3.80}$$

Let us choose

$$\beta_2(z_1, z_2) = -\bar{z}_1 + \frac{\partial\beta_1}{\partial z_1}z_2 \tag{3.81}$$

$$\bar{z}_3 = z_3 - \beta_2(z_1, z_2) \tag{3.82}$$

It follows that

$$\dot{V}_2 = -\left[\bar{z}_1\xi_3 + \bar{z}_2\xi_2 - \bar{z}_2\frac{\partial\beta_1}{\partial z_1}\xi_3\right](\alpha_1 - \alpha_{1d})z_5 + \alpha_{1d}\bar{z}_2\bar{z}_3 \tag{3.83}$$

Step 3*:* We consider now the (z_1, z_2, z_3) subsystem of system (3.73), the time derivative of the following function

$$V_3(\bar{z}_1, \bar{z}_2, \bar{z}_3) = V_2(\bar{z}_1, \bar{z}_2) + \frac{1}{2}\bar{z}_3^2 \tag{3.84}$$

satisfies

$$\dot{V}_3 = -\left[\bar{z}_1\xi_3 + \bar{z}_2\xi_2 - \left(\bar{z}_2\frac{\partial\beta_1}{\partial z_1}\xi_3 + \bar{z}_3\frac{\partial\beta_2}{\partial z_1}\xi_3 + \bar{z}_3\frac{\partial\beta_2}{\partial z_2}\xi_2\right)\right]$$

$$.(\alpha_1 - \alpha_{1d})z_5 - \bar{z}_3 z_5\alpha_2 + \alpha_{1d}\bar{z}_3\left[\bar{z}_2 + z_4 - \left(\frac{\partial\beta_2}{\partial z_1}z_2 + \frac{\partial\beta_2}{\partial z_2}z_3\right)\right] \tag{3.85}$$

Let us choose

$$\beta_3(z_1, z_2, z_3) = -\bar{z}_2 + \frac{\partial \beta_2}{\partial z_1} z_2 + \frac{\partial \beta_2}{\partial z_2} z_3 \tag{3.86}$$

$$\bar{z}_4 = z_4 - \beta_3(z_1, z_2, z_3) \tag{3.87}$$

It follows that

$$\dot{V}_3 = \bar{z}_4 \bar{z}_3 \alpha_{1d} - \bar{z}_3 z_5 \alpha_2 - \left[\bar{z}_1 \xi_3 + \bar{z}_2 \xi_2 - \left(\bar{z}_2 \frac{\partial \beta_1}{\partial z_1} \xi_3 + \bar{z}_3 \frac{\partial \beta_2}{\partial z_1} \xi_3 + \bar{z}_3 \frac{\partial \beta_2}{\partial z_2} \xi_2\right)\right](\alpha_1 - \alpha_{1d}) z_5 \tag{3.88}$$

Step 4*:* Let us consider the (z_1, z_2, z_3, z_4) subsystem of (3.73) and let us choose the function

$$V_4(\bar{z}_1, \bar{z}_2, \bar{z}_3, \bar{z}_4) = V_3(\bar{z}_1, \bar{z}_2, \bar{z}_3) + \frac{1}{2}\bar{z}_4^2 = \sum_{i=1}^{4} \frac{1}{2}\bar{z}_i^2 \tag{3.89}$$

According to (3.73) and (3.88), the time derivative of V_4 along the solutions of (3.73) satisfies

$$\begin{aligned} \dot{V}_4 = {} & \bar{z}_4 \left[\alpha_{1d} \bar{z}_3 + \alpha_2 - \alpha_{2d} - \left(\frac{\partial \beta_3}{\partial z_1} \alpha_{1d} z_2 + \frac{\partial \beta_3}{\partial z_2} \alpha_{1d} z_3 + \frac{\partial \beta_3}{\partial z_3} \alpha_{1d} z_4\right)\right] \\ & - \left[\bar{z}_3 - \bar{z}_4 \frac{\partial \beta_3}{\partial z_3}\right] \alpha_2 z_5 - \left[\bar{z}_1 \xi_3 + \bar{z}_2 \xi_2 - \left(\bar{z}_2 \frac{\partial \beta_1}{\partial z_1} \xi_3 + \bar{z}_3 \frac{\partial \beta_2}{\partial z_1} \xi_3 + \bar{z}_3 \frac{\partial \beta_2}{\partial z_2} \xi_2\right)\right. \\ & \left. - \left(\bar{z}_4 \frac{\partial \beta_3}{\partial z_1} \xi_3 + \bar{z}_4 \frac{\partial \beta_3}{\partial z_2} \xi_2\right)\right](\alpha_1 - \alpha_{1d}) z_5 \end{aligned} \tag{3.90}$$

We can obtain α_2 by applying the following control law

$$\alpha_2 = \alpha_{2d} - c_4 \bar{z}_4 - \alpha_{1d} \bar{z}_3 + \frac{\partial \beta_3}{\partial z_1} \alpha_{1d} z_2 + \frac{\partial \beta_3}{\partial z_2} \alpha_{1d} z_3 + \frac{\partial \beta_3}{\partial z_3} \alpha_{1d} z_4 \tag{3.91}$$

where $c_4 > 0$ is chosen to be constant, we obtain:

$$\dot{V}_4 = -c_4 \bar{z}_4^2 - \left(\bar{z}_3 - \bar{z}_4 \frac{\partial \beta_3}{\partial z_3}\right) \alpha_2 z_5 - \Delta_1 (\alpha_1 - \alpha_{1d}) z_5 \tag{3.92}$$

where $\Delta_1(z_1, z_2, z_3, z_4, \tilde{\xi}_d)$ is a smooth function given by

$$\Delta_1 = \left[\bar{z}_1 \xi_3 + \bar{z}_2 \xi_2 - \left(\bar{z}_2 \frac{\partial \beta_1}{\partial z_1} \xi_3 + \bar{z}_3 \frac{\partial \beta_2}{\partial z_1} \xi_3 + \bar{z}_3 \frac{\partial \beta_2}{\partial z_2} \xi_2\right) - \left(\bar{z}_4 \frac{\partial \beta_3}{\partial z_1} \xi_3 + \bar{z}_4 \frac{\partial \beta_3}{\partial z_2} \xi_2\right)\right] \tag{3.93}$$

Step 5*:* In the final step, the objective is to design α_1 such that $\bar{z}_1, \bar{z}_2, \bar{z}_3, \bar{z}_4$ and z_5 converge to zero. Toward this end, consider the positive definite and proper function V_5 which serves as Lyapunov function candidate for the complete system (3.73)

$$V_5(\bar{z}) = \frac{1}{2}\bar{z}_1^2 + \frac{1}{2}\bar{z}_2^2 + \frac{1}{2}\bar{z}_3^2 + \frac{1}{2}\bar{z}_4^2 + \frac{\kappa}{2}z_5^2 \tag{3.94}$$

where $\kappa > 0$ is a design parameter.

Differentiating V_5 along the solutions of (3.73) gives

$$\dot{V}_5 = -c_4\bar{z}_4^2 + z_5(\kappa - \Delta_1)\left[(\alpha_1 - \alpha_{1d}) - (\bar{z}_3 - \bar{z}_4\frac{\partial\beta_3}{\partial z_3})\alpha_2\right] \tag{3.95}$$

By choosing the following control law

$$\alpha_1 = \alpha_{1d} + (\kappa - \Delta_1)^{-1}\left[-c_5 z_5 + (\bar{z}_3 - \bar{z}_4\frac{\partial\beta_3}{\partial z_3})\alpha_2\right] \tag{3.96}$$

with $c_5 > 0$, is a chosen constant, we obtain

$$\dot{V}_5(\bar{z}) = -c_4\bar{z}_4^2 - c_5 z_5^2 \tag{3.97}$$

Thus $\dot{V}_5$ is negative which proves the stability of the controlled system (3.73). The described five steps permit us to find the kinematic control laws α_1 and α_2 which produce input signals (or set points) signals for the dynamic controller in the next section.

Preliminary analysis

In this section, we prove the tracking control performance for system (3.67).

Proposition 3.1*:* Assume that $\xi_{id}(2 \le i \le 4)$, α_d, and $\dot{\alpha}_{1d}$ are bounded over $[0, \infty)$. Then, the tracking control problem is semi globally solvable for system (3.67). This means that using coordinates transformation and applying the design procedure described in the above section to system (3.73), given any compact neighborhood S of the origin in $\mathbb{R}^5$, we can find a sufficiently large $\kappa > 0$ so that, for any initial conditions $\xi_e(0)$ in S, all the solutions of the closed loop system, (3.69), (3.91), and (3.96) are uniformly bounded. Furthermore, if $\alpha_{1d}(t)$ does not converge to zero, we have $\lim_{t\to+\infty}|\xi_e(t)| = 0$.

The idea of the proof proposition 3.1 may be found in paper [120].

As we mentioned before, the main purpose of this subsection is to design the kinematic control laws α_1 and α_2 in (3.91) and (3.96) for trajectory tracking of the considered system in (3.73).

From the transformation of parameters, we can obtain

$$\alpha = T_\alpha \eta \tag{3.98}$$

where

$T_{\alpha 11} = cos\,\theta_3$, $\qquad T_{\alpha 12} = 0$,

$$T_{\alpha 21} = \frac{1}{d_1 d_2} sec^4\theta_3 tan(\theta_1 - \theta_2) sec^4(\theta_2 - \theta_3)[\frac{1}{d_1} 3tan(\theta_2 - \theta_3) tan(\theta_1 - \theta_2) + sec^2(\theta_1 - \theta_2) + \frac{1}{d_2}(6tan\theta_3 sin(\theta_2 - \theta_3) - 2tan(\theta_2 - \theta_3) sin(\theta_2 - \theta_3) - sec(\theta_2 - \theta_3))],$$

$$T_{\alpha 22} = (1/d_1 d_2) sec^4\theta_3 sec^2(\theta_1 - \theta_2) sec^3(\theta_2 - \theta_3)$$

Define a virtual kinematic control signal

$$\alpha_c = T_\alpha \eta_c \tag{3.99}$$

and the velocity tracking error

$$\eta_e = \eta - \eta_c \tag{3.100}$$

Then we have

$$\alpha_e = \alpha - \alpha_c = T_\alpha \eta_e \tag{3.101}$$

Now, we design the virtual kinematic control law α_c as

$$\alpha_{2c} = \alpha_{2d} - c_4 \bar{z}_4 - \alpha_{1d} \bar{z}_3 + \frac{\partial \beta_3}{\partial z_1} \alpha_{1d} z_2 + \frac{\partial \beta_3}{\partial z_3} \alpha_{1d} z_3 + \frac{\partial \beta_3}{\partial z_3} \alpha_{1d} z_4 \tag{3.102}$$

$$\alpha_{1c} = \alpha_{1d} + (\kappa - \Delta_1)^{-1} \left[-c_5 z_5 + \left(\bar{z}_3 - \bar{z}_4 \frac{\partial \beta_3}{\partial z_3} \right) \alpha_{2c} \right] \tag{3.103}$$

where $c_4 > 0$ and $c_5 > 0$ are chosen to be constant.

From equation (3.99) the kinematic control law is

$$\boldsymbol{\eta_c = T_\alpha^{-1} \alpha_c} \tag{3.104}$$

Substituting (3.101), (3.102) and (3.103) into equation (3.97) yields

$$\dot{V}_5 = -c_4 \bar{z}_4^2 - c_5 z_5^2 + z_5 (k - \Delta_1) \alpha_{e1} + z_5 \left(\bar{z}_4 \frac{\partial \beta_3}{\partial z_3} - \bar{z}_3 \right) \alpha_{e2} \tag{3.105}$$

By letting the $f_\eta = \left[z_5(\kappa - \Delta_1), z_5 \left(\bar{z}_4 \frac{\partial \beta_3}{\partial z_3} - \bar{z}_3 \right) \right]^T$ we get

$$\dot{V}_5 = -c_4 \bar{z}_4^2 - c_5 z_5^2 + f_\eta^T T_\alpha \eta_e \tag{3.106}$$

It is clear that from this equation if $f_\eta^T T_\alpha \eta_e \to 0$, then $\dot{V}_5 \leq 0$, which means that the system is stable. To implement this and to ensure desired system performance, a dynamic controller will be designed in the next section.

3.3.1.3.2 Multiple dynamic controller design

Since the failures are uncertain it is difficult to ensure system stability and asymptotic tracking by using a single control law. To cover all possible failure patterns, we will design one specific control law for each failure pattern. Then, we will establish a control switching mechanism to select an appropriate control law to be the applied one.

Dynamic control laws

We are going to design the dynamic control law using the same control structure presented for the case of two-linked mobile robots. For three-linked mobile robots, the differences are in the dimensions of the matrices $\bar{M}_1$, $\bar{M}_2$, $\bar{C}$, and $\bar{B}$ and on the parameters related to the kinematic controller f_η, T_α, η_c.

Then, the dynamic control law is

$$\boldsymbol{u_{(k)} = \left(\bar{M}_1^{-1}\bar{B}\sigma_{(k)}\right)^{+}\left[-c_6\eta_e - T_\alpha^T f_\eta + \bar{M}_1^{-1}\bar{M}_2\eta + \bar{M}_1^{-1}\bar{C} + \dot{\eta}_c\right]} \quad (3.107)$$

for $k = 1, 2, \dots, N$, where $c_6 > 0$ is chosen to be constant, and $\left(\bar{M}_1^{-1}\bar{B}\sigma_{(k)}\right)^{+}$ is a generalized inverse matrix.

Performance analysis

The performance of the designed dynamic control laws is given as follows

Lemma 3.2*: If the applied control law matches with the actual failure pattern matrix, i.e., $\sigma = \sigma_{(a)}$ and $u = u_{(a)}$ for $a = 1, 2, \dots, N$, then the boundedness of all closed loop signals is ensured, and $\lim_{t\to\infty}(x(t) - x_d(t)) = 0$, $\lim_{t\to\infty}(y(t) - y_d(t)) = 0$, $\lim_{t\to\infty}(\theta_3(t) - \theta_{3d}(t)) = 0$, $\lim_{t\to\infty}(\theta_2(t) - \theta_{2d}(t)) = 0$, $\lim_{t\to\infty}(\theta_1(t) - \theta_{1d}(t)) = 0$ and $\lim_{t\to\infty}(\eta(t) - \eta_c(t)) = 0$.*

Proof*:* Consider $\sigma = \sigma_{(a)}$ and $u = u_{(a)}$ and choose the global Lyapunov function as follows

$$V_{6(a)} = V_5 + \frac{1}{2}\eta_e^T\eta_e \quad (3.108)$$

Deriving equation (3.108) and using (3.106) and (3.34) lead to

$$\dot{V}_{6(a)} = -c_4\bar{z}_4^2 - c_5 z_5^2 + {f_\eta}^T T_\alpha\eta_e + \eta_e^T[-\bar{M}^{-1}\bar{M}_2\,\eta - \bar{M}_1^{-1}\bar{C} + \bar{M}^{-1}\bar{B}\,\sigma u - \dot{\eta}_c] \quad (3.109)$$

Substituting the dynamic control law in (3.107) with $k = a$ in the equation (3.109), we have

$$\dot{V}_{6(a)} = -c_4\bar{z}_4^2 - c_5 z_5^2 - c_6\eta_e^T\eta_e \leq 0 \tag{3.110}$$

where $(z_1, \cdots, z_5)$ are used to derive the kinematic control law, η_e is the velocity tracking error.

The proof of equation (3.110) is as follows:

$z_1, z_2, z_3, z_4, z_5, \bar{z}_1, \bar{z}_2, \bar{z}_3, \bar{z}_4, \eta_e \in L^\infty$, and $\bar{z}_4, z_5, \eta_e \in L^2$. The definitions of L^∞ and L^2 can be found in [131]. It follows from equations (2.89), (2.90) and (2.91), that $cos\,\theta_3 \neq 0$, $cos(\theta_2 - \theta_3) \neq 0$ and $tan(\theta_1 - \theta_2) \in L^\infty$ which means $cos(\theta_1 - \theta_2) \neq 0$. Then from the equations (3.69), (3.73), and also from (3.99)-(3.104) and (3.107), we obtain the following: T_α is bounded and nonsingular, and $\alpha_c, \alpha_e, \alpha, \eta_c, \eta_e, \eta, \dot{z}_1, \dot{z}_2, \dot{z}_3, \dot{z}_4, \dot{z}_5, \dot{\bar{z}}_1, \dot{\bar{z}}_2, \dot{\bar{z}}_3, \dot{\bar{z}}_4, \dot{\alpha}_c, \dot{\eta}_c, u_{(k)}, \dot{\eta}, \dot{\eta}_e, \dot{\alpha}, \dot{\alpha}_e \in L^\infty$.

According to Barbalat's Lemma [131], it is concluded that all the closed loop system signals are bounded, and $\lim_{t\to\infty} \bar{z}_4 = 0$, $\lim_{t\to\infty} z_5 = 0$ and $\lim_{t\to\infty} \eta_e = 0$, which also implies $\lim_{t\to\infty} \alpha_e = 0$. With equation (3.101) and according to the proposition 1, we have $\lim_{t\to\infty} z_1 = 0$, $\lim_{t\to\infty} z_2 = 0$, $\lim_{t\to\infty} z_3 = 0$, $\lim_{t\to\infty} z_4 = 0$, $\lim_{t\to\infty} z_5 = 0$, $\lim_{t\to\infty} \bar{z}_1 = 0$, $\lim_{t\to\infty} \bar{z}_2 = 0$, $\lim_{t\to\infty} \bar{z}_3 = 0$, $\lim_{t\to\infty} \bar{z}_4 = 0$, and $|\alpha_{1d}| \geq 0$, then we can further obtain $\lim_{t\to\infty} \alpha_{2c} = \alpha_{2d}$ from equation (3.102), it follows that $\lim_{t\to\infty} \alpha_2 = \alpha_{2d}$, and also $\lim_{t\to\infty} \alpha_{1c} = \alpha_{1d}$ and from equation (3.103), it follows that $\lim_{t\to\infty} \alpha_1 = \alpha_{1d}$.

Finally, all the closed loop system signals are uniformly bounded, furthermore $\lim_{t\to\infty} z_i(t) = 0$, $(i = 1, \ldots 5)$ and $\lim_{t\to\infty} \xi_{ie}(t) = 0$, $(i = 1, \ldots 5)$ and $\lim_{t\to\infty} (\eta(t) - \eta_c(t)) = 0$, which also means $\lim_{t\to\infty} (x(t) - x_d(t)) = 0$, $\lim_{t\to\infty} (y(t) - y_d(t)) = 0$, $\lim_{t\to\infty} (\theta_3(t) - \theta_{3d}(t)) = 0$, $\lim_{t\to\infty} (\theta_2(t) - \theta_{2d}(t)) = 0$, $\lim_{t\to\infty} (\theta_1(t) - \theta_{1d}(t)) = 0$.

This concludes the proof of *lemma 3.2*. ■

3.3.1.3.3 Control switching mechanism design

As the actual failure pattern matrix is unknown, the system equation for η will be reconstructed considering all the possible fault scenarios. Then, in the next steps, the fault failure pattern matrix that gives the best signal reconstruction will be selected in order to select the most suitable control signal. So, the steps presented in subsection 3.2.2.3 can be used.

3.3.1.3.4 Overall system performance analysis

Theorem 3.2*: The developed multiple-model actuator failure compensation control scheme, constituted by the kinematic control law in (3.102) and (3.103), multiple dynamic control laws in (3.107) and the control switching mechanism implemented by (3.47) and (3.48) with multiple reconstructed signals in (3.42) and multiple cost functions in (3.46), applied to three-linked 2WD mobile robots, guarantees that all closed-loop signals are bounded and* $\lim_{t\to\infty}(x(t)-x_d(t))=0$, $\lim_{t\to\infty}(y(t)-y_d(t))=0$, $\lim_{t\to\infty}(\theta_3(t)-\theta_{3d}(t))=0$, $\lim_{t\to\infty}(\theta_2(t)-\theta_{2d}(t))=0$, $\lim_{t\to\infty}(\theta_1(t)-\theta_{1d}(t))=0$, *despite the presence of actuator failures that are uncertain in time instants and patterns.*

Proof*:* Consider $\sigma=\sigma_{(a)}$ From (3.44) and (3.46), we have $J_{(a)}=0$ for the matched cost function. But for the unmatched functions $J_{(b)}, b=1,2,\dots N, b\neq a$, these zero properties may not hold due to (3.45). Since all cost functions are nonnegative, the matched cost function will generically become smaller than the other ones. Then, the matched control law $u_{(a)}$ will be selected as the applied one with (3.47) and (3.48). According to Lemma 3.2, the selected control law can guarantee that all closed-loop signals are bounded and $\lim_{t\to\infty}(x(t)-x_d(t))=0$, $\lim_{t\to\infty}(y(t)-y_d(t))=0$, $\lim_{t\to\infty}(\theta_3(t)-\theta_{3d}(t))=0$, $\lim_{t\to\infty}(\theta_2(t)-\theta_{2d}(t))=0$, $\lim_{t\to\infty}(\theta_1(t)-\theta_{1d}(t))=0$, despite the presence of actuator failures. This is the generic (generally true) matched case. On the other hand, if the unmatched control law $u_{(b)}, b\neq a$ is selected as the applied one meaning $J_{(b)}(t)\leq J_{(a)}$, then there is a time interval $[T_1,T_2]$ such that $J_{(b)}(t)=0$ for $t\in[T_1,T_2]$, as $J_{(a)}=0$. From (3.45), $J_{(b)}(t)=0$ means $\bar{M}_1^{-1}\bar{B}\,\sigma_{(a)}u_{(a)}-\bar{M}_1^{-1}\bar{B}\,\sigma_{(b)}u_{(b)}=0$ for $t\in[T_1,T_2]$, together with $\bar{M}_1^{-1}\bar{B}\sigma_{(b)}u_{(b)}=\bar{M}_1^{-1}\bar{B}\sigma_{(a)}u_{(a)}=-c_6\eta_e-T_\alpha^T f_\eta+\bar{M}_1^{-1}\bar{M}_2\eta+\bar{M}_1^{-1}\bar{C}+\dot{\eta}_c$, it also means that: if $\sigma_{(a)}$ but $u_{(b)}$ is selected, then $u_{(b)}$ has the same control effectiveness as compared with the matched control law $u_{(a)}$.

This concludes the proof of *Theorem 3.2*. ■

3.3.1.4 Simulation studies

In this simulation studies, we assume that the three wheeled driven robots are the ones used in [34], then the physical parameters of the three robots are chosen as: $a_1=a_2=a_3=$

$0.3\ m$, $b_1 = b_2 = b_3 = 0.75\ m$, $r_1 = r_2 = r_3 = 0.15\ m$, $m_1 = m_2 = m_3 = 30\ kg$, $I_{m1} = I_{m2} = I_{m3} = 15.625\ kg \cdot m^2$. The length of the link between each two robots is assumed to be $d = 1\ m$. $x_d, y_d, \theta_{3d}, \theta_{2d}, \theta_{1d}, \upsilon_{3d}$ and ω_{1d}, are the reference trajectories with $x_d(0) = y_d(0) = \theta_{3d}(0) = \theta_{2d}(0) = \theta_{1d}(0) = 0$. In order to verify the fault compensation effectiveness of the developed multiple model scheme, the following fault cases are simulated

- No fault: $\sigma_{(1)} = \text{diag}\{1, 1, 1, 1, 1, 1\}$, $0 \leq \text{t} < 20\text{s}$;
- τ_{1r} fails: $\sigma_{(2)} = \text{diag}\{0, 1, 1, 1, 1, 1\}$, $20\text{s} \leq \text{t} < 40\text{s}$;
- τ_{2l}, τ_{3l} fail: $\sigma_{(3)} = \text{diag}\{1, 1, 1, 0, 1, 0\}$, $40\text{s} \leq \text{t} < 60\text{s}$;
- τ_{1l},τ_{2r}, τ_{3r} fail: $\sigma_{(4)} = \text{diag}\{1, 0, 0, 1, 0, 1\}$, $60\text{s} \leq \text{t} < 80\text{s}$;
- $\tau_{1l}, \tau_{2r}, \tau_{2l}, \tau_{3r}$ fail: $\sigma_{(5)} = \text{diag}\{1, 0, 0, 0, 0, 1\}$, $\text{t} \geq 80\text{s}$.

There are 5 failure patterns satisfying the actuation redundancy condition. Then we need 5 control laws in (3.107), reconstructed signals in (3.42) and cost functions in (3.46). The initial conditions are chosen as: $x(0) = y(0) = 0.5$, $\theta_3(0) = \theta_2(0) = \theta_1(0) = 30\ deg$, and the control gains are chosen as: $C_4 = C_5 = C_6 = 2$ and $\kappa = 5$.

Fig. 3.10, shows the positions of robots 1, 2, 3 and reference trajectory, and Fig. 3.11, shows the tracking errors of all the states. From them, we can see that the desired system stability and asymptotic tracking are ensured despite the presence of actuator failures.

Fig. 3.12, shows the control torques generated by the wheels in robot 1, robot 2, and robot 3 respectively, from which we can see that the actuator failures are consistent with the failure cases in simulation conditions.

Fig. 3.13, shows the control switching index, the sequence is 1→2→3→4→5. We can see that the control switching index matches with the actual failure pattern index, although there is some wrong switching at some short time intervals after the failure occurring time instants. This wrong control switching does not affect system stability and asymptotic tracking properties. For the short time interval after 20s, in which the control signal has a wrong switching to 3, this case is consistent with the unmatched case in the proof of *Theorem 3.2.*

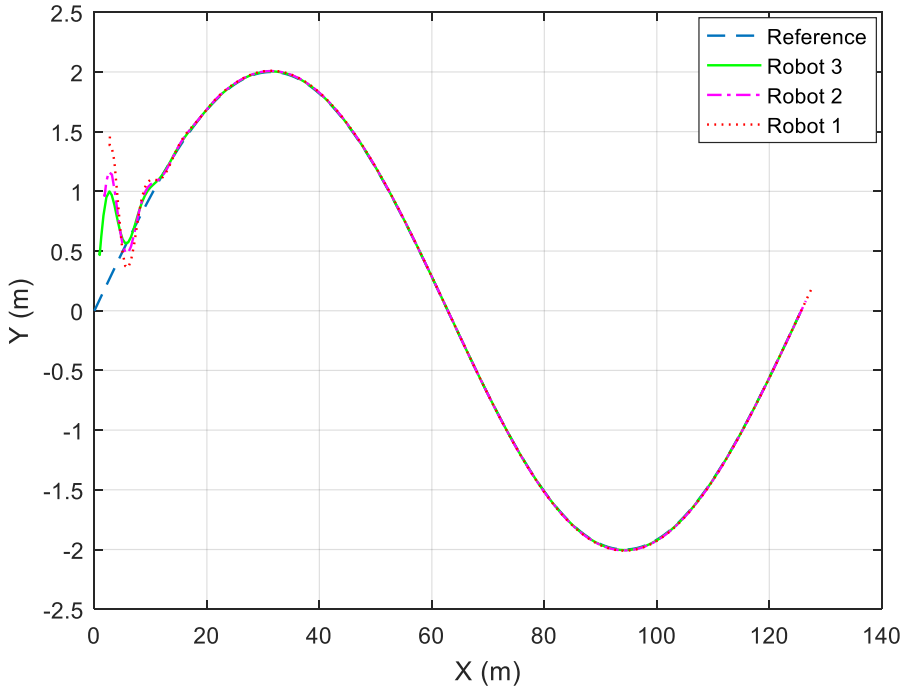

Figure 3.10: Robot trajectories in (x, y) plane.

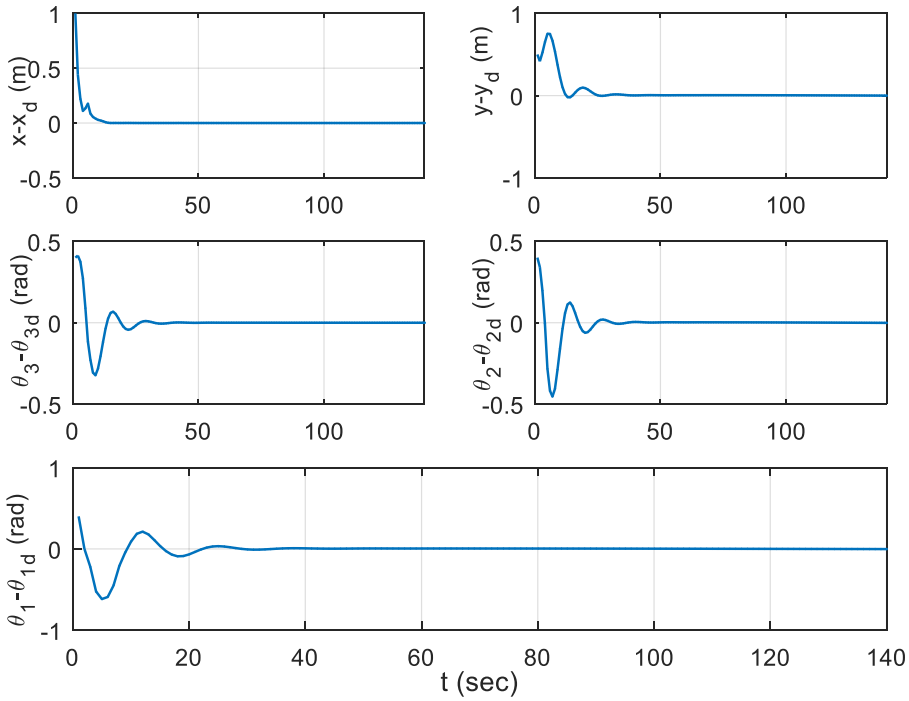

Figure 3.11: Tracking errors.

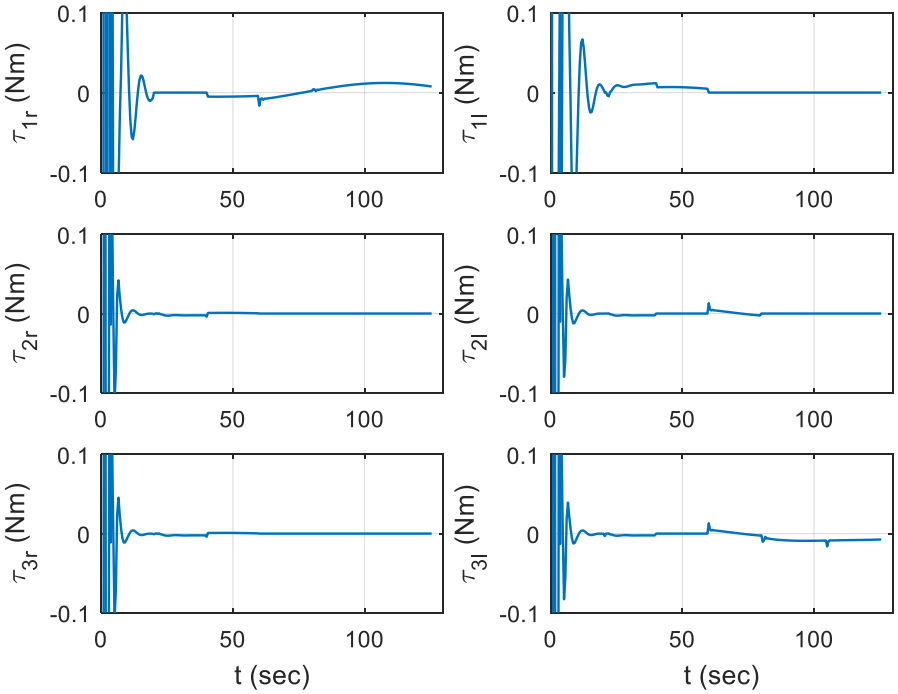

Figure 3.12: Control torques generated by robot 1, robot 2 and robot 3.

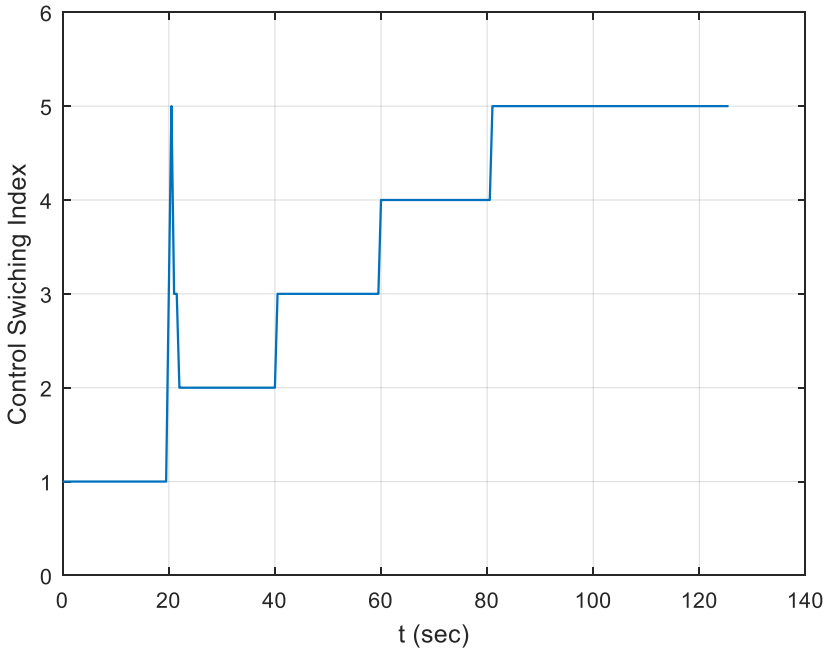

Figure 3.13: Control switching index.

3.3.2 Multi-design integration based adaptive FTC for three-linked robots

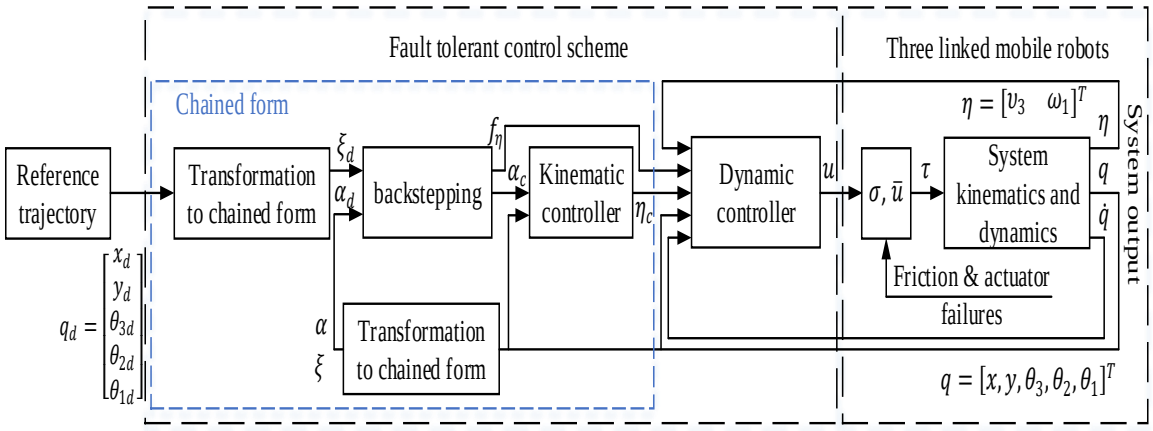

Figure 3.14: Block diagram of the fault compensation control scheme with coordinate and feedback transformations, for the case of three-linked robots.

In this subsection, a multi-design integration based adaptive actuator failure compensation scheme is developed for three linked 2WD mobile robots including a kinematic controller and a dynamic controller.

In order to design a FTC for three-linked 2WD mobile robots with friction and actuator faults, the same kinematic control law proposed in subsection 3.3.1 is used, but the dynamic control avoid the control switching mechanism used in the multiple dynamic controllers method. These frictions and actuator faults introduce additional uncertainties, especially the uncertainties of the control gain. To cover all possible actuator faults and to deal with uncertainties, a multi design integration based adaptive method is used. We employ adaptive laws to compensate uncertain friction coefficients and faults, in order to adapt online the single control law.

3.3.2.1 Problem formulation and fault-tolerant control objective 3

Our fault-tolerant control objective 3 is to design a feedback control signal $u(t)$ for the system despite the presence of actuator faults that satisfy redundancy condition, such that all the closed loop system signals are bounded and the system output $q(t)$ tracks a given reference output $q_d(t) = [x_d, y_d, \theta_{3d}, \theta_{2d}, \theta_{1d}]$, in the presence of actuator faults.

Design issues: The structure of the proposed actuator fault compensation scheme is shown in Fig. 3.14. To design such a fault tolerant control scheme, the following steps need to be solved:

1. The kinematic controller is the same as presented in Section 3.3.1.
2. For the dynamic controller, a multi-design integration based adaptive method is employed, to handle the problems of uncertain system friction and multiple actuator faults.

Remark 3.6*: The possible failure patterns of the three-linked 2WD mobile robots during the system operation, which satisfy the redundancy condition, are the fault free case and the multiple fault cases where up to any four actuators are simultaneously faulty.*

Key technical issues*:* The key feature of our actuator fault compensation scheme, as shown in Fig. 3.14, is the use of multiple control designs (which are capable of dealing with individual faults) and a control integration to form the composite control law. To handle system uncertainties and faults, both the control designs and their integration mechanism are adaptively updated based on the system performance errors, without using an explicit fault diagnosis algorithm.

3.3.2.2 Fault-tolerant control design

In this subsection, in order to achieve the desired control objective 3, we propose an adaptive compensation control scheme, consisting of a kinematic and dynamic control design. The structure of the proposed scheme is shown in Fig. 3.14.

3.3.2.2.1 Kinematic controller design

The design of the kinematic control is based on the transformation of model into the chained form.

The chained form of the kinematic model [40] and a recursive technique based on the classical integrator backstepping [120] give the following kinematic control law already presented in Section 3.3.1:

$$\boldsymbol{\eta_c = T_\alpha^{-1} \alpha_c} \tag{3.111}$$

where T_α and α_c as described in section 3.3.1 are

$$T_\alpha = \begin{bmatrix} T_{\alpha 11} & T_{\alpha 12} \\ T_{\alpha 21} & T_{\alpha 22} \end{bmatrix} \tag{3.112}$$

$$\alpha_c = \begin{bmatrix} \alpha_{1c} \\ \alpha_{2c} \end{bmatrix} \tag{3.113}$$

This kinematic control law is a function of the measured and desired generalized coordinates q and q_d, respectively. It is shown in previous section, that a dynamic controller can be applied in jointly with (3.111) in order to assure closed loop stability and performance. In the sequence, a suitable dynamic controller is presented.

3.3.2.2.2 Dynamic controller design

To cover all possible faults and to handle the uncertainties of system frictions and faults, a multi-design integration based adaptive dynamic controller is developed in this subsection.

Multi design integration

Substituting (2.102) into (2.55) (see chapter 2), the multi-robot system dynamic is described by the following dynamic equation when considering actuator faults as follows

$$\dot{\eta} = -\bar{M}_1^{-1}\bar{M}_2\eta - \bar{M}_1^{-1}\bar{C} + \bar{M}_1^{-1}\bar{B}\sigma u + \bar{M}_1^{-1}\bar{B}\bar{u}_f \tag{3.114}$$

where $\bar{u}_f = (I_6 - \sigma)\bar{u}$ is the unknown friction value that is introduced by loss of control failure, and $u = [u_{1\mathrm{r}}, u_{1\mathrm{l}}, u_{2\mathrm{r}}, u_{2\mathrm{l}}, u_{3\mathrm{r}}, u_{3\mathrm{l}}]^{\mathrm{T}}$ is the control signal to be designed.

Let $\sigma_{(k)}$, $k = 1, 2, \ldots, N$ denote the kth possible fault pattern matrix satisfying actuation redundancy condition, where N is the number of all possible fault pattern matrices that are under consideration.

For each $\sigma_{(k)}$, a corresponding dynamic control signal $u_{(k)}$ is designed such that the desired system performance can be ensured if $u = u_{(k)}$ and $\sigma = \sigma_{(k)}$. Then, to cover all possible failure patterns, a nominal multi-design integration based dynamic signal is constructed as follows

$$u^* = \sum_{k=1}^{N} \chi_{(k)} u_{(k)} \tag{3.115}$$

where

$$\chi_{(k)} = \begin{cases} 1 & \text{if } \sigma = \sigma_{(k)} \\ 0 & \text{otherwise} \end{cases} \tag{3.116}$$

with $\chi_{(k)}$ may be 1 or 0, equation (3.115) can be rewritten as

$$u^{*}=\sum_{k=1}^{N}\mathrm{diag}\{\chi_{(k)1r},\chi_{(k)1l},\chi_{(k)2r},\chi_{(k)2l},\chi_{(k)3r},\chi_{(k)3l}\}u_{(k)} \tag{3.117}$$

where

$$\chi_{(k)1r}=\chi_{(k)1l}=\chi_{(k)2r}=\chi_{(k)2l}=\chi_{(k)3r}=\chi_{(k)3l}$$

Since the actual failure pattern σ is uncertain, $\chi_{(k)}$ is also uncertain for $k=1,2,\dots,N$. Let $\hat{\chi}_{(k)}$ denote the estimates of $\chi_{(k)}$, and $\hat{\bar{u}}_f$ denotes the estimate of $\bar{u}_f$, and where $k=1,2,\dots,N$. Then the dynamic control law is designed to deal with such uncertainties as follows

$$\boldsymbol{u}=\sum_{\boldsymbol{k=1}}^{\boldsymbol{N}}\widehat{\boldsymbol{\chi}}_{\boldsymbol{(k)}}\boldsymbol{u}_{\boldsymbol{(k)}} \tag{3.118}$$

where

$\hat{\chi}_{(k)}=\mathrm{diag}\{\hat{\chi}_{(k)1r},\hat{\chi}_{(k)1l},\hat{\chi}_{(k)2r},\hat{\chi}_{(k)2l},\hat{\chi}_{(k)3r},\hat{\chi}_{(k)3l}\}$ is the estimated matrix that will be described later.

The time derivative of the velocity tracking error in (3.25) is

$$\dot{\eta}_e=\dot{\eta}-\dot{\eta}_c \tag{3.119}$$

Substituting (3.114) into (3.119), we get the following equation

$$\dot{\eta}_e=-\bar{M}_1^{-1}\bar{M}_2\eta-\bar{M}_1^{-1}\bar{C}+\bar{M}_1^{-1}\bar{B}\sigma u+\bar{M}_1^{-1}\bar{B}\bar{u}_f-\dot{\eta}_c \tag{3.120}$$

Then, the dynamic control signal $u_{(k)}$ is designed as

$$\boldsymbol{u_{(k)}}=\left(\boldsymbol{\bar{M}_1^{-1}\bar{B}\sigma_{(k)}}\right)^{+}\left[-\boldsymbol{c_6\eta_e}-\boldsymbol{T_\alpha^T f_\eta}+\boldsymbol{\bar{M}_1^{-1}\bar{M}_2\eta}+\boldsymbol{\bar{M}_1^{-1}\bar{C}}-\boldsymbol{\bar{M}_1^{-1}\bar{B}\hat{\bar{u}}_f}+\boldsymbol{\dot{\eta}_c}\right] \tag{3.121}$$

for $\sigma_{(k)}$, $k=1,2,\dots,N$, where $c_6>0$ is chosen to be constant, and $\left(\bar{M}_1^{-1}\bar{B}\sigma_{(k)}\right)^{+}$ is a generalized inverse matrix satisfying $\bar{M}_1^{-1}\bar{B}\sigma_{(k)}\left(\bar{M}_1^{-1}\bar{B}\sigma_{(k)}\right)^{+}=I_3$.

Remark 3.7*: Some elements of some $u_{(k)}$ may be zero. For example, if $\sigma_{(k)}=diag\{0,1,1,1,1,1\}$ and $\left(\bar{M}_1^{-1}\bar{B}\sigma_{(k)}\right)^{+}=\sigma_{(k)}(\bar{M}_1^{-1}\bar{B})^T\left(\bar{M}_1^{-1}\bar{B}\sigma_{(k)}(\bar{M}_1^{-1}\bar{B})^T\right)^{-1}$, then $u_{(k)1r}=0$. In this sense, some $\hat{\chi}_{(k)}$ in (3.131) can be simplified. For instance, for $\sigma_{(k)}=diag\{0,1,1,1,1,1\}$, $\hat{\chi}_{(k)}=\{0,\hat{\chi}_{(k)1l},\hat{\chi}_{(k)2r},\hat{\chi}_{(k)2l},\hat{\chi}_{(k)3r},\hat{\chi}_{(k)3l}\}$; and for $\sigma_{(k)}=diag\{0,1,1,1,1,0\}$, $\hat{\chi}_{(k)}=\{0,\hat{\chi}_{(k)1l},\hat{\chi}_{(k)2r},\hat{\chi}_{(k)2l},\hat{\chi}_{(k)3r},0\}$.*

Let $\hat{\bar{u}}_f$ denote the estimate of $\bar{u}_f$, and $\hat{\chi}_{(k)}$ denote the estimates of $\chi_{(k)}$, where $k = 1, 2, \dots, N$. Define the estimation error as

$$\tilde{\bar{u}}_f = \bar{u}_f - \hat{\bar{u}}_f,$$

$$\tilde{\chi}_{(k)1r} = \chi_{(k)} - \hat{\chi}_{(k)1r}, \quad \tilde{\chi}_{(k)1l} = \chi_{(k)} - \hat{\chi}_{(k)1l},$$

$$\tilde{\chi}_{(k)2r} = \chi_{(k)} - \hat{\chi}_{(k)2r}, \quad \tilde{\chi}_{(k)2l} = \chi_{(k)} - \hat{\chi}_{(k)2l},$$

$$\tilde{\chi}_{(k)3r} = \chi_{(k)} - \hat{\chi}_{(k)3r}, \quad \tilde{\chi}_{(k)3l} = \chi_{(k)} - \hat{\chi}_{(k)3l} \tag{3.122}$$

for $k = 1, 2, \dots, N$. Then, substituting (3.117), (3.118) and (3.121) into (3.120), we have

$$\dot{\eta}_e = -\bar{M}_1^{-1}\bar{M}_2\eta - \bar{M}_1^{-1}\bar{C} + \bar{M}_1^{-1}\bar{B}\sigma u^* + \bar{M}_1^{-1}\bar{B}\bar{u}_f - \dot{\eta}_c + \bar{M}_1^{-1}\bar{B}\sigma(u - u^*)$$

$$\dot{\eta}_e = -c_6\eta_e - T_\alpha^T f_\eta + \bar{M}_1^{-1}\bar{B}\tilde{\bar{u}}_f - \sum_{k=1}^{N}(\bar{M}_1^{-1}\bar{B})_{c1}\sigma_{1r}\tilde{\chi}_{(k)1r}u_{(k)1r}$$

$$- \sum_{k=1}^{N}(\bar{M}_1^{-1}\bar{B})_{c2}\sigma_{1l}\tilde{\chi}_{(k)1l}u_{(k)1l} - \sum_{k=1}^{N}(\bar{M}_1^{-1}\bar{B})_{c3}\sigma_{2r}\tilde{\chi}_{(k)2r}u_{(k)2r}$$

$$- \sum_{k=1}^{N}(\bar{M}_1^{-1}\bar{B})_{c4}\sigma_{2l}\tilde{\chi}_{(k)2l}u_{(k)2l} - \sum_{k=1}^{N}(\bar{M}_1^{-1}\bar{B})_{c5}\sigma_{3r}\tilde{\chi}_{(k)3r}u_{(k)3r}$$

$$- \sum_{k=1}^{N}(\bar{M}_1^{-1}\bar{B})_{c6}\sigma_{3l}\tilde{\chi}_{(k)3l}u_{(k)3l} \tag{3.123}$$

where $(\bar{M}_1^{-1}\bar{B})_{ci}$ $(i = 1, \dots, 6)$ denotes the ith column vector of matrix $\bar{M}_1^{-1}\bar{B}$.

Adaptive law

Based on the error equation in (3.123), we now design the adaptive law to construct the control signal $u_{(k)}$ in (3.121), as

$$\dot{\hat{\bar{u}}}_f = \Gamma_f + (\bar{M}_1^{-1}\bar{B})^T\eta_e \tag{3.124}$$

where $\Gamma_f = \Gamma_f^T \in \Re^{6\times 6}$ is the positive-definite adaptation gain matrix that is chosen to be constant.

To construct the dynamic control law u in (3.118), the adaptive law of $\hat{\chi}_{(k)1r}, \hat{\chi}_{(k)1l}, \hat{\chi}_{(k)2r}, \hat{\chi}_{(k)2l}, \hat{\chi}_{(k)3r}$ and $\hat{\chi}_{(k)3l}$ are chosen as

$$\dot{\hat{\chi}}_{(k)1r} = -\gamma_{k1r} u_{(k)1r} \eta_e^T (\bar{M}_1^{-1} \bar{B})_{c1} + f_{k1r,}$$

$$\dot{\hat{\chi}}_{(k)1l} = -\gamma_{k1l} u_{(k)1l} \eta_e^T (\bar{M}_1^{-1} \bar{B})_{c2} + f_{k1l,}$$

$$\dot{\hat{\chi}}_{(k)2r} = -\gamma_{k2r} u_{(k)2r} \eta_e^T (\bar{M}^{-1} \bar{B})_{c3} + f_{k2r,}$$

$$\dot{\hat{\chi}}_{(k)2l} = -\gamma_{k2l} u_{(k)2l} \eta_e^T (\bar{M}_1^{-1} \bar{B})_{c4} + f_{k2l,}$$

$$\dot{\hat{\chi}}_{(k)3r} = -\gamma_{k3r} u_{(k)3r} \eta_e^T (\bar{M}_1^{-1} \bar{B})_{c5} + f_{k3r,}$$

$$\dot{\hat{\chi}}_{(k)3l} = -\gamma_{k3l} u_{(k)3l} \eta_e^T (\bar{M}_1^{-1} \bar{B})_{c6} + f_{k3l,} \quad (3.125)$$

for $k = 1, 2, \dots, N$, where $\gamma_{k1r} > 0, \gamma_{k1l} > 0, \gamma_{k2r} > 0, \gamma_{k2r} > 0, \gamma_{k3r} > 0$, and $\gamma_{k3l} > 0$, are the adaptation gains.

Standard parameters projection functions [131] $f_{k1r,}\ f_{k1l,}\ f_{k2r,}\ f_{k2l,}\ f_{k3r}$ and f_{k3l} are set to ensure the boundedness of the parameters errors $\tilde{\chi}_{(k)1r}, \tilde{\chi}_{(k)1l}, \tilde{\chi}_{(k)2r}, \tilde{\chi}_{(k)2l}, \tilde{\chi}_{(k)3r}, \tilde{\chi}_{(k)3l}$ that are defined in the following. Let

$$p_{k1r} = -\gamma_{k1r} u_{(k)1r} \eta_e^T (\bar{M}_1^{-1} \bar{B})_{c1},$$

$$p_{k1l} = -\gamma_{k1l} u_{(k)1l} \eta_e^T (\bar{M}_1^{-1} \bar{B})_{c2},$$

$$p_{k2r} = -\gamma_{k2r} u_{(k)2r} \eta_e^T (\bar{M}_1^{-1} \bar{B})_{c3},$$

$$p_{k2l} = -\gamma_{k2l} u_{(k)2l} \eta_e^T (\bar{M}_1^{-1} \bar{B})_{c4},$$

$$p_{k3r} = -\gamma_{k3r} u_{(k)3r} \eta_e^T (\bar{M}_1^{-1} \bar{B})_{c5},$$

$$p_{k3l} = -\gamma_{k3l} u_{(k)3l} \eta_e^T (\bar{M}_1^{-1} \bar{B})_{c6} \quad (3.126)$$

The projection functions are given as follows

$$f_{kj} = \begin{cases} 0, & \begin{array}{c} \text{if } \hat{\chi}_{(k)j} \in (0,1), \text{or} \\ \text{if } \hat{\chi}_{(k)j} = 0 \text{ and } p_{kj} \geq 0, \text{or} \\ \text{if } \hat{\chi}_{(k)j} = 1 \text{ and } p_{kj} \leq 0, \end{array} \\ -p_{kj}, & \text{otherwise} \end{cases} \quad (3.127)$$

Lemma 3.3*: The adaptive laws in (3.126) with the projection functions in (3.127) for* $k = 1, 2, \dots, N$ *guarantee that*

1) $\hat{\chi}_{(k)1r}, \hat{\chi}_{(k)1l}, \hat{\chi}_{(k)2r}, \hat{\chi}_{(k)2l}, \hat{\chi}_{(k)3r}, \hat{\chi}_{(k)3l} \in [0,1]$.

2) $\tilde{\chi}_{(k)1r} f_{k1r} \geq 0$, $\tilde{\chi}_{(k)1l} f_{k1l} \geq 0$, $\tilde{\chi}_{(k)2r} f_{k2r} \geq 0$, $\tilde{\chi}_{(k)2l} f_{k2l} \geq 0$, $\tilde{\chi}_{(k)3r} f_{k3r} \geq 0$, *and* $\tilde{\chi}_{(k)3l} f_{k3l,} \geq 0$. *For* $k = 1, 2, \ldots, N$.

Proof*:* The proofs for the six adaptive laws are similar. Take $\hat{\chi}_{(\mathrm{k})1\mathrm{r}}$ as an example. Choose the initial estimate value as $\hat{\chi}_{(k)1r}(0) \in (0,1)$. The projection functions in (3.127) with $j = 1r$ ensure $\hat{\chi}_{(k)1r}(t) \in (0,1)$, and

$$\left(\chi_{(k)1r} - \hat{\chi}_{(k)1r}\right) f_{k1r} = \tilde{\chi}_{(k)1r} f_{k1r} \geq 0 \tag{3.128}$$

that is analyzed for the following three cases

1) If $\hat{\chi}_{(k)1r} = 0$ and $p_{k1r} < 0$, then $\chi_{(k)1r} - \hat{\chi}_{(k)1r} \geq 0$ and $f_{k1r} = -p_{k1r} > 0$, which means (3.128) is ensured.
2) If $\hat{\chi}_{(k)1r} = 1$ and $p_{k1r} > 0$, then $\chi_{(k)1r} - \hat{\chi}_{(k)1r} \leq 0$ and $f_{k1r} = -p_{k1r} < 0$, which also means (3.128) is ensured.
3) Otherwise, we have $f_{k1r} = 0$, then (3.128) is ensured.

Similarly, we can also obtain the same properties for the other five adaptive laws. The proof is completed. ■

3.3.2.2.3. Stability analysis

In this subsection, the overall system performance is given as follows.

Theorem 3.3*: For three-linked mobile robots subject to actuator failures, the proposed multi-design integration based adaptive actuator failure compensation control scheme, constituted by the kinematic control law in (3.111), and dynamic control law in (3.118) with multiple control signals in (3.121) and updated with projection adaptive laws in (3.124) and (3.125), can guarantee the boundedness of all the closed loop signals and asymptotic tracking despite the actuator failures.*

Proof: According to remark 3.6, there are five compensable cases: no fault and cases from one faulty actuator up to four simultaneously faulty actuators. Therefore, the performance of the system is analyzed as follows

1) ***No fault****:* Let us consider the Lyapunov function candidate as

$$V_6 = V_5 + \frac{1}{2}\eta_e^T\eta_e + \frac{1}{2}\tilde{\tilde{u}}_f^T\Gamma_f^{-1}\tilde{\tilde{u}}_f + \frac{1}{2}\left[\sum_{k=1}^{N}\sigma_{1r}\gamma_{k1r}^{-1}\tilde{\chi}_{(k)1r}^2 + \sum_{k=1}^{N}\sigma_{1l}\gamma_{k1l}^{-1}\tilde{\chi}_{(k)1l}^2 + \sum_{k=1}^{N}\sigma_{2r}\gamma_{k2r}^{-1}\tilde{\chi}_{(k)2r}^2 + \sum_{k=1}^{N}\sigma_{2l}\gamma_{k2l}^{-1}\tilde{\chi}_{(k)2l}^2 + \sum_{k=1}^{N}\sigma_{3r}\gamma_{k3r}^{-1}\tilde{\chi}_{(k)3r}^2 + \sum_{k=1}^{N}\sigma_{3l}\gamma_{k3l}^{-1}\tilde{\chi}_{(k)3l}^2\right] \quad (3.129)$$

Then, the derivative of V_6 is

$$\dot{V}_6 = \dot{V}_5 + \eta_e^T\dot{\eta}_e + \tilde{\tilde{u}}_f^T\Gamma_f^{-1}\dot{\tilde{\tilde{u}}}_f + \sum_{k=1}^{N}\gamma_{k1r}^{-1}\tilde{\chi}_{(k)1r}\dot{\tilde{\chi}}_{(k)1r} + \sum_{k=1}^{N}\gamma_{k1l}^{-1}\tilde{\chi}_{(k)1l}\dot{\tilde{\chi}}_{(k)1l} + \sum_{k=1}^{N}\gamma_{k2r}^{-1}\tilde{\chi}_{(k)2r}\dot{\tilde{\chi}}_{(k)2r} + \sum_{k=1}^{N}\gamma_{k2l}^{-1}\tilde{\chi}_{(k)2l}\dot{\tilde{\chi}}_{(k)2l} + \sum_{k=1}^{N}\gamma_{k3r}^{-1}\tilde{\chi}_{(k)3r}\dot{\tilde{\chi}}_{(k)3r} + \sum_{k=1}^{N}\gamma_{k3l}^{-1}\tilde{\chi}_{(k)3l}\dot{\tilde{\chi}}_{(k)3l} \quad (3.130)$$

Substituting (3.106) and (3.119)-(3.125) into (3.130), and with $\dot{\tilde{\tilde{u}}}_f = -\dot{\hat{\tilde{u}}}$, $\dot{\tilde{\chi}}_{(k)1r} = -\dot{\hat{\chi}}_{(k)1r}$, $\dot{\tilde{\chi}}_{(k)1l} = -\dot{\hat{\chi}}_{(k)1l}$, $\dot{\tilde{\chi}}_{(k)2r} = -\dot{\hat{\chi}}_{(k)2r}$, $\dot{\tilde{\chi}}_{(k)2l} = -\dot{\hat{\chi}}_{(k)2l}$, $\dot{\tilde{\chi}}_{(k)3r} = -\dot{\hat{\chi}}_{(k)3r}$, and $\dot{\tilde{\chi}}_{(k)3l} = -\dot{\hat{\chi}}_{(k)3l}$,

we have

$$\dot{V}_6 = -c_4\bar{z}_4^2 - c_5z_5^2 - c_6\eta_e^T\eta_e - \sum_{k=1}^{N}\gamma_{k1r}^{-1}\tilde{\chi}_{(k)1r}f_{k1r} - \sum_{k=1}^{N}\gamma_{k1l}^{-1}\tilde{\chi}_{(k)1l}f_{k1l} - \sum_{k=1}^{N}\gamma_{k2r}^{-1}\tilde{\chi}_{(k)2r}f_{k2r} - \sum_{k=1}^{N}\gamma_{k2l}^{-1}\tilde{\chi}_{(k)2l}f_{k2l} - \sum_{k=1}^{N}\gamma_{k3r}^{-1}\tilde{\chi}_{(k)3r}f_{k3r} - \sum_{k=1}^{N}\gamma_{k3l}^{-1}\tilde{\chi}_{(k)3l}f_{k3l} \quad (3.131)$$

together with the second property in Lemma 3.3, we obtain

$$\dot{V}_6 \leq -c_4\bar{z}_4^2 - c_5z_5^2 - c_6\eta_e^T\eta_e \leq 0 \quad (3.132)$$

The proof of equation (3.132) is as follows:

$z_1, z_2, z_3, z_4, z_5, \bar{z}_1, \bar{z}_2, \bar{z}_3, \bar{z}_4, \eta_e \in L^\infty$, and all estimates are bounded, and $\bar{z}_4, z_5, \eta_e \in L^2$. The definitions of L^∞ and L^2 can be found in [131]. It follows from equations (2.89),

(2.90) and (2.91), that $cos\,\theta_3 \neq 0$, $cos(\theta_2 - \theta_3) \neq 0$ and $tan(\theta_1 - \theta_2) \in L^\infty$ which means $cos(\theta_1 - \theta_2) \neq 0$.

Then from equations (3.69), (3.73), and also from (3.99) -(3.104) and (3.107), and according to Barbalat's Lemma [131], it is concluded that all the closed loop system signals are bounded, and $\lim_{t\to\infty} \bar{z}_4 = 0$, $\lim_{t\to\infty} z_5 = 0$ and $\lim_{t\to\infty} \eta_e = 0$, which also implies $\lim_{t\to\infty} \alpha_e = 0$, with equation (3.101). and also, we have $\lim_{t\to\infty} z_1 = 0$, ⋯, $\lim_{t\to\infty} z_5 = 0$, $\lim_{t\to\infty} \bar{z}_1 = 0$, ⋯, $\lim_{t\to\infty} \bar{z}_4 = 0$, and $|\alpha_{1d}| \geq 0$. Then we can further obtain $\lim_{t\to\infty} \alpha_{2c} = \alpha_{2d}$ from equation (3.102), it follows that $\lim_{t\to\infty} \alpha_2 = \alpha_{2d}$, and also $\lim_{t\to\infty} \alpha_{1c} = \alpha_{1d}$ and from equation (3.103), it follows that $\lim_{t\to\infty} \alpha_1 = \alpha_{1d}$.

Finally, we can conclude that all the closed loop system signals are uniformly bounded, furthermore $\lim_{t\to\infty} z_i(t) = 0$, $(i = 1, \dots 5)$ and $\lim_{t\to\infty}(\eta(t) - \eta_c(t)) = 0$, which also means $\lim_{t\to\infty}(q(t) - q_d(t)) = 0$

2) ***One actuator fails:*** Suppose the left actuator of robot 1 is faulty, that is $\sigma = \text{diag}\{1, 0, 1, 1, 1, 1\}$ with $\sigma_{(1l)} = 0$. In this case, we consider the Lyapunov function candidate as

$$V_6 = V_5 + \frac{1}{2}\eta_e^T\eta_e + \frac{1}{2}\tilde{\tilde{u}}_f^T\Gamma_f^{-1}\tilde{\tilde{u}}_f + \frac{1}{2}\left[\sum_{k=1}^{N}\sigma_{1r}\gamma_{k1r}^{-1}\tilde{\chi}_{(k)1r}^2 + \sum_{k=1}^{N}\sigma_{1r}\gamma_{k1r}^{-1}\tilde{\chi}_{(k)1r}^2 + \sum_{k=1}^{N}\sigma_{2l}\gamma_{k2l}^{-1}\tilde{\chi}_{(k)2l}^2 + \sum_{k=1}^{N}\sigma_{3r}\gamma_{k3r}^{-1}\tilde{\chi}_{(k)3r}^2 + \sum_{k=1}^{N}\sigma_{3l}\gamma_{k3l}^{-1}\tilde{\chi}_{(k)3l}^2\right] \quad (3.133)$$

Then, according to (3.106), (3.120) -(3.125) and Lemma 3.3, we have

$$\dot{V}_6 \leq -c_4\bar{z}_4^2 - c_5 z_5^2 - c_6\eta_e^T\eta_e \leq 0 \quad (3.134)$$

Note that, although there is no $\tilde{\chi}_{(k)1l}$ for $k = 1, 2, \dots, N$, in (3.133) they are also bounded according to the first property in Lemma 3.3 Then, from (3.134), we can conclude that stability and asymptotic tracking are established compared with first case (fault free case). The performance analysis of the system for the other cases with one fault is similar.

3) ***Two actuators fail:*** Suppose the left wheel of robot 1 and the right wheel of robot 2 are faulty, that is $\sigma = \text{diag}\{1, 0, 0, 1, 1, 1\}$ with $\sigma_{(1l)} = 0$, $\sigma_{(2r)} = 0$. The following Lyapunov function candidate is chosen here

$$V_6 = V_5 + \frac{1}{2}\eta_e^T\eta_e + \frac{1}{2}\tilde{\tilde{u}}_f^T\Gamma_f^{-1}\tilde{\tilde{u}}_f + \frac{1}{2}\left[\sum_{k=1}^{N}\sigma_{1r}\gamma_{k1r}^{-1}\tilde{\chi}_{(k)1r}^2 + \sum_{k=1}^{N}\sigma_{2l}\gamma_{k2l}^{-1}\tilde{\chi}_{(k)2l}^2 + \sum_{k=1}^{N}\sigma_{3r}\gamma_{k3r}^{-1}\tilde{\chi}_{(k)3r}^2 + \sum_{k=1}^{N}\sigma_{3l}\gamma_{k3l}^{-1}\tilde{\chi}_{(k)3l}^2\right] \quad (3.135)$$

Then, according to (3.106), (3.120) -(3.125) and Lemma 3.3, we have

$$\dot{V}_6 \leq -c_4\bar{z}_4^2 - c_5 z_5^2 - c_6\eta_e^T\eta_e \leq 0 \quad (3.136)$$

Which denotes that the desired system stability and asymptotic tracking properties are ensured. The performance analysis for the other cases with two faulty actuators is similar.

4) ***Three actuators fail****:* Suppose the left wheel of robot 1, the right wheel of robot 2, and the right wheel of robot 3 are faulty, that is $\sigma = \text{diag}\{1,0,0,1,0,1\}$ with $\sigma_{(1l)} = 0, \sigma_{(2r)} = 0, \sigma_{(3r)} = 0$, we consider the Lyapunov function candidate as

$$V_6 = V_5 + \frac{1}{2}\eta_e^T\eta_e + \frac{1}{2}\tilde{\tilde{u}}_f^T\Gamma_f^{-1}\tilde{\tilde{u}}_f\frac{1}{2}\left[\sum_{k=1}^{N}\sigma_{1r}\gamma_{k1r}^{-1}\tilde{\chi}_{(k)1r}^2 + \sum_{k=1}^{N}\sigma_{2l}\gamma_{k2l}^{-1}\tilde{\chi}_{(k)2l}^2 + \sum_{k=1}^{N}\sigma_{3l}\gamma_{k3l}^{-1}\tilde{\chi}_{(k)3l}^2\right] \quad (3.137)$$

Then, according to (3.106), (3.120) -(3.125) and Lemma 3.3, we have

$$\dot{V}_6 \leq -c_4\bar{z}_4^2 - c_5 z_5^2 - c_6\eta_e^T\eta_e \leq 0 \quad (3.138)$$

From equation (3.138), we can conclude that the closed-loop stability and asymptotic tracking can be established. The performance analysis for the other cases with three faulty actuators is similar.

5) ***Four actuators fail****:* Suppose the left wheel of robot 1, the right wheel of robot 2, and the right and left wheel of robot 3 are faulty, that is $\sigma = \text{diag}\{1,0,0,1,0,0\}$ with $\sigma_{(1l)} = 0$, $\sigma_{(2r)} = 0, \sigma_{(3r)} = 0, \sigma_{(3l)} = 0$, we consider the Lyapunov function candidate as

$$V_6 = V_5 + \frac{1}{2}\eta_e^T\eta_e + \frac{1}{2}\tilde{\tilde{u}}_f^T\Gamma_f^{-1}\tilde{\tilde{u}}_f + \frac{1}{2}\left[\sum_{k=1}^{N}\sigma_{1r}\gamma_{k1r}^{-1}\tilde{\chi}_{(k)1r}^2 + \sum_{k=1}^{N}\sigma_{2l}\gamma_{k2l}^{-1}\tilde{\chi}_{(k)2l}^2\right] \quad (3.139)$$

Then, according to (3.106), (3.120) -(3.125) and Lemma 3.3, we have

$$\dot{V}_6 \leq -c_4\bar{z}_4^2 - c_5 z_5^2 - c_6\eta_e^T\eta_e \leq 0 \tag{3.140}$$

From equation (3.140), it can be concluded that the closed-loop stability and asymptotic tracking can be established.

3.3.2.3 Simulation studies

The case of two-linked 2WD mobile robots

To verify the effectiveness of the developed multi-design integration based adaptive actuator fault compensation scheme for two-linked 2WD mobile robots, the following simulation study is presented.

1) Simulation conditions: In this simulation, we assume that each of the two robots is the one used in [34], then the physical parameters are $a_1 = a_2 = 0.3\,m$, $b_1 = b_2 = 0.75\,m$, $r_1 = r_2 = 0.15\,m, m_1 = m_2 = 30\,kg, I_{m1} = I_{m2} = 15.625\,kg\cdot m^2$. The length of the link is assumed to be $d = 1.7\,m$.

To verify the system tracking property, an eight-like reference trajectory and a circle reference trajectory are considered, the velocities v_d and ω_d are chosen as:

$$v_d = 0.5 \text{ m/s}, \omega_d = 0.5 \text{ rad/s}$$

for the circle reference trajectory; and

$$v_d = \sqrt{0.81cos^2(0.3t) + 0.5625cos^2(0.15t)} \text{ m/s}, \omega_d = \frac{f_{\omega_{r1}}(t) - f_{\omega_{r2}}(t)}{v_d^2} \text{ rad/s}$$

for the eight-like reference trajectory, where

$$f_{\omega_{r1}}(t) = 0.2025 \sin(0.3\text{t}) \cos(0.15\text{t}), f_{\omega_{r2}}(t) = -0.10125 \sin(0.15\text{t}) \cos(0.3\text{t}).$$

Then, x_d, y_d and θ_d are generated by: $\dot{x}_d = v_d \cos\theta_d$, $\dot{y}_d = v_d \sin\theta_d$, $\dot{\theta}_d = \omega_d$, with $x_d(0) = y_d(0) = 0$ and $\theta_d(0) = 45$ deg.

In order to verify the fault compensation effectiveness of the developed adaptive control scheme, the following fault cases are simulated.

- no fault: $\sigma_{(1)} = \text{diag}\{1, 1, 1, 1\}$, for $0 \leq \text{t} < 10\text{s}$;
- τ_{1r} fails: $\sigma_{(2)} = \text{diag}\{0, 1, 1, 1\}$, $\tau_{1r} = 0$, $10\text{s} \leq \text{t} < 20\text{s}$;
- τ_{1r}, τ_{2l} fail: $\sigma_{(3)} = \text{diag}\{0, 1, 1, 0\}, \tau_{1r} = 0, \tau_{2l} = -2$ Nm, $20\text{s} \leq \text{t} < 30\text{s}$;
- τ_{2l} fails: $\sigma_{(4)} = \text{diag}\{1, 1, 1, 0\}$, $\tau_{2l} = -2$ Nm, $30\text{s} \leq \text{t} < 40\text{s}$;
- τ_{2r}, τ_{2l}, fail: $\sigma_{(5)} = \text{diag}\{1, 1, 0, 0\}$, $\tau_{2r} = -1$ Nm, $\tau_{2l} = -2$ Nm, $\text{t} \geq 40\text{s}$.

There are 5 fault pattern matrices which satisfy the actuation redundancy condition, covering the cases of fault free, one actuator fails, both two actuators of robot 2 fail, and one actuator of each robot fails.

The initial conditions are chosen as: $x(0) = 0, y(0) = 1\ m$, $\theta_2(0) = 10\ deg, \theta_2(0) = 0$, $v_2(0) = 0$, $\omega_1(0) = 0$, $\hat{\chi}_{(1)}(0) = \text{diag}\{1,1,1,1\}$, $\hat{\chi}_{(2)}(0) = \hat{\chi}_{(3)}(0) = \hat{\chi}_{(4)}(0) = \hat{\chi}_{(5)}(0) = 04 \times 4$, and $\bar{u}_f = [0,0,0,0]^T$.

The adaptation gains are chosen as: $\Gamma_f = I_4$, and $\gamma_{k1r} = \gamma_{k1l} = \gamma_{k2r} = \gamma_{k2l} = 1$ for k = 1, 2, 3, 4, 5. The control gains are chosen as: $k_1 = 10$, $: k_2 = 10, k_3 = 2$ and $k_4 = 10$ for the eight-like reference; $k_1 = 1$, $: k_2 = 1, k_3 = 0.2$ and $k_4 = 20$ for the circle reference trajectory.

Remark 3.8*:* For actual situations, choosing small adaptation gains in the adaptive laws and control gains in the control laws may contribute to a smooth system transient response but make the tracking errors converge slowly, while choosing large ones may shorten the convergence time of the tracking errors but result in a large transient response. To fully utilize such advantages and disadvantages, parameters may be fixed empirically. The controlled system may be simulated with different parameter gains (small ones and large ones). We may choose the most appropriate ones to be applied, which can ensure a good smooth system transient response and an acceptable convergence speed of tracking errors.

2) Simulation results: The developed multi-design integration based adaptive actuator fault compensation scheme is applied, and the following simulation results are given to show its effectiveness.

Fig. 3.15 and 3.19 show the positions of the robot 2, the reference robot and the robot 1. Fig. 3.16 and Fig. 3.20 shows the tracking errors. Fig. 3.17 and Fig. 3.21 show the orientation error between two robots, from which we can see that $\theta_1 - \theta_2$ does not go to $\frac{\pi}{2}$ that guarantees the nonlinearity of T_α in 3.124. Fig. 3.18 and Fig. 3.22 show the control torques generated by the four wheels, which are consistent with the faulty cases in simulation conditions. From them, we can see that the desired system stability and asymptotic tracking properties are ensured by the developed multi-design integration based adaptive fault compensation scheme for both the circle and the eight-like reference trajectories, despite the presence of some actuator faults.

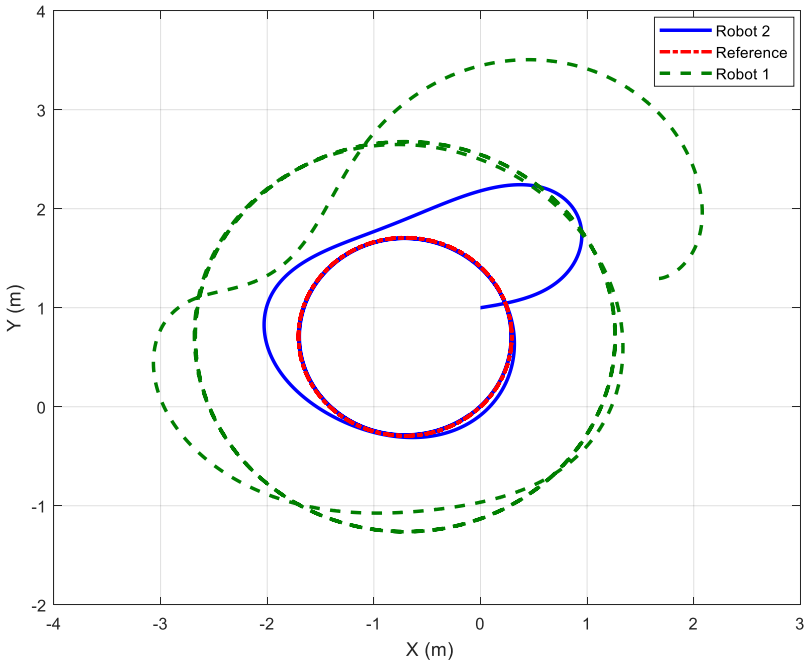

Figure 3.15: Robot trajectories for the circle reference in (X, Y) plane

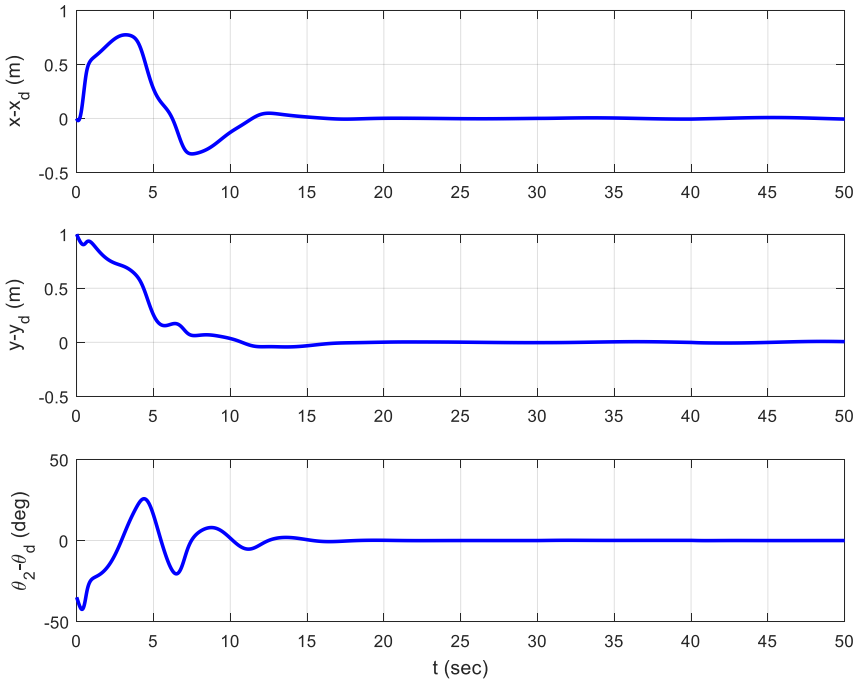

Figure 3.16: Tracking errors for the circle reference.

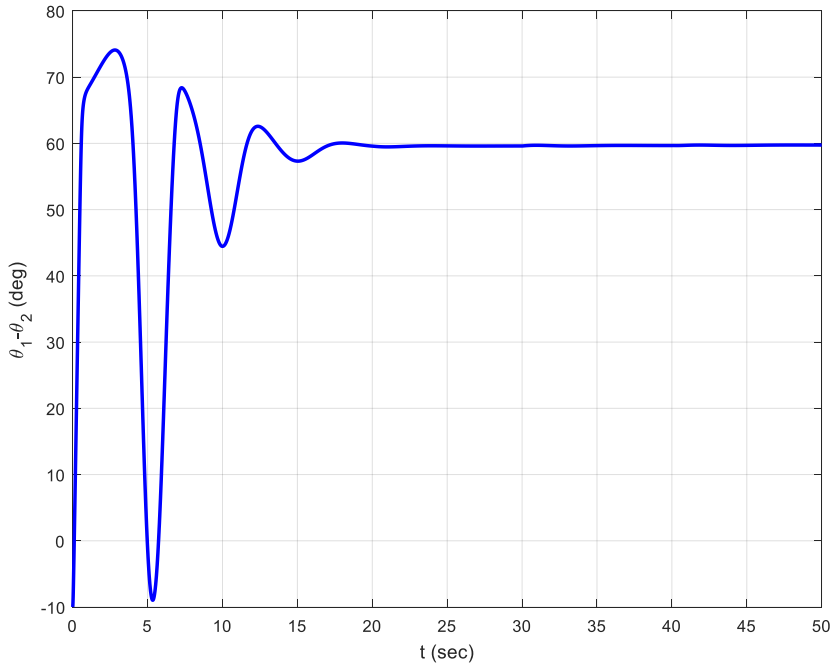

Figure 3.17: Orientation error between two robots for the circle reference.

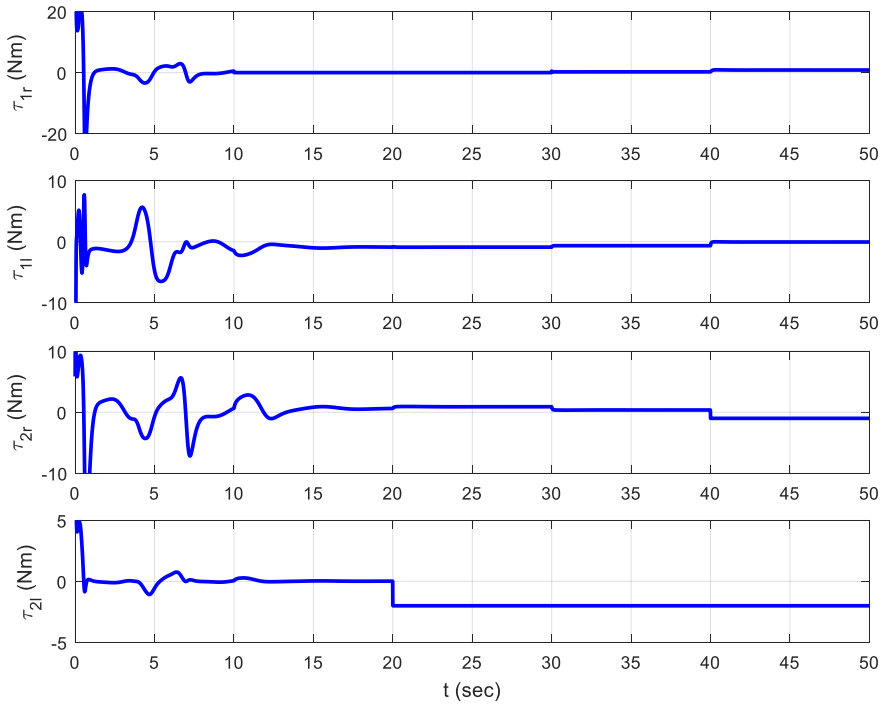

Figure 3.18: Control torques for the circle reference.

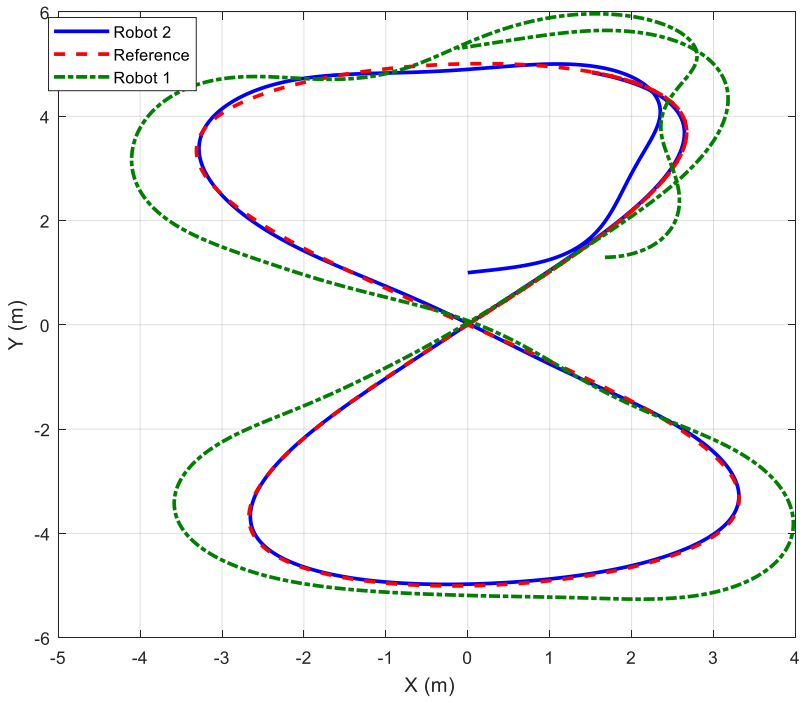

Figure 3.19: Robot trajectories for the eight-like reference in (X, Y) plane.

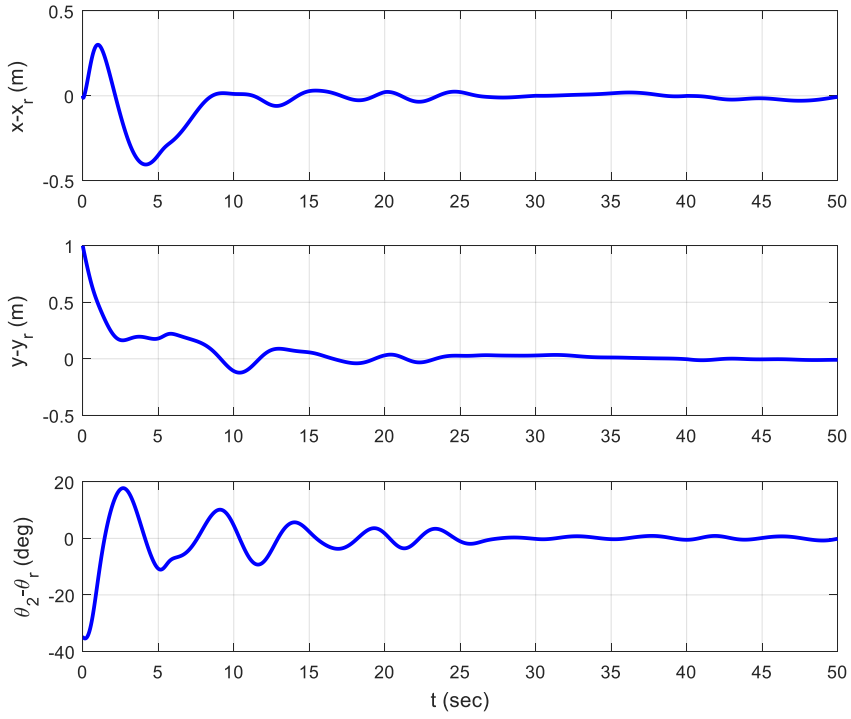

Figure 3.20: Tracking errors for the eight-like reference.

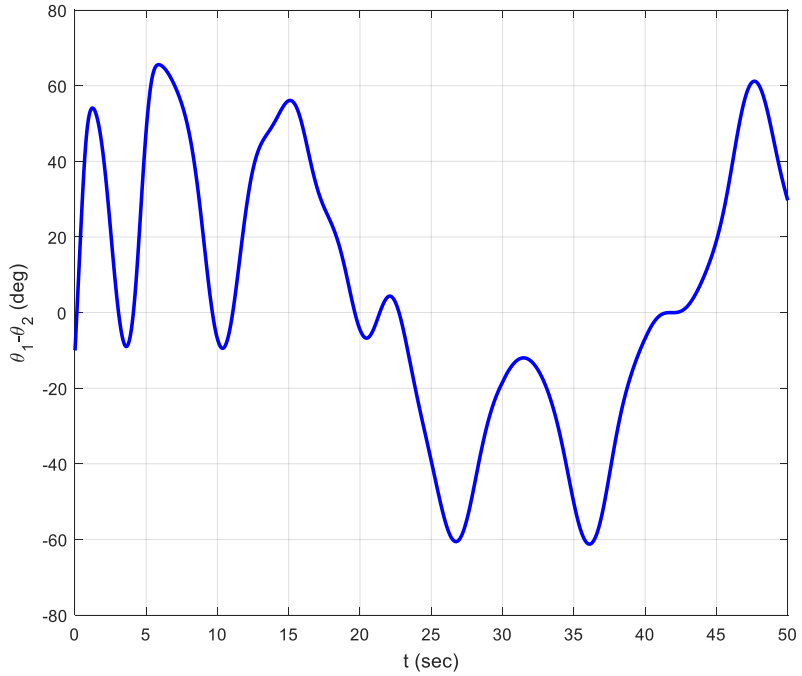

Figure 3.21: Orientation error between two robots for the eight-like reference.

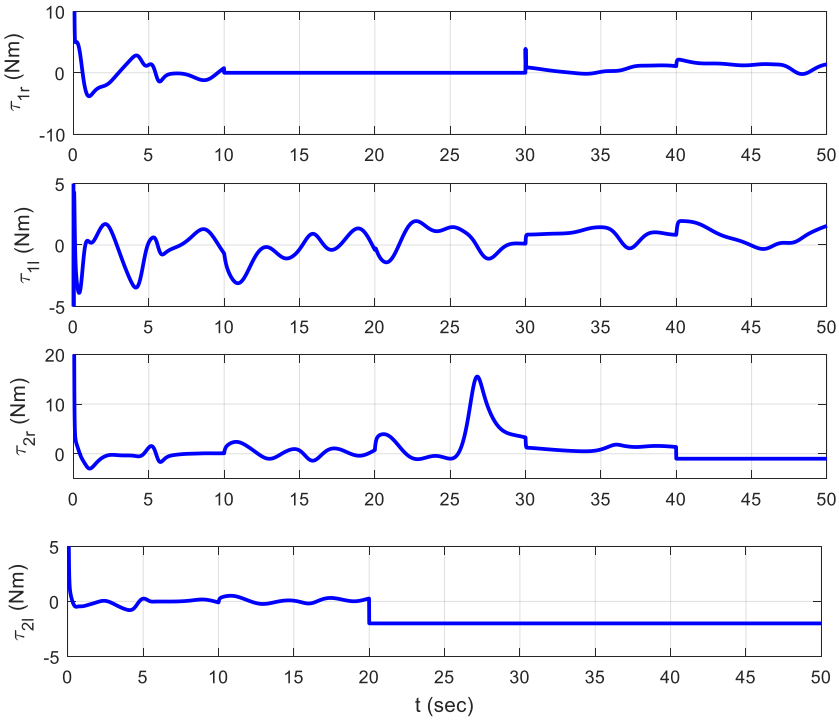

Figure 3.22: Control torques for the eight-like reference.

The case of three-linked 2WD mobile robots

In this simulation studies, we assume the three wheeled driven robots are the one used in [34], then the physical parameters of the three robots are chosen as: $a_1 = a_2 = a_3 = 0.3\ m,\ \ b_1 = b_2 = b_3 = 0.75\ m,\ \ r_1 = r_2 = r_3 = 0.15\ m,\ \ m_1 = m_2 = m_3 = 30\ kg,\ I_{m1} = I_{m2} = I_{m3} = 15.625\ kg \cdot m^2$. The length of the link between each two robots is assumed to be $d = 1\ m$.

The reference trajectory is generated by (6)-(13) with $x_d(0) = y_d(0) = \theta_{3d}(0) = \theta_{2d}(0) = \theta_{1d}(0) = 0$.

In order to verify the fault compensation effectiveness of the adaptive scheme, the following failure cases are simulated:

- no fault: $\sigma_{(1)} = \text{diag}\{1, 1, 1, 1, 1, 1\}$, $0 \leq t < 20s$;
- τ_{1r}, fails: $\sigma_{(2)} = \text{diag}\{0, 1, 1, 1, 1, 1\}$, $\tau_{1r} = 0$, $20s \leq t < 40s$;
- τ_{1r},τ_{3l}, fail: $\sigma_{(3)} = \text{diag}\{0, 1, 1,1, 1, 0\}, \tau_{1r} = 0, \tau_{3l} = -2\ Nm$,$40s \leq t < 60s$;
- τ_{3l}, fails: $\sigma_{(4)} = \text{diag}\{1, 1, 1, 1, 1,0\},\ \tau_{3l} = -2\ Nm,\ 60s \leq t < 80s$;
- τ_{3r}, τ_{3l}, fail: $\sigma_{(5)} = diag\{1, 1, 1, 1, 0, 0\}, \tau_{3r} = -1\ Nm, \tau_{3l} = -2\ Nm,\ t \geq 80s$.

There are 5 failures pattern satisfying the actuation redundancy condition, covering the cases of fault free, one actuator fails, one actuator of robots 1 and 3 fails, one actuator of robot 3 fails, both two actuators of robot 3 fail.

The initial conditions are chosen as: $x(0) = y(0) = 0.5,\ \theta_3(0) = \theta_2(0) = \theta_1(0) = 30\ deg$. The adaptation gains are chosen as: $\Gamma_f = I_6$, and $\gamma_{k1r} = \gamma_{k1l} = \gamma_{k2r} = \gamma_{k2l} = \gamma_{k3r} = \gamma_{k3l} = 1$, for $k = 1, 2, 3, 4, 5$. The control gains are chosen as: $C_4 = C_5 = C_6 = 2$ and $\kappa = 5$.

Fig. 3.23, shows the positions of robot 1, 2, 3 and reference trajectory. Fig. 3.24, shows the control torques generated by the wheels in robot 1, robot 2, and robot 3 respectively, from which we can see that the actuator faults are consistent with the fault cases in simulation conditions.

Fig. 3.25, shows the tracking errors of the states. Fig. 3.26, shows the orientation error between each two robots. From them, we can see that the desired system stability and asymptotic tracking are ensured despite the presence of actuator faults.

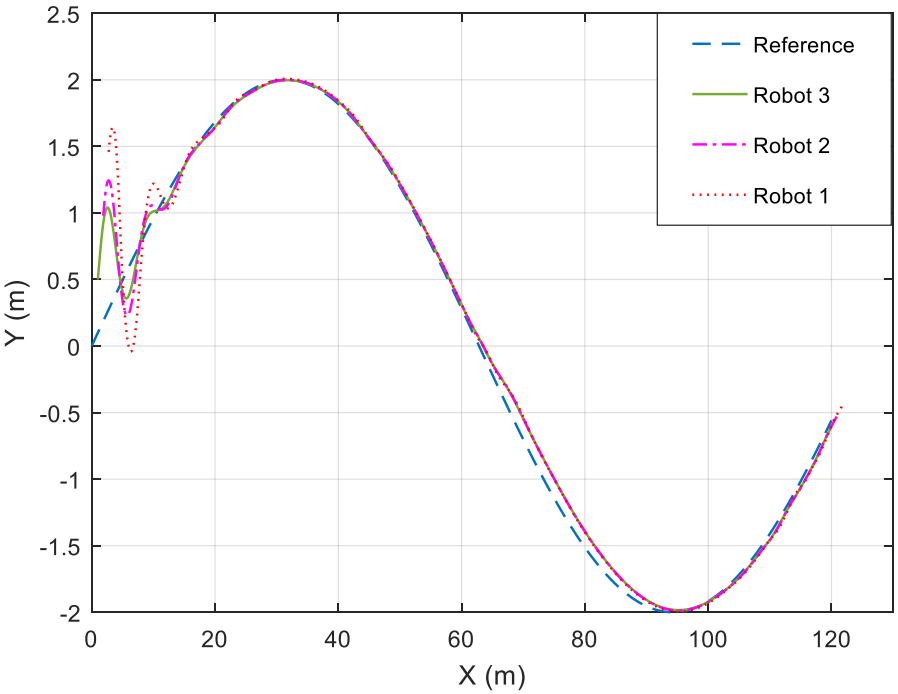

Figure 3.23: Robot trajectories in (x, y) plane.

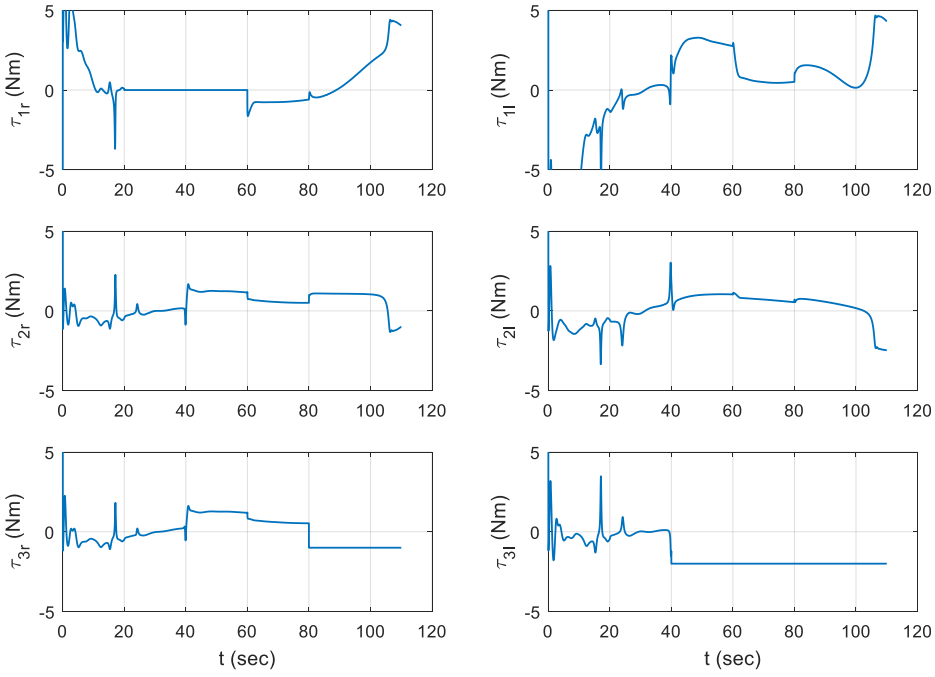

Figure 3.24: Control torques generated by robot 1, robot 2 and robot 3.

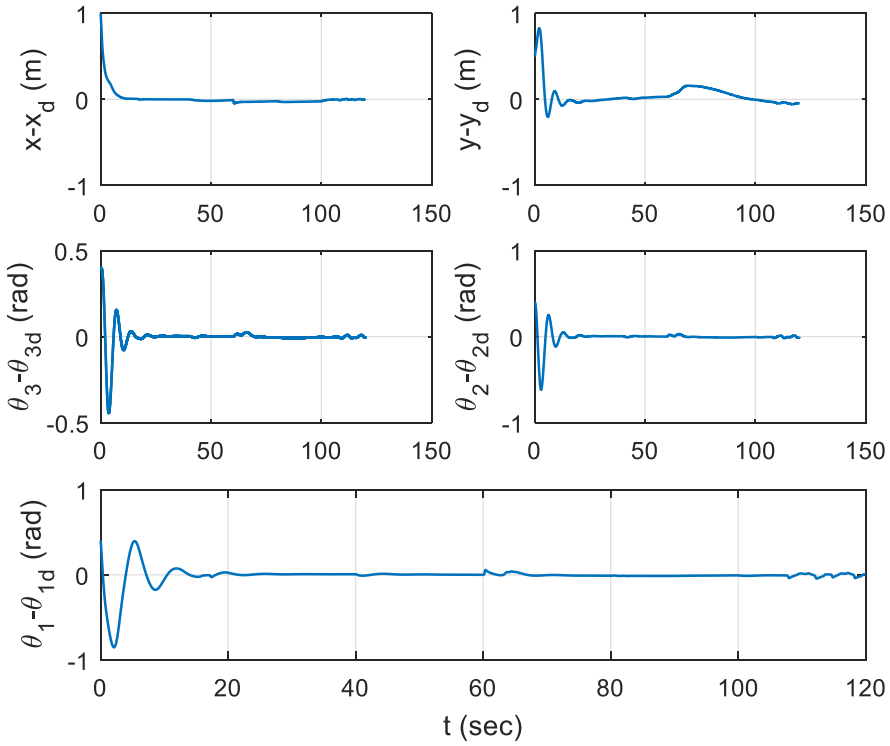

Figure 3.25: Tracking errors.

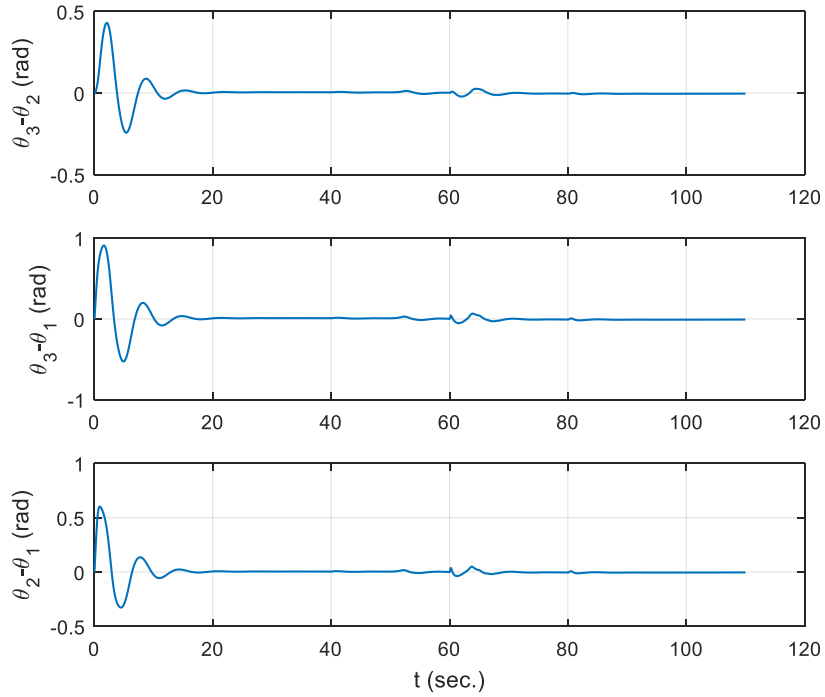

Figure 3.26: Orientation errors between each two robots.

3.4 Design steps of a passive FTC for n-linked 2WD mobile robots (n>1)

In this section, we summarize the steps to design the passive FTC scheme for n-linked 2WD mobile robots (for any $n > 1$).

1) The kinematic model of multi-linked 2WD mobile robots is first transformed into the chained form (transformation of coordinates). It consists in transforming the nonlinear model into an equivalent linear one through a change of variables and a feedback transformation. The transformation of the kinematic model into the chained form has been presented for n-linked robots in chapter 2, Section 2.5, page 38 (Theorem 2.1). It has been applied for three-linked robots in Section 2.5.1, page 41.
2) A recursive algorithm is used to design the kinematic controller for n ($n > 1$) linked robots to guarantee that all the system's states converge to their desired trajectories [86]. This algorithm is presented in Section 3.3, page 71, for three-linked robots. The same methodology may be applied easily for any n-linked robots.
3) General dynamic control laws including actuator fault have to be finally designed, each of which is designed using one possible failure pattern matrix. If the failure pattern which is used in the controller is consistent with the actual one, then the applied control signal can ensure the desired system performance. Different dynamic control laws may be chosen including, multiple dynamic fault tolerant controllers in Section 3.3.1, page 76 and adaptive fault tolerant dynamic controller in Section 3.3.2, page 85, both applied for three-linked robots.

3.5 Conclusion

In this chapter, a brief review of tracking control for mobile robots and multi-linked wheeled mobile robots was first presented. Then, based on the transformation of the kinematic model into the chained form, the kinematic controller was designed for two-linked and three-linked 2WD mobile robots.

For fault compensation, a multiple model dynamic controller is designed. Two techniques are proposed to apply the correct dynamical control law. A control switching

mechanism is first used, then a multi-integration based adaptive law is proposed. The effectiveness of the proposed passive FTC methods have been illustrated using numerical simulations.

The fault tolerant control methods that were presented in this chapter are passive ones and do not give any information on the faults that occur. This information on the faults would be useful for maintenance operations. Moreover, only limited fault cases may be considered with such passive FTC techniques. In the next chapter, we propose an Active FTC technique which includes a fault estimation observer and adapts the control action to the faulty case.

CHAPTER 4

Active Fault Tolerant Control

Contents

4.1 Introduction..... 104

4.2 FD and FTC in three-linked 2WD mobile robots..... 105

4.2.1 Problem formulation 105

4.2.2 Nonlinear adaptive observer and fault diagnosis 107

4.2.2.1 State-space representation of the system..... 107

4.2.2.2 Nonlinear adaptive observer 108

4.2.2.3 Fault estimation..... 109

4.2.3 Fault tolerant control design 109

4.2.3.1 Kinematic controller..... 109

4.2.3.2 Dynamic controller 109

4.2.4 Simulations studies 110

4.3 Generalization of FD and FTC for *n*-linked 2WD mobile robots 128

4.3.1 Nonlinear adaptive observer and fault diagnosis..... 128

4.4.1.1 Nonlinear adaptive observer 129

4.4.1.2 Fault estimation 129

4.3.2 Fault tolerant control design..... 129

4.4 Conclusion 130

Chapter content

An Active Fault Tolerant Control scheme is presented and designed in this chapter for multiple physically-linked mobile robots. A nonlinear dynamic observer is used not only to estimate the actuator fault signal (to realize the Fault Diagnosis) but also to estimate the states that are needed in the feedback control law.

Firstly, we consider a system with three 2WD mobile robots subject to multiplicative and additive actuators faults. Secondly, we generalize the method for n mobile robots, for any $n > 1$.

4.1 Introduction

In general, a number of different faults may occur in complex systems like mobile robots, and the likelihood of multiple faults occurrence increases in harsh operating environments.

In systems and control research, various theoretical results and methodologies on fault diagnosis have been proposed during the last two decades. These results aim to improve system reliability and fault tolerance, specifically by detecting, isolating, identifying and accommodating faults in linear and non-linear centralized and distributed systems, utilizing model-free and model-based approaches [133-135]. The problem of joint estimation of non-measured states, system's parameters and fault signals in linear and nonlinear state space systems with observers has motivated a lot of work for adaptive and fault tolerant control [134], [136].

The observer-based methods play a key role in model-based fault diagnosis [137]. Such techniques were considered for WMR (Wheeled Mobile Robots) diagnosis in [71], where an observer is designed for actuator fault detection, isolation and estimation, following the approach presented in [72].

Based on the fault information, a fault tolerant control is designed to compensate for the effect of faults. By estimating the fault, it is possible to change the control input to accommodate the fault in operation [138].

4.2 FD and FTC in three-linked 2WD mobile robots

In this section, an actuator fault estimation and compensation scheme in a three-linked 2WD mobile robots system is designed. For the reference trajectory tracking, the control scheme which was proposed in Section 3.3.1, is adopted where a kinematic controller and a dynamic controller are associated. An observer is used to estimate the actuator multiplicative faults corrupting the applied torques, and also to estimate the non-measured states of the system, which are needed to apply the feedback control law. The dynamic control law is modified by incorporating the faults and the system states estimations.

4.2.1 Problem formulation

The kinematic and dynamic models for a three-linked 2WD mobile robots were derived in Section 2 of Chapter 2, and are recalled below

Kinematic model:

$$\dot{q} = S(q)\eta \tag{4.1}$$

Dynamic model:

$$\bar{M}_1(q)\dot{\eta} + \bar{M}_2(q)\eta + \bar{C}(q,\dot{q}) = \bar{B}(q)\tau \tag{4.2}$$

where

$q = [x, y, \theta_3, \theta_2, \theta_1]$, is the generalized coordinate vector; $\eta = [v_3 \quad \omega_1]^T$, where v_3 is the linear velocity of robot 3, and ω_1 is the rotational velocity of robot 1; the matrices $\bar{M}_1(q)$, $\bar{M}_2(q)$, $\bar{C}(q,\dot{q})$, and $\bar{B}(q)$ are given pages 33 and 34.

Two types of actuator faults are considered: 1) Partial loss of effectiveness of the wheel motor, that can make it impossible to apply the torque input corresponding to the control signals; 2) Some motors totally lose power or are stuck which will introduce additional frictions. This actuator malfunction can be seen as a multiplicative and additive fault modeled as

$$\tau(t) = \sigma(t)u(t) + \bar{u} \tag{4.3}$$

where $\tau = [\tau_{1r}, \tau_{1l}, \tau_{2r}, \tau_{2l}, \tau_{3r}, \tau_{3l}\ ]^T$ is the torque vector generated by the motors, $u = [u_{1r}, u_{1l}, u_{2r}, u_{2l}, u_{3r}, u_{3l}\ ]^T$ is the control signals vector to be designed, $\sigma = \text{diag}\{\sigma_{1r}, \sigma_{1l}, \sigma_{3r}, \sigma_{3l}\}$ is the uncertain control effectiveness matrix, and $\bar{u} = [\bar{u}_{1r}, \bar{u}_{1l}, \bar{u}_{2r}, \bar{u}_{2l}, \bar{u}_{3r}, \bar{u}_{3l}\ ]^T$ is the friction vector caused by actuator faults.

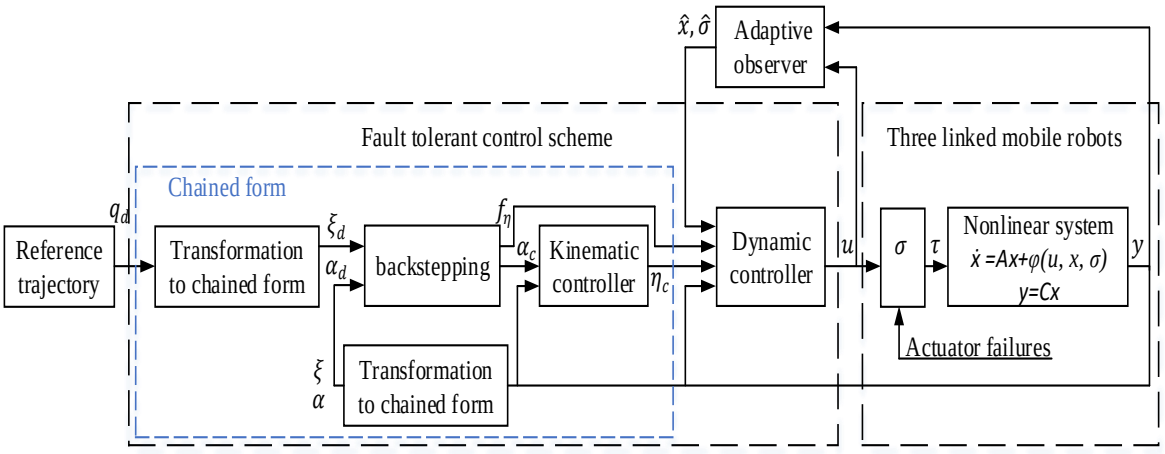

Figure 4.1: Active fault tolerant control scheme for fault estimation.

In the following, based on the proposed actuator fault model (4.3), some fault scenarios are discussed. The fault-free situation can be represented by $\sigma_j = 1$ and $\bar{u}_j = 0$; the loss of control is given by $\sigma_j = 0$ and it is associated with a freely rotating wheel or a stuck motor, represented by $\bar{u}_j = 0$ or $\bar{u}_j \neq 0$, respectively; $0 < \sigma_j < 1$ denotes partial loss of effectiveness of the actuator.

Using Assumption 2.3 defined in Chapter 2 page 43, the dynamic subsystem in (4.2) for three-linked 2WD mobile robots has two control inputs (υ_3, ω_1) to be controlled.

Fault-tolerant control and diagnosis objectives

The control objective is to asymptotically track the reference trajectory, despite the presence of actuators' faults, and the diagnosis objective is to estimate the actuators faults. The control objective can take advantage of the fault estimation, using this information to update the control law.

The control design is based on the approach proposed in Section 3.3.1 of Chapter 3. The same kinematic control law is adopted here but a different version of the dynamic control law is proposed.

In Section 3.3.1 of Chapter 3, multiple dynamic controllers are designed, each one aiming at the compensation of a specific combination of actuators faults, then a switching mechanism selects the proper controller. Besides the undesirable effects of a control switching, by this way only a finite set of possible faults, i.e., $\rho_k(t)$ takes its values in a discrete set, can be considered. On the other hand, here we propose to use an Active FTC

scheme, as shown in Fig. 4.1, which is composed of an adaptive nonlinear observer and an adaptive dynamic control law that uses the estimated fault values for the compensation/accommodation of a set of possible continuous faults, i.e., $\rho_k(t)$ takes any value in the interval [0, 1]. A general scheme for this diagnosis and FTC scheme can be seen in Fig. 4.1. Moreover, we consider here that only the generalized coordinates q are measured and the velocities $\dot{q}$ and η used in the control law are estimated by the observer.

The kinematic controller is designed using a transformation of coordinates (chained form) in combination with a recursive method (backstepping) to derive the control law as in Section 3.3.1 of Chapter 3. The dynamic controller is designed to guarantee system stability and also fault accommodation. The nonlinear adaptive observer provides estimates of the system states and the parameters related to the actuator faults, both used in the dynamic control law and available for fault diagnosis.

4.2.2 Nonlinear adaptive observer and fault diagnosis

4.2.2.1 State-space representation of the system

Let us introduce the following state-space representation of a nonlinear system

$$\dot{x} = Ax(t) + \varphi(u(t), x(t), \bar{\rho})$$
$$y(t) = Cx(t) \tag{4.4}$$

where $x(t) \in \mathbb{R}^n$ is the state vector, $u(t) \in \mathbb{R}^m$ is the control input, $y(t) \in \mathbb{R}^p$ is the system output, $\varphi(u(t), x(t), \bar{\rho}) \in \mathbb{R}^n$ is a nonlinear function; $A \in \mathbb{R}^{n\times n}$ and $C \in \mathbb{R}^{p\times n}$ are time-independent system matrices.

For the three-linked mobile robots described by the kinematic and dynamic models given in (4.1) and (4.2) respectively, we can define the state variables $x_1 = q$ and $x_2 = \dot{q}$ such that the state vector is $x = [x_1^T \quad x_2^T]^T$. The output vector of the system is $y = q = x_1$ which means that only the generalized coordinates are measured.

From (4.1), (4.2) and (4.3), it is easy to express a state-space representation of the system in the form of (4.4) considering

$$A = \begin{bmatrix} 0_{5\times5} & I_{5\times5} \\ 0_{5\times5} & 0_{5\times5} \end{bmatrix}, C = [I_{5\times5} \quad 0_{5\times5}] \tag{4.5}$$

$$\varphi(u,x,\bar{\rho}) = [\varphi_1(u,x,\bar{\rho})^T \quad \varphi_2(u,x,\bar{\rho})^T]^T \tag{4.6}$$

where $\bar{\rho} = [\rho^T, \bar{u}^T]^T$, $I_{5\times5}$ is a 5 × 5 identity matrix, $0_{5\times5}$ is a null square matrix of dimension 5, and

$$\varphi_1(u,x,\bar{\rho}) = 0_{5\times1}$$

$$\varphi_2(u,x,\bar{\rho}) = S(x_1)(\bar{M}_1^{-1}(x_1)(-\bar{M}_2(x_1)(S^+(x_1)x_2 - \bar{C}(x_1,x_2) + \bar{B}(x_1)\bar{\sigma}v))$$

$$+\dot{S}(x_1)S^+(x_1)x_2 \tag{4.7}$$

where $\bar{\sigma} = [\mathrm{diag}(\rho), \mathrm{diag}(\bar{u})]$ and $v = [u^T, 1, 1, 1, 1, 1, 1]^T$.

Note that $S^+(.)$ represents the pseudo-inverse of $S(.)$.

4.2.2.2 Nonlinear adaptive observer

A nonlinear adaptive observer was proposed in [136] to estimate the state x and parameter $\bar{\rho}$ in a nonlinear system (4.4) which respects the following *Assumption 4.1*.

Assumption 4.1: *Considering the nonlinear system represented by (4.4):*

(a) The state x, the control signal u and the unknown parameters ρ are bounded.

(b) The function $\varphi(u,x,\bar{\rho})$ is Lipschitz with respect to x and $\bar{\rho}$, uniformly in u.

(c) The nonlinear parameterization $\varphi(u,x,.)$ is one to one.

Remark 4.1 [136]: *The following notations are adopted for the subsequent definition of the observer equations:*

(a) Given $\Theta > 0$, it is defined:

$$\Delta_\Theta = diag\left[I_P, \frac{1}{\Theta}I_P, \cdots, \frac{1}{\Theta^{q-1}}I_p\right] \tag{4.8}$$

(b) Considering A and C as in (4.4), S_o is the solution of:

$$S_o + A^T S_o + S_o A - C^T C = 0 \tag{4.9}$$

(c) $\forall\tilde{y}(t)\epsilon\,\mathbb{R}^m$, $K(\tilde{y}(t)) = k_1\tanh(k_0\tilde{y}(t))$ with k_1, $k_0 > 0$, is a function that satisfies

$$\tilde{y}^T(t)K(\tilde{y}(t)) \geq \frac{1}{2}\tilde{y}^T(t)\tilde{y}(t) \tag{4.10}$$

Theorem 4.1 [136]: *Considering the class of nonlinear systems (4.4) with Assumption 4.1 and adopting the notations and definitions in Remark 4.1, the estimations $\hat{x}$ of the states x and $\hat{\rho}$ of the parameters $\bar{\rho}$ can be given by the nonlinear adaptive:*

$$\dot{\hat{x}}(t) = A\hat{x}(t) + \varphi\big(u(t), \hat{x}(t), \hat{\rho}(t)\big) - \Theta\Delta_{\theta}^{-1}\big(S_o^{-1} + \Upsilon(t)P(t)\Upsilon^T(t)\big)C^T K(\tilde{y}(t))$$

$$\dot{\hat{\rho}} = -\Theta P(t)\Upsilon^T(t)C^T K(\tilde{y}(t))$$

$$\dot{\Upsilon}(t) = \Theta(A - S_o^{-1}C^T C)\Upsilon(t) + \Delta_{\Theta}\frac{\partial \varphi}{\partial \rho}(u(t), \hat{x}(t), \hat{\rho})$$

$$\dot{P}(t) = -\Theta P(t)\Upsilon^T(t)C^T C\Upsilon(t)P(t) + \Theta P(t) \tag{4.11}$$

with $\Upsilon(t) \in \mathbb{R}^{n\times m}$, $P(t) \in \mathbb{R}^{m\times m}$, $\Upsilon(0) = 0$, $P(0)=P^T(0) > 0$, and $\tilde{y}(t) = y(t) - C\hat{x}(t)$.

The proof of *Theorem 4.1* may be found in [136].

4.2.2.3 Fault estimation

As we mentioned in subsection 4.2.1, the actuators faults are directly related to the actuators gains ρ and additive terms $\bar{u}$. Thus, the estimation of $\bar{\rho} = [\rho^T, \bar{u}^T]^T$ provided by the nonlinear adaptive observer (4.11) can be also interpreted as a fault estimation. Notice that it is possible to estimate simultaneous faults in all the actuators, multiplicative and additive ones. Although, as discussed in this subsection, the system requires a minimum number of actuators to provide sufficient torques, which limits the set of possible faults.

4.2.3 Fault tolerant control design

4.2.3.1 Kinematic controller

The chained form of the kinematic model introduced in Chapter 2, Section 2.5 [40] and a recursive technique based on the classical integrator backstepping [120] give the following kinematic control law which was described in chapter 3:

$$\eta_c = T_{\alpha}^{-1}(\alpha_c - f_{\alpha}) \tag{4.12}$$

where T_{α}, f_{α} and α_c are given in Section 3.3 of chapter 3 (see equations 3.98, 3.102, and 3.103 in chapter 3). This kinematic control law is a function of the measured and desired generalized coordinates q and q_d, respectively. The parameters of this kinematic controller, as well as a performance analysis, are described in details in Section 3.3 of chapter 3.

4.2.3.2 Dynamic controller

Let us consider the dynamic control law as in Section 3.3, equation 3.121. The control signal is given by

$$u = (\bar{M}_1^{-1}\bar{B}\sigma)^{+}\left[-c_6\eta_e - T_\alpha^T f_\eta + \bar{M}_1^{-1}\bar{M}_2\eta + \bar{M}_1^{-1}\bar{C} - \bar{M}_1^{-1}\bar{B}\bar{u} + \dot{\eta}_c\right] \tag{4.13}$$

where $f_\eta = [z_5(\kappa - (z_3 + 2z_1)\xi_3 - (2z_4 + 5z_1)\xi_2), z_5(-z_1 - z_3)]^T$ with $(\kappa, z_1, z_2, z_3, z_4, z_5, \xi_2, \xi_3)$ being as referred in section 3.3.

The control law (4.13) depends on the unknown parameter σ and $\bar{u}$.

The nonlinear adaptive observer (4.11) provides estimates of σ and $\bar{u}$ that can be used in the dynamic control law.

From (4.1) it can be seen that $x_2 = S(x_1)\eta$, which means that $\eta = S^{+}(x_1)x_2$. It is assumed that just the state x_1 is measured ($y = x_1$). Also, an estimation of the state x_2 is provided by the observer. So, an estimation of η can be given by $\hat{\eta} = S^{+}(x_1)\hat{x}_2$. Based on the estimated signals $\hat{x}_2$, $\hat{\eta}$ and also $\hat{\sigma}$ and $\hat{\bar{u}}$ the dynamic control law can be reformulated as:

$$u = (\bar{M}_1^{-1}\bar{B}\hat{\sigma})^{+}[-c_6\hat{\eta}_e - T_\alpha^T f_\alpha + \bar{M}_1^{-1}\bar{M}_2\hat{\eta} + \bar{M}_1^{-1}\bar{C} - \bar{M}_1^{-1}\bar{B}\hat{\bar{u}} + \dot{\eta}_c] \tag{4.14}$$

where $\hat{\eta}_e = \hat{\eta} - \eta_c$.

4.2.4 Simulation studies

The case of two-linked 2WD mobile robots

We consider a two-linked 2WD mobile robots system, where each of the two 2WD mobile robots are as described in [34]. The parameters of the robots are: $a_1 = a_2 = 0.3\ m$, $b_1 = b_2 = 0.75\ m$, $r_1 = r_2 = 0.15\ m$, $m_1 = m_2 = 30\ kg$, $I_{m1} = I_{m2} = 15.625\ kg \cdot m^2$. The length of the link between the two robots is $d = 1\ m$.

In order to verify the effectiveness of the fault compensation control and the fault estimation, the actuators' faults described in Table 4.1 is considered. Only the actuator $1r$ is healthy at the beginning of the simulation but at time 35 (s) the gain of this actuator also changes to totally lose effectiveness.

The parameters of the kinematic and dynamic controllers are chosen as $k_1 = 1$ $k_2 = 1$, $k_3 = 0.2$, and $k_4 = 20$. The initial conditions are $x_1(0) = q(0) = [0, 1, 0]^T$ and

$x_2(0) = \dot{q}(0) = [0,1,0]^T$. For the observer, the initial conditions are $P(0) = 0.1I_{4\times4}$, $x(0) = [0,0,0,0,]^T, \rho(0) = [1,1,1,1], \bar{u} = [0,0,0,0]$; the other parameters are $k_0 = k_2 = 1\ and\ \Theta = 1.6$. The parameter Θ is freely selected in order to provide convergence. The simulation was performed in MATLAB/SIMULINK with total simulation time $T = 70\ [s]$, sampling time $T_s = 10\ [ms]$, and solver ode4 (runge-kutta).

Fig. 4.2(a) shows the reference trajectory in plane (x, y), which is defined for robot 2, and the achieved trajectories for each robot. Despite the severe actuators' faults profile, it can be seen that the controlled system asymptotically tracks the desired trajectory. The tracking error $q_d - q$ is presented in Fig. 4.2(b).

The nonlinear adaptive observer provides accurate state estimations as shown in Fig. 4.3(a). At time $t = 35\ [s]$, due to the faults, a transient behavior appears, which is shown in Fig. 4.3(b).

The estimated multiplicative and additive actuators faults can be seen in Fig. 4.4(a) and Fig. 4.4(b), respectively. It is clear that the estimated values of ρ and $\bar{u}$ converge to the actual values described in TABLE 4.1.

The simulations were performed considering a saturation of the torque signals at 5 [N. m]. So, the increasing values during the transients, as shown in Fig. 4.5 and Fig. 4.6, are truncated at 5 [N. m], but rapidly decreases to small values.

Fig. 4.7 and Fig. 4.8, show the linear and angular velocities of each robot.

Table 4.1: Actuators' faults.

$0 \leq t < 35$	$35 \leq t \leq 70$
$\rho_{1r} = 1$	$\rho_{1r} = 1$
$\rho_{2l} = 1$	$\rho_{2l} = 0$
$\rho_{2r} = 1$	$\rho_{2r} = 0.8$
$\rho_{2l} = 0.5$	$\rho_{2l} = 0.5$
$\bar{u}_{1r} = 0$	$\bar{u}_{1r} = -0.5$
$\bar{u}_{1l} = 0$	$\bar{u}_{1l} = 0$
$\bar{u}_{2r} = 0$	$\bar{u}_{2r} = 0$
$\bar{u}_{2l} = 0$	$\bar{u}_{2l} = 0$

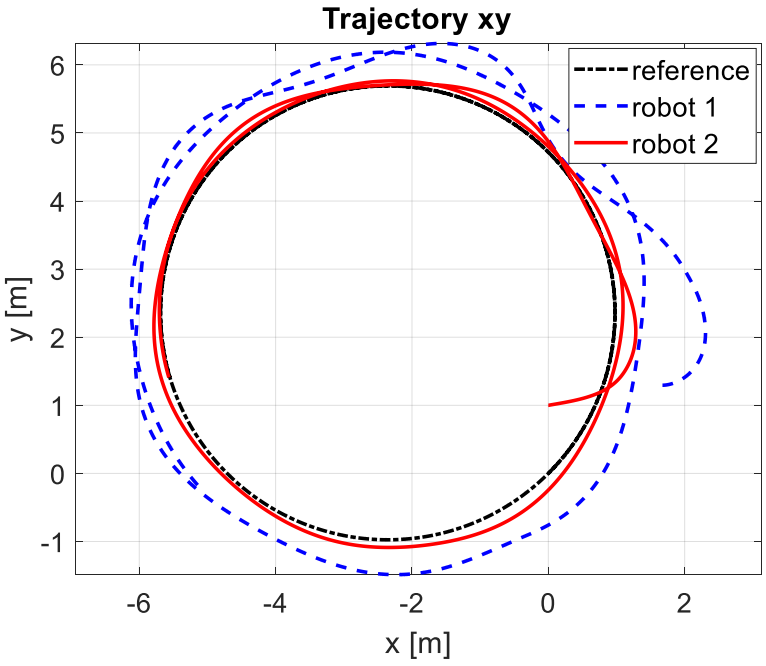

(a) Trajectories (reference, robot 1 and robot 2) in the plane $x - y$. The control objective is the reference tracking by robot 2.

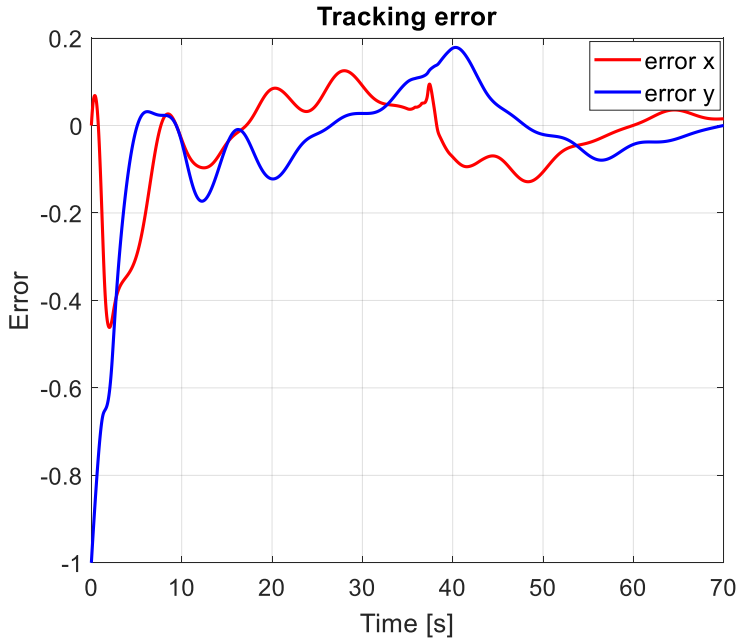

(b) Transient behavior of the tracking error between reference and simulated trajectories.

Figure 4.2: Trajectories of the mobile robots and tracking errors

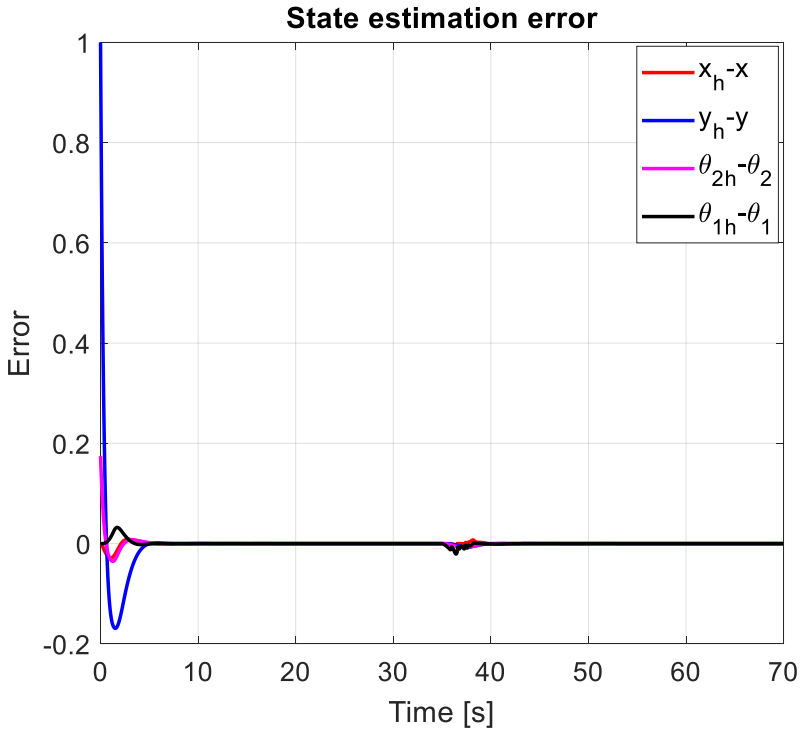

(a) State estimation error.

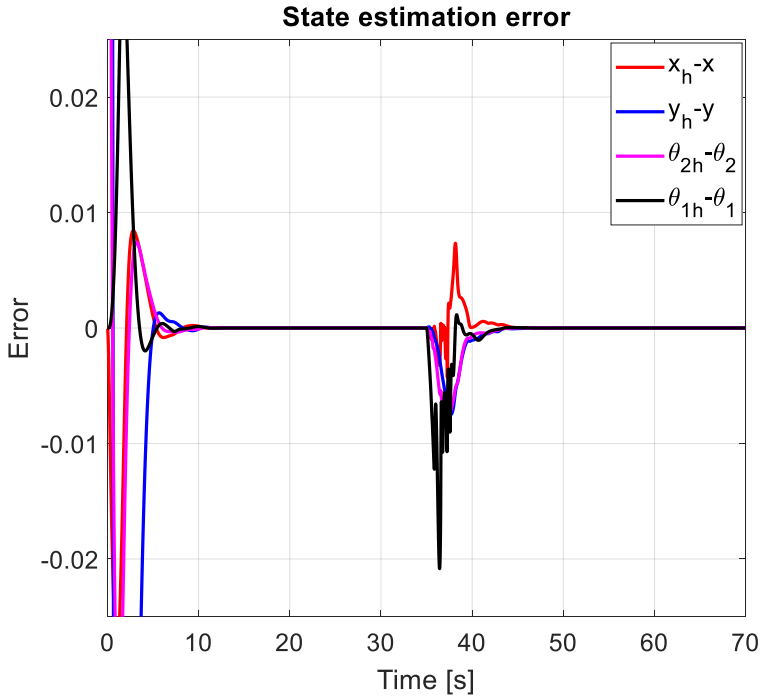

(b) Zoom of the state estimation error.

Figure 4.3: State estimation error.

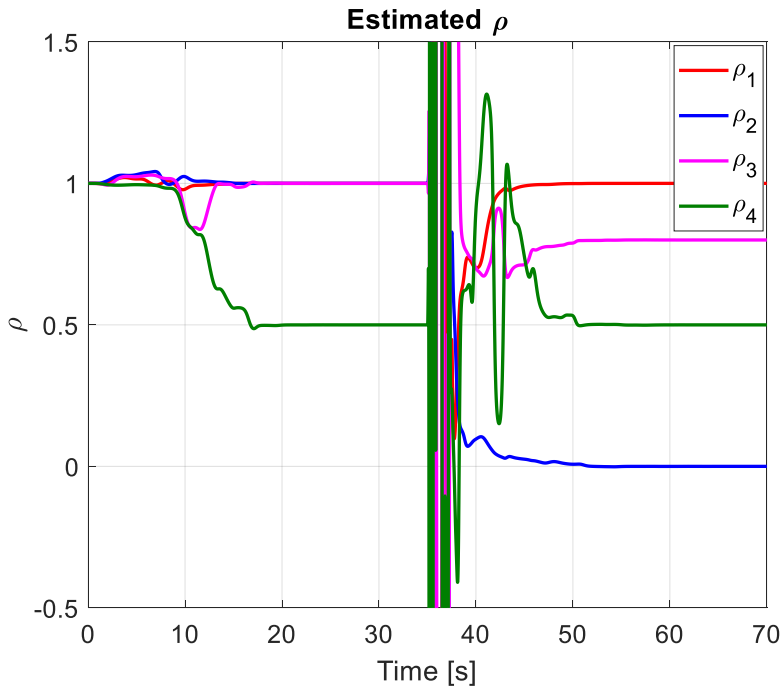

(a) Estimated ρ

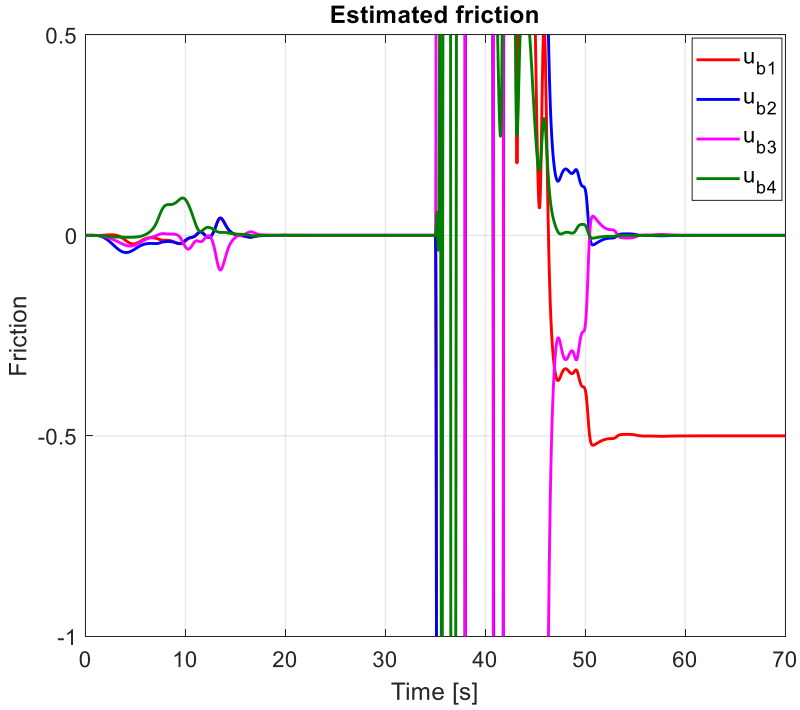

(b) Estimated $\bar{u}$.

Figure 4.4: Estimations of ρ and $\bar{u}$.

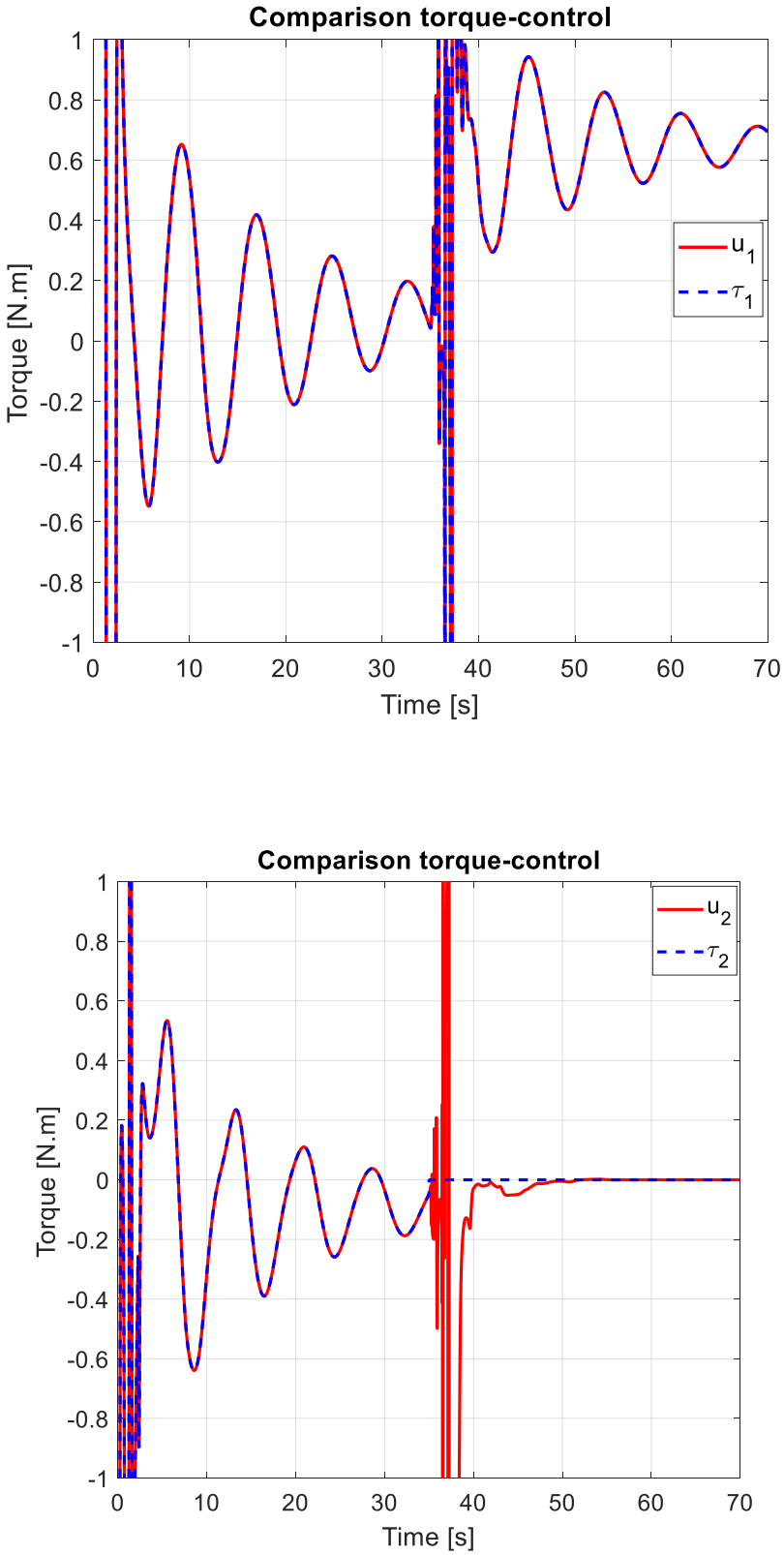

Figure 4.5: Applied torques and control signals of robot 1.

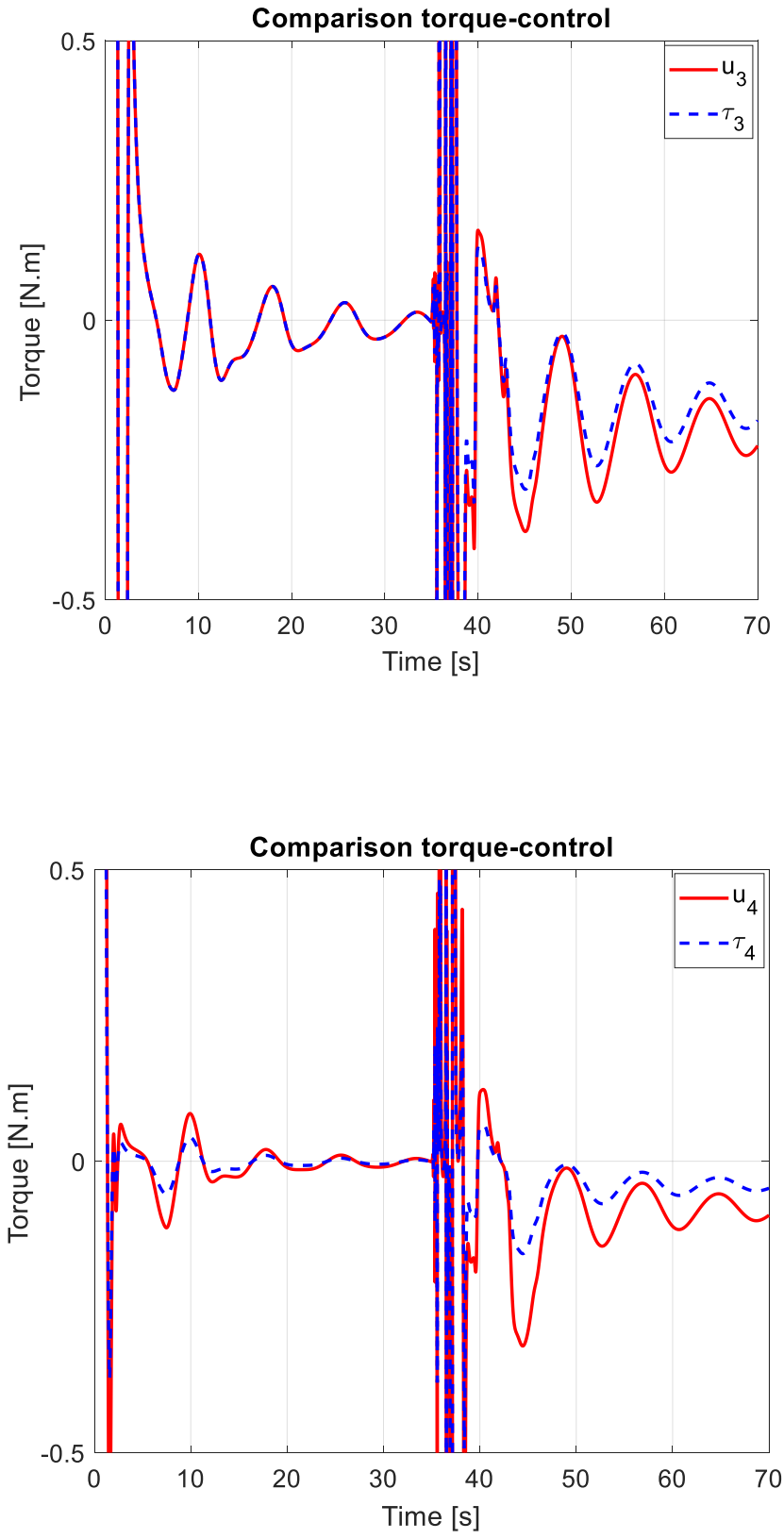

Figure 4.6: Applied torques and control signals of robot 2.

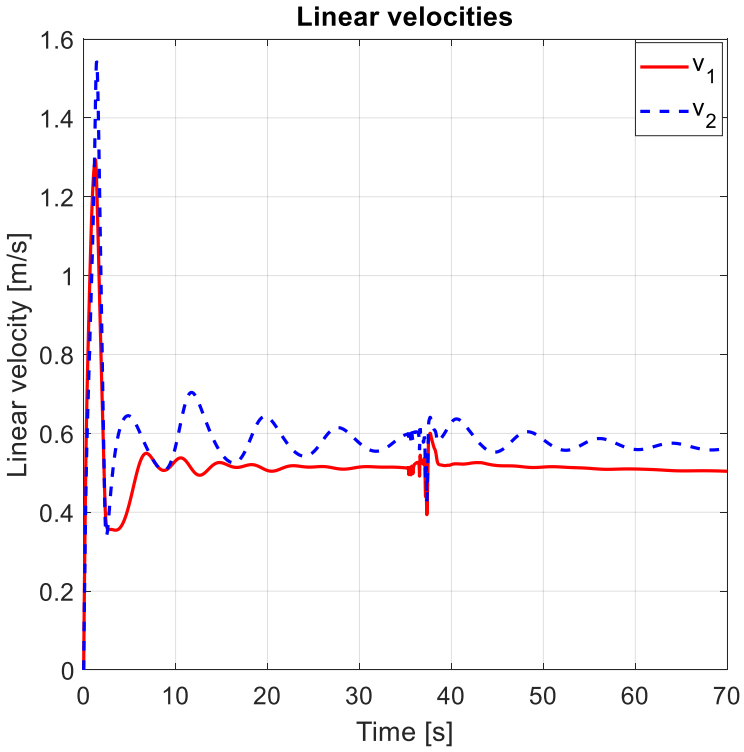

Figure 4.7: Linear velocities of robot 1 and robot 2.

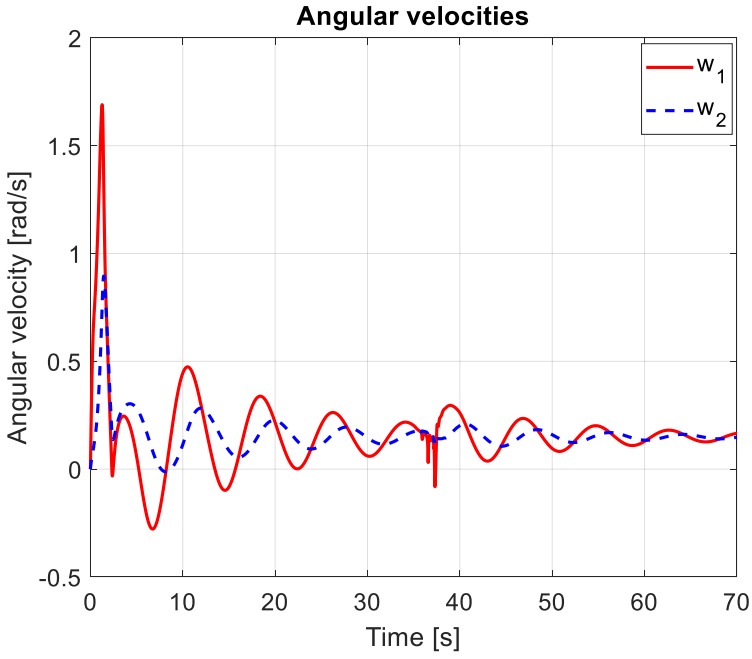

Figure 4.8: Angular velocities of robot 1 and robot 2.

The case of three-linked 2WD mobile robots

We consider now a three-linked 2WD mobile robots system, where each of the three 2WD mobile robots are as described in [34]. The parameters of the robots are: $a_1 = a_2 = a_3 = 0.3\ m$, $b_1 = b_2 = b_3 = 0.75\ m$, $r_1 = r_2 = r_3 = 0.15\ m$, $m_1 = m_2 = m_3 = 30\ kg$, $I_{m1} = I_{m2} = I_{m3} = 15.625\ kg \cdot m^2$. The length of the link between each two robots is $d = 1\ m$.

In order to verify the effectiveness of the fault compensation control and the fault estimation, the actuators' faults described in Table 4.2 are considered. We are considering a fault condition characterized by a severe loss of effectiveness (multiplicative fault), without considering friction (additive fault). The control objective is that each robot should track a sinusoidal trajectory. Only the actuator $1r$ is healthy at the beginning of the simulation but at time 1100 (s) the gain of this actuator also changes.

The parameters of the kinematic and dynamic controllers are chosen as $C_4 = 2$, $C_5 = 2$, $C_6 = 5$ and $\kappa = 5$. For the observer, the chosen parameters are $\theta = 0.9$ and $k_0 = k_1 = 1$. The parameter Θ is selected in order to provide convergence.

The reference trajectories for the generalized coordinates q are sinusoidal ones. Fig. 4.9 (a), shows the trajectories in plane (x, y): desired, simulated (output of the controlled system) and estimated. Despite the severe faults, the controlled system asymptotically tracks the desired planar trajectory. Considering the full vector q and the desired trajectory $q_d = (x_d, y_d, \theta_{3d}, \theta_{2d}, \theta_{1d})$, a detailed view of the tracking error is presented in Fig. 4.9 (b).

The nonlinear adaptive observer provides accurate state estimation as shown in Fig. 4.10 (a), where the state estimation error is shown during the transient response at the beginning of the simulation ($t < 50\ (s)$). At time $t = 220\ (s)$, due to the faults, a transient behavior appears, which is shown in Fig. 4.10 (b).

The estimated actuator gains can be seen in Fig. 4.11 and Fig. 4.12. It is clear that the estimated values of ρ converge to the actual values described in TABLE 4.2. We can see in Fig 4.13, the filtered version of the estimations, using a first-order low-pass filter whose transfer function is 1/(30s+1). The estimations are filtered to make the signal smooth and reduce the rapid oscillations. It will also be useful to reduce the noise influence and the high-frequency disturbances in practical situation. These filtered estimations are used in the feedback controller.

The control signals have relatively high values during the first transient, as shown in Fig. 4.14, Fig. 4.15 and Fig. 4.16, but rapidly decrease to small values. The linear and angular velocities of each robot are shown in Fig 4.17 and 4.18.

Table 4.2: Actuators' faults.

$0 \leq t < 220$	$220 \leq t \leq 400$
$\rho_1 = 1$	$\rho_1 = 0.8$
$\rho_2 = 0.3$	$\rho_2 = 0.3$
$\rho_3 = 0.4$	$\rho_3 = 0.4$
$\rho_4 = 0.2$	$\rho_4 = 0.2$
$\rho_5 = 0.1$	$\rho_5 = 0.1$
$\rho_6 = 0.7$	$\rho_6 = 0.7$

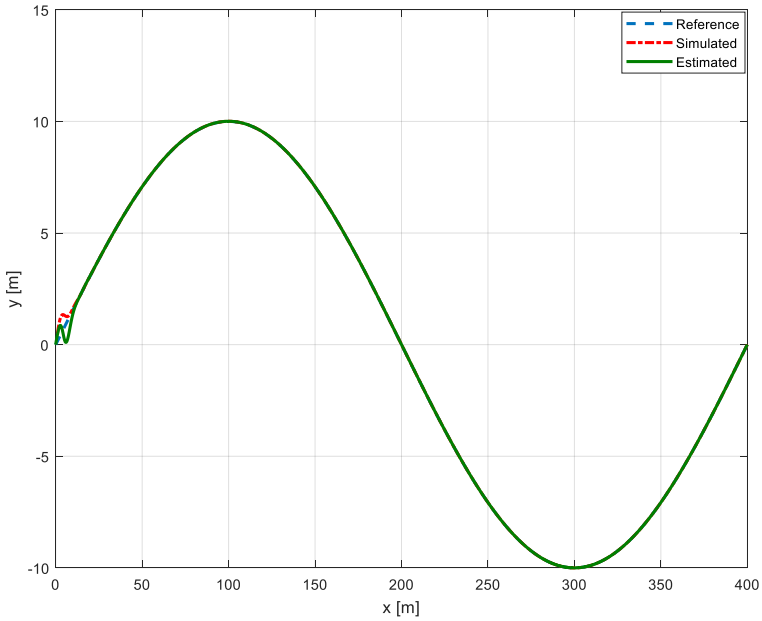

(a) Trajectories (reference, simulated) in the plane $\boldsymbol{x} - \boldsymbol{y}$.

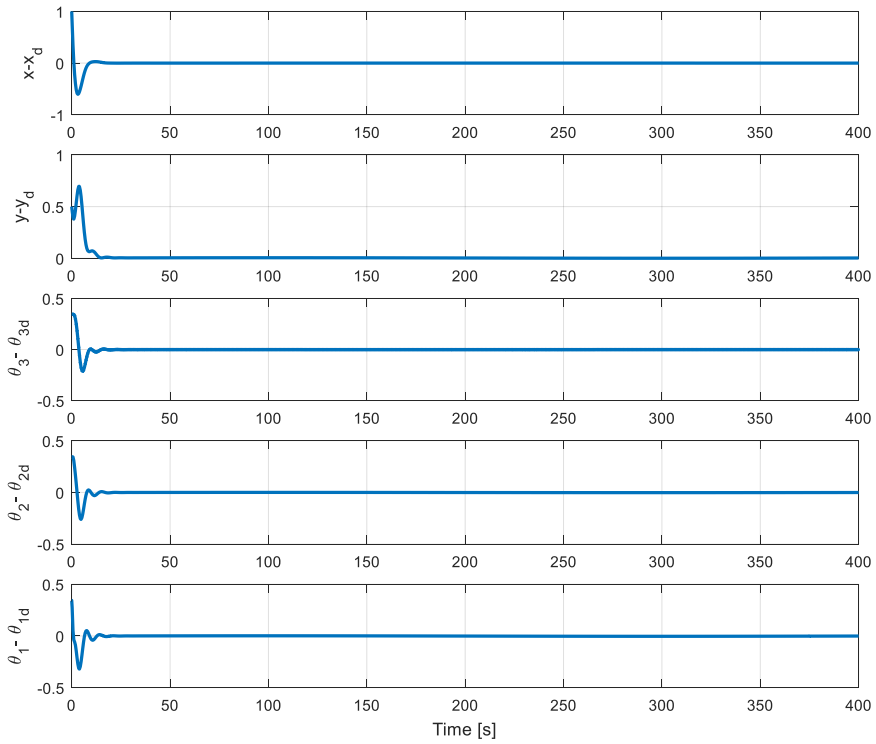

(b) Tracking error between reference and simulated trajectories.

Figure 4.9: Trajectories of the mobile robots and tracking errors.

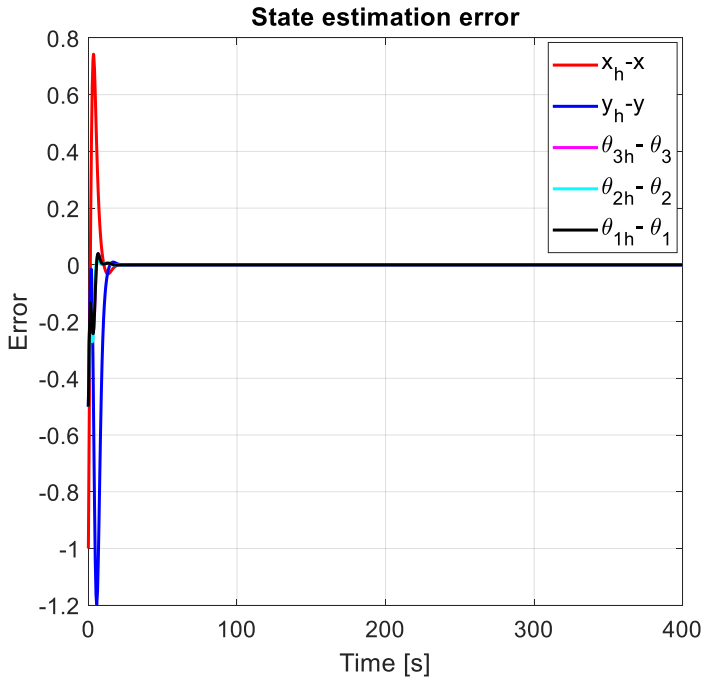

(a) State estimation error - the transient behavior after the change in ρ_1.

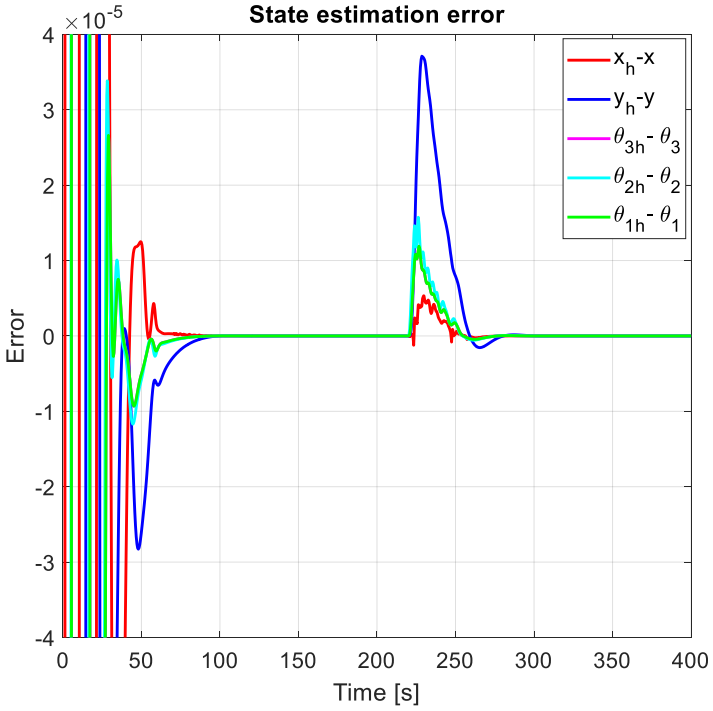

(b) State estimation error – zoom on the transient behavior at the initial time instants.

Figure 4.10: State estimation error.

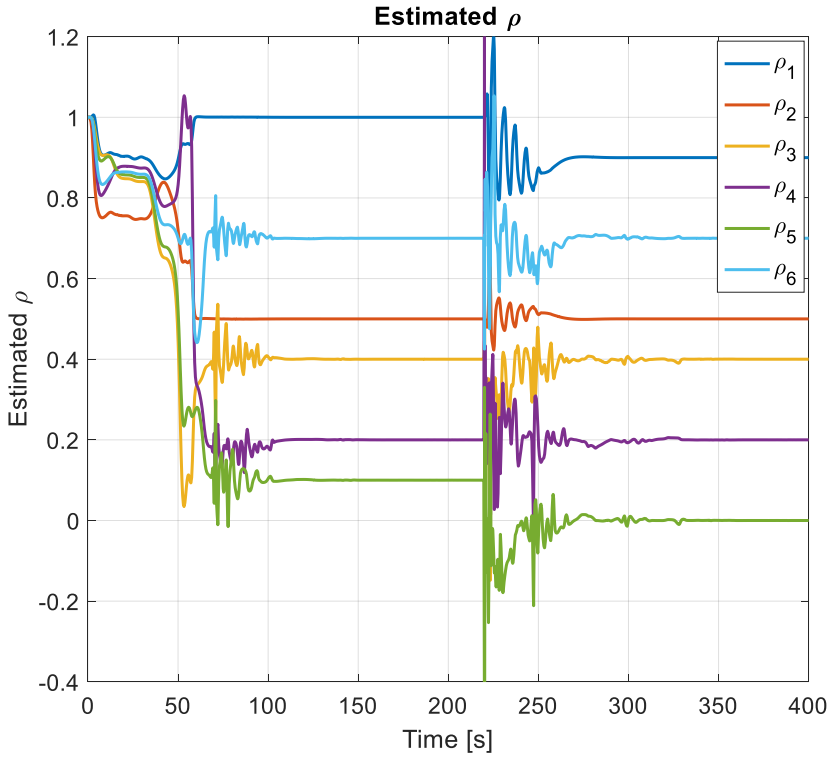

Figure 4.11: Estimated ρ (unfiltered).

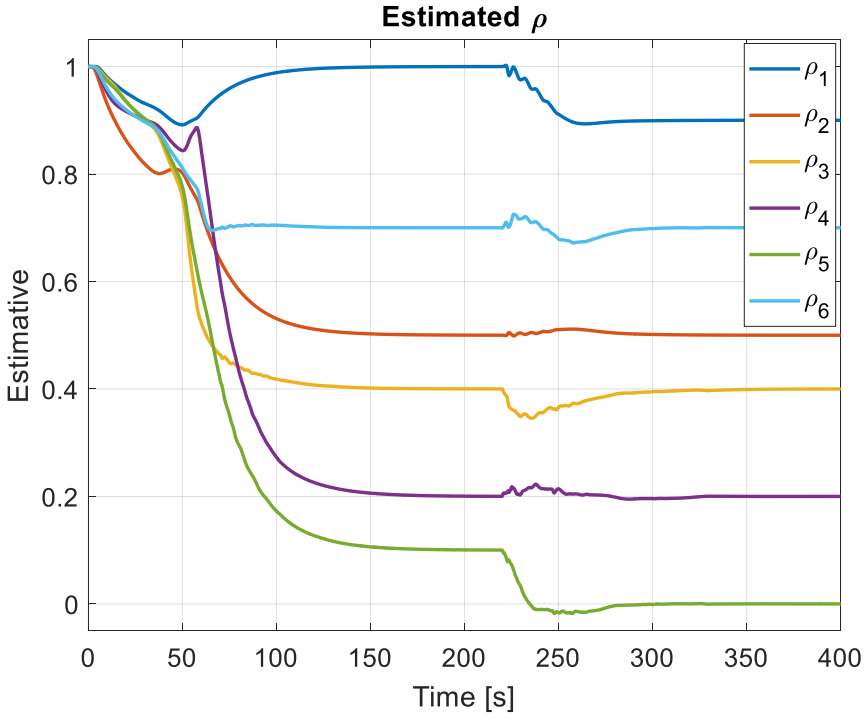

Figure 4.12: Estimated ρ (filtered).

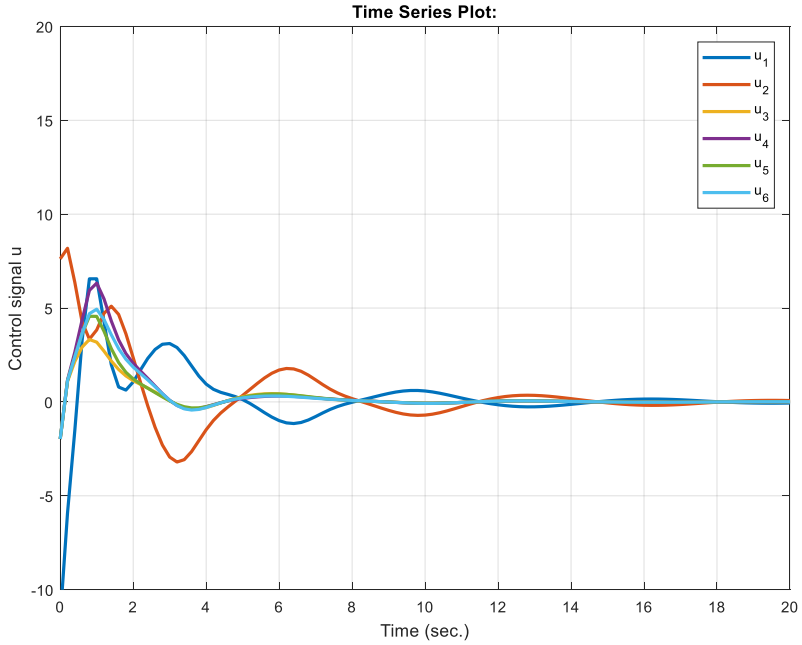

(a) Control signals at first transitory behavior.

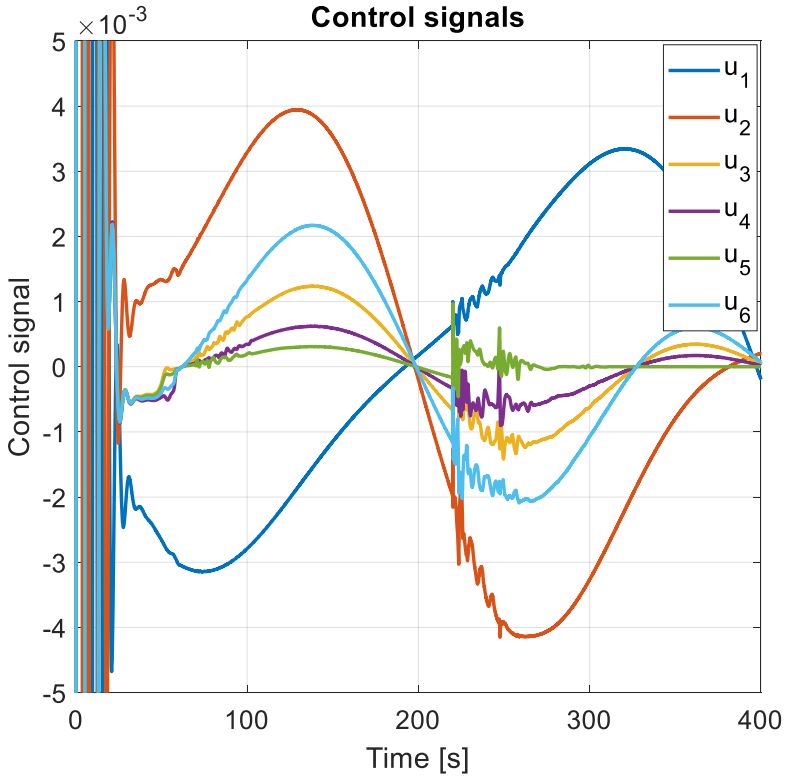

(b) Control signals with zoom in the y-axis emphasizing the behavior after the transient.

Figure 4.13: Control signal.

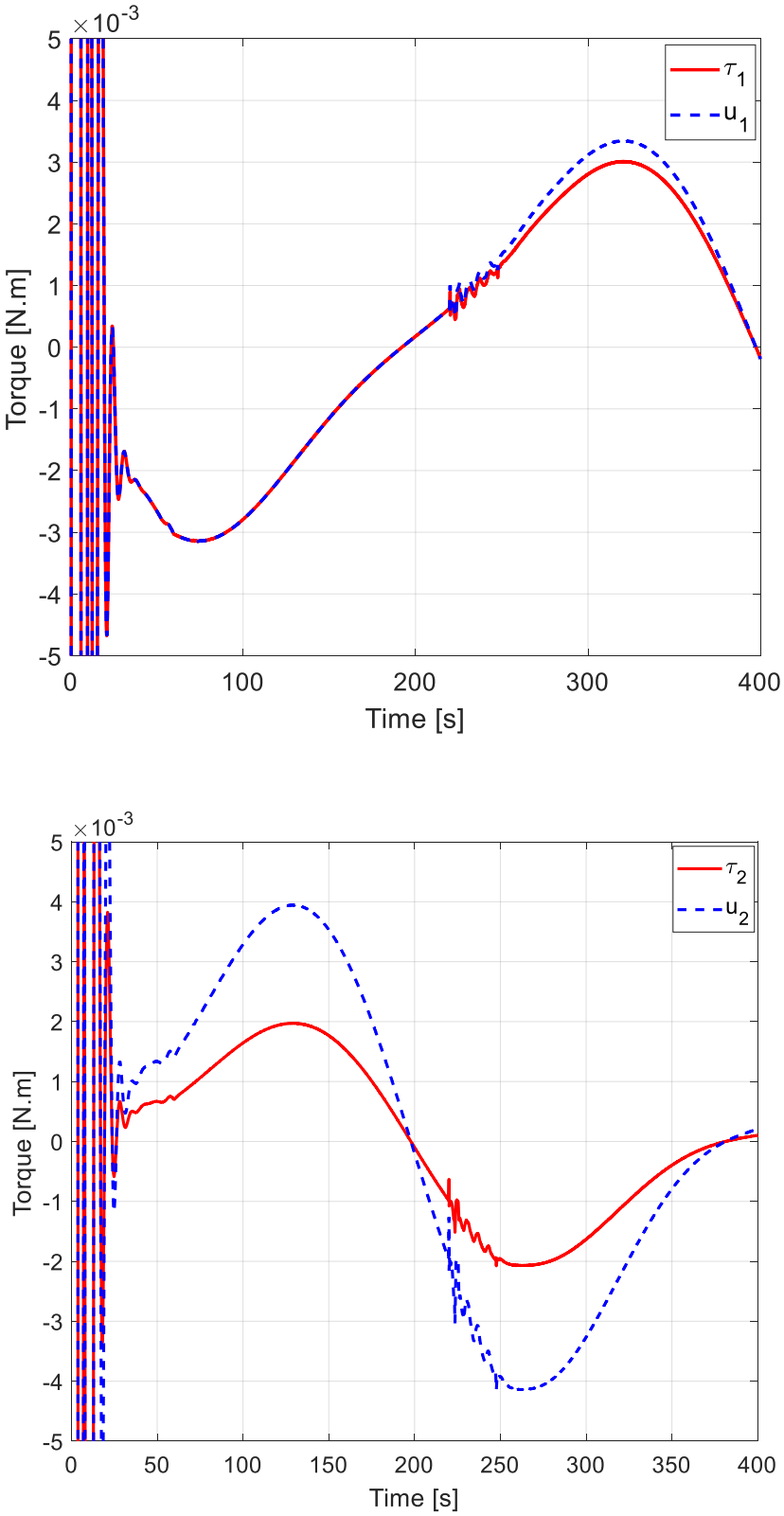

Figure 4.14: Comparison torque-control of robot 1.

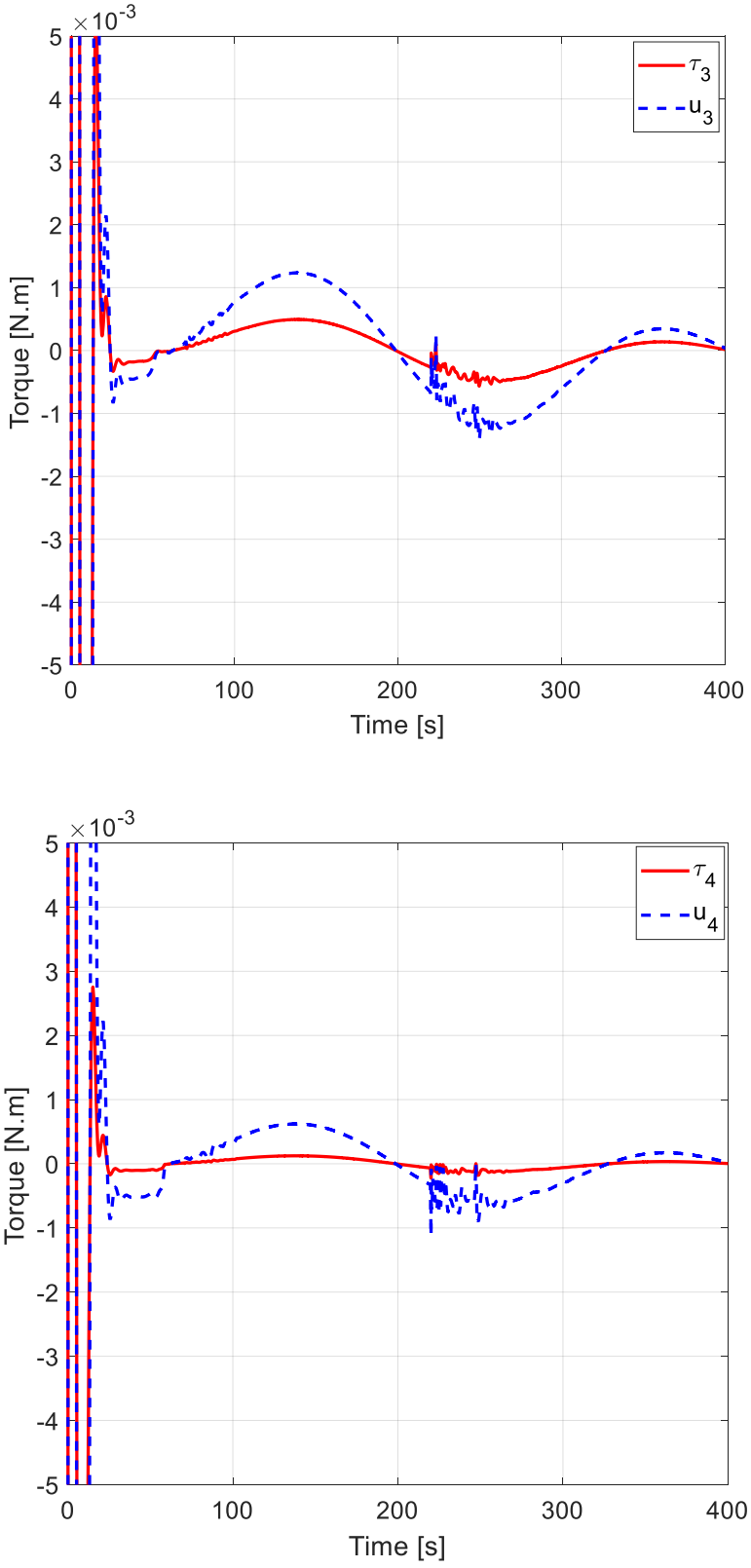

Figure 4.15: Comparison torque-control of robot 2.

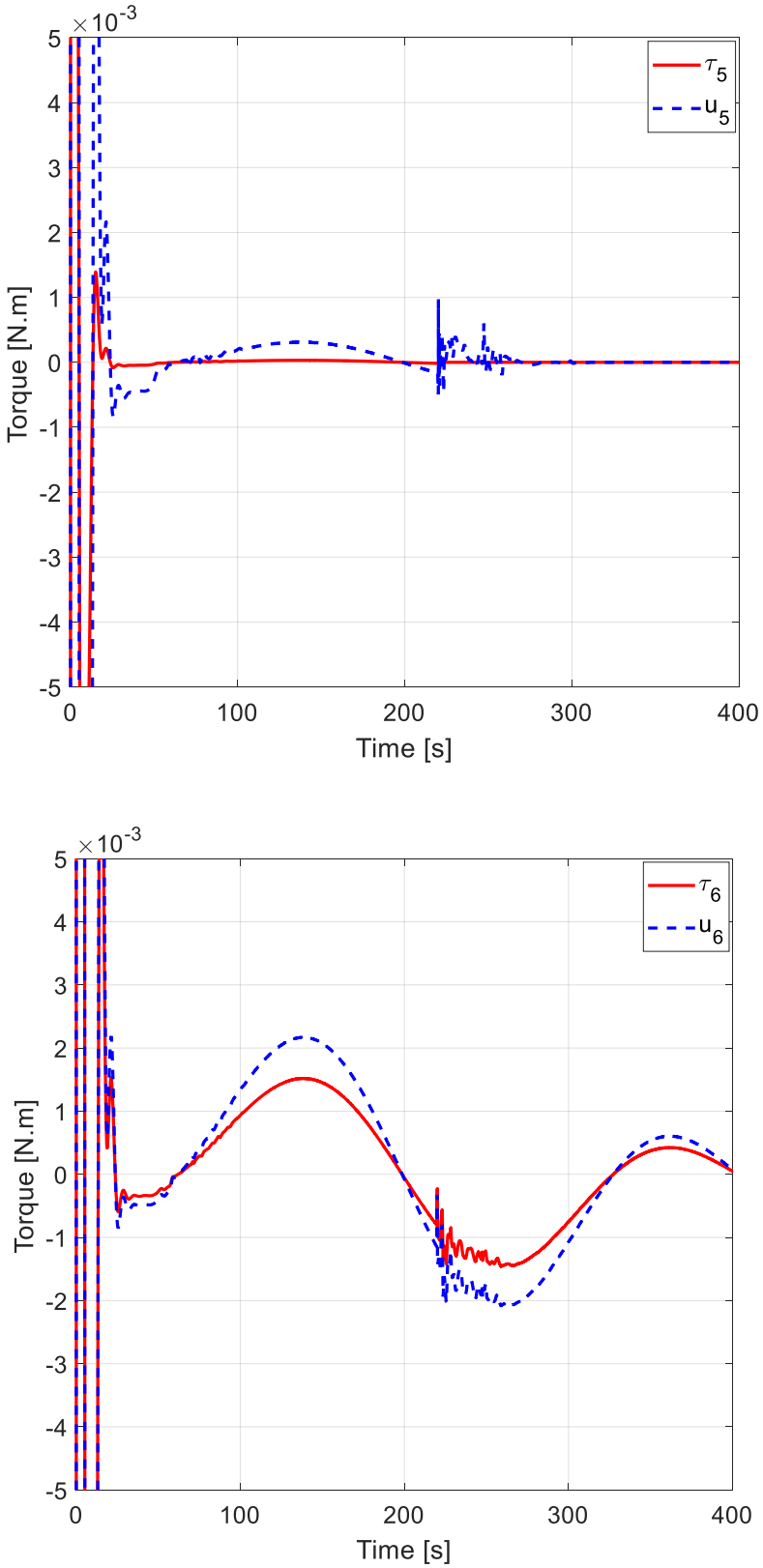

Figure 4.16: Comparison torque-control of robot 3.

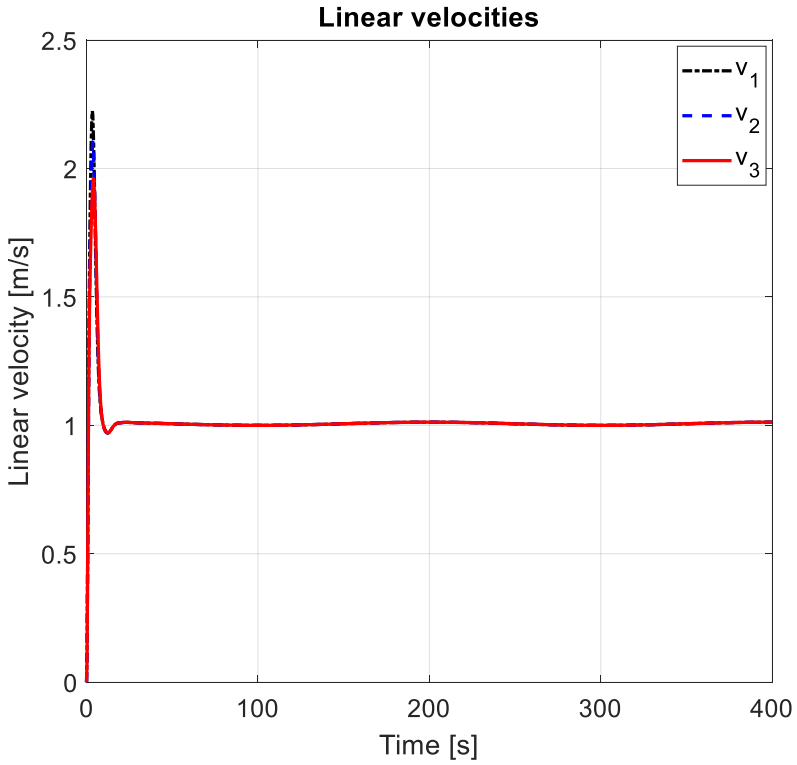

Figure 4.17: Linear velocities of robot 1, 2 and robot 3.

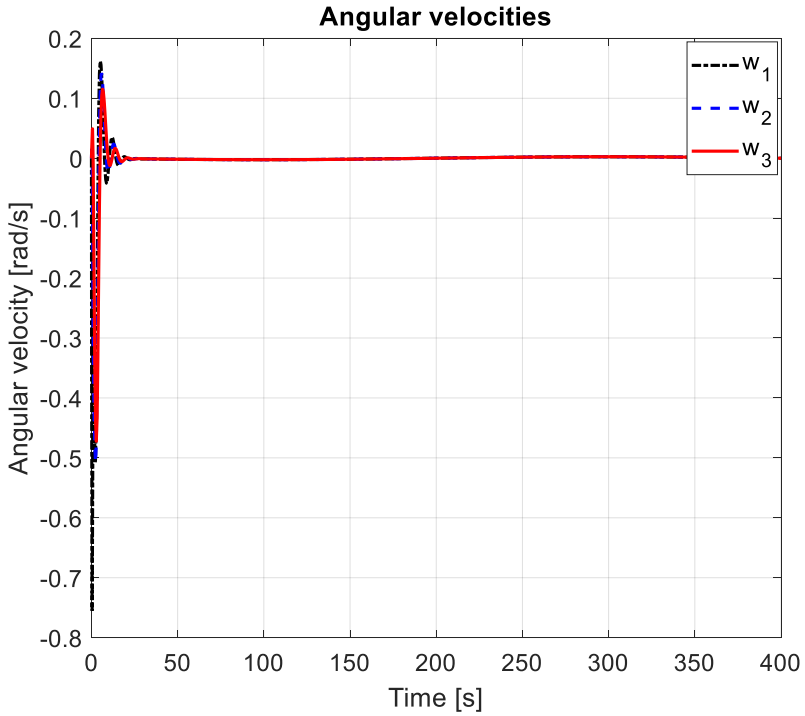

Figure 4.18: Angular velocities of robot 1, 2 and robot 3.

4.3 Generalization of FD and FTC for n-linked 2WD mobile robots

The active FTC method which has been designed for three-linked 2WD mobile robots in Section 4.2, can be directly generalized for n-linked 2WD robots for any n greater than one. For the reference trajectory tracking, the control scheme developed in Chapter 3 is adopted, the dynamic control law is modified by incorporating the faults and system states estimations. The observer is used to estimate the multiplicative and additive actuator faults corrupting the applied torques, and also to estimate the non-measured states of the system, which are needed to apply the feedback control law.

4.3.1 Nonlinear adaptive observer and fault diagnosis

For the n-linked 2WD mobile robots described by the kinematic and dynamic models given in Section 2.4.3, in equations (2.63) and (2.70) respectively, we choose the state variables $x_1 = q$ and $x_2 = \dot{q}$. The state vector of the system is $x = [x_1^T \quad x_2^T]^T$. Then, using (2.63), (2.70), and also the actuator fault model given for n-linked 2WD mobile robots in (2.102), it is possible to give a state-space representation of the system in the form of (4.6) with

$$\dot{x} = Ax(t) + \varphi(u(t), x(t), \bar{\rho})$$
$$y(t) = Cx(t) \tag{4.15}$$

where

$$A = \begin{bmatrix} 0_{N\times N} & I_N \\ 0_{N\times N} & 0_{N\times N} \end{bmatrix}, C = [I_N \quad 0_{N\times N}] \tag{4.16}$$

$$\varphi(u, x, \rho) = [\varphi_1(u, x, \rho)^T \quad \varphi_2(u, x, \rho)^T]^T \tag{4.17}$$

where I_N is a $N \times N$ identity matrix, the zeros in A and C are matrices of proper dimensions such that $A \in \mathbb{R}^{2N\times 2N}$ and $C \in \mathbb{R}^{N\times 2N}$,

and

$$\varphi_1(u, x, \rho) = 0_{N\times 1}$$
$$\varphi_2(u, x, \rho) = S(x_1)(\bar{M}_1^{-1}(x_1)(-\bar{M}_2(x_1)(S^+(x_1)x_2 - \bar{C}(x_1, x_2)$$
$$+\bar{B}(x_1)\sigma u)) + \dot{S}(x_1)S^+(x_1)x_2 \tag{4.18}$$

where N is the dimension vector of the generalized coordinates of the system q, and $N = n + 2$.

4.3.1.1 Nonlinear adaptive observer

A nonlinear adaptive observer as proposed in [136] is used to estimate the state x and parameter $\bar{\rho}$ in a nonlinear system (4.4) which respects the properties given in *Assumption 4.1*, *Remark 4.1*, and *Theorem 4.1* in the Section 4.2.

4.3.1.2 Fault estimation

As we mentioned in subsection 4.2.1, the actuators faults are directly related to the actuators gains ρ and additive terms $\bar{u}$. Thus, the estimation of $\bar{\rho} = [\rho^T, \bar{u}^T]^T$ provided by the nonlinear adaptive observer (4.11) can be also interpreted as a fault estimation. Notice that it is possible to estimate simultaneous faults in all the actuators. Although, as discussed in subsection 4.2.1, the system requires a minimum number of actuators to provide sufficient torques, which limits the set of possible faults.

4.3.2 Fault tolerant control design

The control design is based on the approach proposed in Section 3.2.1 of Chapter 3. For the kinematic control law, a generalization of the FTC for n-linked 2WD mobile robots can be performed as discussed in Chapter 3, Section 3.4. By this way, the kinematic controller is designed using a transformation of coordinates (chained form) [40] in combination with a recursive method (backstepping) [120].

General dynamic control laws including actuator fault are designed, each of which is designed using one possible failure pattern matrix. If the failure pattern which is used in the controller is consistent with the actual one, then the applied control signal can ensure desired system performance. We can find different dynamic control law including, multiple and adaptive fault tolerant dynamic controllers.

The nonlinear adaptive observer gives estimates of the system states and the parameters related to the actuator faults, both are used in the dynamic control law and available for fault diagnosis. By this way, the proposed control and diagnosis scheme allows fault estimation and fault tolerant control.

4.4 Conclusion

The nonlinear adaptive observer adopted in this work is capable of estimating actuators multiplicative and additive constant faults on n physically linked 2WD mobile robots. In the control scheme composed of a kinematic and a dynamic controller, the estimated actuator faults and the estimated state-space variables are used to update the dynamic control law, guaranteeing trajectory tracking with fault tolerance. By this way, the proposed control and diagnosis scheme allows fault estimation and fault tolerant control. We illustrated the effectiveness of the overall approach by simulations for two-linked and three-linked robots.

CHAPTER 5

Conclusions and Future Work

The work presented in this manuscript was dedicated to the trajectory tracking control of multi-linked 2WD mobile robots with actuator faults. The different passive and active fault tolerant control schemes that have been proposed are based on common theoretical tools related to WMR kinematic and dynamic models, and also nonlinear adaptive control, and nonlinear adaptive observer theories. The proposed passive and active FTC schemes have been validated in simulation for two-linked and three-linked 2WD robots.

One of the contributions of this thesis concerns to the development of a general control strategy for the multi-linked 2WD mobile robots to compensate for actuator fault. The configuration of n $(n > 1)$ physically linked 2WD mobile robots was proposed in Chapter 2, Section 2.4 to deal with the actuator faults. The kinematic and dynamic models of the multi-linked 2WD mobile robots have been proposed, and a generalization of the FTC compensation method for multi-linked 2WD mobile robots was elaborated in Chapter 3, Section 3.4. Using a chained form representation, a recursive algorithm was proposed to design the kinematic controller for n linked robots to guarantee that all the system's states converge to their desired trajectories. Furthermore, a general dynamic control law including actuator fault was designed considering the unknown failure pattern matrix.

Different passive FTC strategies were proposed to deal with the unknown failure pattern matrix in the dynamic control law.

A multiple model actuator failure compensation scheme for two-linked 2WD mobile robots was developed in Chapter 3, Section 3.2, to compensate for actuator failures, consisting of a kinematic controller, multiple dynamic controllers and a control switching mechanism, which ensure system stability and asymptotic tracking properties. Indeed, the approach proposed for the design of the kinematic controller is suitable only for the specific case of two-linked 2WD mobile robots. A diffeomorphism relating the kinematic and dynamic controllers was found. However, it is very difficult to find in the same way a diffeomorphism for more than two-linked 2WD mobile robots. Furthermore, even if we

can find this diffeomorphism, the control objective will be always designed only for the last robot of the 2WD multi-linked mobile robots. Moreover, the switching mechanism in the dynamic controller can produce undesirable effects on the control signal. As a consequence, a control solution which is well-suited for n-linked ($n > 2$) 2WD mobile robots was presented in Chapter 3, Section 3.3.1. The provided solution is based on the chained form model introduced in Chapter 2, Section 2.5. Using the transformed system representation, a recursive technique was proposed in Chapter 3, Section 3.3.1 to derive the kinematic control law. The fault compensation is provided by multiple dynamic controllers that are designed considering a fixed set of possible failure cases. Although providing a kinematic controller adequate for the n-linked system, this method still has the switching problem related to the dynamic controller. Besides, the method does not consider model uncertainties and disturbance inputs, as for instance the friction.

In order to design a FTC for multi-linked 2WD mobile robots with friction and actuator faults, the same kinematic control law derived in Chapter 3, Section 3.3.1 is used, but the dynamic control is different. Therefore, a multi-design integration based adaptive actuator failure was presented in Chapter 3, Section 3.3.2, to avoid the control switching mechanism and also conveniently deal with the friction. Nevertheless, this multi-design integration-based method is still based on a fixed discrete set of possible failure pattern matrices.

The control methods presented in passive FTC do not give any information on the faults that occur. This information on the faults would be useful for maintenance operations. Moreover, only limited fault cases were considered with the passive FTC techniques. In order to improve the work on this direction, an Active Fault Tolerant Control scheme was presented and designed in Chapter 4. A nonlinear dynamic observer was used not only to estimate the actuator fault signal but also to estimate the states that are needed in the feedback control law.

Future work

Based on existing researches, this thesis gives some preliminary solutions for FTC and FD for multi-linked 2WD mobile robots with actuator fault. However, some problems are still not solved in the thesis. They are presented as follows:

We worked only with simulations, without experiments with the real robots, which should be an obvious extension of this work. During the thesis period we have not been able to apply the different FTC algorithms on real robots because in our experimental platform composed of TurtleBot 2 robots, it was not possible to access the wheel motors control inputs. Recently, we have bought new TurtleBot 3 robots which makes it possible to access these control signal.

In order to guarantee the robustness of the controllers, the uncertainties related to the kinematic and dynamic model should be taken into account. In future works, adaptive robust control design methods for nonlinear systems, such as in [139], should be applied to the multi-linked 2WD mobile robots. Other FTC technique that could be used, for instance sliding mode control as in [126, 140], predictive control as in [141], to improve and give better performance.

The robot configuration that we considered has the form of a snake-like robot (or a tractor-trailer), with a leader and followers. However, many other configurations for the linked mobile robots could be used, such as star-like, triangular, etc. The leader-follower based configurations have the disadvantage of requiring that the leader must have at least one actuator working, a limitation that could be solved by a different configuration that doesn't require a leader.

Another limitation of the FTC laws proposed in this thesis is that they are designed without considering the saturation of the controller. Methods including constraints of the control signal in the controller design [142] may be useful to overcome this problem and should be considered in future works.

We worked only with the actuator faults. Other types of faults, such as sensor fault, communication faults, component faults, etc., can also be included in the FTC and FD scheme. For example, the observer used in the Active FTC scheme proposed on this thesis could be modified, as suggested in [143, 144], in order to simultaneously estimate actuator and sensor faults.

APPENDIX A

INPUT TRANSFORMATION MATRIX $B(q)$ IN (2.43)

Define the unit vectors for the directions of the two robots in forward movements as

$$U_1 = [cos\,\theta_1\,, sin\,\theta_1]^T\,, \quad U_2 = [cos\,\theta_2\,, sin\,\theta_2]^T \tag{A.1}$$

where $cos\,\theta_i$ and $sin\,\theta_1$ $(i = 1, 2)$ are the components in the X and Y directions, respectively. Then, the control force and torque vectors generated by actuators are

$$F_1 = \frac{\tau_{1r} + \tau_{1l}}{r_1} U_1, \qquad F_2 = \frac{\tau_{2r} + \tau_{2l}}{r_2} U_2$$

$$M_{t1} = \frac{\tau_{1r} - \tau_{1l}}{r_1} b_1\,, \quad M_{t2} = \frac{\tau_{2r} - \tau_{2l}}{r_2} b_2 \tag{A.2}$$

where M_{ti} $(i = 1, 2)$ are in the Z direction.

Let

$$r_{p1} = [x + d\,cos\,\theta_2\,, y + d\,sin\,\theta_2]^T\,, \quad r_{p2} = [x, y]^T \tag{A.3}$$

be the position vectors of P_1 and P_2. Then, the variation of the work done by the applied generalized forces is

$$\delta W = F_1^T \delta r_{p1} + F_2^T \delta r_{p2} + M_{t1}\delta\theta_1 + M_{t2}\delta\theta_2 \tag{A.4}$$

where δr_{p1}, δr_{p2}, $\delta\theta_1$ and $\delta\theta_2$ are variations of r_{p1}, r_{p2}, θ_1, and θ_2.

With $q = [x, y, \theta_2, \theta_1]^T$, equation (A.4) can be rewritten as

$$\delta W = F_1^T \frac{\partial r_{p1}}{\partial q}\delta q + F_2^T \frac{\partial r_{p2}}{\partial q}\delta q + M_{t1}\frac{\partial \theta_1}{\partial q} + M_{t2}\frac{\partial \theta_2}{\partial q}$$

$$= Q^T \delta q \tag{A.5}$$

where δq is the variation of q, and

$$Q = \left(\frac{\partial r_{p1}}{\partial q}\right)^T F_1 + \left(\frac{\partial r_{p2}}{\partial q}\right)^T F_2 + \left(\frac{\partial \theta_1}{\partial q}\right)^T M_{t1} + \left(\frac{\partial \theta_2}{\partial q}\right)^T M_{t2} \tag{A.6}$$

is the vector of the generalized forces corresponding to the generalized system coordinates. Therefore, the injection matrix is given as

$$B(q) = \frac{\partial Q}{\partial \tau} \tag{A.7}$$

where $\tau = [\tau_{1r}, \tau_{1l}, \tau_{2r}, \tau_{2l}]$ is the control torque vector.

APPENDIX B

SYSTEM INERTIA MATRIX $M(q)$ AND CORIOLIS FORCES VECTOR $C(q,\dot{q})$ IN (2.43)

Define the position vectors of C_1 and C_2 as

$$\begin{aligned} r_{c1} &= r_{p1} + a_1 U_1 \\ &= [x + d\cos\theta_2 + a_1\cos\theta_1 , y + d\sin\theta_2 + a_1\sin\theta_1]^T \\ r_{c2} &= r_{p2} + a_2 U_2 = [x + a_2\cos\theta_2 , y + a_2\sin\theta_2]^T \end{aligned} \tag{B.1}$$

The system kinematic energy is

$$T(q,\dot{q}) = \tfrac{1}{2}\left(m_1 \dot{r}_{c1}^T \dot{r}_{c1} + m_2 \dot{r}_{c2}^T \dot{r}_{c2} + I_{m1}\dot{\theta}_1^2 + I_{m2}\dot{\theta}_2^2\right) \tag{B.2}$$

The time derivative of r_{c1} and r_{c2} can be written as

$$\dot{r}_{c1} = \frac{\partial r_{c1}}{\partial q}\dot{q} = T_1\dot{q} , \quad \dot{r}_{c2} = \frac{\partial r_{c2}}{\partial q}\dot{q} = T_2\dot{q} \tag{B.3}$$

where T_1 and T_2 are the Jacobian matrices. Then, the system kinematic energy in (B.2) can be rewritten as

$$\begin{aligned} T(q,\dot{q}) &= \frac{1}{2}\left(m_1\dot{q}^T T_1^T T_1\dot{q} + m_2\dot{q}^T T_2^T T_2\dot{q} + I_{m1}\dot{\theta}_1^2 + I_{m2}\dot{\theta}_2^2\right) \\ &= \tfrac{1}{2}\dot{q}^T M(q)\dot{q} \end{aligned} \tag{B.4}$$

where

$$M(q) = m_1 T_1^T T_1 + m_2 T_2^T T_2 + \text{diag}\{0, 0, I_{m1}, I_{m2}\} \tag{B.5}$$

is the inertia matrix that is symmetric positive definite.

The Lagrange formulation for the system is

$$\frac{d}{dt}\left(\frac{\partial T}{\partial \dot{q}}\right) - \frac{\partial T}{\partial q} = Q + A^T(q)\lambda \tag{B.6}$$

From (B.4), we have

$$\frac{\partial T}{\partial \dot{q}} = M\dot{q} \tag{B.7}$$

Then,

$$\frac{d}{dt}\left(\frac{\partial T}{\partial \dot{q}}\right) - \frac{\partial T}{\partial q} = M\ddot{q} + \dot{M}\dot{q} - \frac{\partial T}{\partial q}$$

$$= M\ddot{q} + C(q, \dot{q}) \tag{B.8}$$

where

$$C(q, \dot{q}) = \dot{M}\dot{q} - \frac{\partial T}{\partial q} \tag{B.9}$$

is the centripetal and Coriolis vector.

APPENDIX C

INPUT TRANSFORMATION MATRIX $B(q)$ IN (2.69)

Define the unit vectors for the directions of the n robots in forward movements as

$$U_1 = [cos\,\theta_1\,, sin\,\theta_1]^T\,,\; U_2 = [cos\,\theta_2\,, sin\,\theta_2]^T\,,\; \cdots,\; U_n = [cos\,\theta_n\,, sin\,\theta_n]^T \qquad \text{(C.1)}$$

where $cos\,\theta_i$ and $sin\,\theta_1$ $(i = 1, 2, \cdots, n)$ are the components in the X and Y directions, respectively.

The control force and torque vectors generated by actuators are

$$F_1 = \frac{\tau_{1r}+\tau_{1l}}{r_1} U_1,\;\; F_2 = \frac{\tau_{2r}+\tau_{2l}}{r_2} U_2, \cdots,\;\; F_N = \frac{\tau_{nr}+\tau_{nl}}{r_n} U_n$$

$$M_{t1} = \frac{\tau_{1r}-\tau_{1l}}{r_1} b_1\,,\;\; M_{t2} = \frac{\tau_{2r}-\tau_{2l}}{r_2} b_2, \cdots,\;\; M_{tN} = \frac{\tau_{nr}-\tau_{nl}}{r_n} b_n \qquad \text{(C.2)}$$

where M_{ti} $(= 1, 2, \cdots, n)$ are in the Z direction.

Let

$$r_{p1} = (x + \textstyle\sum_{i=1}^{n} d_i\, cos\,\theta_i)\hat{\mathrm{I}} + (y + \sum_{i=1}^{n} d_i \sin\theta_i)\hat{\mathrm{J}},\quad r_{pn} = [x, y]^T \qquad \text{(C.3)}$$

The variation of the position vector (C.3) can be written as

$$\delta r_{p1} = (\delta x - \textstyle\sum_{i=1}^{n} d_i \sin\theta_i\, \delta\theta_i)\hat{\mathrm{I}} + (\delta y + \sum_{i=1}^{n} d_i \cos\theta_i\, \delta\theta_i)\hat{\mathrm{J}},\; \delta r_{pn} = [\delta x, \delta y]^T \qquad \text{(C.4)}$$

be the position vectors of $P_1, \cdots, P_n$. Then, the variation of the work done by the applied generalized forces is

$$\delta W = F_1^T \delta r_{p1} + F_2^T \delta r_{p2} + \cdots + F_N^T \delta r_{pn} + M_{t1}\delta\theta_1 + M_{t2}\delta\theta_2 + \cdots + M_{tN}\delta\theta_n \qquad \text{(C.5)}$$

where $\delta r_{p1}, \delta r_{p2}, \cdots, \delta r_{pn}$ and $\delta\theta_1, \delta\theta_2, \cdots, \delta\theta_n$ are variations of $r_{p1}, \cdots, r_{pn}$, and $\theta_1, \cdots, \theta_n$. With $q = [x, y, \theta_n, \theta_{n-1}, \ldots, \theta_1]^T$, equation (C.5) can be rewritten as

$$\delta W = F_1^T \frac{\partial r_{p1}}{\partial q}\delta q + F_2^T \frac{\partial r_{p2}}{\partial q}\delta q + \cdots + F_n^T \frac{\partial r_{pn}}{\partial q}\delta q + M_{t1}\frac{\partial \theta_1}{\partial q} + M_{t2}\frac{\partial \theta_2}{\partial q} + \cdots + M_{tn}\frac{\partial \theta_n}{\partial q}$$

$$= Q^T \delta q \qquad \text{(C.6)}$$

where δq is the variation of q, and

$$Q = \left(\frac{\partial r_{p1}}{\partial q}\right)^T F_1 + \cdots + \left(\frac{\partial r_{pn}}{\partial q}\right)^T F_n + \left(\frac{\partial \theta_1}{\partial q}\right)^T M_{t1} + \cdots + \left(\frac{\partial \theta_n}{\partial q}\right)^T M_{tn} \tag{C.7}$$

is the vector of the generalized forces corresponding to the generalized system coordinates. Therefore, the injection matrix is given as

$$B(q) = \frac{\partial Q}{\partial \tau} \tag{C.8}$$

where $\tau = [\tau_{1r}, \tau_{1l}, \tau_{2r}, \tau_{2l}, \cdots, \tau_{nr}, \tau_{nl}]$ is the control torque vector.

APPENDIX D

SYSTEM INERTIA MATRIX $M(q)$ IN (2.67) AND CORIOLIS FORCES $C(q,\dot{q})$ IN (2.68)

Define the position vectors of C_1 and C_n as

$$r_{c1} = r_{p1} + a_1 U_1$$

$$= [x + d\cos\theta_2 + a_1\cos\theta_1\,, y + d\sin\theta_2 + a_1\sin\theta_1]^T$$

$$r_{cn} = r_{pn} + a_n U_n = [x + a_n\cos\theta_n\,, y + a_n\sin\theta_n]^T \tag{D.1}$$

The system kinematic energy is

$$T(q,\dot{q}) = \tfrac{1}{2}\textstyle\sum_{i=0}^{n}\{m_i\dot{r}_{ci}^T\dot{r}_{ci} + I_{mi}\dot{\theta}_i^2\} \tag{D.2}$$

The time derivative of $r_{c1}, \cdots, r_{cn}$ can be written as

$$\dot{r}_{c1} = \frac{\partial r_{c1}}{\partial q}\dot{q} = T_1\dot{q}\,, \quad \dot{r}_{cn} = \frac{\partial r_{cn}}{\partial q}\dot{q} = T_n\dot{q} \tag{D.3}$$

where $T_1, \cdots, T_n$ are the Jacobian matrices. Then, the system kinematic energy in (D.2) can be rewritten as

$$T(q,\dot{q}) = \tfrac{1}{2}\textstyle\sum_{i=0}^{n}\{m_i\dot{q}^T T_i^T T_i\dot{q} + I_{mi}\dot{\theta}_i^2\} \tag{D.4}$$

where

$$M(q) = \textstyle\sum_{i=0}^{n}\{m_i T_i^T T_i\} + \mathrm{diag}(\{0, 0, I_{m1}, I_{m2}, \cdots, I_{mn}\}) \tag{D.5}$$

is the inertia matrix that is symmetric positive definite.

The Lagrange formulation for the system is

$$\frac{d}{dt}\left(\frac{\partial T}{\partial\dot{q}}\right) - \frac{\partial T}{\partial q} = Q + A^T(q)\lambda \tag{D.6}$$

From (D.4), we have

$$\frac{\partial T}{\partial \dot{q}} = M\dot{q} \tag{D.7}$$

Then,

$$\frac{d}{dt}\left(\frac{\partial T}{\partial \dot{q}}\right) - \frac{\partial T}{\partial q} = M\ddot{q} + \dot{M}\dot{q} - \frac{\partial T}{\partial q}$$

$$= M\ddot{q} + C(q, \dot{q}) \tag{D.8}$$

where

$$C(q, \dot{q}) = \dot{M}\dot{q} - \frac{\partial T}{\partial q} \tag{D.9}$$

is the centripetal and Coriolis vector.

APPENDIX E

PROOF OF THEOREM 2.1

The kinematic model for n-linked 2WD mobile robots were derived in Section 2.4.3 (see chapter 2), and is

$$\dot{q} = S(q)\eta \tag{E.1}$$

where

$\eta = [v \quad \omega_1]^T$

System (E.1) can be represented (locally) as follows

$$\dot{x} = v$$

$$\dot{\theta}_1 = \omega_1$$

$$\dot{\theta}_2 = \frac{1}{d_2}\frac{tan(\theta_1 - \theta_2)}{p_2(\theta_2)}v$$

$$\vdots$$

$$\dot{\theta}_i = \frac{1}{d_i}\frac{tan(\theta_{i-1} - \theta_i)}{p_i(\theta_i)}v$$

$$\dot{y} = tan\theta_n v \tag{E.2}$$

for $i \in \{1, \cdots, n\}$

where v is given by (2.76).

Let us denote, for $i \in \{1, \cdots, n\}$

$$f_i(\theta_{i-1}) = \frac{1}{d_i}\frac{tan(\theta_{i-1} - \theta_i)}{p_i(\theta_i)} \tag{E.3}$$

This means that we can write

$$\dot{\theta}_i = f_i(\theta_{i-1})v \tag{E.4}$$

After a reordering of the state variables, we denote the state by the vector

$$[\xi_1, \xi_2, \cdots, \xi_{n+2}]^T = [x, y, \theta_n, \theta_{n-1}, \ldots, \theta_1]^T$$

which has dimension $n + 2$.

We note from (E.2) that this kinematic model has a special triangular structure where $\dot{\xi}_i$ is not a function of $\xi_1, \cdots, \xi_{i-2}$, where $i \in \{3, \cdots, n+2\}$
and let us define

$$\xi_{n+3} = y \tag{E.5}$$

Using (E.2), the differentiation (E.5) with respect to time gives

$$\dot{\xi}_{n+3} = \dot{y} = \tan\theta_n \, v \tag{E.6}$$

We get $\dot{\xi}_{n+3} = \xi_{n+2} v$ by choosing

$$\xi_{n+2} = \tan\theta_n \tag{E.7}$$

Using (E.2), the differentiation of (E.7) with respect to time gives

$$\dot{\xi}_{n+2} = \frac{1}{cos^2\theta_n}\dot{\theta}_n = \frac{tan(\theta_{n-1} - \theta_n)}{d_n cos^3\theta_n} v \tag{E.8}$$

We get $\dot{\xi}_{n+2} = \xi_{n+1} v$ by choosing

$$\xi_{n+1} = \frac{tan(\theta_{n-1} - \theta_n)}{d_n cos^3\theta_n} \tag{E.9}$$

It can be shown by induction that $\dot{\xi}_{i+2} = \xi_i v$ by choosing

$$\xi_i = \frac{tan(\theta_{i-2} - \theta_{i-1})}{c_i(\theta_{i-1})} + r_i(\theta_{i-1}) \tag{E.10}$$

for $i \in \{2, \cdots, n\}$ where

$$c_i(\Theta_{i-1}) = \prod_{j=1}^{n+1} cos^{j-i+3}\big(\theta_{j-1} - \theta_j\big) d_{n+i-j} = p_{i-1}^2(\theta_{i-1}) \prod_{j=i-1}^{n} d_j p_j\big(\Theta_j\big) \tag{E.11}$$

$$r(\Theta_{i-1}) = \frac{\partial \xi_{i+1}}{\partial \theta_i} f_i(\Theta_{i-1}) \tag{E.12}$$

where $i \in \{1, \cdots, n\}$. This means that $\xi_i = \xi_i(\theta_{i-2})$.
Assume that (E.10) is satisfied for $i = m$. Equations (2.80), (E.2), (E.11) and (E.12) imply

$$\dot{\xi}_m = \frac{\partial \xi_m}{\partial \theta_{m-2}} \dot{\theta}_{m-2} + \frac{\partial \xi_m}{\partial \theta_{m-1}} \dot{\theta}_{m-1}$$

$$= \frac{1}{cos^2(\theta_{m-2} - \theta_{m-1}) c_m(\theta_{m-1})}$$

$$= \frac{1}{d_{m-2}} \frac{tan(\theta_{m-3} - \theta_{m-2})}{p_{m-2}(\theta_{m-2})} v + \frac{\partial \xi_m}{\partial \theta_{m-1}} f_{m-1}(\theta_{m-2}) v$$

$$= \left(\frac{tan(\theta_{m-3} - \theta_{m-2})}{c_{m-1}(\theta_{m-2})} + r_{m-1}(\theta_{m-2}) \right) v$$

Note from (2.80) and (E.10) that

$$c_{m-1} = cos^2 \alpha_{m-2} c_m d_{m-2} p_{m-2}$$

$$= cos^2 \alpha_{m-2} p_{m-1}^2 \left(\prod_{j=m-1}^{n} d_j p_j \right) d_{m-2} p_{m-2}$$

$$= p_{m-2}^2(\theta_{m-2}) \prod_{j=m-2}^{n} d_j p_j(\theta_j)$$

where $\alpha_{m-2} = \theta_{m-2} - \theta_{m-1}$, $c_m = c_m(\theta_{m-1})$, and $p_j = p_j(\theta_j)$.

We have thus shown that if ξ_i is given by (E.9) for $i = m$ then

$$\dot{\xi}_m = \xi_{m-1} v$$

Let choose ξ_{m-1} as in (E.9) with $i = m - 1$. It remains to show that if ξ_n is given by (E.9) with $i = n$ and ξ_{n-1} is given by (E.8) then

$$\dot{\xi}_{n+1} = \xi_n v$$

From (E.2), (E.9), (E.11) and (E.12), we get

$$\dot{\xi}_{n+1} = \frac{\partial \xi_{n+1}}{\partial \theta_{n-1}} \dot{\theta}_{n-2} + \frac{\partial \xi_{n+1}}{\partial \theta_n} \dot{\theta}_n$$

$$= \frac{1}{cos^2(\theta_{n-1} - \theta_n) d_n cos^3 \theta_n}$$

$$= \frac{1}{d_{n-1}} \frac{tan(\theta_{n-2} - \theta_{n-1})}{cos\, \theta_n \, cos(\theta_{n-1} - \theta_n)} v + \frac{\partial \xi_{n+1}}{\partial \theta_n} f_n(\theta_{n-1}) v$$

$$= \left(\frac{tan(\theta_{n-2} - \theta_{n-1})}{c_n(\theta_{n-1})} + r_n(\theta_{n-1}) \right) v$$

This means that

$$\dot{\xi}_{n+1} = \xi_n v$$

by choosing

$$\xi_n = \frac{tan(\theta_{n-2} - \theta_{n-1})}{c_n(\theta_{n-1})} + r_n(\theta_{n-1}) \tag{E.13}$$

Therefore, ξ_i is given by (E.9) for all $i \in \{1, \cdots, n\}$ and the transformation (2.81)-(2.91) (see chapter 2) imply that

$$\dot{\xi}_i = \xi_{i-1} v, \qquad \forall i \in \{3, \cdots, n+3\}$$

To complete the proof, we have shown that

$$\dot{\xi}_2 = \alpha_2, \qquad \dot{\xi}_1 = \alpha_1$$

ξ_2 is given by (E.9) with $i = 2$.

By differentiating (E.9), we obtain

$$\begin{aligned}\dot{\xi}_2 &= \frac{\partial \xi_2}{\partial \theta_0}\dot{\theta}_1 + \frac{\partial \xi_2}{\partial \theta_1}\dot{\theta}_2 \\ &= \frac{1}{cos^2(\theta_1 - \theta_2)c_2(\theta_2)}\omega + \frac{\partial \xi_2}{\partial \theta_2} f_1(\theta_1) v \\ &= \frac{1}{cos^2(\theta_1 - \theta_2)c_2(\theta_1)}\omega + r_1(\theta_1) f_1(\theta_1) v_1\end{aligned}$$

since $v = p_1(\theta_1)v_1$. This implies that the transformation (2.91) (see chapter 2) implies

$$\dot{\xi}_2 = \alpha_2 \tag{E.14}$$

From (E.6) it follows directly that

$$\dot{\xi}_1 = \alpha_1 \tag{E.15}$$

By choosing $\xi_1 = x$ and $\alpha_1 = v = p_1(\theta_1)v_1$.

Finally one can conclude that the transformation (2.81)-(2.86) implies that

$$\begin{aligned}\dot{\xi}_1 &= \alpha_1 \\ \dot{\xi}_2 &= \alpha_2 \\ \dot{\xi}_1 &= \xi_2 \alpha_1 \\ &\vdots \\ \dot{\xi}_n &= \xi_n \alpha_1\end{aligned} \tag{E.16}$$

APPENDIX F

DIFFEOMORPHISM IN (3.19)-(3.22)

It is easy to obtain $\dot{z}_1$, $\dot{z}_2$ and $\dot{z}_4$ from (3.11)-(3.18). From $z_3 = \tan e_\theta$ in (3.16) and with (3.15), (3.17), and (3.18), we have

$$\dot{z}_3 = \frac{1}{\cos^2 e_\theta}\dot{e}_\theta = \frac{v_2 \tan(\theta_1 - \theta_2)}{d\cos^2 e_\theta} - \frac{\omega_r}{\cos^2 e_\theta}$$

$$= \frac{\tan(\theta_1 - \theta_2)}{d\cos^3 e_\theta} v_2 \cos e_\theta - \frac{\omega_r}{v_r \cos^2 e_\theta} v_2 \cos e_\theta + \frac{\omega_r}{v_r \cos^2 e_\theta}(v_2 - v_r)$$

$$= (z_4 - z_2) v_2 \cos e_\theta + \frac{\omega_r}{v_r \cos^2 e_\theta}\alpha_1$$

$$= v_r(z_4 - z_2) + \alpha_1\left(z_4 - z_2 + \frac{\omega_r}{v_r}(1 + z_3^2)\right) \quad \text{(F.1)}$$

APPENDIX G

OBTAINING T_α AND f_α IN (3.23)

From $z_4 = \frac{\tan(\theta_1-\theta_2)}{d\cos^2 e_\theta} - \frac{\omega_d}{v_d\cos^2 e_\theta}$ in (3.17), and with (3.3), (3.4), (3.12) and (3.13), we have

$$\begin{aligned}\dot{z}_4 = \frac{1}{\cos^2 e_\theta} &= \frac{\frac{(\dot{\theta}_1-\dot{\theta}_2)}{\cos^2(\theta_1-\theta_2)}\cos^2 e_\theta + 3\tan(\theta_1-\theta_2)\cos^2 e_\theta \sin e_\theta \dot{e}_\theta}{d\cos^2 e_\theta} \\ &- \frac{\dot{\omega}_d v_d\cos^2 e_\theta - \omega_d(\dot{v}_d\cos^2 e_\theta - 2v_d\cos e_\theta \sin e_\theta \dot{e}_\theta)}{v_d^2\cos^4 e_\theta} + \dot{e}_y \\ &= \frac{\omega_1 - \frac{v_2}{d}\tan(\theta_1-\theta_2)}{d\cos^3 e_\theta \cos^2(\theta_1-\theta_2)} + \frac{3\tan(\theta_1-\theta_2)\sin e_\theta\left(\frac{v_2}{d}\tan(\theta_1-\theta_2)-\omega_d\right)}{d\cos^4 e_\theta} \\ &- \frac{\dot{\omega}_r}{v_d\cos^2 e_\theta} + \frac{\omega_d\dot{v}_d}{v_d^2\cos^2 e_\theta} - \frac{2\omega_d\sin e_\theta\left(\frac{v_2}{d}\tan(\theta_1-\theta_2)-\omega_d\right)}{v_d\cos^3 e_\theta} - \omega_d e_x + v_d\sin e_\theta \\ &= \left(\frac{3\tan^2(\theta_1-\theta_2)\sin e_\theta}{d^2\cos^4 e_\theta} - \frac{\tan(\theta_1-\theta_2)}{d^2\cos^3 e_\theta\cos^2(\theta_1-\theta_2)} - \frac{2\omega_d\tan(\theta_1-\theta_2)\sin e_\theta}{dv_d\cos^3 e_\theta} + \sin e_\theta\right)v_2 \\ &+ \frac{1}{d\cos^3 e_\theta\cos^2(\theta_1-\theta_2)}\omega_d - \frac{3\omega_d\tan(\theta_1-\theta_2)\sin e_\theta}{d\cos^4 e_\theta} \\ &- \frac{\dot{\omega}_d}{v_d\cos^2 e_\theta} + \frac{\omega_d\dot{v}_d}{v_d^2\cos^2 e_\theta} + \frac{2\omega_d^2\sin e_\theta}{v_d\cos^3 e_\theta} - \omega_d e_x \end{aligned} \quad \text{(G.1)}$$

together with $\alpha_1 = v_2\cos e_\theta - v_d$ and $\alpha_2 = \dot{z}_4$, we can finally obtain

$$\begin{aligned}\alpha = \begin{bmatrix}\alpha_1\\ \alpha_2\end{bmatrix} &= T_\alpha\eta + f_\alpha \\ &= \begin{bmatrix}T_{11} & T_{12}\\ T_{21} & T_{22}\end{bmatrix}\begin{bmatrix}v_2\\ \omega_1\end{bmatrix} + \begin{bmatrix}f_{\alpha1}\\ f_{\alpha2}\end{bmatrix}\end{aligned} \quad \text{(G.2)}$$

where

$$T_{\alpha11} = \cos e_\theta,\ T_{\alpha12} = 0,$$

$$T_{\alpha21} = \frac{3\tan^2(\theta_1-\theta_2)\sin e_\theta}{d^2\cos^4 e_\theta} - \frac{\tan(\theta_1-\theta_2)}{d^2\cos^3 e_\theta\cos^2(\theta_1-\theta_2)} - \frac{2\omega_d\tan(\theta_1-\theta_2)\sin e_\theta}{dv_d\cos^3 e_\theta} + \sin e_\theta,$$

$$T_{\alpha22} = \frac{1}{d\cos^3 e_\theta\cos^2(\theta_1-\theta_2)},\quad f_{\alpha1} = -v_d,$$

$$f_{\alpha2} = -\frac{3\omega_d\tan(\theta_1-\theta_2)\sin e_\theta}{d\cos^4 e_\theta} - \frac{\dot{\omega}_d}{v_d\cos^2 e_\theta} + \frac{\omega_d\dot{v}_d}{v_d^2\cos^2 e_\theta} + \frac{2\omega_d^2\sin e_\theta}{v_d\cos^3 e_\theta} - \omega_d e_x \quad \text{(G.3)}$$

BIBLIOGRAPHY

[1] V. Verma, G. Gordon, R. Simmons and S. Thrun, "Real-time fault diagnosis [robot fault diagnosis]," *in IEEE Robotics & Automation Magazine*, vol. 11, no. 2, pp. 56-66, June 2004. 1

[2] https://mars.nasa.gov/ask-nasa-mars/#/. 1

[3] B. Siciliano, and O. Khatib, "Handbook of Robotics," *Springer-Verlag Berlin Heidelberg*, 2008. 1, 9, 22

[4] L. T. Dauer, P. Zanzonico, R. M. Tuttle, D. M. Quinn, and H. W. Strauss, "The Japanese tsunami and resulting nuclear emergency at the Fukushima Daiichi power facility: technical, radiologic, and response perspectives," *Journal of Nuclear Medicine*, 52(9):1423-1432, 2011. 2

[5] K. Nagatani, S. Kiribayashi, Y. Okada, K. Otake, K. Yoshida, S. Tadokoro, T. Nishimura, T. Yoshida, E. Koyanagi, M. Fukushima and S. Kawatsuma, "Emergency response to the nuclear accident at the Fukushima Daiichi nuclear power plants using mobile rescue robots," *Journal of Field Robotics*, vol. 30, Issue 1, pp. 44-63, 2013. 2

[6] D. Cynthia, S. Evans, E. Geist, S. W. Harold, V. R. Koym, S. Savitz and L. Thrall, Technological Lessons from the Fukushima Dai-Ichi Accident, *Santa Monica, CA: RAND Corporation*, 2016. https://www.rand.org/pubs/research_reports/RR857.html. 2

[7] S. Kawatsuma, M. Fukushima, and T. Okada, "Emergency response by robots to Fukushima-Daiichi accident: summary and lessons learned," *Industrial Robot: An International Journal*, vol. 39, Issue 5, pp. 428-435, 2012. 2

[8] S. Kawatsuma, R. Mimura and H. Asama, Unitization for portability of emergency response surveillance robot system: experiences and lessons learned from the deployment of the JAEA-3 emergency response robot at the Fukushima Daiichi Nuclear Power Plants, *ROBOMECH Journal*, 4:6, February 2017. 3

[9] M. Defoort, T. Floquet, A. Kokosy and W. Perruquetti, "Sliding-mode formation control for cooperative autonomous mobile robots," in *IEEE Transactions on Industrial Electronics*, vol. 55, no. 11, pp. 3944-3953, November 2008. 3

[10] F. Xie, "Model predictive control of nonholonomic mobile robots," *Ph.D. Thesis, Oklahoma State University*, USA, December 2007. 3

[11] F. Mondada, L. M. Gambardella, D. Floreano, S. Nolfi, J. L. Deneuborg and M. Dorigo, "The cooperation of swarm-bots: physical interactions in collective robotics," in *IEEE Robotics & Automation Magazine*, vol. 12, no. 2, pp. 21-28, June 2005. 4

[12] R. O'Grady, A. L. Christensen and M. Dorigo, "SWARMORPH: multirobot morphogenesis using directional self-assembly," in *IEEE Transactions on Robotics*, vol. 25, no. 3, pp. 738-743, June 2009. 4

[13] T. L. Huntsberger, A. T. Ollennu, H. Aghazarian, P. S. Schenker, P. Pirjanian and H. D. Nayar, "Distributed control of multi-robot systems engaged in tightly coupled tasks," in *Autonomous Robots*, vol. 17, Issue 1, pp. 79-92, July 2004. 5

[14] A. Stroupe, A. Okon, M. Robinson, T. Huntsberger, H. Aghazarian and E. Baumgartner, "Sustainable cooperative robotic technologies for human outpost infrastructure construction and maintenance," in *Springer Science, Autonomous Robots*, vol. 20, Issue 2, pp. 113-123, April 2006. 5

[15] M. A. Kamel, X. Yu and Y. Zhang, "Fault-tolerant cooperative control design of multiple wheeled mobile robots," in *IEEE Transactions on Control Systems Technology*, vol. PP, no. 99, pp.1-9, March 2017. 5

[16] J. Yuan, F. Sun and Y. Huang, "Trajectory generation and tracking control for double-steering tractor-trailer mobile robots with on-axle hitching," *IEEE Transactions on Industrial Electronics*, vol. 62, no. 12, pp. 7665-7677, July 2015. 6, 9, 13

[17] G. Grzegorz, "Hypermobile robots the survey," *Journal of Intelligent & Robotic Systems*, vol. 75, no. 1, pp. 147-169, July 2014. 7

[18] M. Delrobaei and K. McIsaac, "Design and steering control of a center-articulated mobile robot module," *Journal of Robotics*, vol. 2011, article ID 621879, 14 pages. 8

[19] M. Yim, W. Shen, B. Salemi, D. Rus, M. Moll, H. Lipson, E. Klavins and G. Chirikjian, "Modular Self-Reconfigurable Robot Systems [Grand Challenges of Robotics]," in *IEEE Robotics & Automation Magazine*, vol. 14, no. 1, pp. 43-52, March 2007. 8

[20] M. Delrobaei and K. A. McIsaac, "Connection mechanism for autonomous self-assembly in mobile robots," in *IEEE Transactions on Robotics*, vol. 25, no. 6, pp. 1413-1419, December 2009. 8

[21] P. Ritzen, E. Roebroek, N. van de Wouw, Z. P. Jiang and H. Nijmeijer, "Trailer steering control of a tractor-trailer robot," in *IEEE Transactions on Control Systems Technology*, vol. 24, no. 4, pp. 1240-1252, July 2016. 9

[22] M. M. Michałek and M. Kiełczewski, "The concept of passive control assistance for docking maneuvers with n-trailer vehicles," in *IEEE/ASME Transactions on Mechatronics*, vol. 20, no. 5, pp. 2075-2084, October 2015. 9

[23] F. Sanfilippo, J. Azpiazu, G. Marafioti, A. Transeth, Q. Stavdahi and P. Lilijeback, "Perception-driven obstacle-aided locomotion for snake robots: the state of the art, challenges and possibilities," *Applied Sciences*, 7(4): 336, March 2017. 10

[24] O. Shmakov, "Snakelike robots locomotions control, *Course 5: Mechatronics-Foundations and Applications*, May 2006. 10

[25] I. Kolmanovsky and N. McClamroch, "Developments in nonholonomic control problem," *IEEE Control Systems Magazine*, vol. 15, no. 6, pp. 20-36, November 1995. 12

[26] G. Yuan, S. X. Yang and G. S. Mittal, "Tracking control of a mobile robot using a neural dynamic based approach," *Proceedings 2001 ICRA, IEEE International Conference on Robotics and Automation*, Seoul, South Korea, pp. 163-168, 2001. 12

[27] Y. Hu and S. X. Yang, "A fuzzy neural dynamics-based tracking controller for a nonholonomic mobile robot," *Proceedings 2003 IEEE/ASME International Conference on Advanced Intelligent Mechatronics (AIM 2003)*, Kobe, Japan, pp. 205-210, 2003. 12

[28] Y. Kanayama, Y. Kimura, F. Miyazaki and T. Noguchi, "A stable tracking control method for an autonomous mobile robot," Proceedings, *IEEE International Conference on Robotics and Automation*, Cincinnati, USA, vol. 1, pp. 384-389, 1990. 12

[29] B. Chen, T. Lee and W. Chang, "A robust H infinity model reference tracking design for nonholonomic mechanical control systems," *International Journal of Control*, vol. 63, no. 2, pp. 283-306, 1996. 12

[30] M. Fliess, J. Lévine, P. Martin and P. Rouchon, "Flatness and defect of non-linear systems: introductory theory and examples," *International Journal of Control*, vol. 61, no. 6, 1327-1361, February 2007. 12

[31] R. Fierro and F. L. Lewis, Control of a nonholonomic mobile robot: back stepping kinematics into dynamics, *Journal of Robotic Systems* 14: 149-163, 1997. 12

[32] R. Fierro and F. L. Lewis, "Control of a nonholonomic mobile robot using neural networks," in *IEEE Transactions on Neural Networks*, vol. 9, no. 4, pp. 589-600, July 1998. 12, 49

[33] W. Dong and K. D. Kuhnert, "Robust adaptive control of nonholonomic mobile robot with parameter and nonparameter uncertainties," in *IEEE Transactions on Robotics*, vol. 21, no. 2, pp. 261-266, April 2005. 12

[34] T. Fukao, H. Nakagawa and N. Adachi, "Adaptive tracking control of a nonholonomic mobile robot," *IEEE Transactions on Robotics and Automation*, vol. 16, no. 6, pp. 609-615, 2000. 12, 60, 78, 92, 98, 110, 118

[35] W. Dong, W. Huo, S. K. Tso and W. L. Xu, "Tracking control of uncertain dynamic nonholonomic system and its application to wheeled mobile robots," in *IEEE Transactions on Robotics and Automation*, vol. 16, no. 6, pp. 870-874, December 2000. 12

[36] J. David and P. Manivannan, "Control of truck-trailer mobile robots: a survey," *Intelligent Service Robotics*, vol. 7, Issue 4, pp. 245-258, October 2014. 12

[37] J. Laumond, "Controllability of a multibody mobile robot," *IEEE Transactions on Robotics and Automation*, vol. 9, no. 6, pp. 755-763, December 1993. 12, 66

[38] F. Lamiraux and J. Laumond, "Flatness and small-time controllability of multibody mobile robots: Application to motion planning," *IEEE Transactions on Automatic Control*, vol. 45, no. 10, pp. 1878-1881, October 2000. 12, 66

[39] J. Laumond, S. Sekhavat and F. Lamiraux, "Guidelines in nonholonomic motion planning for mobile robots," in *Robot Motion Planning and Control*, vol. 229, pp. 1-54, Berlin, Germany: Springer-Verlag, 1998. 12

[40] O. J. Sørdalen, "Conversion of the kinematics of a car with n trailers into a chained form," *IEEE Conference on Robotics and Automation*, pp. 382-387, 1993. 12, 38, 39, 69, 83, 109, 129

[41] P. Morin and C. Samson, "Transverse function control of a class of non-invariant drift less systems. Application to vehicles with trailers", *Proceedings 47th IEEE Conference on Decision and Control*, Cancun, 4312-4319, 2008. 13

[42] A. Keymasi Khalaji and S. A. A. Moosavian, "Robust Adaptive Controller for a Tractor-Trailer Mobile Robot," in *IEEE/ASME Transactions on Mechatronics*, vol. 19, no. 3, pp. 943-953, June 2014. 13, 20, 44

[43] A. Khalaji, M. Bidgoli and S. A. Moosavian , "Non-model-based control for a wheeled mobile robot towing two trailers," *Proceedings of the Institution of Mechanical Engineers, Part K: Journal of Multi-body Dynamics*, vol. 229, no. 1, 2014. 13

[44] Y. Zhang and J. Jiang, "Bibliographical review on reconfigurable fault-tolerant control systems," *Annual Reviews in Control*, vol. 32, no. 2, pp. 229-252, 2008. 13

[45] X. Yu and J. Jiang, "A survey of fault-tolerant controllers based on safety-related issues," *Annual Reviews in Control*, vol. 39, pp. 46-57, 2015. 13

[46] D. Ye and G. H. Yang, "Adaptive fault-tolerant tracking control against actuator faults with application to flight control," *IEEE Transactions on Control Systems Technology*, vol. 14, no. 6, pp. 1088-1096, November 2006. 13

[47] J. Fang, W. Li, H. Li and X. Xu, "Online inverter fault diagnosis of buck-converter BLDC motor combinations," *IEEE Transactions on Power Electronics*, vol. 30, no. 5, pp. 2674-2688, 2015. 13

[48] K. Zhang, B. Jiang, and V. Cocquempot, "Fuzzy unknown input observer-based robust fault estimation design for discrete-time fuzzy system," *Signal Processing, Elsevier*, vol. 128, pp. 40-47, November 2016. 13

[49] M. Luo, D. Wang, M. Pham, C. B. Low, J. B. Zhang, D. H. Zhang, and Y. Z. Zhao, "Model-based fault diagnosis/prognosis for wheeled mobile robots: a review," *Proceedings of 31st Annual Conference of IEEE Industrial Electronics Society*, pp. 6-12, 2005. 13

[50] Z. H. Duan, Z. X. Cai, and J. X. Yu, "Fault diagnosis and fault tolerant control for wheeled mobile robots under unknown environments: a survey," *Proceedings of the IEEE International Conference on Robotics and Automation*, pp. 3428-3433, 2005. 13

[51] M. Ji and N. Sarkar, “Supervisory fault adaptive control of a mobile robot and its application in sensor-fault accommodation,” *IEEE Transactions on Robotics*, vol. 23, no. 1, pp. 174-178, February 2007. 13

[52] A. Stancu, E. Codres and V. Puig, "A fault hiding approach for the sliding mode fault-tolerant control of a non-holonomic mobile robot," *2016 3rd Conference on Control and Fault-Tolerant Systems (SysTol)*, Barcelona, 2016, pp. 7-14. 13

[53] A. C. Leite, B. Schäfer and M. L. de OLiveira e Souza, Fault-Tolerant Control Strategy for Steering Failures in Wheeled Planetary Rovers, *Journal of Robotics*, vol. 2012, Article ID 694673, 15 pages. 13

[54] D. Stavrou, D. G. Eliades, C. G. Panayiotou and M. M. Polycarpou, Fault detection for service mobile robots using model-based method, *Springer, Autonomous Robots*, February 2016, vol. 40, Issue 2, pp. 383-394. 13

[55] Z. Shen, Y. Ma and Y. Song, "Robust adaptive fault-tolerant control of mobile robots with varying center of mass," in *IEEE Transactions on Industrial Electronics*, vol. PP, no. 99, August 2016. 13

[56] M. Ji, Z. Zhang, G. Biswas, and N. Sarkar, “Hybrid fault adaptive control of a wheeled mobile robot,” *IEEE/ASME Transactions on Mechatronics*, vol. 8, no. 2, pp. 226-233, June 2003. 13

[57] Y. H. Chang, C. I. Wu and C. Y. Yang, “Adaptive output-feedback fault-tolerant tracking control for mobile robots under partial loss of actuator effectiveness,” *2015 54th IEEE Conference on Decision and Control*, Osaka, pp. 6306-6311, 2015. 13

[58] W. E. Dixon, I. D. Walker and D. M. Dawson, “Fault detection for wheeled mobile robots with parametric uncertainty,” *2001 IEEE/ASME International Conference on Advanced Intelligent Mechatronics*, vol. 2, pp. 1245-1250, 2001. 13

[59] M. Bisgaard, D. Vinther, and K. Z. Østergaard, Modelling and fault-tolerant control of an autonomous wheeled robot, *Institute of Control Engineering, University of Aalbog*, 2004, Project Group 04gr1030a. 13

[60] D. Rotondo, V. Puig, F. Nejjari, and J. Romera, “A fault-hiding approach for the switching Quasi-LPV fault-tolerant control of a four-wheeled omnidirectional mobile robot,” *IEEE Transactions on Industrial Electronics*, vol. 62, no. 6, pp. 3932-3944, November 2014. 13

[61] M. Koh, M. Noton and S. Khoo, “Robust fault-tolerant leader-follower control of four-wheel-steering mobile robots using terminal sliding mode,” *Australian Journal of Electrical and Electronics Engineering*, vol. 9, no. 4, pp. 247-254, 2012. 13

[62] T. Kim, J. Park and H. Jin Kim, “Actuator reconfiguration control of a robotic vehicle with four independent wheel driving,” *The 15th International Conference on Control, Automation and Systems*, Busan, Korea, pp. 1767-1770, 2015. 13

[63] D. Rotondo, A. Cristofaro, T. Johansen, F. Nejjari, and V. Puig, "Diagnosis of icing and actuator faults in UAVs using LPV unknown input observers," *Journal of Intelligent & Robotic Systems*, pp. 1-15, October 2017. 14

[64] M. Blanke, M. Kinnaert, J. Lunze, and M. Staroswiecki, "Diagnosis and Fault-Tolerant Control," 3rd edition, *Springer-Verlag Berlin Heidelberg*, 2016. 14

[65] S. Ding, "Model-Based Fault Diagnosis Techniques: Design Schemes Algorithms and Tools," 2nd edition, *series Advances in Industrial Control, Springer-Verlag London*, 2013. 14

[66] J. Chen and R. Patton, "Robust Model-Based Fault Diagnosis for Dynamic Systems," *Springer Publishing Company, Incorporated*, 2012. 14

[67] V. Venkatasubramanian, R. Rengaswamy, K. Yin, and S. N. Kavuri, "A review of process fault detection and diagnosis: Part i: Quantitative model-based methods," *Computers & Chemical Engineering*, vol. 27, no. 3, pp. 293-311, 2003. 14

[68] V. Venkatasubramanian, R. Rengaswamy, and S. N. Kavuri, "A review of process fault detection and diagnosis: Part ii: Qualitative models and search strategies," *Computers & Chemical Engineering*, vol. 27, no. 3, pp. 313-326, 2003. 14

[69] V. Venkatasubramanian, R. Rengaswamy, S. N. Kavuri, and K. Yin, "A review of process fault detection and diagnosis: Part iii: Process history-based methods," *Computers & Chemical Engineering*, vol. 27, no. 3, pp. 327-346, 2003. 14

[70] Z. Gao, C. Cecati, and S. X. Ding, "A survey of fault diagnosis and fault-tolerant techniques - part ii: Fault diagnosis with model-based and signal-based approaches," *IEEE Transactions on Industrial Electronics*, vol. 62, no. 6, pp. 3757–3767, June 2015. 14

[71] N. Hoang and H. Kang, "Model-based fault diagnosis scheme for wheeled mobile robots," *International Journal of Control, Automation, and Systems*, vol. 12, no. 3, pp. 637-651, June 2014. 14, 104

[72] X. Zhang, M. Polycarpou and T. Parisini, "A robust detection and isolation scheme for abrupt and incipient faults in nonlinear systems," in *IEEE Transactions on Automatic Control*, vol. 47, no. 4, pp. 576-593, April 2002. 14, 104

[73] E. N. Skoundrianos and S. G. Tzafestas, "Finding fault - fault diagnosis on the wheels of a mobile robot using local model neural networks," in *IEEE Robotics & Automation Magazine*, vol. 11, no. 3, pp. 83-90, September 2004. 14

[74] G. K. Fourlas, S. Karkanis, G. C. Karras and K. J. Kyriakopoulos, "Model based actuator fault diagnosis for a mobile robot," *2014 IEEE International Conference on Industrial Technology (ICIT)*, Busan, South Korea, pp. 79-84, 2014. 14

[75] M. Yu, S. Chen, H. Xia, M. Li and H. Wang, "Intelligent multiple-fault diagnosis of a mobile robot system in the presence of hide effect," *2016 IEEE International*

Conference on Mechatronics and Automation, Harbin, China, pp. 1572-1577, 2016. 14

[76] J. M. G. de-Gabriel, A. Mandow, J. F. Lozano and A. G. Cerezo, "Mobile robot lab project to introduce engineering students to fault diagnosis in mechatronic systems," in *IEEE Transactions on Education*, vol. 58, no. 3, pp. 187-193, August 2015. 14

[77] Z. Li and W. Jiang, "Active fault-tolerant control for two-wheeled differential drive mobile robot based on fault compensation method," *2013 Chinese Automation Congress*, Changsha, pp. 359-363, 2013. 14

[78] S. I. Roumeliotis, G. S. Sukhatme and G. A. Bekey, "Sensor fault detection and identification in a mobile robot," *Proceedings. 1998 IEEE/RSJ International Conference on Intelligent Robots and Systems, Innovations in Theory, Practice and Applications*, Victoria, BC, pp. 1383-1388 vol. 3, 1998. 14

[79] D. Stavrou, D. G. Eliades, C. G. Panayiotou and M. Polycarpou, "A path correction module for two-wheeled service robots under actuator faults," *21st Mediterranean Conference on Control and Automation*, Chania, Greece, pp. 1119-1126, 2013. 14

[80] A. L. Christensen, R. O'Grady, M. Birattari, & M. Dorigo, "Fault detection in autonomous robots based on fault injection and learning," *Autonomous Robots*, vol. 24, Issue 1, pp. 49-67, January 2008. 14

[81] Y. Ma, V. Cocquempot, M. El Badaoui El Najjar and B. Jiang, "Multi design integration based adaptive actuator failure compensation control for two linked 2WD mobile robots," in *IEEE/ASME Transactions on Mechatronics*, vol. 22, no. 5, pp. 2174-2185, October 2017. 15

[82] Y. Ma, V. Cocquempot, M. El Badaoui El Najjar and B. Jiang, "Adaptive compensation of multiple actuator faults for two physically linked 2WD robots," in *IEEE Transactions on Robotics*, vol. PP, no. 99, pp. 1-8, October 2017. 15

[83] Y. Ma, V. Cocquempot, M. El Badaoui El Najjar and B. Jiang, "Actuator Failure Compensation for Two Linked 2WD Mobile Robots Based on Multiple-Model Control," *International Journal of Applied Mathematics and Computer Science (AMCS)*, vol. 27, no. 4, 2017. 15, 49

[84] Y. Ma, A. Al-Dujaili, V. Cocquempot, and M. El Badaoui El Najjar, "An Adaptive Actuator Failure Compensation Scheme for Two Linked 2WD Mobile Robots," Advanced *Control and Diagnosis, ACD 2016*, Lille, 17-18 November 2016. 17

[85] A. Al-Dujaili, Y. Ma, M. El Badaoui El Najjar, and V. Cocquempot, "Actuator Fault Compensation in Three Linked 2WD Mobile Robots Using Multiple Dynamic Controllers," IFAC *WC*, Toulouse, 9-14 July, 2017. 17, 65

[86] A. Al-Dujaili, V. Cocquempot, M. El Badaoui El Najjar, Y. Ma, "Actuator Fault Compensation Tracking Control for Multi Linked 2WD Mobile Robots," IEEE *MED 2017, 25th Mediterranean Conference on Control and Automation*, Valletta, Malta,

July 3-6, 2017. 17

[87] P. F. Muir, "Modeling and control of wheeled mobile robots," *PhD Thesis, Carnegie Mellon University,* August 1988. 19

[88] G. Campion, G. Bastin, B. D'Andrea-Novel, "Structural properties and classification of kinematic and dynamic models of wheeled mobile robot," *IEEE Transactions on Automatic Control*, vol. 12, pp. 47-62, 1996. 19

[89] J. C. Alexander and J. H. Maddocks, "On the kinematics of wheeled mobile robots," *International Journal of Robotics Research*, vol. 8, no. 5, pp. 15-27, May 1989. 19

[90] B. D'Andrea-Novel and G. Bastin, and G. Campion, "Modeling and control of nonholonomic wheeled mobile robots," *Proceedings of IEEE Conference on Robotics and Automation*, Sacramento, CA, USA, pp.1130-1135, April 1991. 19

[91] N. Chakraborty and A. Ghosal, "Kinematics of wheeled mobile robots on uneven terrain," *Mechanism and Machine Theory*, vol. 39, no.12, pp. 1273-1287, December 2004. 19

[92] N. Chakraborty and A. Ghosal, "Dynamic modeling and simulation of a wheeled mobile robot for traversing uneven terrain without slip," *Journal of Mechanical Des*ign, vol. 127, no. 5, pp. 901-909, October 2004. 19

[93] L. Gracia and J. Tornero, Kinematic modeling and singularity of wheeled mobile robots, *Advanced Robotics*, vol. 21, no. 7, pp. 793-816, 2012. 20

[94] Z. G. Hou, A. M. Zou, L. Cheng and M. Tan, Adaptive control of an electrically driven nonholonomic mobile robot via back stepping and fuzzy Approach, *IEEE Transactions on Control Systems Technology,* vol. 17, no. 4, pp. 803-815, 2009. 20

[95] X. Yun, Y. Yamamoto, On feedback linearization of mobile robots, *Technical Report* No. MS- CIS-92-45, Philadelphia, PA, June 1992. 20

[96] Y. Yamamoto, X. Yun, Coordinating locomotion and manipulation of a mobile manipulator, *Technical Report*, No. MS-CIS-92-18 Philadelphia, PA, March 1992. 20

[97] N. Sarkar, X. Yun, V. Kumar, Control of mechanical systems with rolling constraints: application to dynamic control of mobile robots, *International Journal of Robotics*, vol. 13, no. 1, pp. 55-69, 1994. 20

[98] R. M. DeSantis, Modeling and path-tracking control of a mobile wheeled robot with a differential drive, *Robotica*, vol. 13, Issue 4, pp. 401-410, July 1995. 20

[99] A. Albagul and Wahyudi A, Dynamic modeling and adaptive traction control for mobile robots, *International Journal of Advanced Robotic Systems*, vol. 1, no. 3, pp. 149-154, 2004. 20

[100] K. Thanjavur, R. Rajagopalan, Ease of dynamic modeling of wheeled mobile robots (WMRs) using Kane's approach, *Proceedings of International Conference on Robotics and Automation*, vol. 4, pp. 2926-2931, 1997. 20

[101] R. P. Chan, K. A. Stol and C. Roger Halkyard, Review of modeling and control of two-wheeled robots, *Annual Reviews in Control*, vol. 37, no. 1, pp. 89-103, April 2013. 20

[102] Y. Nakamura, H. Ezaki, Y. Tan and W. Chung, "Design of steering mechanism and control of nonholonomic trailer systems," in *IEEE Transactions on Robotics and Automation*, vol. 17, no. 3, pp. 367-374, Jun 2001. 20

[103] J. C. Ryu, S. K. Agrawal and J. Franch, Motion planning and control of a tractor with a steerable trailer using differential flatness, *Journal of Computational and Nonlinear Dynamics*, vol. 3, Issue 3, April 2008. 20

[104] A. K. Khalaji and S. A. A. Moosavian, Dynamic modeling and tracking control of a car with *n* trailers, *Multibody System Dynamics*, vol. 37, no. 2, pp. 211-225, 2016.

[105] A. C. Matos, Optimization and control of nonholonomic vehicles and vehicles formations, *PhD Thesis, University of Porto*, 2011. 20

[106] R. M. Murray, Z. Li, S. S. Sastry, A mathematical introduction to robotic manipulation, *Textbook by CRC Press, ISBN 9780849379819*, 480 Pages, March, 1994. 20, 21

[107] O. Mohareri, R. Dhaouadi, A. Rad, “Indirect adaptive tracking control of a nonholonomic mobile robot via neural networks,” *Neurocomputing*, vol. 88, pp. 54-66, July 2012. 22

[108] J. M. Yang and J. H. Kim, “Sliding mode control for trajectory tracking of nonholonomic wheeled mobile robots,” *IEEE Transactions on Robotics and Automation*, vol. 15, Issue 3, pp. 578-587, June 1999. 24

[109] L. G. Bushnell, D. M. Tilbury, and S. S. Sastry, Steering three-input nonholonomic systems: the fire truck example, *The International Journal of Robotics Research*, vol. 14, no. 4, August 1995. 37

[110] A. Isidori, Nonlinear control systems: an introduction (2nd edition), *Springer-Verlag New York, Inc.* New York, NY, USA 1989, ISBN:0-387-50601-2. 37, 38

[111] R. Murray and S. Sastry, “Nonholonomic motion planning: steering using sinusoids,” *IEEE Transactions on Automatic Control*, vol. 38, no. 5, pp. 700-716, 1993. 37, 38

[112] R. Murray and S. Sastry, Steering nonholonomic systems in chained forms, *In Proceedings of the 30th Conference on Decision and Control*, Brighton, England, vol. 2, pp. 1121-1126, 1991. 37

[113] G. Oriolo, A. D. Luca, M. Vendittelli, WMR control via dynamic feedback linearization: design, implementation, and experimental validation, *IEEE Transaction on Control Systems Technology*, vol. 10, Issue 6, pp. 835-852, November 2002. 47

[114] W. Dong, W. L. Xu, Adaptive tracking control of uncertain nonholonomic dynamic system, *IEEE Transactions on Automatic Control*, vol. 46, Issue 3, pp. 450-454, March 2001. 47

[115] T. Kuc, S. Baek, K. Park, Adaptive learning controller for autonomous mobile robots, *IEE Proceedings Control Theory and Applications*, vol. 148, Issue 1, pp 49-54, January 2001. 48

[116] P. Morin, C. Samson, Control of nonholonomic mobile robots based on the transverse function approach, *IEEE Transactions on Robotics*, vol. 25, Issue 5, pp. 1058-1073, April 2009. 48

[117] D. Buccieri, D. Perritaz, P. Mullhaupt, Z. P. Jiang, D. Bonvin, Velocity-scheduling control for a unicycle mobile robot: theory and experiments, *IEEE Transactions on Robotics*, vol. 25, Issue 2, pp. 451-458, April 2009. 48

[118] W. E. Dixon, D. M. Dawson, F. Zhang, E. Zergeroglu, Global exponential tracking control of a mobile robot system via a PE condition, *IEEE Transactions on Systems, Man, and Cybernetics*, vol. 30, Issue 1, pp. 129-142, February 2000. 48

[119] R. S. Ortigoza, G. S. Ortigoza, V. M. Guzman, V. R. Sotelo, J. M. Jimenez, V. M. Garcia, Trajectory tracking in a mobile robot without using velocity measurement for control of wheels, *IEEE Latin America Transaction*, vol. 6, Issue 7, pp. 598-607, December 2008. 48

[120] Z. P. Jiang and H. Nijmeijer, A recursive technique for tracking control of non-holonomic systems in chained form, *IEEE Transactions on Automatic Control*, vol. 44, no. 2, pp. 265-279, 1999. 48, 70, 71, 74, 83, 109, 129

[121] T. J. Huang, Adaptive tracking control of high-order nonholonomic mobile robot systems, *IET Control Theory & Applications*, vol. 3, Issue 6, pp. 681-690, May 2009. 48

[122] W. E. Dixon, D. M. Dawson, E. Zargeroglu, A. Behal, Adaptive tracking control of a wheeled mobile robot via an uncalibrated camera system, *IEEE Transactions on Systems, Man, and Cybernetics*, vol. 31, pp. 341-352, 2001. 48

[123] W. E. Dixon, M. S. de Queiroz, D. M. Dawson, T. J. Flynn, Adaptive tracking and regulation of a wheeled mobile robot with controller/update law modularity, *IEEE Transactions on Control Systems Technology*, vol. 12, Issue 1, pp. 138-147, February 2004. 48

[124] P. Coelho, U. Nunes, Path-following control of mobile robots in presence of uncertainties, *IEEE Transactions on Robotics*, vol. 21, Issue 2, pp. 252-261, April 2005. 48

[125] J. M. Yang, J. H. Kim, Sliding mode motion control of nonholonomic mobile robots, *IEEE Control Systems*, vol. 19, Issue 2, pp. 15-23, April 1999.

[126] C. Chwa, Sliding-mode tracking control of nonholonomic wheeled mobile robots in polar coordinates, *IEEE Transactions on Control Systems Technology*, vol. 12, Issue 4, pp. 637-644, June 2004. 48, 133

[127] H. Chen, M. M. Ma, H. wang, Z. Y. Liu, Z. X. Cai, Moving horizon H_∞ tracking control of wheeled mobile robots with actuator saturation, *IEEE Transaction on Control Systems Technology*, vol. 17, Issue 2, pp. 449-457, February 2009. 48

[128] S. Akhavan, M. Jamshidi, A NN-based sliding mode control for nonholonomic mobile robots, in: *Proceedings of the IEEE International Conference on Control Applications*, Anchorage, 2000, pp. 664-667. 48

[129] N. A. Martins, D. Bertol, E. R. De Pieri, E. B. Castelan, M. M. Dias, Neural dynamic control of a nonholonomic mobile robot incorporating the actuator dynamics, in: *Proceedings of the International Conference on Computational Intelligence for Modeling Control and Automation*, Vienna, pp. 563-568, 2008. 48

[130] J. Ye, Tracking control for nonholonomic mobile robots: Integrating the analog neural network into the backstepping technique, *Neurocomputing*, vol. 71, Issues 16-18, pp. 3373-3378, October 2008. 48

[131] G. Tao, Adaptive Control Design and Analysis, *John Wiley & Sons*, New Jersey, 2003. 48, 55, 57, 77, 87, 89, 90,

[132] K. S. Narendra and J. Balakrishnan, "Adaptive control using multiple models," *IEEE Transactions on Automatic Control*, vol. 42, no. 2, pp. 171-187, February 1997. 60

[133] R. Isermann, "Supervision, fault-detection and fault-diagnosis methods an introduction," *Control Engineering Practice*, 5(5), 639-652, 1997. 104

[134] M. Blanke, M. Kinnaert, J. Lunze, and M. Staroswiecki, "Diagnosis and fault-tolerant control (2nd edition)," *Berlin: Springer*, 2006. 104

[135] J. Chen, and R. J. Patton, "Robust model-based fault diagnosis for dynamic systems," *Boston: Kluwer Academic Publishers*, 1999. 104

[136] M. Farza, M. M'Saad, T. Maatoug, and M. Kamoun, "Adaptive observers for nonlinearly parameterized class of nonlinear systems," *Automatica, Elsevier*, vol. 45, no. 10, pp. 2292-2299, October 2009. 104, 108, 109, 129

[137] K. Zhang, B. Jiang, P. Shi, V. Cocquempot, Observer-Based Fault Estimation Techniques, *Springer Nature, Series: Studies in Systems, Decision and Control*, Volume 127, 2018. 104

[138] M. M. Polycarpou, and A. J. Helmicki, "Automated fault detection and accommodation: a learning systems approach," *IEEE Transactions on Systems Man*

and Cybernetics, vol. 25, no. 11, pp. 1447-1458, 1995. 104

[139] J. Liao, Z. Chen and B. Yao, "Performance-oriented coordinated adaptive robust control for four-wheel independently driven skid steer mobile robot," in *IEEE Access*, vol. 5, pp. 19048-19057, 2017. 133

[140] B. S. Park, S. J. Yoo, J. B. Park and Y. H. Choi, "Adaptive neural sliding mode control of onholonomic wheeled mobile robots with model uncertainty," in *IEEE Transactions on Control Systems Technology*, vol. 17, no. 1, pp. 207-214, Jan. 2009. 133

[141] H. Yang, M. Guo, Y. Xia and L. Cheng, "Trajectory tracking for wheeled mobile robots via model predictive control with softening constraints," in *IET Control Theory & Applications*, vol. 12, no. 2, pp. 206-214, 1 30 2018. 133

[142] X. Zhang, Fault-tolerant control scheme for linear systems with input constraints and actuator faults, *PHD Thesis, University of Lille 1*, March 2015. 133

[143] H. J. Ma, G. H. Yang, Simultaneous fault diagnosis for robot manipulators with actuator and sensor faults, *Information Sciences*, vol. 366, pp. 12-30, October 2016. 133

[144] J. AL Hage, M. El Badaoui El Najjar, D. Pomorski, Multi-sensor fusion approach with fault detection and exclusion based on the Kullback-Leibler Divergence: application on collaborative multi-robot system, *Information Fusion*, vol. 37, pp. 61-76, January 2017. 133

Diagnostic et commande tolérante aux fautes pour un système de robots mobiles liés physiquement

Résumé: Dans les environnements difficiles résultant de catastrophes naturelles ou d'accidents industriels, des robots mobiles peuvent être utilisés pour réduire les interventions humaines. Ces robots doivent pouvoir parcourir de longues distances, suivre des trajectoires précises, transporter des matériels et instruments, tout en étant robustes aux perturbations et aux défaillances éventuelles de leurs composants (capteurs, actionneurs).

Dans cette thèse, nous considérons des systèmes composés de robots mobiles à deux roues motrices (2WD), reliés physiquement entre eux. Nous proposons des lois de commande permettant au système multi-robot de suivre une trajectoire de référence malgré la présence de défauts d'actionneurs. Différentes commandes tolérantes aux fautes (FTC: Fault Tolerant Control) sont proposées. Certaines sont des commandes dîtes passives, qui sont conçues pour être robustes à des défauts actionneurs sélectionnés, d'autres sont dîtes actives puisqu'elles intègrent un algorithme de diagnostic (observateur adaptatif non linéaire) qui détecte, localise et estime les défauts.

Des résultats de simulation sont présentés tout au long de la thèse pour vérifier la validité et montrer les performances des algorithmes de commande tolérante proposés.

Mots clés: Commande tolérante aux fautes, Diagnostic, Forme chainée, Système multi-robot, Robotique mobile, Modélisation.

Fault Diagnosis and Fault Tolerant Control Design for Physically Linked 2WD Mobile Robots Systems

Abstract: In harsh environments resulting from natural disasters or industrial accidents, reducing human interventions by increasing robotic operations is desirable. The main challenges to be considered are not only that the robots should be able to go over long distances and operate for relatively long periods, but also make the global system tolerant to actuators' failures. In this thesis, to overcome these challenges, systems composed of multi-linked two-wheel drive (2WD) mobile robots are considered. The objective of these multi-robot systems is to asymptotically track a reference trajectory, despite the presence of actuator faults. In this thesis, we design original Fault Tolerant Control (FTC) schemes. Some of them are passive methods, i.e. robust control laws to given failures, and other ones are active FTC which include a Fault Diagnosis (FD) algorithm (nonlinear adaptive observer) that detects, localizes and estimates the faults, and finally adapt the control actions to the faulty situations.

Simulation results are presented all along the thesis to verify the validity of the proposed control algorithms and to show the performance of the FTC schemes.

Keywords: Fault-tolerant control; Fault diagnosis; Chained form; Multi-linked mobile robots, Mobile robotics, Modeling.